SWINGS Cruise Report MD229- N/O Marion-Dufresne- Jan 11th -March 8th 2021

Catherine Jeandel, Hélène Planquette

SWINGS Cruise Report

MD229 | N/O Marion-Dufresne | Jan 11th-March 8th 2021

Catherine Jeandel (CNRS-LEGOS-Toulouse) & **Hélène Planquette** (CNRS-LEMAR-Plouzané)

Co-PIs of SWINGS and Co-chief scientists of the cruise

Figure 0 -1: group picture taken on Feb 28th just before leaving Port-aux-Français, Kerguelen

SCIENTIFIC PERSONNEL

	Name	Surname	Laboratory	Citizenship
1	Barut	Guillaume	LOCEAN/France	France
2	Baudet	Corentin	LEMAR/France	France
3	Belhadj	Moustafa	LEGOS/France	France
4	Berthelot	Hugo	SBR/ France	France
5	Blain	Stéphane	LOMIC/France	France
6	Cardinal	Damien	LOCEAN/France	France
7	Cassou	Christophe	CERFACS/France	France
8	Clerc	Corentin	LMD/France	France
9	Cotard	Edwin	LEMAR/France	France
10	Cotte	Cedric	LOCEAN/France	France
11	De Saint Léger	Emmanuel	DT INSU/France	France
12	D'orgeval	Sybille	Artist/France	France
13	Eldin	Gérard	LEGOS/France	France
14	Fin	Jonathan	LOCEAN/France	France
15	Forrer	Heather	Florida International University	South Africa
16	Fourquez	Marion	M.I.O/France	France
17	Gest	Léa	Université de la Réunion	France
18	Godard	Laurent	Artist/France	France
19	Goddard-Dwyer	Millie	University of Liverpool/U.K.	U.K.
20	Gonzalez-Santana	David	LEMAR/France	Spain
21	Gueneugues	Audrey	LOMIC/France	France
22	Hamelin	Bruno	CEREGE/France	France
23	Izard	Lloyd	LOCEAN/France	France/U.K.
24	Jeandel	Catherine	LEGOS/France	France
25	Kestenare	Elodie	LEGOS/France	France
26	Lagarde	Marion	LEGOS/France	France
27	Landing	Bill	Florida State University/U.S.A.	U.S.A
28	Lemaitre	Nolwenn	ETH/Switzerland	France
29	Leon	Morgane	LEGOS/France	France
30	Leseurre	Coraline	LOCEAN/France	France
31	Liao	Wen-Hsuan	LEMAR/France	Taiwan
32	LoMonaco	Claire	LOCEAN/France	France
33	Lopes	Christian	Florida International University	U.SA
34	Mignon	Claude	LOCEAN/France	France
35	Obernosterer	Ingrid	LOMIC/France	Austria
36	Perault	Fabien	DT INSU/France	France
37	Piejus	Marine	Voluntary/France	France
38	Planchon	Frédéric	LEMAR/France	France
39	Planquette	Hélène	LEMAR/France	France
40	Ryan Keogh	Thomas	CSIR/South Africa	U.K.
41	Sanial	Virginie	Université Toulon/ France	France
42	Sergi	Sara	LOCEAN/France	Italia
43	Torres-Rodriguez	Natalia	M.I.O/France	Colombia
44	Turnbull	Isobel	University of Plymouth/U.K.	U.K.
45	van Beek	Pieter	LEGOS/France	France
46	Vivier	Frédéric	LOCEAN/France	France
47	Vorrath	Maria-Elena	LEMAR/France	Germany
48	Zhang	Rui	LOMIC/France	China

TABLE OF CONTENTS

CRUISE OVERVIEW

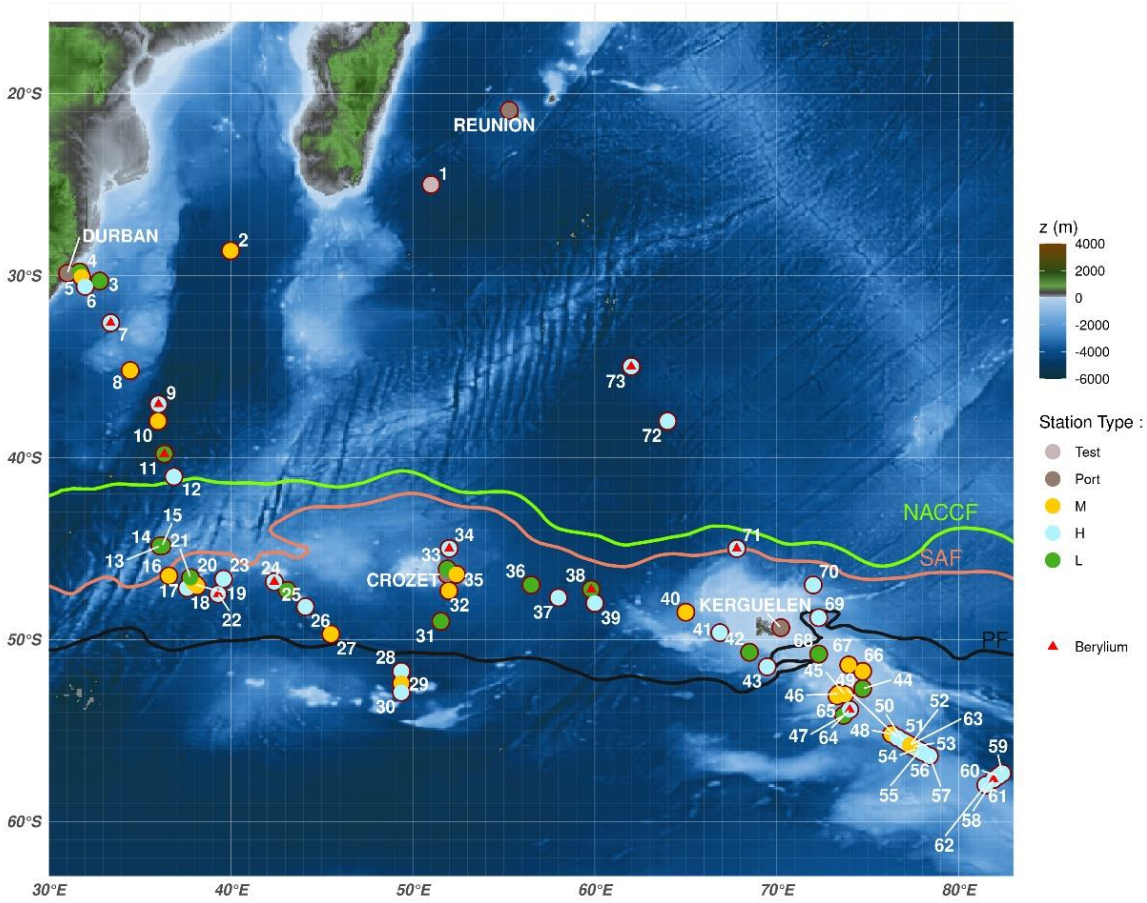

Figure 0-2: Final map of the SWINGS cruise track, edited by Corentin Clerc and Sara Sergi. Location of the Southern Ocean fronts defined by Park et al. (2019[1]) are shown: Green, NACCF, North Antarctic Circumpolar Current Front; Pink, SAF: Sub Antarctic Front; Black, PF: Polar Front. Blue points: station H (Hydrology, only one standard CTD deployment); yellow points: station M (medium, one standard CTD, one clean CTD); green points: station L, same as M with in situ pumps and coring); red triangles: ^{7}Be sampling locations.

Logbook of all sampling operations is available at this link: http://www.obs-vlfr.fr/proof/php/SWINGS/swings_log_basicfiles.php

[1] Park, Y. H., Park, T., Kim, T. W., Lee, S. H., Hong, C. S., Lee, J. H., ... & Provost, C. (2019). Observations of the Antarctic Circumpolar Current over the Udintsev Fracture Zone, the narrowest choke point in the Southern Ocean. *Journal of Geophysical Research: Oceans*, *124*(7), 4511-4528.

Introduction and objectives

SWINGS is a multidisciplinary 4-year project dedicated to elucidate trace element sources, transformations and sinks along a section crossing key areas of the Southern Ocean (SO). Major French contribution to the international GEOTRACES program (www.geotraces.org), SWINGS involves ca 80 scientists (21 international laboratories, 7 countries[2]). As core action of SWINGS, the SWINGS cruise (R/V Marion-Dufresne, MD229, Geotraces section GS02) started from La Reunion on January 11th 2021 and ended at La Reunion 57 days later (March 8th, 2021). This cruise explored a large part of the South Indian Ocean (Figure 0-2) in order to tackle the following objectives:

1) establish the relative importance of sedimentary, atmospheric and hydrothermal sources of TEIs in the Indian sector of the SO

2) investigate the drivers of the internal trace element cycles: biogenic uptake, remineralization, particle fate, and export, and

3) quantify TEI transport by the Antarctic Circumpolar Current and the numerous fronts at the confluence between Indian and Atlantic Oceans.

Cruise Strategy

SWINGS strategy relies on the strong coupling between physical oceanography, biogeochemistry and modeling. During the cruise, a major and original focus has been put on the characterization of the physical, biological and chemical particle speciation in suspended and sinking particles that have been collected during SWINGS.

We realized a high spatial resolution sampling of the dissolved (<0.45 µm) and particulate (>0.45 µm) pools, from the surface to the seafloor. This harvest of data will allow a major step forward in the understanding and quantification of dissolved-particle exchanges, a major recognized bolt for the element cycle modeling. Moreover, samples to analyze dedicated tracers (e.g Th and Pa isotopes) were collected in order to better characterize the particle dynamics. Ra isotope analyses will support the quantification of land-ocean transfers while Nd ones will trace the origin of the dissolved and particulate matter. Both tracers will also help identifying and characterizing hydrothermal source occurrences. Indeed, specific attention was paid to the ocean interfaces: atmospheric and land contacts, and a segment of the South West Indian Ridge suspected to be the home of active hydrothermal sites were explored. Combined with the other suite of trace metals, we will be able to provide an estimation of the lateral and vertical transport of key trace metals from the different sources investigated along the section. We also collected samples in order to describe the taxonomic diversity of heterotrophic microbes, their metabolic potential, gene- and protein expression patterns as well as samples necessary for the enumeration of heterotrophic prokaryotes and small (up to 20 µm) autotrophic phytoplankton,

[2] SWINGS PARTNERS: CNRS_UPS_LEGOS (PI, TOULOUSE), CNRS_UBO_LEMAR (PI, BREST), AMU_MIO (MARSEILLE), CNRS_UVSQ_LSCE (SACLAY), CNRS_SU_LOCEAN (PARIS), CNRS_SU_LOMIC (BANYULS), CNRS_UPS_GET (TOULOUSE), CNRS_SU_AD2M (ROSCOFF), CNRS_CECI (TOULOUSE), CSIR-SOCCO (CAPE TOWN, SOUTH AFRICA), SU-DEAS, ULB_BRUXELLES (BELGIUM), WU-SO (WASHINGTON UNIV, USA), WHOI-MBC (WOODS HOLE, USA), FU-DEOAS (FLORIDA STATE UNIV AND FLORIDA INTERNATIONAL UNIVERSITY, USA), GEOMAR (KIEL, GERMANY), PEO AND ETH (ZURICH, CH)

the concentration of dissolved organic carbon (DOC) and major inorganic nutrients (nitrate and nitrite, phosphate and silicic acid). Finally, dedicated biology experiments, such as nitrification, calcification or iron uptake experiments were conducted throughout the cruise.

The cruise track –at the Atlantic-Indian boundary- did cross up to 6 currents or fronts, among which the 3 majors are reported in Figure 0-2. These jets are major pathways of the general circulation, critical for chemical specie transport: our navigation strategy was regularly adapted using the SOS (Scheduler for Oceanographic Samplings), an interactive navigation tool for adaptive cruise scheduling in order to characterize these current dynamic (geostrophic calculation) as well as their trace element and isotope contents.

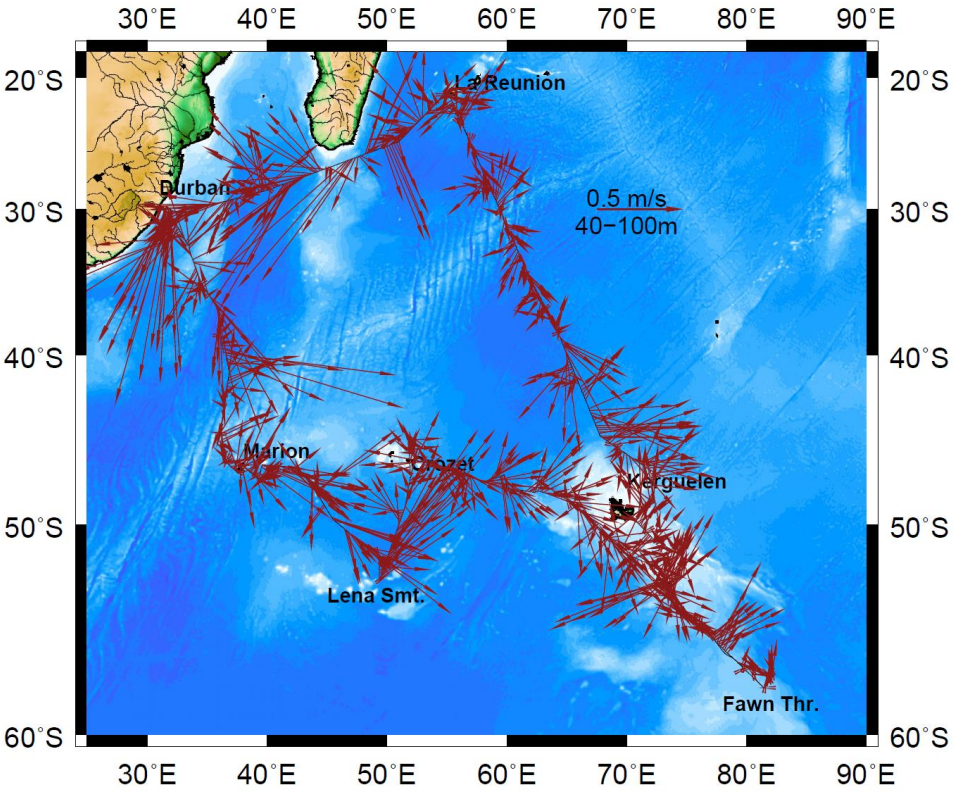

Figure 0-3: Surface currents measured all along the SWINGS cruise (OS75 SADCP data, edited by Gerard Eldin and acquired at time of writing). Arrows show average current in 0.1 x 0.1 degree, 40-100m depth boxes.

First results

For most of the parameters collected during SWINGS, we cannot show any results since these parameters require specific laboratory conditions (clean labs) and dedicated instruments (mass spectrometers) to be analyzed. However, some physical and chemical analyses were conducted on board. We selected preliminary results on the surface currents (SADCP data treatment,

Figure 0-4); a north-south section of T,S and dissolved oxygen non-calibrated data (Figure 0-4); dissolved iron and mercury first results (Figures Figure 0- 5 and Figure 0-6) and ^{223}Ra data (Figure 0-7) above the SWIR.

All these figures are commented in more details in the corresponding chapters of this report, organized as follows: chapter 1: Navigation, Chapter 2: Physical oceanography and circulation; chapter 3: Ancillary parameters; chapter 4: Hydrothermal exploration, chapter 5: Surface and biological parameters; chapter 6: Trace metals; chapter 7: Isotopes and radionucleides; chapter 8 : Particles, export and cores ; chapter 9 : Outreach activity and finally, the appendix.

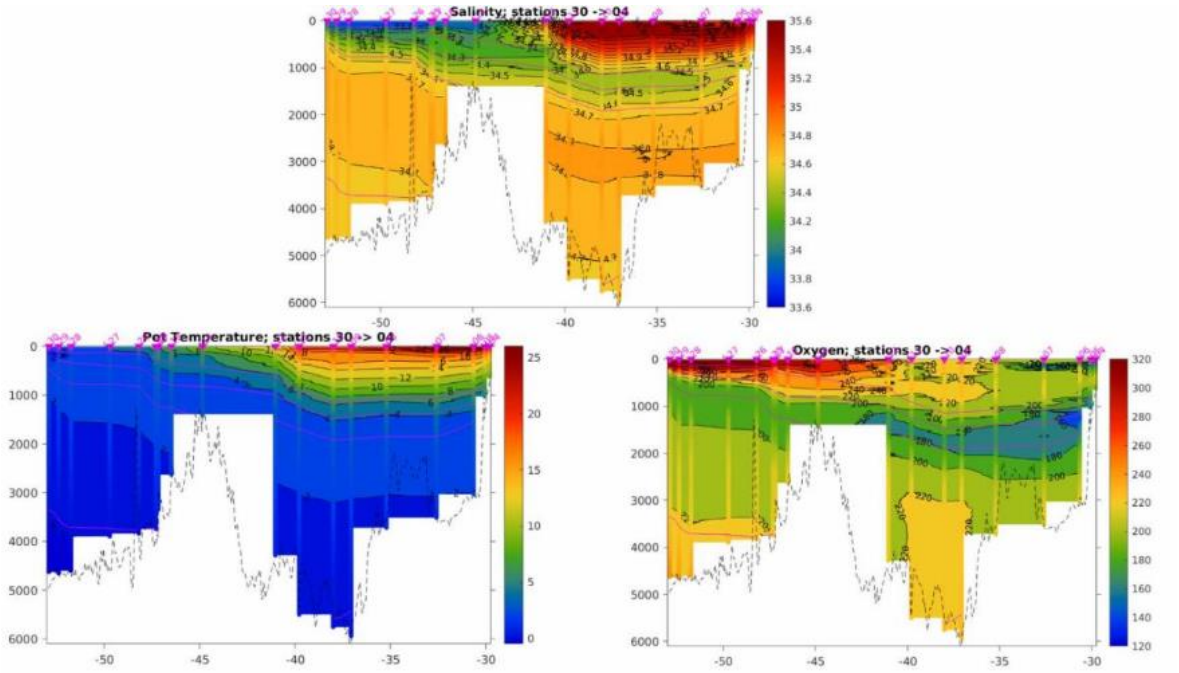

Figure 0-4: North-South T, S and Oxygen data section between SWINGS stations # 04 to #30 (Frédéric Vivier, Elodie Kestenare and Gérard Eldin)

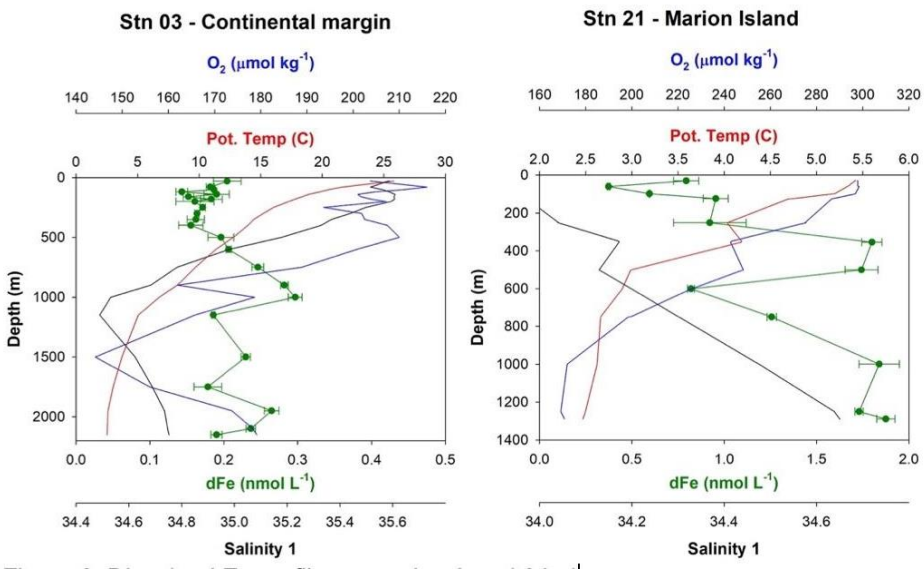

Figure 0-5: Dissolved iron profiles above the South African continental margin and at Marion island (David Gonzalez-Santana)

Post cruise strategy and data management

Just after the cruise, new model experiments will be designed and take place after the first data acquisition, in order to evaluate the sensitivity in TEI distributions to the representation of sources and transports and explore the importance of "the island effect" on the TEI distribution around naturally fertilized islands. Analyses, data validation, interpretation will start in boreal spring 2021.

Post-cruise meetings, communications and peer-reviewed publications will regularly happen until 2024 and likely beyond. SWINGS being a GEOTRACES section (#GS02) will follow the mandatory sampling resolution, intercalibration procedure and data validation: all the acquired data will be granted open access following a rigorous Data Management Plan.

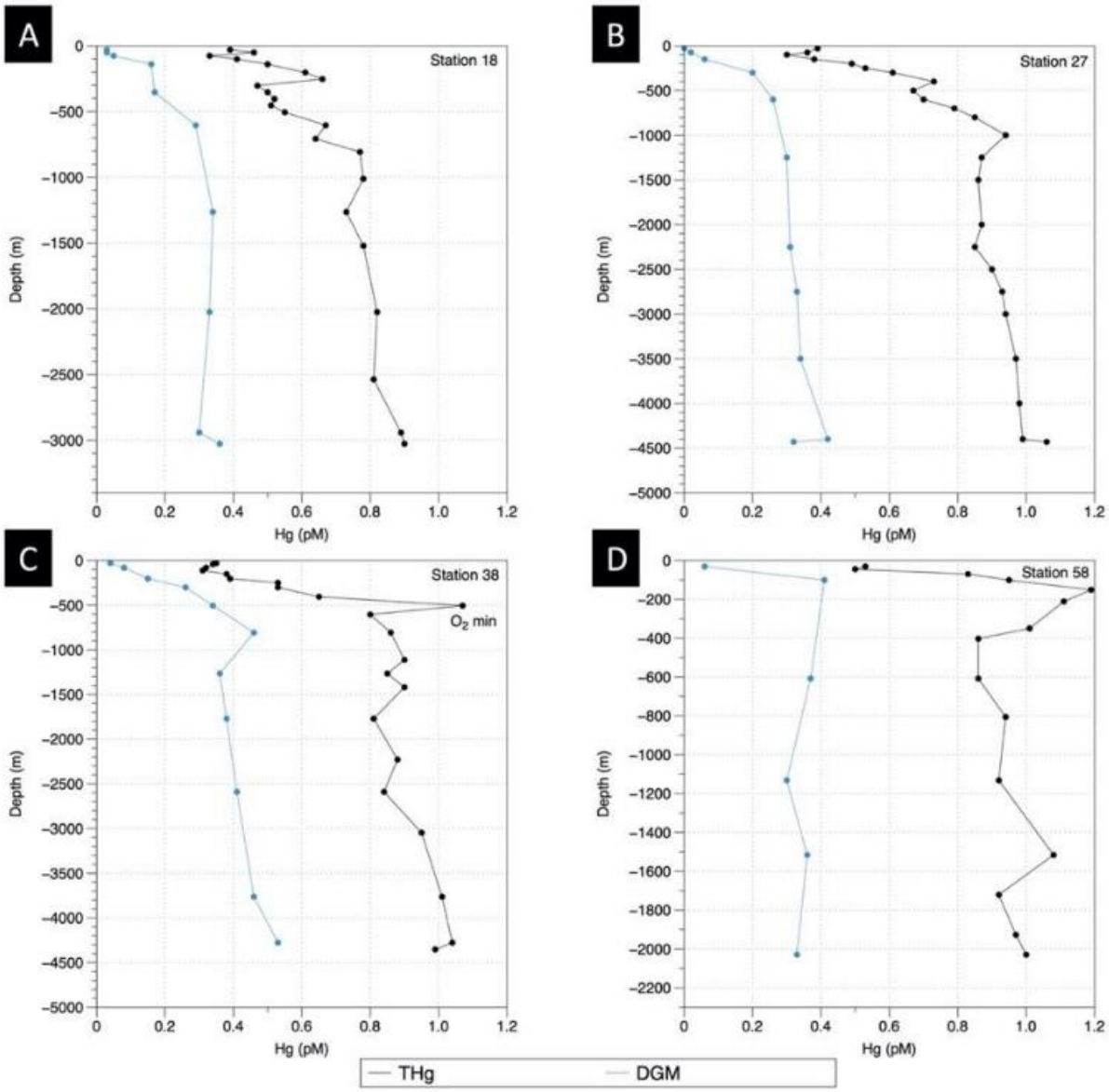

Figure 0-6 First profiles of THg and DGM measured during SWINGS (Natalia Torres-Rodriguez)

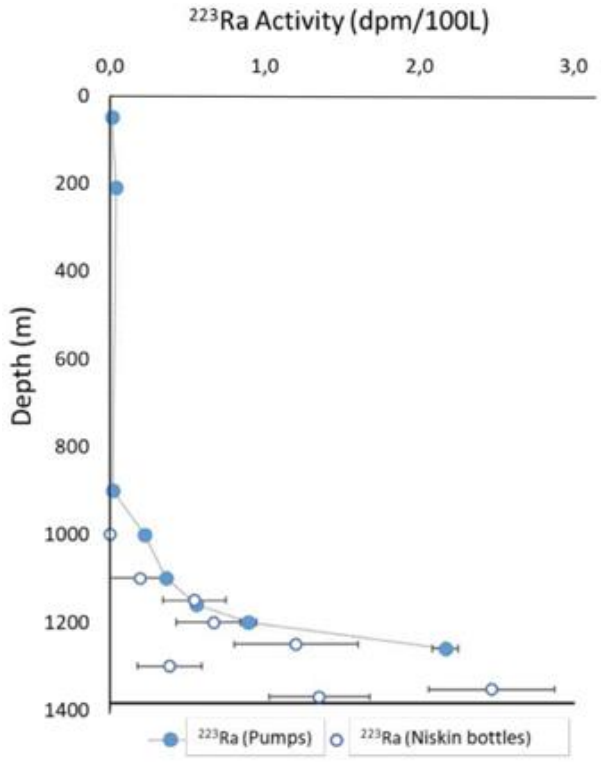

Figure 0-7: ^{223}Ra profiles measured above the South West Indian Ridge. The strong activity increase observed at the bottom clearly signs a hydrothermal activity (Pieter van Beek, Morgane Leon and Virginie Sanial).

To conclude, few numbers

As a whole, during SWINGS, 73 stations were occupied. We realized 105 vertical profiles with the standard rosette including 11 surface casts for the ^{7}Be analysis, 40 with the clean rosette dedicated to the trace metal sampling, 23 *in situ* pumps vertical profiles (12 pumps deployed on average) and 6 successful interface corings. At most clean stations, ultrafiltration was performed to extract the colloidal phase in order to closely document the physical speciation of the particles. We also collected aerosols and rain samples. More than 40 m^3 of water were collected via both rosettes while 190m^3 were filtered with the *in-situ* pumps. Oxygen, dissolved inorganic carbon, pCO_2, Hg and dissolved iron analyses were performed on board. On deck incubations were also conducted to establish the phytoplankton activity in the different biogeochemical areas crossed by the SWINGS track. In addition to this intensive sampling activity, the SWINGS researchers posted 28 articles in 2 languages (Fr and En) on the web site (https://swings.geotraces.org) and edited 8 articles (also bilingual) in the eXploreur on line journal of the Toulouse University (https://exploreur.univ-toulouse.fr/). Among others, this allows irrigating more than 15 schools including a jail's one.

Acknowledgements

All this successful harvest could not have been possible without the strong implication of the 48 scientists who actively participated to the cruise. We know the sampling effort was pretty intense so we wish to deeply and warmly thank all of them for their constant and fruitful effort.

During more than a year, various teams prepared our equipment and sampling bottles: we are infinitely thankful to the various actors on shore. Starting from the design of the new sampling van and geofish (C. Marec, L. Scouarnec, O. Desprez de Gésincourt), the cleaning team for GO-FLO and bottle cleaning at LEMAR (E. Bucciarelli, F. Desprez de Gésincourt, M. Gallinari, G. Sarthou), the wonderful team at DT INSU who prepared carefully our two rosettes and CTDs, as well as the *in-situ* pumps.

An oceanographic cruise is not possible without capable persons operating the vessel, so, in addition to the researchers, engineers and students who shared this scientific venture, we wish to sincerely thank the Master Adrien Eyssautier and the crew of the Marion-Dufresne: without your skills and professionalism, this sampling success would not have been possible. You deployed all our instruments with great care, sometimes in very harsh conditions and you always positively responded to our maniac requests (sleeves, no start of secondary engines during clean operations and so many researchers' "caprices") and our station plan optimizations, sometimes at short notice. We would like to address a special thanks to the very supportive GENAVIR Team: starting with OPEXOs Martin Boudoux d'Hautefeuille and François Réguerre: you provided the necessary expertise, good willing, help and guidance, your role on board was crucial and should be maintained in future cruises; the careful clean winch operators Guillaume Viollette and Alain Jaouen and the electronician Vincent Gabriel. Finally, a special thanks also to the Colson brothers Emmanuel de Saint-Léger and Fabien Pérault (CNRS-INSU), the efficient and reliable engineer tandem, aka our ISP super heroes or fish resuscitators without whom nothing would have been possible.

We would like to also thank on-land colleagues who efficiently help for all the navigation and station position issues (Julie Deshayes, Francesco d'Ovidio) so we could optimize our sampling strategy.

SWINGS is supported by IFREMER (Flotte Oceanographique Francaise), CNRS-INSU (programme LEFE/CYBER), Agence Nationale de la Recherche (ANR-19-CE01-0012-01), Université de Bretagne Occidentale (IsBlue), Université Paul Sabatier (IPO GEOTRACES and web-master, www.swings.geotraces.org) and Université Fédérale de Toulouse (Journal eXploreur: https://exploreur.univ-toulouse.fr/).

Catherine Jeandel

Hélène Planquette

I. SOS (SCHEDULER FOR OCEANOGRAPHIC SAMPLINGS), AN INTERACTIVE NAVIGATION TOOL FOR ADAPTIVE CRUISE SCHEDULING

Principal investigator
Corentin Clerc
ENS Département de Géosciences, 24 rue Lhomond 75005 Paris
corentin.clerc@lmd.ens.fr

Names of other participants
On board: Sara Sergi (LOCEAN), Lloyd Izard (LOCEAN), Catherine Jeandel (LEGOS) Hélène Planquette (LEMAR),
On shore: Julie Deshayes (LOCEAN), Francesco D'Ovidio (LOCEAN)

Abstract

Sea surface satellite observations and 3D model reanalyses provide substantial information of the near real time oceanographic conditions. In a context of increasing access to network onboard, taking profit of those information for oceanographic cruise scheduling is valuable, especially for adapting scientific cruise scheduling to the high dynamics of the ocean. Scheduler for Oceanographic Samplings (SOS) is a visual and interactive tool that combine position and scientific operation information of a cruise to provide an instant schedule, automatically including and considering the bathymetry of the stations. The sampling strategy can be optimally and quickly adapted directly within the tool based on multiple constraints, ranging from technical constraints of the scientific operations to near real time oceanographic information that are also included in the tool. We present in this report how SOS substantially impacted the SWINGS cruise in term of planification efficiency and sampling quality. Based on this first experimentation, SOS-based cruise scheduling should be considered as a promising strategy for further oceanographic campaigns.

I.1 Scientific context

Planning plays a central role in the success of an oceanographic cruise. Indeed, scientific relevance of operations is strongly depending on their timing and location. Pre-cruise planning of operations is usually based on an exhaustive exploration of the literature, with a specific focus on past cruises within the zone of interest. Pre-cruise meetings then constrains the cruise schedule depending on scientific interest of each participant and available time. Timing of cruise operations can be roughly estimated using simple parameterization of scientific operations (*e.g.* time for a bathymetric probe deployment) and transit times. This pre-cruise planification is time costly as it is PI-dependent and strongly depending on the bathymetry which need to be set manually.

Due to the intrinsic highly dynamical conditions of the ocean environment, cruise planning schedules have to be constantly adapted to local and real-time environmental conditions (e.g. Nencioli et al., 2011; Pascual et al., 2017). In this context, the Software Package for an Adaptive Satellite-based Sampling for Oceanographic cruises (SPASSO) program has been developed by Doglioli et al. in 2013 and is freely distributed, hoping to be useful for the oceanographic community. SPASSO relies on Lagrangian diagnostics to provide the monitoring of dynamical and biogeochemical structures at the sub-mesoscale (fronts, eddies and filaments), in addition to chlorophyll *a* and sea surface temperature maps. Its diagnostics are based on model predictions and near real-time acquisition of satellite maps. The software configuration is discussed during pre-cruise meetings and once set up, it runs automatically (retrieving data and generating maps), daily. Nencioli et al. (2011) developed the initial codes of the software, and the implementing code for the Lagrangian analysis has been developed by Francesco d'Ovidio (d'Ovidio et al., 2004). The adaptations for the SWINGS cruise are the result of a collaborative effort between Lloyd Izard, Stéphanie Barrillon, Andrea Doglioli, and Anne Petrenko. Stéphanie Barrillon monitored the program and made sure it kept running during the cruise. Data interpretation and comments were written in daily reports by Julie Deshayes and Francesco d'Ovidio. At sea, the communication with the land team was mainly assured by Sara Sergi, Corentin Clerc, and the cruise's PIs. SPASSO is operated and developed thanks to the support of the SIP (Service Informatique de Pythéas) and, in particular, C.Yohia, J.Lecubin. D.Zevaco et C.Blanpain (Institut Pythéas, Marseille, France)."

SPASSO (https://spasso.mio.osupytheas.fr/) has been implemented for adaptive sampling strategy during more than 10 ocean campaigns since 2010.
Combining on board near real time oceanographic conditions and boat positioning appears as a necessity to optimize the relevancy of operations.

I.2 Overview of the project and objectives

As onboard network access is increasing (100Mo per day is a reasonable and reliable value for daily uploads), satellite-based databases provide a promising framework to consider downloading data and monitor oceanographic conditions while at sea. However, to our knowledge, there is no tool combining cruise scheduling of operations and analysis of near real time oceanographic conditions and that is coupled to the bathymetry, an essential constraint for operation duration.

As it appeared as a promising way of considering cruise scheduling, we developed SOS (Scheduler for Oceanographic Samplings), an interactive and automatic tool for pre-cruise and onboard scheduling based on near real time oceanographic conditions. This tool has been developed for the SWINGS cruise, but aims to be shared with the scientific community in order to: 1. Reduce the time allocated to the planning process 2. Increase the relevance of operation positioning during a cruise 3. Allow an improved reactivity to the environmental condition changes (*e.g.* weather, chlorophyll, mesoscale circulation).

The first version of SOS has been developed between July and December 2020, based on the SWINGS experimental setup planned by C. Jeandel and H. Planquette. A test session simulating the SWINGS cruise was permormed in December 2020, in order to evaluate the potential of the tool based on three criteria: it had to be user-friendly (for non-programmer users), adaptive (able to support quick onboard decision-

making while facing a particular situation) and reliable (consistent and exhaustive use of available information to give the best planning estimates). This simulation allowed us to evaluate the ability of the tool to perform adaptive cruise scheduling and the reliability of the SOS configuration for the SWINGS cruise.

Between January and March 2021, onboard SWINGS' adaptive cruise scheduling has been based on SOS. The schedule was updated each 2-day based on near-real time oceanographic condition and time constraints, in presence of the two chief scientists. Satellite data were downloaded on board (exhaustive description of satellite products is provided in section 1.3.2), while processing of model outputs was produced on land and regularly sent on board (LOCEAN, Julie Deshayes). In addition, two colleagues from the LOCEAN (Julie Deshayes and Francesco d'Ovidio) daily received SPASSO analyses and provided optimal recommendations to the PIs when adjusting sampling strategy.

I.3 Methodology and sampling strategy

SOS is a RShiny application that provide a visual interface from which you can control all the parameters of the cruise schedule and consult near real time oceanographic conditions. A brief description of the structure of the tool is provided below, a more complete description will be available after the cruise with the open access version of the tool.

I.3.1 Schedule

SOS receive as an input a *.csv* file in which each line represents a station. The following information are provided for each station: name, position, type of station, ship velocity and cast parameters (CTD or *in situ* pump specific parameters).

In the framework of SWINGS, three kinds of operations are included: CTD deployment, *in-situ* pump deployment and transit time.

From the station position, SOS extracts the depth based on the 5-minutes-resolution GEBCO bathymetry. From the bathymetry and input cast parameters (such as cable velocity or number of bottles), SOS computes the expected duration of each cast. This was an important request of the chief scientists.

The transit time is computed from the minimal distance between two points on the WGS84 ellipsoid. The boat velocity is set to 12knt by default, but can be increased or reduced depending on weather conditions or instrument deployment or any other reason.

The complete schedule is obtained by summing the different transit and operation times. SOS provides two distinct outputs: a crew and a complete output. The crew output includes all the necessary information for navigation and operation succession. Both outputs have the form of an excel sheet. SOS also generates an updated map of the stations.

SOS also gives the possibility to modify the input file directly from the visual interface: you can move, remove, add and change any parameter of any station.

Scheduling is therefore continuously updated considering internal factors (operations scheduling, technical problems …) but also considering external factors as meteorological conditions.

I.3.2 Near real time oceanographic conditions

Satellite images and models' outputs are daily downloaded during the cruise. SOS read NetCDF files and put it as a background of the cruise maps, allowing to observe real time updated stations' position with the most recent available oceanographic observations. The different products are described below:

Satellite surface Chlorophyll *a* concentration: estimated from Ocean Color maps produced and distributed by the society *Collecte Localisation Satellites* (CLS).

Sea Surface Temperature gradients: estimated from a satellite product run by the UK's Met Office and distributed by the European Copernicus Marine Environment Monitoring Service (CMEMS; product id: SST_GLO_SST_L4_NRT_OBSERVATIONS_010_001-TDS).

Sea surface height and geostrophic currents: estimated from an altimetry multi-satellite global product produced by SSALTO/DUACS and distributed by CMEMS (product id: SEALEVEL_GLO_PHY_L4_REP_OBSERVATIONS_008_047).

Subsurface currents: estimated by the reanalysis product GLORYS current data. The data are averaged over 5 days and integrated over three vertical levels: 0 to 500 m, 500 to 1000 m and 1000 to 2000 m. In addition, the currents estimated at the surface and at the bottom (last vertical level of the model) are also considered.

Ocean fluids dynamics which better appear to suits to SWINGS scientific objectives: evaluation of latitudinal and longitudinal displacement of water masses in order to avoid high mixing regions; Lagrangian dispersion of water masses from shallow topographies or from other regions of interest (as hydrothermal vents). Altimetry-derived geostrophic currents are evaluated with a Lagrangian approach following d'Ovidio et al. (2015).

I.4 Preliminary results

Cruise schedule has been largely adjusted all along the SWINGs expedition. Indeed, while the large-scale cruise track has been conserved, at the regional scale station types and positions have largely been adapted to real time environmental conditions. As for instance, new sections have been added around 50 °E and east of 80°E in order to characterize specific currents and water masses, and total number of stations has been increased from 54 to 73 (Figure 1 1). The cruise schedule was modified in many different oceanographic situations, in order to better suits to SWINGS scientific objectives. These include the measurement of current transport or the sampling of trace elements and isotopes advected from specific sources, as continental shelves and islands. In particular, this was the case close to Marion Islands and Heard Islands, following the sampling strategies developed for similar studies in the same region (d'Ovidio et al., 2015; Sanial et al., 2014).

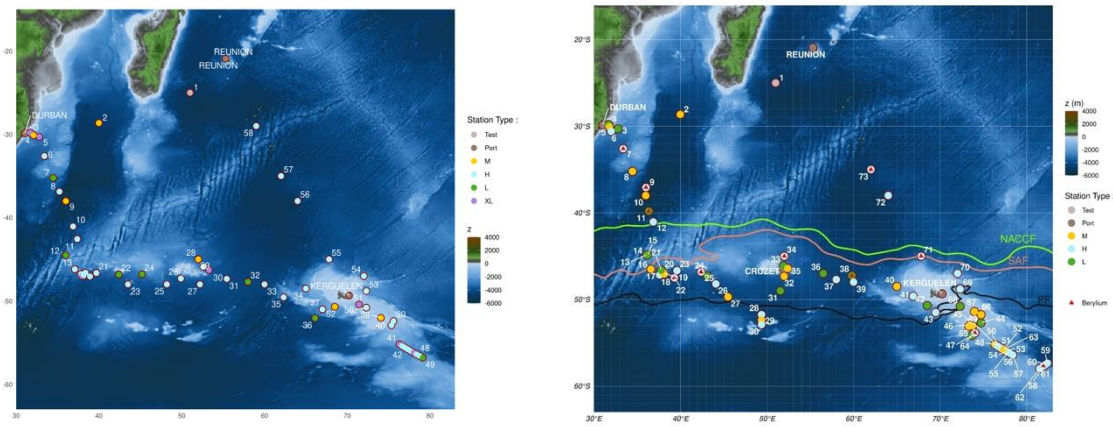

Figure 1 1: Cruise planning map from the SOS tool before the cruise (left) and at the end of the cruise (right). Stations types are classed by colors ("Test", "Port", "H", "M", "L" and "XL"). Final map of the SWINGS cruise track, edited by Corentin Clerc and Sara Sergi. Locations of Southern Ocean fronts defined by Park et al. (2019) are shown in the right panel: Green, NACCF, North Antarctic Circumpolar Current Front; Pink, SAF: Sub Antarctic Front; Black, PF: Polar Front. Blue points: station H (Hydrology, only one standard CTD deployment); yellow points: station M (medium, one standard CTD, one clean CTD); green points: station L, same as M with in situ pumps and coring); red triangles: ^{7}Be sampling locations.

The South Africa shelf region provides an interesting study case where the sampling strategy of the SWINGS cruise was suited to many constraints. One of the main objectives of this study region was to estimate the transport of trace elements and isotopes carried by two currents: the southward Agulhas Current and the deep northward Agulhas Undercurrent. The depths of the sampled stations were also an important constraint: stations should have an increased water depth in order to sample different regions of the continental shelf meanwhile the water depths have to been reduced as much as possible in order to avoid time consuming operations (full depth sample are mandatory for deploying all the instruments).

Figure I-2 shows the sampling strategy adopted in order to fit to the objectives and the operationnal constraints. Positions of stations are illustrated over some oceanographic properties considered with the SOS tool for adjusting the sampling strategy. In particular, the GLORYS reanalysis was used for identifying the two target currents (Figure I-2 A and B), while the chlorophyll *a* concentration and Lagrangian analyses were used as an indicator of transport of sedimentary elements from the continental shelf (Figure I-2 C and D). The latter two were also used for identifying a recirculation region between the coast and 32 °E which has been avoided by the cruise strategy.

The hybrid tool SOS proved its relevance during SWINGS cruise in numerous ways. Taking advantage of the reliable access to the network, it considerably reduced the time allocated to the planning process during the cruise to approximately 3 hours twice a week. The collaboration with modelers strongly increased the reactivity and adaptability of the navigation team. The planning process played an important role in the success of SWINGS, allowing to sample 73 stations instead of the 58 as initially planned. Moreover, those stations are likely to be better positioned than initially, implying a considerable gain in term of quality and relevance of the sampling. Post-cruise evaluation needs to be performed to confirm that assumption.

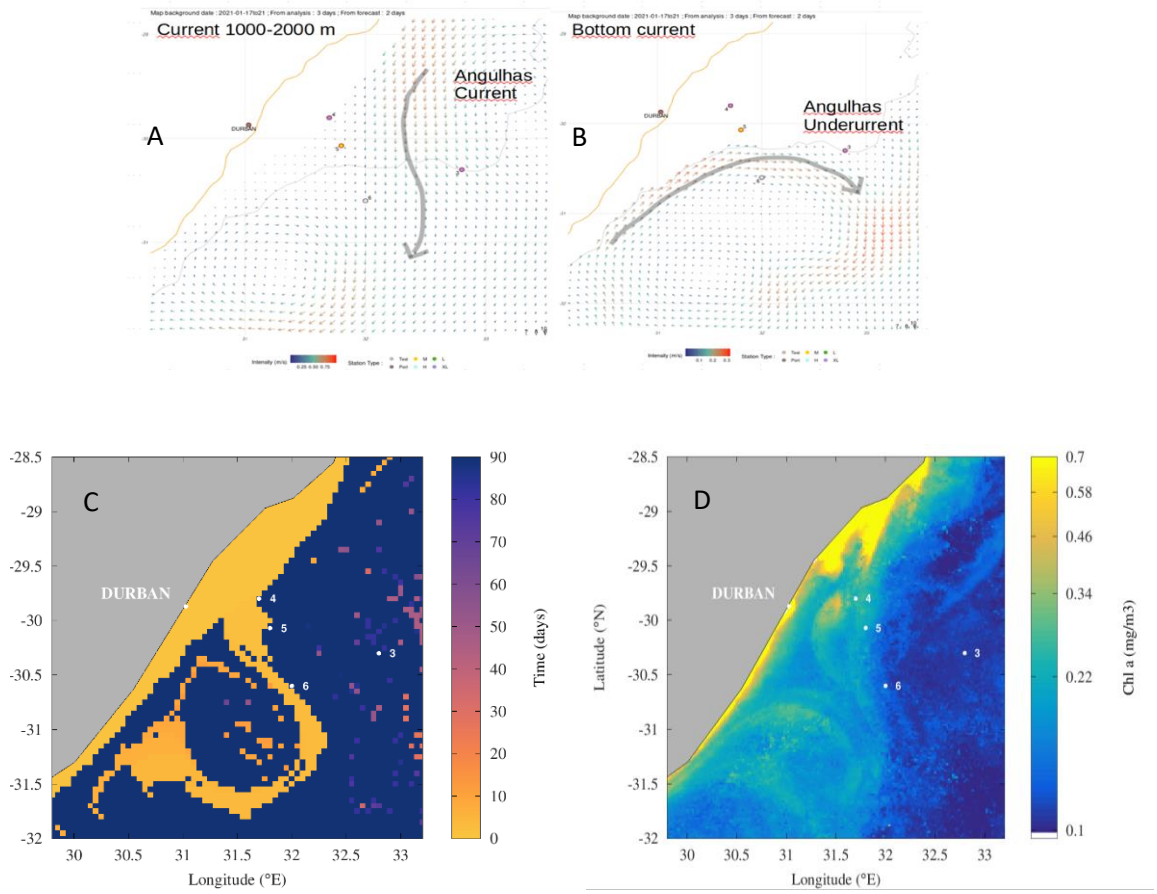

Figure I-2: ***Sampling strategy developed during the SWINGS cruise with the SOS tool in the Agulhas Current Region.*** *(A-B) Identification of the current patterns targeted: the southward Agulhas Current (grey arrow in panel A) and the deep northward Agulhas Undercurrent (grey arrow in panel B). Velocity fields used for identifying the current are issued from GLORYS data averaged between 1000 and 2000 m for the Agulhas Current (panel A) and at the bottom for the Agulhas Undercurrent (panel B) between the 17 and 21 of January, 2021. (C) Distance in time of water masses from the continental shelf (depth shallower than 500 m) since the 17 of January, 2021. (D) Chlorophyll a concentration observed on the 17 of January, 2021. Stations are identified by dots.*

I.5 Post-cruise sampling analyses and envisioned timeline of working plan, people involved on shore

An open source SOS version should be available once the code is ready to share and under license. A maintenance of the tool will be ensured by the main developer during three years after the campaign.

References

Botnikov, V. N. (1963). Geographical position of the Antarctic Convergence Zone in the Antarctic Ocean. Soviet Antarctic Exped. Inform. Bull. 41, 324–327.

d'Ovidio, F., Fernández, V., Hernández-García, E., & López, C. (2004). Mixing structures in the Mediterranean Sea from finite-size Lyapunov exponents. Geophysical Research Letters, 31(17). https://doi.org/10.1029/2004GL020328

d'Ovidio, F., Della Penna, A., Trull, T. W., Nencioli, F., Pujol, M. I., Rio, M. H., et al. (2015). The biogeochemical structuring role of horizontal stirring: lagrangian perspectives on iron delivery downstream of the Kerguelen plateau. Biogeosciences 12, 5567–5581. doi: 10.5194/bg-12-5567-2015

Doglioli, A. M., Nencioli, F., Petrenko, A. A., Rougier, G., Fuda, J.-L., and Grima, N.: A software package and hardware tools for in situ experiments in a Lagrangian reference frame, Journal of Atmospheric and Oceanic Technology, 30, 1940–1950, https://doi.org/10.1175/JTECH-D-12-00183.1, 2013.

GEBCO Compilation Group (2020) GEBCO 2020 Grid (doi:10.5285/a29c5465-b138-234d-e053-6c86abc040b9).

Kim, Y. S. and Orsi, A (2014). On the Variability of Antarctic Circumpolar Current Fronts Inferred from 1992–2011 Altimetry. Journal of Physical Oceanography. 44

Nencioli, F., d'Ovidio, F., Doglioli, A. M., & Petrenko, A. A. (2011). Geophysical Research Letters, 38(17).

Pascual, A., Ruiz, S., Olita, A., Troupin, C., Claret, M., Casas, B., ... & Mason, E. (2017). Frontiers in Marine Science, 4, 39.

Park, Y.-H., Park, T., Kim, T.-W., Lee, S.-H., Hong, C.-S., Lee, J.-H., Rio, M.-H., Pujol, M.-I., Ballarotta, M., Durand, I., & Provost, C. (2019). Observations of the Antarctic Circumpolar Current Over the Udintsev Fracture Zone, the Narrowest Choke Point in the Southern Ocean. Journal of Geophysical Research: Oceans, 124(7), 4511–4528. https://doi.org/10.1029/2019JC015024

Sanial, V., van Beek, P., Lansard, B., d'Ovidio, F., Kestenare, É, Souhaut, M., et al. (2014). J. Geophys. Res. Oceans 119, 2227–2237. doi: 10.1002/2013jc009305

II. HYDROGRAPHY

II.1 Transport and Water Masses in the Antarctic Circumpolar Current region

Principal investigator
VIVIER Frédéric
LOCEAN Paris
+33 (0)1 44 27 70 77
frederic.vivier@locean.ipsl.fr

Names of other participants: The CTD team on board included: Elodie Kestenare (IRD/LEGOS), Gerard Eldin (IRD/LEGOS-retiring), Corentin Clerc (PhD student, LMD), Lloyd Izard (PhD student, LOCEAN), Sara Sergi (PhD student, LOCEAN)

Abstract:

The Southern Ocean, hosting the Antarctic Circumpolar Current, is a central component of the meridional overturning circulation, and as such, has a major influence on the World Ocean and climate. Despite its disproportionate influence the Southern Ocean remains undersampled. The overall objective regarding physical oceanography is to investigate the water masses distribution and circulation with a quantification of the transport of the different current branches intercepted by the SWINGS cruise plan. We will specifically focus on the southernmost sections (Fawn Trough section and WOCE I8S) that were occupied previously during the TRACK (TRansport ACross the Kerguelen plateau) cruises in 2009 and 2010 and that have been re-occupied with a fine spatial sampling. The modification of water masses that may have occurred over the past 10 years will be in particular carefully analyzed. We will examine as well other sections that were sampled with a coarser spatial resolution and estimate as accurately as possible the transport and water masses associated with the different fronts and plumes.

II.1.1 Scientific context

The Southern Ocean (SO), hosting the Antarctic Circumpolar Current (ACC), is a central component of the meridional overturning circulation, and as such, has a major influence on the world's ocean and climate. The SO has been rapidly changing over the past decades, storing in its subsurface water masses almost half of the heat associated with climate change. The response of the ACC to an increase of the westerlies remains unclear yet. Changes in the strength or a meridional shift of the ACC pathway may greatly impact water mass transformation, and thus the meridional overturning circulation. The large-scale 3D circulation of the SO is strongly shaped by the interaction of the flow with topography. This is particularly so in the Indian sector with the South West Indian Ridge and first and foremost with the Kerguelen Plateau, which stands out as the largest topographic feature barring the way of the ACC. There, sixty percent of the flow is diverted to the north in the merged Sub Antarctic Front and Subtropical Front, while the remainder of the ACC flows across the plateau, primarily funneled in the Fawn Trough (40 Sv)

along the Southern ACC Front. Regarding the deep circulation, the Kerguelen Plateau (KP) blocks the inter-basin exchange of AABW, forming two separated abyssal gyres on each side of the plateau: the Weddell Gyre to the west and the Australian-Antarctic Gyre to the east. The latter closes in a deep western boundary current shouldering the eastern flank of the southern KP, which is one of the main equatorward routes of AABW. The latter, which sources in Adélie Land and Ross Sea, has freshened and warmed over the past decades. Despite its disproportionate influence on climate, the Southern Ocean remains under sampled. While this is true for the Indian sector in general, this is particularly so for the Fawn Trough current, measured for the first time 11 years ago with the TRACK program (Park et al 2009), and which had not been revisited since.

II.1.2 Overview of the project and objectives

The overall objective of the project is to investigate the water mass distribution and circulation with a quantification of the transport of the different current branches intercepted by the cruise plan. We will specifically focus on the southernmost sections (Fawn Trough section and WOCE I8S) that were occupied previously during the TRACK cruises in 2009 and 2010. Regarding the branch of the ACC flowing in the Fawn Trough, we benefit from a 25-year long time series of transport estimates based on altimetry (Vivier et al., 2015) built from the statistics stemming from one year worth of current meter data from the 3 moorings deployed during TRACK underneath a TOPEX/Jason satellite ground track. The transport estimated from the synoptic section of the current will be compared to the satellite estimate. The modification of water masses will be carefully examined.

II.1.3 Methodology and sampling strategy

The SWINGS cruise plan encompasses the full span of the ACC frontal system, which provides a rare opportunity to investigate the current and water masses. Because of the different sampling strategy required for geochemistry and biogeochemistry objectives, the system of current is not crossed in a straight meridional section with high spatial resolution, but an overall good trade-off has been found by the cruise leaders, and most appreciably, specific ship time has been dedicated to a refined survey of the regions south of Heard Island (Fawn Trough section, and WOCE I8S section) that were formerly occupied during the two TRACK cruises. We thus expect a fairly good estimate of the transport associated with the different current branches there, whereas estimates will probably be cruder elsewhere. While a specific focus will obviously be on the Fawn trough and WOCE I8S section, for which we can directly compare with our previous observations, we will also carefully examine the other sections, and estimate as accurately as possible the transport and water masses associated with the different fronts and plumes that were sampled during the cruise.

The measured parameters regarding physical oceanography are classical and include T, S, O_2, and the horizontal velocity over a total of 139 casts as detailed in Table 1.

Table 1: List of measured parameters allowing characterizing the SWINGS hydrography

Parameter	Code of operation (Station-cast)	Number of samples
1. T, S O_2, Fluo	All stations (139 casts)	105 Standard (including 5 OISO Kerguelen-Réunion) 40 Clean
2. LADCP (U, V)	Most stations (on standard casts)	62 casts
3. SADCP (U, V)	Underway	

II.1.4 Preliminary results

Operational assessment

Overall the operational assessment is excellent with the collection of high-quality data over most profiles. A major drawback is the absence of the deep reaching shipborne-ADCP (OS 38kHz) which was out of order from start.

The CTD and LADCP provided by DT-INSU worked properly during the entire cruise. Incidents were experienced but were quickly and efficiently fixed by the DT-INSU team or Genavir team and did not hamper the cruise (noise in the data due to bad electric contact in the cable, deck unit breakdown...).

CTD data:

CTD data have been processed onboard by Elodie Kestenare, which required to adjust the processing tools that were provided (the reader is referred to her technical report in Appendix 1 of this cruise report for further detail).

The different conductivity sensors from the CTD, calibrated only a few months before the cruise matched to within less than 0.003 mS/cm (manufacturer accuracy). Samples for salinity were taken by the OISO team throughout the cruise, but an initial assessment suggests that a correction may not be necessary.

A preliminary assessment of the shift of [O_2] data from the CTD compared with samples analyzed by the OISO team has been performed by F. Vivier et C. Lo Monaco (the corresponding report, proposed in Appendix 2 of this cruise report, is by no mean a proposed correction but may be useful for the person in charge; these preliminary crude corrections do not meet WOCE recommendations of 1.7 umol/kg).

L-ADCP data:

The processing of LADCP, which has been performed by Elodie Kestenare, has encountered several obstacles, and has proven much more difficult than anticipated for a variety of reasons (the reader is referred to her report in Appendix 1). A final dataset will not be available until further on shore processing. The acquisition of LADCP worked on all casts except for a few.

S-ADCP data:

The acquisition of S-ADCP data from the OS150 and OS 75kHz was set up and supervised by Gérard Eldin who also ensured the processing onboard. The reader is referred to his report.

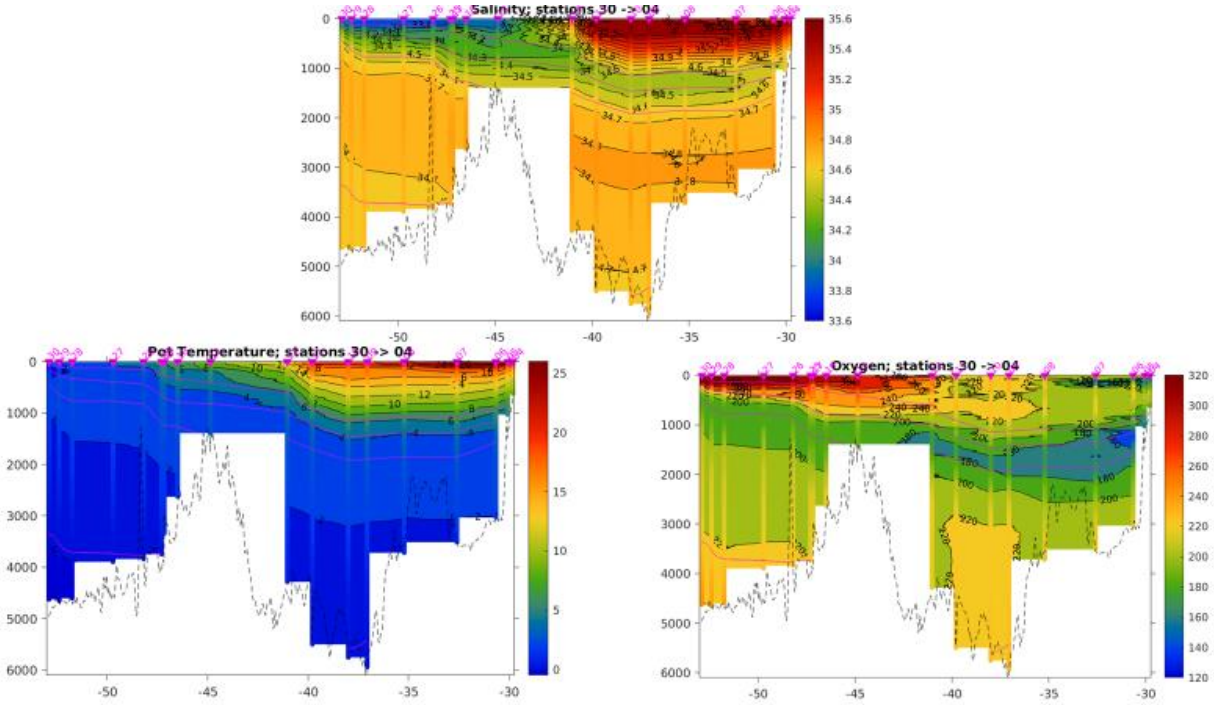

Figure II-1: Meridional section of potential temperature, salinity and dissolved oxygen from the Aghulas Current to the Polar Front (Station 4->30) displaying the main water masses of the Southern Ocean (AAIW, NADW/ CDW, AABW,..).

II.1.5 Post-cruise sampling analyses and envisioned timeline of working plan, people involved on shore

Scientific analyses on shore will be carried out in collaboration with Young-Hyang Park (LOCEAN/MNHN), who initiated the TRACK program 11 years ago, and who is one of the finest specialists of the region as far as physical oceanography is concerned.

A final dataset is yet to be processed. This includes correction of the dissolved oxygen concentration profiles collected with the CTD based on the samples titrated with the modified Winkler method by the OISO team. This shall be done carefully by a specialist. Processing of the LADCP dataset initiated onboard by Elodie Kestenare still requires as well a fairly significant amount of work (please refer to Appendix 1 of this cruise report). An estimated timeline for scientific analyses and budgets should be on the order of one year or so, depending on the availability of a final dataset.

References

Park, Y-H, Vivier, F, Roquet, F, and E. Kestenare. Direct observation of the ACC transport across the Kerguelen Plateau. Geophys Res. Letters, 2009, vol 36, L18603, doi :10.1029/2009GL039617

Park, Y-H and F Vivier. Circulation and hydrography over the Kerguelen Plateau, In "The Kerguelen Plateau: Marine Ecosystem and Fisheries", proceedings of the 1st international Science Symposium on the Kerguelen Plateau (Duhamel G. & Welsford D. Eds). Société Francaise d'Ichtyologie. 2011, pp. 43-55.

Vivier, F ; Y-H Park, H Sekma, and J Le Sommer (2015). Variability of the Antarctic Circumpolar Current transport through the Fawn Trough, Kerguelen Plateau, Deep-Sea Res.II. Topical Studies in Oceanography: Southern Ocean Dynamics and Biogeochemistry in a Changing Climate. Volume 114, Pages 12-26.doi :10.1016/j.dsr2.2014.01.017

II.2 Data acquisition and processing from Ship-mounted Acoustic Doppler Current Profilers (SADCP).

Principal investigator
Gérard Eldin
LEGOS, Toulouse
gerard.eldin@ird.fr

II.2.1 Introduction

N/O Marion-Dufresne is equipped with 3 ADCPs manufactured by RD Instruments (RDI), CA, USA. They provide vertical profiles of horizontal current velocity along the ship track, both en-route and during stations. Each ADCP has its own working frequency and delivers data in specific vertical resolution and depth range, as shown in Table 2 . Data acquisition was performed by RDI VmDAS program, v. 1.49, on PCs running Windows 7. Navigation data from the CINNA system (ship heading, GPS position) was also recorded through the ship Ethernet network. The data aimed at scientific exploitation were obtained as Long Term Average (LTA) profiles.

SADCP models and configurations			
	OS150 (150 kHz)	OS75 (75 kHz)	OS38 (38 kHz)
Blanking interval	6m	8m/16m	16m
Bin length	4m	8m/16m	16m
Depth of 1st bin	16.5m	22.4m/38m	38.4m
LTA profiles	600s	600s	600s
Recording start	2021/01/13 09:00 UT	2021/01/13 04:00 UT	2021/01/13 08:30 UT
Recording end	End of cruise	End of cruise	2021/01/19 08:30 UT
Nominal range	300m	750m	1000m

Table 2: SADCP models and configurations.

II.2.2 Data acquisition

The acoustic transmissions of SADCPs and onboard echo sounder (EK80) need to be synchronized to prevent interferences. Triggering is provided by an external synchronizing device (OSEA). The triggering interval is defined to both prevent spurious bottom detections on the EK80 and allows a sufficient number of "pings" for SADCP LTA profiles (> 100). A triggering interval of 3.5 to 4.5s was chosen, varying with bottom depth. The number of pings in each LTA interval thus remained at 133-170 during the cruise.

From the start of cruise, data quality on the OS38 was found very low (PGOOD <50 most of the time), making the already acquired data unusable. Several days of troubleshooting, in coordination with GENAVIR and RDI-Europe led to the conclusion that the OS38 transducer was faulty. Since it could not be repaired at sea, data acquisition of the OS38 had to be definitively stopped.

For the OS150 and OS75 data acquisition was performed without noticeable problems. Figure 0- shows the along-track OS150/OS75 ADCP data acquisition at time of writing of this report.

II.2.3 Data processing

Only a preliminary processing could be performed on board; a final version of the data will be completed after the cruise. Processing was done using the CODAS system (Common Oceanographic Data Access System), developed at the University of Hawaii (e.g. Bahr et al., 1989, http://currents.soest.hawaii.edu). The "CODAS-bionic-64" version was used. The main steps were:

1) Feeding the data base
The LTA files obtained from VMDAS were loaded every day in CODAS format database

2) Checking profiles
The SADCP provides profiles of water velocity relative to the ship. Before computing of absolute currents, it is necessary to check profiles quality. Some profiles can be affected by a high level of noise or reflections on the bottom: statistics tests are applied to detect these problems, and profiles are visually inspected and corrected if necessary.

3) Integration of navigation
The GPGGA messages provided by the GPS receiver are recorded in the LTA files. They allow computing of the absolute current velocity in a reference layer (here 50 to 180 m). This current is filtered (Blackman filter, 30mn half width) and the ship velocity relative to that layer is recorded in the data base. The absolute current at every level is then computed from these data.

4) Calibration
Two main types of error can affect ADCP data: an error on the transducer orientation in geographic coordinates, or an error in the current velocity amplitude from the computation of the Doppler effect. The orientation error could originate from an error in heading data (variable error) or an error in the orientation of the transducer relative to the ship keel (fixed error). The amplitude error can be associated with a problem in electronics or transducer evolution in time. It has been shown (Pollard and Read, 1989) that a comparison of absolute current velocities before or after a large change in the ship velocity (e. g., stations) allows an estimation of the above-mentioned error. This calculation can only be done after the cruise, using the whole data base, after the previous steps have been performed.

5) Data distribution
Final data can be distributed in different formats: ASCII, Matlab or NetCDF. Contours of current are presented here as examples (*Figure II-2*). These are preliminary data only, and will likely change to some extent after the final calibration is performed.

References

Bahr, F., E. Firing and S. Jiang, Acoustic Doppler current profiling in the western Pacific during the US-PRC TOGA Cruises 5 and 6, JIMAR Contr. 90-0228, U. of Hawaii, 162 pp., 1990.

Pollard, R. and J. Read, A method for calibrating ship-mounted acoustic Doppler profilers, and the limitations of gyro compasses, J. Atmos. Oceanic Technol., 6, 859-865, 1989.

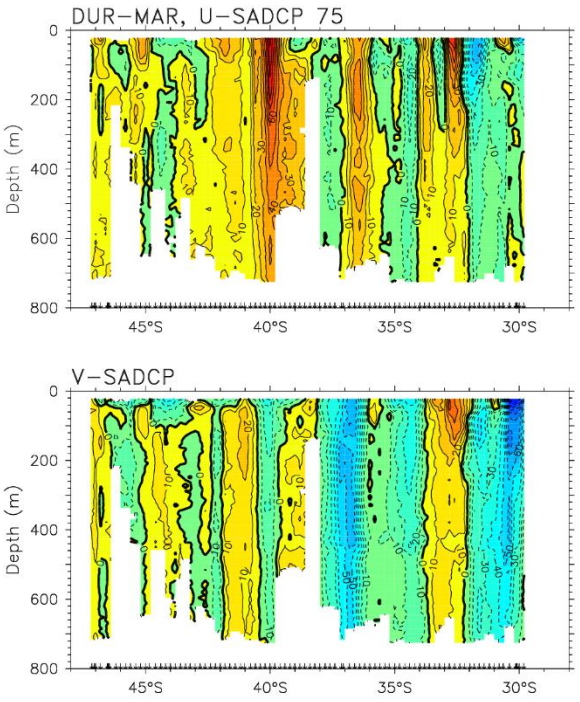

Figure II-2: Example of a meridional current section from the OS75, here from Durban to Marion Island (see Figure 0-2). Zonal (U) and meridional (V) component are presented, with Eastward/Northward and Westward/Southward flows in yellow-red and blue-green color shades, respectively.

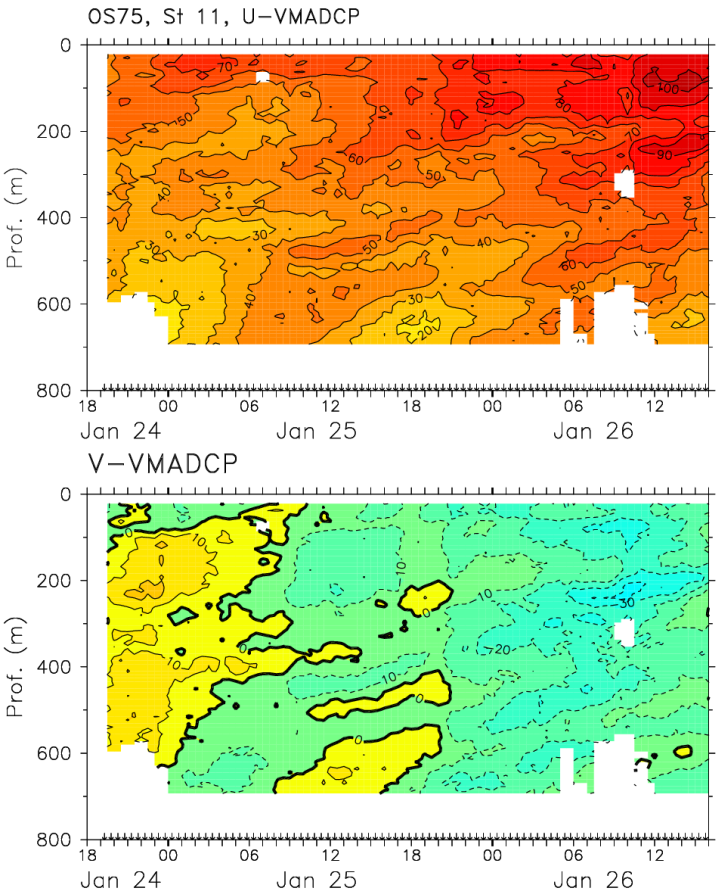

Figure II-3: *Time series of OS75 currents during Station 11, one of the longest of the cruise. Color palette is same as for Figure II-2*

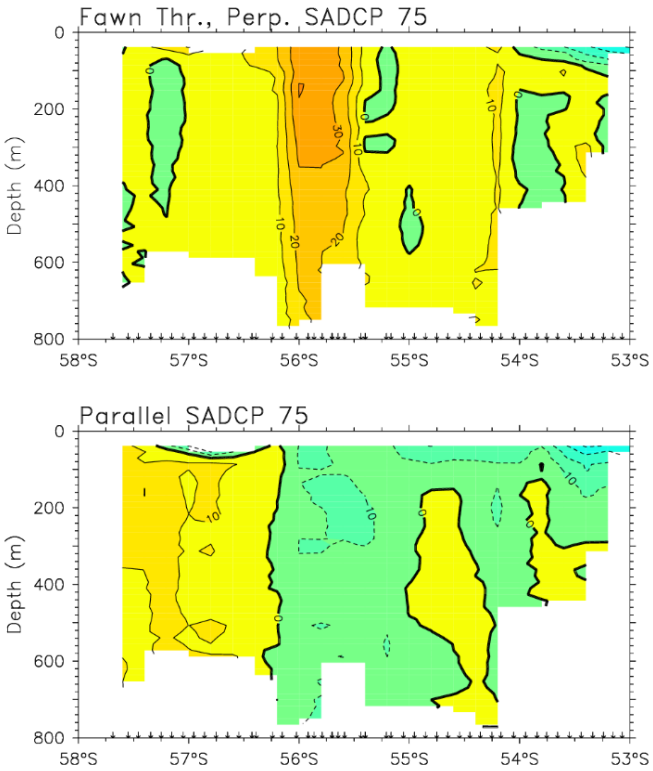

Figure II-4: Current section across the Fawn Through, presented as perpendicular and parallel components relative to the ship track (heading 161°). On the first panel yellow-red is oriented along 71° heading, and blue-green toward 251°.

III. ANCILLARY PARAMETERS (S, O2, DIC, FCO2, TALK AND NUTRIENTS)

III.1 Salinity, O_2 and carbonate chemistry (in the framework of the Océan Indien Service d'Observations, OISO)

Principal investigator
LO MONACO Claire
LOCEAN Sorbonne Université, case 100 – 4 place jussieu – 75252 Paris cedex 05
+33 (1) 44 27 48 68
Claire.lomonaco@locean.ipsl.fr

Names of other participants
BARUT Guillaume (LOCEAN), CASSOU Christophe (CERFACS), FIN Jonathan (LOCEAN), LESEURRE Coraline (LOCEAN), MIGNON Claude (LOCEAN)

Abstract: The OISO program aims at monitoring the variability and changes in oceanic CO_2. The OISO31 cruise was coupled to SWINGS in order to collect underway surface measurements of the fugacity of CO_2 and associated parameters (total CO_2, total alkalinity, dissolved oxygen, nutrients, chlorophyll-a, carbon and water isotopes). Samples were also collected in the water column at most of the stations for total CO_2, total alkalinity, dissolved oxygen and salinity, as well as isotopes on some casts. The samples were measured on board, except for isotopes and nutrients that will be measured at LOCEAN and LOMIC, respectively. The OISO31 observations will be included in the international data syntheses SOCAT, GLODAP and GOAON, therefore contributing to a better understanding of changes in air-sea CO_2 fluxes, in the sequestration of anthropogenic CO_2 and ocean acidification. They will also be included in the GEOTRACES data base with the other SWINGS parameters.

III.1.1 Scientific context

About 30% of the CO_2 emitted by human activities since the industrial revolution was absorbed by the ocean (Sabine et al., 2004). A recent study also showed that the capacity of the ocean to sequester anthropogenic CO_2 was not (yet) altered at the global scale, despite climate change (Gruber et al., 2019). However, regional changes occurred, notably in the Southern Ocean that would have become less efficient in the storage of anthropogenic CO_2 in recent years. The Southern Ocean plays an important role in the regulation of climate change, being the primary conduit for anthropogenic CO_2 entering the ocean (accounting for about 40% of the contemporary oceanic uptake in 2012, DeVries et al., 2014). Observations showed that the uptake of CO_2 by the Southern Ocean could vary substantially on decadal scales in response to climate changes, with a decrease in the sink in the 1990's and a reinvigoration at the beginning of the years 2000 (Landschützer et al., 2015).
The accumulation of anthropogenic CO_2 in the ocean has a major counterpart, as the increase in oceanic CO_2 leads to ocean acidification. Model simulations suggest that pH dropped by 0.1 unit since the industrial revolution (e.g. Jiang et al 2019). Thanks to the international effort for collecting and qualifying oceanic CO_2 observations it has been possible to estimate the decrease in pH in recent decades in different regions of the ocean. In surface waters, the decrease in pH was estimated between 0.01 and 0.03 unit per decade in most regions (e.g. Takahashi et al., 2014; Bates et al., 2015; Lauvset et al., 2015).

In the context of climate change and ocean acidification, it is essential to maintain the monitoring of oceanic CO_2 and related parameters in different regions of the ocean in order to document and understand decadal changes and spatial variability in the uptake and storage of anthropogenic CO_2 and in the rate of ocean acidification. These observations are also crucial to validate model predictions.

III.1.2 Overview of the project and objectives

The main objective of the OISO long-term monitoring program is to provide oceanic CO_2 observations in order to contribute to a better understanding of changes in air-sea CO_2 fluxes and in the sequestration of anthropogenic CO_2, and to evaluate ocean acidification. To this aim, 1 or 2 cruises are conducted every year (since 1998) in the South Indian Ocean and the corresponding Southern sector. Most of the cruises were conducted along the same transects (La Réunion – Crozet – 56.6°S – Amsterdam – La Réunion) in January/February in order to better understand the interannual variability during austral summer.
In January/February 2021 the OISO31 cruise was coupled with the SWINGS cruise conducted in the same region. This collaboration provides mutual benefits with the shared objective of improving our understanding of water transport and biogeochemical processes in the Southern Indian Ocean.

III.1.3 Methodology and sampling strategy

Observations were collected underway in surface waters and in the water column at most of the stations. In addition to underway continuous measurements of the fugacity of CO_2 (fCO_2), total CO_2 (CT) and total alkalinity (AT), seawater samples were collected every 4h for chlorophyll-a (Chl-a) and nutrients (silicate, nitrate and phosphate) and every 8h for dissolved oxygen (O_2) and salinity (to validate/correct the continuous sensor data) and for carbon and water isotopes. Samples were collected from the Niskin bottles at most stations for CT, AT, O_2 and salinity, and 27 stations for isotopes (Table 3).
Underway surface measurements were obtained from the MD pumping system collecting seawater continuously at about 7m deep. The technique for fCO_2 measurements was described in detail by Poisson et al. (1993), Metzl et al. (1995, 1999) and Jabaud-Jan et al. (2004). This instrumentation was also part of the international at-sea intercomparison of fCO_2 systems conducted in the late 1990's (Kürtzinger et al., 2000). In short, sea surface water was continuously equilibrated using a "thin film" type equilibrator thermostated with surface seawater. The CO_2 in the dried gas was then measured with a non-dispersive infrared analyser (Siemens Ultramat 6F). Standard gases were used for calibration with pCO_2 values of 267 ppm, 351 ppm and 490 ppm (values determined at LSCE, Gif/Yvette, France). The precision of the gas detector is 0.5 µatm. Data accuracy is estimated at 2 µatm (including *in situ* temperature correction).
CT and AT samples were obtained from the MD pumping system for underway automated measurements. Water column samples were also collected at 50 stations using 500 ml glass bottles. Samples were poisoned with 300 µl of $HgCl_2$ (saturated solution) and stored in a cool dark place before measurement. CT and AT were measured simultaneously, onboard, following a potentiometric titration method in a closed cell (Edmond, 1970; Goyet et al., 1991).
We used two home-made automated cells equipped with a Metrohm pHmeter (Basic Titrino 794), one for underway measurements, the other one for station samples. The equivalence point was determined using a non-linear regression method (D.O.E., 1994). The accuracy is better than 3 µmol/kg for both TA and DIC (based on the analysis of CRMs).
O_2 samples were collected in surface waters every 8h to correct the continuous data obtained with an Aanderaa optode. O_2 concentrations in the water column were measured using a Sea- Bird oxygen sensor fixed on the standard and clean rosette. Samples were collected at most stations on the standard CTD to correct the sensor data. Ten samples were also collected on two clean casts (38 and 47). Samples were measured onboard within 3 days following the Winkler titration method using a Metrohm titrator (Compact Titrator G10S). Winkler measurements were calibrated using iodate standards provided by Ocean Scientific International Ltd (UK) to ensure an accuracy of 2 µmol/kg.
Sea surface temperature was measured using a Sea-Bird SBE38 sensor at the beginning of the pumping system to avoid warming in the ship. Sea surface salinity was calculated from conductivity measured

using a SBE21 thermosalinograph and *in situ* temperature from the SBE38 sensor. Surface seawater samples were collected every 8h to validate/correct the salinity data. Samples were also collected at most stations to validate/correct the standard and clean CTD data. Samples were measured onboard using a Guidline salinometer (AUTOSAL) calibrated by the analysis of standards provided by Ocean Scientific International Ltd (UK).
The measurement error is estimated at 0.005.
Samples were collected in surface water every 4h for nutrients and Chl-a analysis using the MD pumping system. Samples for nutrient were collected in 100 ml plastic bottles, filtered on 0.45 µm Whatman filters, poisoned with 100 µl of $HgCl_2$ for 20 ml and stored at 4°C. These samples will be measured at LOMIC (Banyuls), together with samples collected from the Niskin and Go-Flo bottles. For Chl-a, between 500 ml and 2 l were collected and filtered on 25 mm GF/F Whatman filters (porosity 0.2 µm). The filters were stored at -80°C until the analysis performed onboard by Thomas Ryan-Keogh (together with samples collected from the Niskin bottles).
Samples were collected in surface water every 8h (MD pumping system) and from the Niskin bottles at 27 stations for isotopes analysis: 125 ml and 20 ml were collected in glass bottles for carbon (total CO_2) and oxygen (H_2O) isotopes, respectively. Samples for carbon isotopes were poisoned with 1.5 ml of $HgCl_2$ and stored at 4°C. These samples will be measured at LOCEAN (Paris).

Table 3: Parameters investigated by the OISO team

Parameter	Code of operation	Number of samples
1. Fugacity of CO_2 in surface waters	MD pumping system	every 5 minutes
2. Total CO_2	MD pumping system	every 25 minutes
3. Total CO_2	Standard CTD	828 samples
4. Total alkalinity	MD pumping system	every 25 minutes
5. Total alkalinity	Standard CTD	828 samples
6. Dissolved oxygen	MD pumping system	every 8h
7. Dissolved oxygen	Standard CTD	649 samples
8. Dissolved oxygen	Clean CTD	20 samples
9. Salinity	MD pumping system	every 8h
10. Salinity	Standard CTD	450 samples
11. Salinity	Clean CTD	230 samples
12. Nutrients	MD pumping system	every 4h
13. Chlorophyll-a	MD pumping system	every 4h
14. Carbon isotope ($\delta^{13}C_{CT}$)	MD pumping system	every 8h
15. Carbon isotope ($\delta^{13}C_{CT}$)	Standard CTD	254 samples
16. Water isotope ($\delta^{18}O_{H2O}$)	MD pumping system	every 8h
17. Water isotope ($\delta^{18}O_{H2O}$)	Standard CTD	218 samples

III.1.4 Preliminary results

Figure III-1 and Figure III-2 show the air-sea CO_2 disequilibrium (oceanic fCO_2 - atmospheric fCO_2): positive values indicate an outgassing of CO_2 to the atmosphere (CO_2 source) and negative values indicate an uptake of atmospheric CO_2 by the ocean (CO_2 sink).

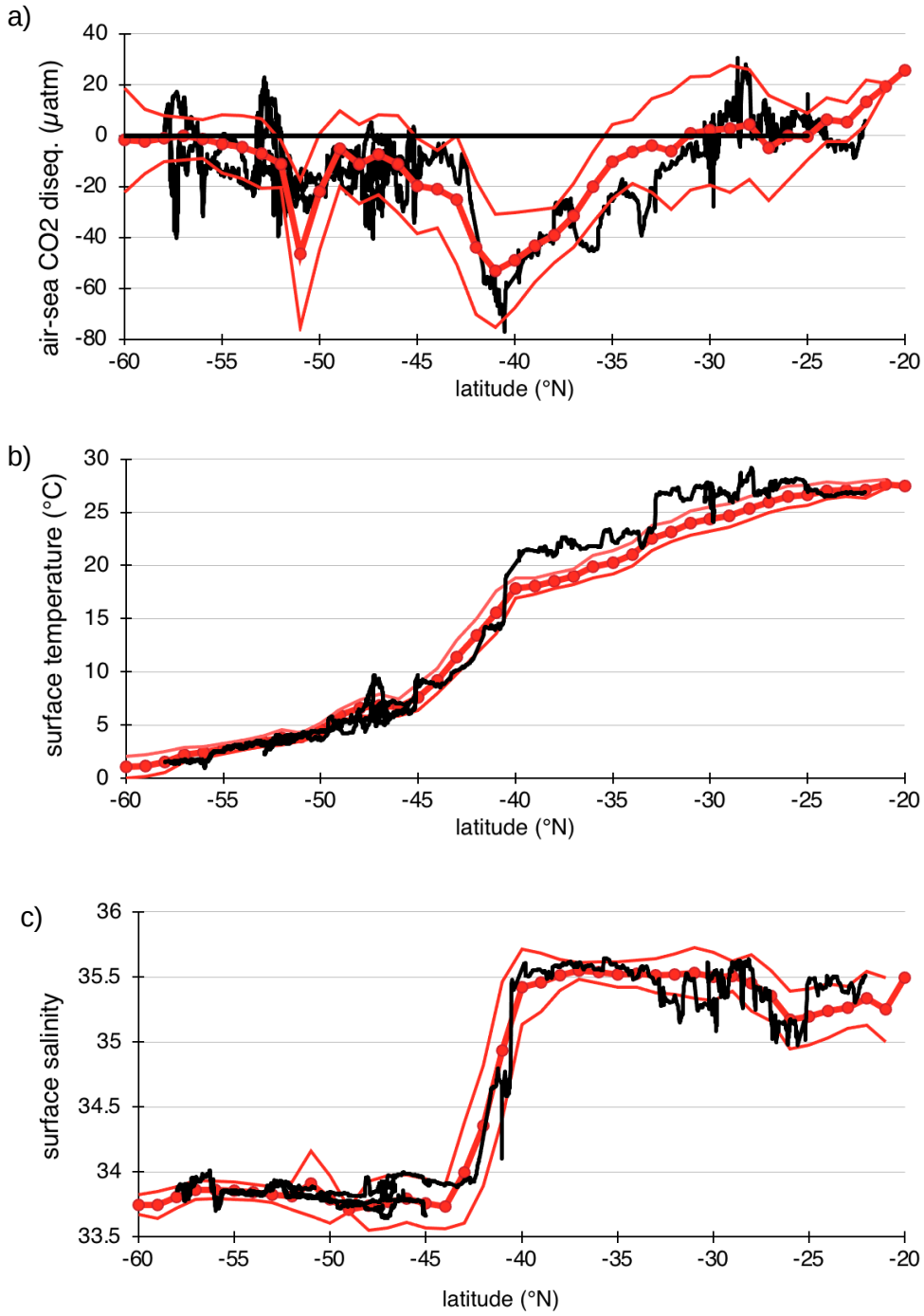

Figure III-1: Underway observations obtained in January/February 2021 (in black) compared to climatological values (in red) computed for January/February over the period 1998-2019 (OISO dataset between La Réunion, Crozet, 56.6°S and Kerguelen)) for a) air-sea CO_2 disequilibrium, b) sea surface temperature and c) sea surface salinity. The thin red lines show the standard deviation of the mean climatological values.

In January/February 2021, the CO_2 source and sink regions were similar to what is usually observed during the OISO cruises conducted in austral summer, with only a few exceptions (Figure III-1 and Figure III-2).

A larger CO_2 sink was observed in 2021 around 35°S on the Durban – Marion Island transect (despite warmer waters, Figure III-1b) compared to the usual OISO transect between La Réunion and Crozet. This signal could be related to the Agulhas Return Current that is stronger to the west.

At 47°S we observed low fCO_2 values between Crozet and Kerguelen that was associated to a patch of high chlorophyll-a concentration (satellite and *in situ* data).

In the Antarctic zone (south of 50°S), we observed a small outgassing of CO_2 above the plateau North of Heard Island (53°S), both on the way down and on the way up (Figure III-2), whereas South of Heard Island the ocean was absorbing CO_2 from the atmosphere.

Most of the area visited over the southern part of the plateau (south of Heard Island) acted as a relatively large CO_2 sink on the way down (compared to the climatology obtained west of the plateau). A local minimum in sea surface fCO_2 was observed in the Fawn Trough (55.8°S). On the way up, we were hit by an explosive storm, which very likely explains the increase in sea surface fCO_2 (due to increased mixing with subsurface waters enriched with CO_2) that led to CO_2 outgassing to the atmosphere between 58°S and 56°S (Figure III-2). It is very surprising that the storm did not impact the uptake of CO_2 at the Fawn Trough (55.8°S).

At the Kerguelen bloom station A3 (51°S on the way up) sea surface fCO_2 was only slightly lower than what we measured at the Kerfix station (51°S on the way down) upstream Kerguelen plateau (outside of the bloom). This could be explained by the decline of the bloom as the A3 station was visited at the end of February, while it is usually visited at the end of January during the OISO cruises. A larger CO_2 sink was measured in the plume North of Kerguelen (station O12 at 47°S on the way up).

In the Polar Front zone North of the plume sea surface fCO_2 was close to equilibrium with the atmosphere.

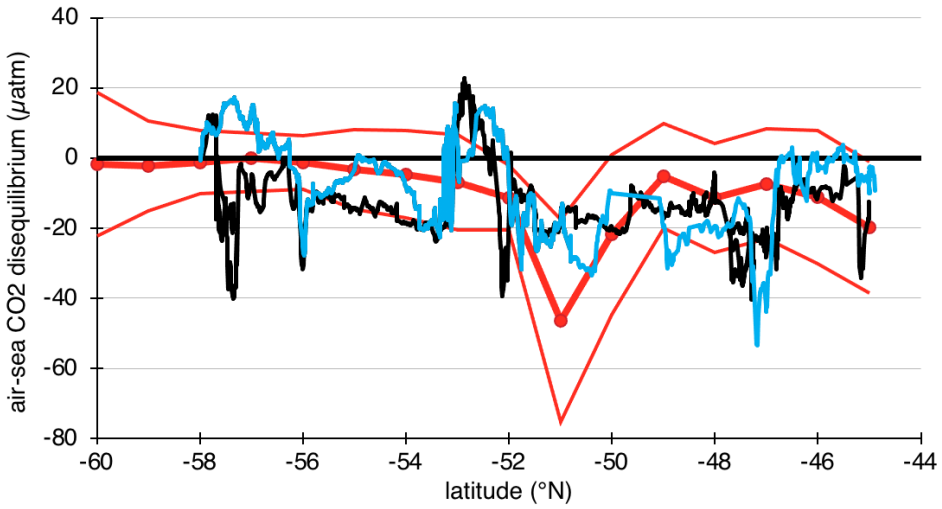

Figure III-2: Air-sea CO_2 disequilibrium observed in January/February 2021 on the way down between Crozet, Kerguelen and 58°S (in black) and on the way back between 58°S and Kerguelen (in blue). The red lines show the OISO climatology (same as Figure III-1).

Column water measurements collected during the cruise show a clear increase in anthropogenic CO_2 compared to estimates from 1996 (Figure III-3). The larger increase (by 20 to 40 µmol/kg) is observed in

Mode Waters (300m-800m) and in the Antarctic Intermediate Water (around 1000m). In 2021, only the core of the North Atlantic Deep Water (around 3000m north of 40°S) is still free of anthropogenic CO_2. An increase by 5-7 µmol/kg is also detected in the Antarctic Bottom Water (below 4000m).

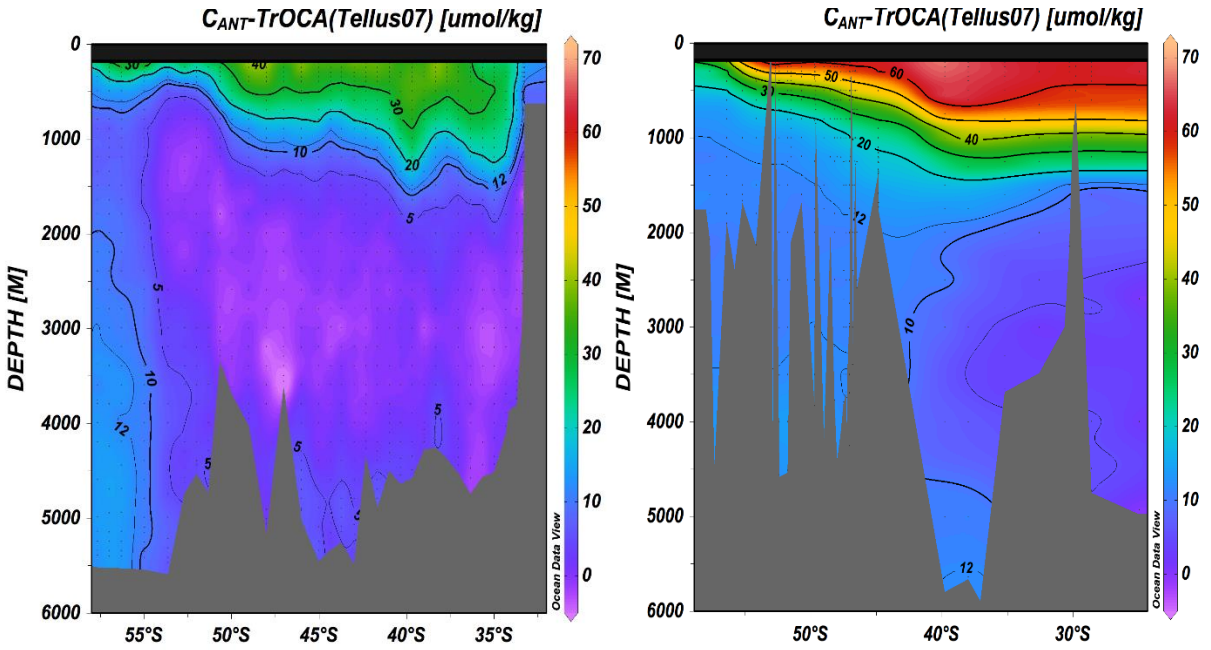

Figure III-3: Concentration of anthropogenic CO_2 estimated from CT, AT and O_2 measurements (TrOCA method) collected a) in January/February 1996 (CIVA-2 cruise along 30°E) and b) 25 years later during the SWINGS/OISO31 cruise.

III.1.5 Post-cruise sampling analyses and envisioned timeline of working plan, people involved on shore

Nutrients (silicate, nitrate and phosphate) will be measured at LOMIC (Banyuls). *People involved in measurements and control quality: Stéphane Blain, Olivier Crispi and Audrey Gueneugues.*

Carbon and water isotopes will be measured at LOCEAN (Paris) following the methods described by Racapé et al. (2010) and Pierre et al. (2001).

People involved in measurements and control quality: Jerome Demange, Coraline Leseurre, Nicolas Metzl and Gilles Reverdin

References

Bates, N.R., Astor, Y.M., Church, M.J., Currie, K., Dore, J.E., Gonzalez-Davila, M., Lorenzoni, L., Muller-Karger, F., Olafsson, J., and Magdalena Santana-Casiano, J. (2014). A time-series view of changing surface ocean chemistry due to ocean uptake of anthropogenic CO2 and ocean acidification, Oceanography, 27(1), 126-141, doi: 10.5670/oceanog.2014.16.

DeVries, T. (2014), The oceanic anthropogenic CO2 sink: Storage, air-sea fluxes, and transports over the industrial era, Global Biogeochem. Cycles, 28 ,631–647, doi:10.1002/2013GB004739.

D.O.E. (1994). Handbook of methods for analysis of the various parameters of the carbon dioxide system in sea water; version 2, A.G. Dickson and C.Goyet, eds. ORNL/CDIAC-74.

Edmond J. M. (1970). High precision determination of titration of alkalinity and total CO2 of seawater by potentiometric titration, Deep-Sea Research, 17, 737-750.

Goyet C., C. Beauverger, C. Brunet and A. Poisson, 1991. Distribution of carbon dioxide partial pressure in surface waters of the southwest Indian Ocean, Tellus, 43B, 1-11.

Gruber, N., D. Clement, B. R. Carter, R. A. Feely, S. van Heuven, M. Hoppema, M. Ishii, R. M. Key, A. Kozyr, S. K. Lauvset, C. Lo Monaco, J. T. Mathis, A. Murata, A. Olsen, F. F. Perez, C. L. Sabine, T. Tanhua, and R. Wanninkhof (2019). The oceanic sink for anthropogenic CO2 from 1994 to 2007, Science, 363 (6432), 1193-1199, doi: 10.1126/science.aau5153.

Jabaud-Jan A., N. Metzl, C. Brunet, A. Poisson and B. Schauer (2004). Variability of the Carbon Dioxide System in the Southern Indian Ocean (20°S-60°S): the impact of a warm anomaly in austral summer 1998. Global Biogeochemical Cycles, 18 (1), GB1042, doi: 10.1029/2002GB002017.

Jiang, L.-Q., Carter, B. R., Feely, R. A., Lauvset, S. K. and Olsen, A. (2019). Surface ocean pH and buffer capacity: past, present and future. Sci Rep, 9, 18624, doi:10.1038/s41598-019-55039-4.

Körtzinger, A., L. Mintrop, D.W.R. Wallace, K.M. Johnson, C. Neill, et al. (2000). The international at-sea intercomparison of fCO2 systems during the R/V Meteor Cruise 36/1 in the North Atlantic Ocean. Marine Chemistry 2 (2–4), 171–192.

Landschützer, P., N. Gruber, F. A. Haumann, C. Rödenbeck, D. C. E. Bakker, S. van Heuven, M. Hoppema, N. Metzl, C. Sweeney, T. Takahashi, B. Tilbrook, R. Wanninkhof (2015). The reinvigoration of the Southern Ocean carbon sink. Science, 349 (6253), 1221-1224, doi:10.1126/science.aab2620.

Lauvset, S. K., N. Gruber, P. Landschützer, A. Olsen, and J. Tjiputra (2015). Trends and drivers in global surface ocean pH over the past 3 decades, Biogeosciences, 12, 1285-1298, doi:10.5194/bg-12-1285-2015.

Metzl, N., A.Poisson, F. Louanchi, C. Brunet, B. Schauer, B. Brès (1995). Spatio-temporal distributions of air-sea fluxes of CO2 in the Indian and Antarctic Oceans: a first step. Tellus, 47B, 56-69.

Metzl, N., B.Tilbrook and A. Poisson (1999). The annual fCO2 cycle and the air-sea CO2 flux in the sub-Antarctic Ocean. Tellus, 51B, 4, 849-861.

Poisson, A., N. Metzl, C. Brunet, B. Schauer, B. Brès, D. Ruiz-Pino and F. Louanchi (1993). Variability of sources and sinks of CO2 and in the western Indian and Southern Oceans during the year 1991. J. Geophys. Res., 98 (C12), 22759-22778.

Pierre C., J-F. Saliege, M-J. Urrutiaguer, and J. Giraudeau, 2001. Stable isotope record of the last 500 ky at site 1087 (Southern Cape Basin). in: Wefer G., Berger W.H., Richter C. et al., Proceedings of the ocean Drilling Program, Scientific Results, vol. 175, chapter 12, 1-22.

Racapé, V., C. Lo Monaco, N. Metzl, and C. Pierre, 2010. Summer and winter distribution of δ13CDIC in surface waters of the South Indian Ocean (20°S-60°S). Tellus B, 62 (5), 660-673. DOI: 10.1111/j.1600-0889.2010.00504.x

Sabine, C., and 14 co-authors (2004). The oceanic sink for anthropogenic CO2. Science, 305, 367-371.

Takahashi, T., S C. Sutherland, C. Sweeney, A.Poisson, N.Metzl, B.Tilbrook, N.Bates, R.Wanninkhof, R.A. Feely, C.Sabine and J.Olafsson and Y. Nojiri, 2002. Global Sea-Air CO2 Flux Based on Climatological Surface Ocean pCO2, and Seasonal Biological and Temperature Effect. Deep Sea Res. II, 49 (9-10), 1601-1622.

III.2 Inorganic nutrients

Principal investigator
On-board : Stéphane Blain
CNRS, Laboratoire d'Océanographie Microbienne (LOMIC), 1 ave Pierre Fabre, 66650 Banyuls sur mer, France
+ 33 (4) 68 88 73 53
Stephane.blain@obs-banyuls.fr

Names of other participants
On-board : Ingrid Obernosterer, Sorbonne University, Laboratoire d'Océanographie Microbienne (LOMIC), Banyuls sur mer, France
Audrey Guéneugues, CNRS, Laboratoire d'Océanographie Microbienne (LOMIC), Banyuls sur mer, France

Abstract:

Inorganic nutrients are ancillary parameters of any oceanographic study. SWINGS cruise targeted the characterization of specific water masses from surface to bottom, such as the wind mixed surface layer, oxygen and salinity minima and maxima, Upper and Lower Circumpolar Deep Water, and Antarctic Bottom Water. We have further collected samples for the major inorganic nutrients (nitrate and nitrite, phosphate and silicic acid) in these different layers. The concurrent detailed description of trace elemental distributions across ocean provinces and depth layers will provide the contextual data for the observations of the microbial functional and taxonomic diversity.

III.2.1 Methodology and sampling strategy

Seawater samples were collected using trace metal clean GoFlo bottles and standard Niskin bottles. For samples collected by GoFlo bottles, seawater was filtered (0.45 µm) in the trace metal clean van. For samples collected with standard Niskin bottles, 125 mL of raw seawater was collected in HDPE flasks, and 60 mL were filtered (0.45 µm Acetate Cellulose filters) (Table 4). All samples were preserved with $HgCl_2$ (4g/l; 300 µL in 20mL) in 60 mL LDPE bottles. They are stored in the dark and at room temperature until analysis back in the laboratory 5 months later. The analyses of nitrate (NO_3^-), nitrite (NO_2^-), phosphate (PO_4^{3-}) and silicic acid $Si(OH)_4$ will be carried out in the laboratory with a segmented flow analyzer (Skalar) equipped with colorimetric detection using methods described in (Aminot and Kérouel, 2007; Blain et al. 2018). The accuracy of the methods is assessed using reference material (Certipur, Merck).

Table 4: Exhaustive list of measured nutrients

Parameter	Code of operation (Station-cast)	Number of samples
1. Inorganic nutrients	SWG_S_002_006	19
	SWG_C_002_007	21
	SWG_C_003_011	23
	SWG_C_004_014	12
	SWG_C_005_018	11
	SWG_S_007_021	21
	SWG_C_008_023	17
	SWG_S_009_025	9
	SWG_C_010_027	23
	SWG_S_010_028	20

	SWG_C_011_034	24
	SWG_C_014_040	6
	SWG_C_014_041	21
	SWG_S_015_044	7
	SWG_C_016_047	21
	SWG_S_017_048	11
	SWG_C_018_049	22
	SWG_C_019_051	12
	SWG_C_020_053	5
	SWG_C_021_058	12
	SWG_C_025_068	21
	SWG_S_026_073	10
	SWG_C_027_074	24
	SWG_C_029_077	23
	SWG_S_030_079	11
	SWG_C_031_082	23
	SWG_C_032_084	23
	SWG_C_033_087	17
	SWG_S_034_091	21
	SWG_C_035_093	15
	SWG_C_036_098	23
	SWG_S_037_101	21
	SWG_C_038_102	23
	SWG_S_039_107	21
	SWG_S_040_108	18
	SWG_C_040_109	20
	SWG_S_042_111	22
	SWG_C_042_112	19
	SWG_S_043_115	10
	SWG_C_044_117	6
	SWG_C_045_122	2
	SWG_C_046_125	3
	SWG_C_047_130	18
	SWG_C_048_134	23
	SWG_S_053_139	13
	SWG_C_058_144	16
	SWG_S_062_154	11
	SWG_C_063_156	22
	SWG_C_065_159	3
	SWG_C_066_163	11
	SWG_C_067_167	11
	SWG_S_068_168	21
	SWG_C_068_169	10

IV. HYDROTHERMAL EXPLORATION

Principal investigator
Cédric Boulart (AD2M, OOR, Roscoff), Valérie Chavagnac (GET, OMP, Toulouse) and the cruise PIs, Catherine Jeandel and Hélène Planquette
cedric.boulart@sb-roscoff.fr; Valerie.chavagnac@get.omp.eu

Names of other participants
On board: Cedric Cotté (LOCEAN), Vincent Gabriel (Genavir), Lloyd Izard (LOCEAN), Alain Jaouen (Genavir), Sara Sergi (LOCEAN), Guillaume Violette (Genavir)

On shore : Hervé Biscaye (Ifremer), Anne Briais (Domaine Océaniques, Brest), Cyrille Poncelet (Ifremer), Carla Scalabrin (Ifremer)

Abstract:

As part of SWINGS, we explored the possible occurrence of hydrothermal activity above the South West Indian Ridge (SWIR). We first dedicated time to a high resolution (15 m) multibeam bathymetric exploration of the targeted area. Having identified potential hydrothermal activity, we decided to do two stations.
The first ^{223}Ra results measured on the bottom are consistent with the geological features, indicating that we clearly detected a hydrothermal activity as detailed in Chapter VII.

IV.1 Scientific context

Hydrothermal inputs of dFe and other TEIs have been overlooked and underestimated so far, mostly above the slow spreading ridges. The SWIR is an ultra-slow spreading ridge. However, hydrothermal sites have been identified at 37ºS but north of the SWINGS track and at its western end providing the first direct evidence for widespread distribution of hydrothermal activity. The SWINGS transect crossed the SWIR between the Prince Edwards (35ºE) and Eric Simpson (40ºE) Fracture Zones where a detailed geophysical survey (bathymetry, gravity and magnetism) has been carried out by the SWIFT cruise (Hummler et al, 2001) and more recently Sato et al (2013), allowing the suspicion of hydrothermal activity. Thus, identifying the possible occurrence of hydrothermal active sites was one of the SWINGS goals.

IV.2 Methodology and sampling strategy

Based on the rough bathymetric data of Sato et al (2013) and on the SWIFT cruise report, we decided to explore the area centered around the DR5 site (Figure IV-1).

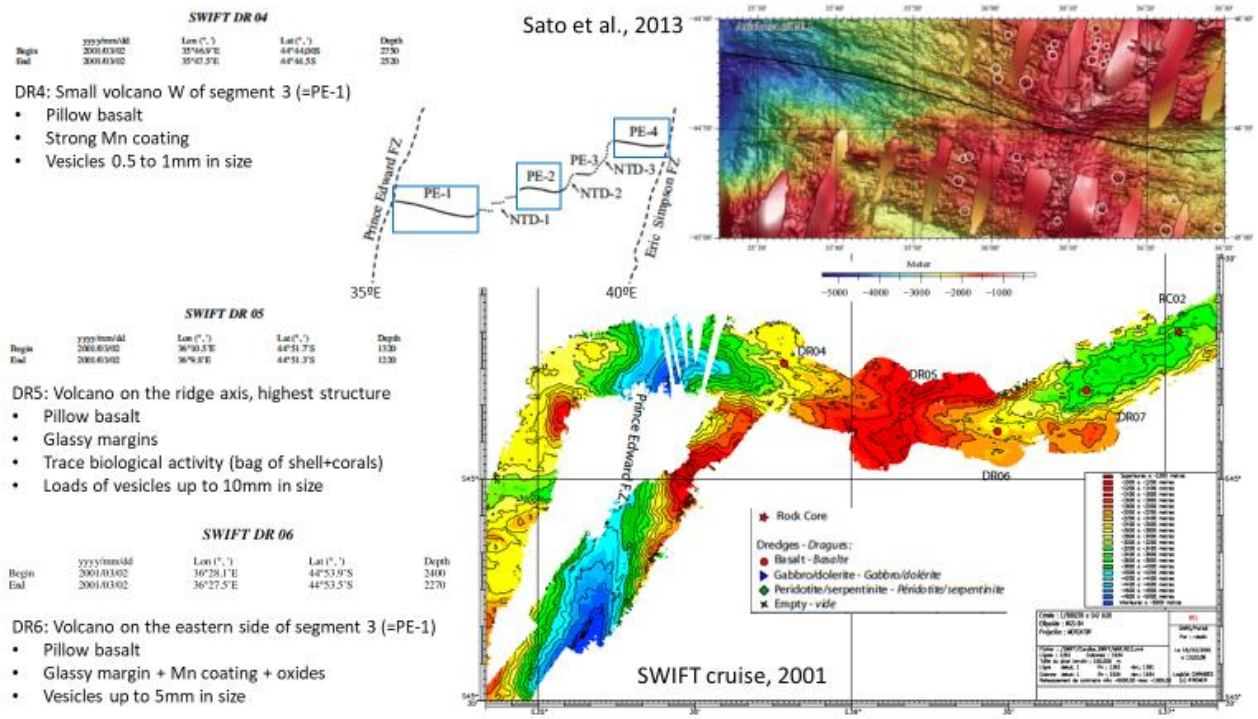

Figure IV-1: Main results from trawls and bathymetric features from the SWIFT cruise

IV.2.1 Bathymetric exploration

The multibeam sensor was set up following the "colonne d'eau" exploration criteria (see the Table 5 below) but using 80 instead of 120 as angular range, in order to keep an optimal bathymetry record while trying to detect "bubbles" in the water column signal, these bubbles tracing potential hydrothermal plumes. We conducted a "radiator" track above the targeted area for 25 hours, starting on January 27 th, at 00h10 UT.

IV.2.1 Water column sampling

Having detected what could be hydrothermal sources, in other words traces of bubbles consistent with geological features (volcanoe shapes) and literature information (SWIFT cruise report, Hummler et al, 2001, Sato et al, 2013) we decided to do two stations: stations #14 and #15 respectively located as described in Table 6 (extraction from the log book). Actually, the location of station #15 was decided following the first extremely high ^{223}Ra activity observed by the "radium team" of Pieter van Beek, immediate results from the first sampling conducted at station #14. We hypothesized that the detected "source" could spread eastward, centered around depths of 1500 m.

Table 5: Setting criteria of the multi beam sounder for the SWINGS hydrothermal exploration

Paramètre	Cartographie + colonne d'eau
Secteur	
Distance de l'écho au nadir (m)	
Navire	
Speed (knots)	8.0
Dist inter ping (m)[1]	
Recurrence inter ping (s)[2]	
EM122	
Mode	
NbSwaths	Dual swath
FM	non
WC	oui
Angular Range (deg)[3]	120 (±60)
Sector Tracking	
Aeration Filter	
Interference Filter	ON
Penetration Filter	
WC TVGFunctionApplied	**30**
WC TVGOffset (dB)	**40**

Table 6: Location and instrument deployments made at stations #14 and #15.

	14	CTD-S_Ra_Ac	SWG_14_040	28/01/2021	15:47	44°51,690	36°10.46	1 388 m	28/01/2021	17:37	44°51,690	36°10.46	1 357 m
	14	CTD-C	SWG_14_041	28/01/2021	18:47	44°51,694	36°10,473	1 388 m	28/01/2021		44°51,696	36°6.465	1 395 m
	14	CTD S_All	SWG_14_042	28/01/2021	20:03	44°51.699	36°10.463	1 389 m	28/01/2021	21:50	44°51.691	36°10.450	1 372 m
	14	P_All	SWG_14_043	29/01/2021	21:56	44°51.699	36°10.463	1 389 m	29/01/2021	03:15	44°51.691	36°10.450	1 285 m
	4:02, reprise du survey hydrothermal			29/01/2021	04:02	44°54.139	36°10.193		29/01/2021				
	15:20, arret définitif du survey hydrothermal								29/01/2021	15:20			
	15	CTD S_All	SWG_15_044	29/01/2021	15:48	44°51,177	36°13,841	1 770 m	29/01/2021	17:52	44°51,200	36°13,8	1 734 m
	15	P_All	SWG_15_045	29/01/2021	18:00	44°51,177	36°13,841	1 749 m	30/01/2021	0h15	44°51,200	36°13,8	1 710 m

IV.3 Preliminary results

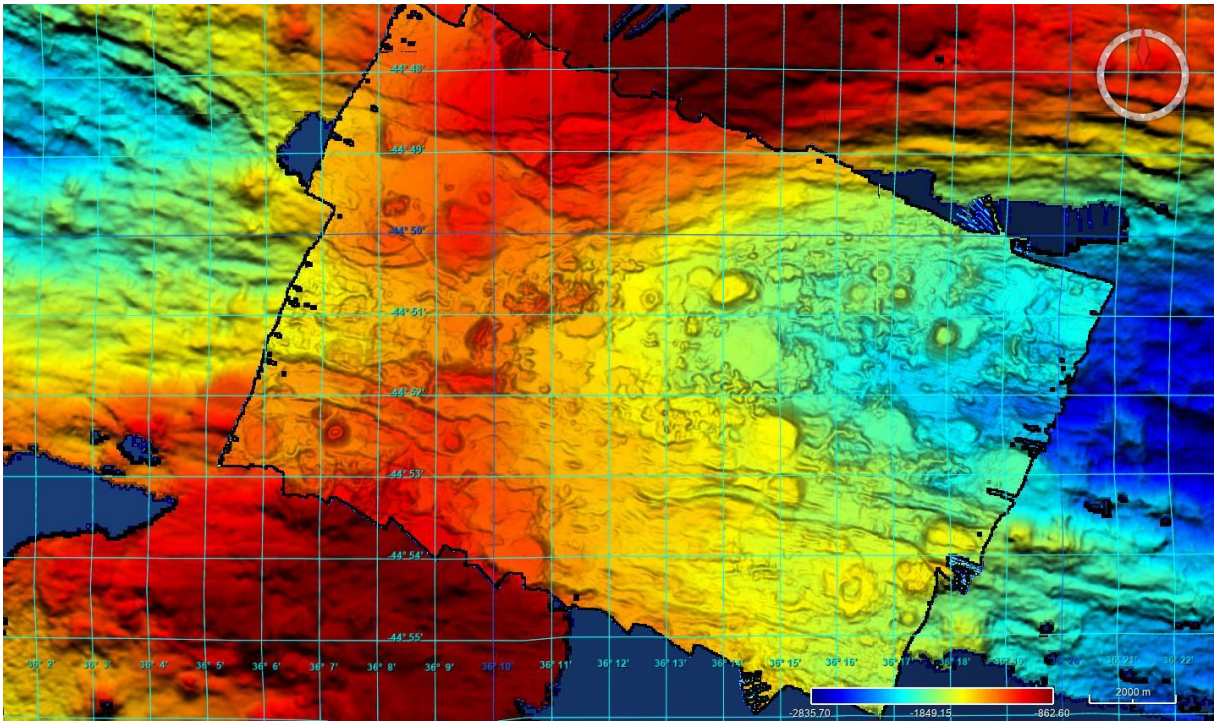

Figure IV-2: High resolution (15m) bathymetry of the investigated segment of the SWIR during SWINGS.

The high resolution (15 m) of the bathymetric map is reported in the Figure IV-2 above. The first radium data are presented and discussed in the "Isotope and radionuclide" chapter.

References

Saito, M. A. *et al.* *Nat. Geosci.* 6, 775 (2013)

Hummler et al., SWIFT rapport de campagne, Ifremer, 2001

V. SURFACE WATER ACTIVITY

V.1 MAP-IO: Marion Dufresne Atmospheric Program in the Indian Ocean

Principal investigator onboard
Léa Gest
LACy, 15 avenue René Cassin, 97400 Saint-Denis, La Réunion.
+262 6 93 32 63 97
lea.gest@univ-reunion.fr

Names of other participants (on shore, framework of MAP IO project)

Pierre Tulet, pierre.tulet@aero.obs-mip.fr ; Nicolas Marquestaut, LACy, nicolas.marquestaut@univ-reunion.fr ; Dominique Mekies, LACy, dominique.mekies@gmail.com ; Olivier Picard, LACy, olivier.picard2@univ-reunion.fr ; Jean-Marc Metzger, OSUR, jean-marc.metzger@univ-reunion.fr ; François Rigaud-Louise, LACy, francois.rigaud-louise@univ-reunion.fr ; Thierry Portafaix, LACy, thierry.portafaix@univ-reunion.fr ; Joël Van-Baelen, LACy, joel.van-baelen@univ-reunion.fr ; Melilotus Thyssen, MIO, melilotus.thyssen@mio.osupytheas.fr

Abstract: MAP-IO program (Marion Dufresne Atmospheric Program in the Indian Ocean) uses the boat as a platform for physical measurements of aerosols distribution (optical depths, granulometry), greenhouse gases (O_3, NO_x, CO_2, H_2O, CH_4, CO), weather parameters (nebulosity, temperature, pressure, humidity, wind), radiation (UV, Sun/Moonlight spectrometry) in the atmosphere, and surface marine biology (phytoplankton by flux cytometry) on the Southern and Indian Ocean.

V.1.1 Overview of the project and objectives

The atmosphere over the oceans lacks observations, and could only be done using ship's navigation routes. The R/V Marion Dufresne mainly steams in the Indian and Southern Ocean, taking the same routes to supply the sub Antarctic French islands 4-5 times a year. Some oceanographic cruises take place roughly twice a year in the same area with this ship, but no atmospheric studies were performed so far on these occasions. The onboard equipment installed by the project MAP-IO is now filling this gap, and the SWINGS cruise was an excellent opportunity to participate. This equipment measures greenhouse gases, aerosols, weather parameters, sunlight, clouds and marine biology. All these measurements are continuously done. They will bring new sets of data above places rarely visited, and will help to constrain atmospheric and oceanographic models on these distant regions

V.1.2 Methodology and sampling strategy

Greenhouse gases (CO_2, CH_4, CO, H_2O, O_3 and NOX) and aerosols are measured by *in-situ* analyzers. They sample directly above the upper deck (i). The weather parameters, Trimble GNSS and photometer are installed on the top of the boat. All these instruments are directly connected in the MAP-IO room, next to the bridge on port side (Table 7).

The flow cytometer is installed in a thermoregulated lab (e deck), where fresh sea water can be sampled continuously.

Table 7: Exhaustive list of measured parameters for the MAP-IO program

Parameter	Number of samples
1. CO2, CH4, CO	Continuous
2. NO, NO2, NOx	Continuous
3. O3	Continuous
4. Aerosols	Continuous
5. Sun/Moon AOD	Continuous
6. Weather (T, P, H%, Pp, Wd, Ws)	Continuous
7. Water vapor column	Continuous
8. Boat position	Continuous
9. Surface sea water particles	Continuous

V.1.3 Preliminary results

Most of the results were sent daily to La Réunion University, and distributed to the different PI labs of MAP IO to be treated and validated. The project being at its first campaign, the data visualizations are still in progress.

At half-cruise, due to weather conditions, the weather station of the ship went down. Unfortunately, few days after, the MAP-IO station crashed as well. On these occasions, we noticed that it would be easier to be able to share weather data (at least) if any of the instrument went to crash again. This would mean some rearrangements from all working teams, to be able to switch from one dataset to the other, and maybe provide some comparisons?

V.1.4 Post-cruise sampling analyses and envisioned timeline of working plan

A nebulosity camera and radiometers will be installed up the front mast, connected to a thermo-regulated room below. The continuous use of the Ifremer ferrybox is also currently discussed, to obtain sea water temperature, alcalinity and pCO_2 measurements.

V.2 THEMISTO Toward Hydroacoustics and Ecology of Mid-trophic levels in Indian and SouThern Ocean

Principal investigator
On board: Cédric Cotté, MNHN, LOCEAN, Paris,

cedric.cotte@locean.ipsl.fr

Participants: on board: Lloyd Izard, LOCEAN, Paris, lloyd.izard@locean.ipsl.fr

The THEMISTO (Toward Hydroacoustics and Ecology of Mid-trophic levels in Indian and SouThern Ocean, PI: Cédric Cotté) research program aims to understand and quantify the processes by which environmental variability structures pelagic ecosystems in the Indian Ocean. It focuses on the mesopelagic ecosystem, as it is still poorly known despite its critical importance in the trophic network and the carbon cycle. To address this knowledge gap, THEMISTO proposes using active acoustic as an observation method. During the SWINGS cruise, a Simrad EK80 echosounder operating at five frequencies (18, 38, 70, 120 and 200 kHz) allowed high-frequency monitoring of micronekton organisms

dynamics in the water column. In the Appendix, section X-3 "Eléments techniques à rapporter en lien avec l'exploitation de l'EK80 et l'acquisition de données de qualité" develops more technical aspects and issues to address.

V.3 Mapping methane concentration in the Southern sector of the Indian Ocean

Principal investigator *(on shore)*
Cedric BOULART
Sorbonne Université, CNRS - UMR7144
Station Biologique de Roscoff,
Place Georges Tessier, BP74
29680 Roscoff, France.
+33 2 98 29 23 17
cedric.boulart@sb-roscoff.fr

Names of other participants
Hugo Berthelot *(on board),* Laboratoire des sciences de l'environnement marin, IUEM, Université de Brest-UMR 6539 CNRS/UBO/IRD/Ifremer, Plouzané, France.

V.3.1 Scientific context

Methane (CH_4) is the second greenhouse gas after CO_2 with a radiative power 20 to 30 times more effective than CO_2 on a 100-yr period. At the global scale, oceans are considered as a minor source of CH_4 but marine contribution has proven difficult to quantify with great certainty due to the scarcity of data available and the inability to capture the spatiotemporal dynamics of CH_4 emissions. In the open ocean, CH_4 is supersaturated relative to atmospheric concentrations, which is known as the ocean methane paradox. Several mechanisms have been proposed to explain this paradox but there is still a lack of data on the different ways of CH_4 production, especially in the mixed layer, as well as on the optimal environmental conditions.

V.3.2 Overview of the project and objectives

The objectives of the study are 1) to evaluate the spatiotemporal dynamics of CH_4 concentrations in the mixed layer, 2) to track the sources of CH_4 and 3) to identify the planktonic populations and the metabolic ways of CH_4 production.

V.3.3 Methodology and sampling strategy

During the SWINGS cruise, we carried out water sampling for the measurement of methane concentrations and the stable carbon isotopic signature of the dissolved CH_4 as well as CO_2 and DIC in the mixed layer.

Samples for CH_4 measurements (duplicates) and $\partial^{13}C$-DIC/CH_4 (monoplicates) in the mixed layer were taken at 23 stations on classical CTD-rosette equipped with Niskin bottles at 5-6 depths from surface to below the DCM. For CH_4, samples were collected in 20 mL glass vials equipped with rubber septum cap and poisoned with $HgCl_2$.

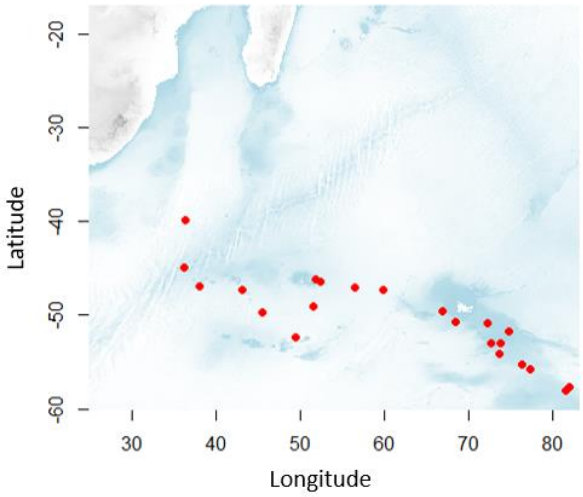

Figure V-1: Location of the sampled stations for methane

In total 262 samples for CH_4 concentrations and 115 for CO_2 $\partial^{13}C$ and CH_4 ∂H were collected (Table 8).

Table 8: List of samples collected

Station Number	Number of samples for CH_4	Number of samples for CO_2 $\partial^{13}C$ and CH_4
11	10	
14	14	7
15	18	9
19	10	5
25	10	5
27	10	5
29	12	6
31	10	5
33	10	5
35	10	5
36	10	5
38	10	5
41	10	5
42	12	2
45	10	2
47	20	5
48	12	6
58	10	5
62	12	6
63	12	6
65	10	5
66	10	5

68	12	6

V.3.4 Post-cruise sampling analyses and envisioned timeline of working plan, people involved on shore

CH_4 and CO_2 $\partial^{13}C$ and CH_4 ∂H will be analyzed using coupled GC – Isotope Mass Ratio Spectroscopy (GC-IRMS). The carbon isotopic signature will allow the determination of the source of CH_4 as well as to evaluate the biogeochemical processes, i.e. mixing, consumption or production.

Dissolved gas (including CH_4) concentrations will be analyzed at the Station Biologique de Roscoff. Gas extraction and analyses will be performed using a Shimadzu Headspace Sampler (HS-20) connected to a Gas Chromatograph (Shimadzu GC-2030) fitted with a barrier discharge ionization detector (BID) and a 30-m SH-Rt-MSieve 5A column and a 30-m RT-Q-Bond column. With this set-up, headspace extraction is entirely automated with pressurization of the sample up to 2 bars, heating at 90°C and equilibration for 10 minutes. Then, an aliquot of the gas sample is transferred to a 1-mL injection loop, maintained at 150°C and injected into a 40°C heated column. The detection threshold of this method is 0.2 nM for CH_4.

∂13C-CH_4 will be analyzed at the METABOMER platform at the Station Biologique de Roscoff (managed by Cédric Leroux) using the newly acquired GC-IRMS facility.

Samples will be analyzed as soon as possible after their return from the cruise. We anticipate that the concentration data should be available by Summer 2021. People involved will be Cédric Boulart, Eric Macé (IE, UMR 7144) and possibly one student. ∂13C-CH_4 should be available later in 2021 after validation of the method of analysis.

V.4 Phytoplankton community characterization

Principal investigator
Thomas Ryan-Keogh (on board)
SOCCO, CSIR, 15 Lower Hope Road, Rosebank, Cape Town, 7700, South Africa
+27 727 535 755
tjryankeogh@gmail.com

Names of other participants

On board: Heather Forrer (Florida State university), Isobel Turnbull (Plymouth Univ.), Goddard-Dwyer Millie (Liverpool Univ.).

On shore: Sarah Fawcett (UCT) & Sandy Thomalla (CSIR)

Abstract

The characterization of the phytoplankton biomass, phytoplankton community structure, organic carbon concentrations, and phytoplankton photo physiology are all necessary to contextualize other parameters collected (i.e. nutrients, trace metals) and provide necessary ancillary information for experiments performed on board.

V.4.1 Overview of the project and objectives

Objective 1: Characterization of phytoplankton biomass and community structure composition.

Objective 2: Characterization of particulate organic carbon concentrations for integration with carbon export flux measurements.

Objective 3: Characterization of phytoplankton photo physiology for determining potential effects of trace metal limitation of photosynthesis.

V.4.2 Methodology and sampling strategy

Chlorophyll-a

Seawater was collected from 6 different depths; 500-1000 mL of seawater was filtered through GF/F filters (Table 9). All filters were placed in glass vials containing 90% acetone and stored at -20°C for ~24 h. Samples were allowed to acclimate to room temperature before the raw chl-*a* fluorescence was measured using a Turner Trilogy Benchtop Fluorometer (non-acidification module).

Particulate Organic Carbon

Seawater was collected from 6 different depths. Approximately 1 - 2 L seawater was filtered through 25 mm ashed (pre-combusted) GF/Fs (0.3 µm nominal pore size). The filters were combusted in a muffle furnace at 400°C overnight, prior to the cruise. Following filtration, filters were placed into pre-combusted tin foil and stored at -80°C until analysis on land.

HPLC

Approximately 1 – 1.5 L of seawater from 6 different depths were filtered through 25 mm GF/Fs GF/Fs (0.7 µm nominal pore size). Filters were placed in cryo-vials, before being flash frozen in liquid nitrogen and stored at -80°C, for analysis on land.

FRRf

Measurements of the photochemical efficiency (F_v/F_m), the effect absorption cross-section of PSII (σ_{PSII}) and electron transport rates were performed with a Chelsea Scientific Instruments FastOcean™ integrated with a FastAct™ laboratory system. Seawater was collected from 6 different depths. Measurements were made in triplicate, using 4 different LED combinations, and corresponding blanks (0.2 µm filtered seawater) were recorded.

Table 9: list of measured parameters for phytoplankton community characterization

Parameter	Code of operation	Number of samples

Chlorophyll-a	Standard CTD	
HPLC	Standard CTD	
FRRf	Standard CTD	
POC	Standard CTD	

No preliminary results yet.

V.4.3 Post-cruise sampling analyses and envisioned timeline of working plan, people involved on shore

POC Analysis

POC filters will be placed into petri-dishes and incubated at 50°C for 24 h. Filters will then be placed in a fume hood, in a desiccation chamber that contains a beaker of concentrated HCl, at room temperature for 24 h. Filters will be punched using a size 13 punch, folded into tin cups, and placed into a labelled 96-well plate, for analysis at the University of Cape Town. As a control, a blank ashed filter will be punched, folded into a tin cup, and placed in the 96-well plate during each round of punching.

HPLC Analysis

HPLC samples will be analyzed at Villefranche/Mer, France. The HPLC pigment data will be run through CHEMTAX to determine relative community structure at each station.

Chlorophyll-a Analysis

The chlorophyll fluorometer will undergo a post cruise calibration and all chlorophyll-a concentrations will be recalculated. The data will be used to calibrate the CTD fluorometers following correction for quenched daytime profiles.

V.5 Primary production and Calcification Rates

Principal investigator
On board: Thomas Ryan-Keogh
SOCCO, CSIR, 15 Lower Hope Road, Rosebank, Cape Town, 7700, South Africa
+27 727 535 755
tjryankeogh@gmail.com

Names of other participants
On board: Heather Forrer (Florida State university)
On shore: Sarah Fawcett (UCT) and Sandy Thomalla (CSIR)

Abstract

Ocean acidification due to the increased uptake of anthropogenic carbon dioxide will impact both marine carbonate chemistry and the physiology of marine photoautotrophs with subsequent effects upon biogeochemical cycling of key nutrients and biological carbon export. The Southern Ocean, an important contributor to global ocean uptake of anthropogenic CO_2, is more susceptible to ocean acidification due to its naturally low buffering capacity with widespread impacts expected before the end of the century

under low to medium mitigation scenarios. Future climate change scenarios suggest that not only will pH decrease in the Southern Ocean, but there will be coincident increases in temperature, light stress and a decrease in upwelled nutrients. Understanding the potential feedback between ocean acidification and these other drivers will provide a more holistic view of the ecosystem level response. With an improved understanding of the physiological implications of ocean acidification we will be able to more accurately model and resolve climate mediated impacts upon both the Southern Ocean ecosystems and the global oceans.

V.5.1 Scientific context

The continued emission of anthropogenic CO_2 is predicted to increase the partial pressure of atmospheric CO_2 (pCO_2) from 400 ppm to ~800 ppm by 2100 (Friedlingstein et al., 2006; 2019; Ciais et al., 2013). The global oceans have absorbed about 30% of global anthropogenic carbon emissions (Sabine and Feely, 2007; Canadell et al., 2007), with 40-50% of this absorbed by the Southern Ocean (Gregor et al., 2019; Gruber et al., 2019), leading to a significant decrease in ocean pH (Bindoff et al., 2019; Oppenheimer et al., 2019). This decrease in pH, known as ocean acidification, is expected to have numerous effects on marine ecosystems, such as changing phytoplankton community composition (Tortell et al. 2008; Beaufort et al. 2011; Hoppe et al. 2013) and driving physiological and evolutionary changes in individual species (Lohbeck et al. 2012). The knock-on effect of which will impact the strength and efficiency of the biological carbon pump, oxygen production and trophic level interactions by grazers and viruses. The Southern Ocean biological carbon pump is an important contributor to global carbon flux, removing 3 Pg C from surface waters south of 30°S each year (Schlitzer, 2002), whilst also regulating the supply of nutrients to low latitude ecosystems (Sarmiento et al., 2004). Climate model predictions suggest that the Southern Ocean will be particularly sensitive to ocean acidification with some ecological impacts already evident in pteropods (Bednarsek et al., 2016) and other significant impacts on calcification before the end of the century (Sasse et al., 2015).

V.5.2 Overview of the project and objectives

Objective 1: Measure net primary production and calcification rates across different seasons and zones in the Southern Ocean to add to global databases for calcification.

Objective 2: Use satellite data to detect any seasonal, interannual and long-term variability in phytoplankton calcification rates and to examine these in line with global databases.

V.5.3 Methodology and sampling strategy

Seawater was collected from 3 different depths, representing the 55%, 10% and 1% light levels. For each light level 2L of seawater was filled into 2 x 1L bottles after passing through a 200 µm mesh to remove large grazers. Each bottle was spiked with 1 mL of ^{13}C representing a 5% enrichment. The bottles were filtered through 25 mm ashed (pre-combusted) GF/Fs (0.3 µm nominal pore size). The ashed filters were then placed in pre-combusted tin foil and placed into ziplock bags in the -80°C freezer.

In total, 20 experiments were performed (Figure V-2 Table 10).

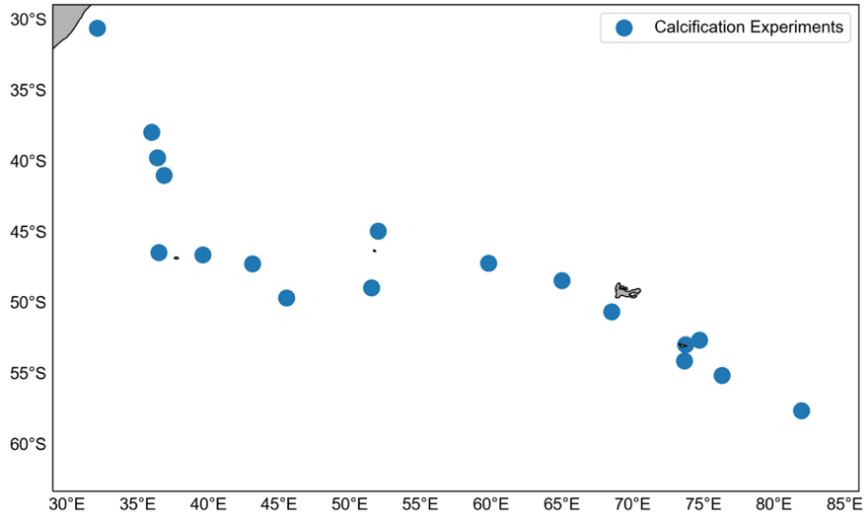

Figure V-2: Map showing the locations of calcification measurements performed.

Samples will be analyzed on land, no preliminary results to present.

Post-cruise sampling analyses and envisioned timeline of working plan, people involved on shore

The filters will be placed into petri dishes and incubated at 50°C for 24 hours, 1 filter from each light level from each experiment will then be placed in a desiccation chamber with a beaker of concentrated HCl at room temperature. Following the acidification process these filters will then be further incubated at 50°C for 24 hours. Filters will be punched using a size 13 punch, folded into tin cups and placed into a labelled 96-well plate. The samples will be sent for analysis on a mass spectrometer at the University of Cape Town. It is envisioned that all the samples will be analyzed within 6 months.

The acidified samples will represent the organic carbon uptake, the non-acidified samples will represent total carbon uptake and the difference between them represents the inorganic carbon uptake for calcification.

Table 10: Location information for calcification measurements performed on SWINGS.

Experiment	Date (UTC)	Station	Cast	Latitude	Longitude
1	21/01/2021	6	20	-30.654	32.151
2	24/01/2021	10	28	-38.018	35.991
3	25/01/2021	11	32	-39.812	36.390
4	27/01/2021	12	38	-41.051	36.870
5	30/01/2021	16	46	-46.500	36.500
6	02/02/2021	23	62	-46.670	39.601
7	04/02/2021	25	69	-47.306	43.107
8	05/02/2021	27	75	-49.714	45.526
9	08/02/2021	31	83	-49.001	51.534
10	10/02/2021	34	91	-45.002	52.001
11	13/02/2021	38	103	-47.257	59.798
12	14/02/2021	40	108	-48.500	65.001
13	16/02/2021	42	114	-50.701	68.501
14	17/02/2021	44	117	-52.698	74.717
15	18/02/2021	45	123	-53.024	73.733
16	19/02/2021	47	131	-54.171	73.655
17	20/02/2021	48	133	-55.199	76.307
18	22/02/2021	58	146	-57.690	81.924
19	24/02/2021	63	159	-55.800	77.320
20	27/02/2021	68	170	-50.800	72.300

References

Beaufort, L., Probert, I., de Garidel-Thoron, T., Bendif, E. M., Ruiz-Pino, D., Metzl, N., et al. (2011). Sensitivity of coccolithophores to carbonate chemistry and ocean acidification. Nature 476, 80–83. doi:10.1038/nature10295.

Bednaršek, N., Harvey, C. J., Kaplan, I. C., Feely, R. A., and Možina, J. (2016). Pteropods on the edge: Cumulative effects of ocean acidification, warming, and deoxygenation. Prog. Oceanogr. 145, 1–24. doi:https://doi.org/10.1016/j.pocean.2016.04.002.

Bindoff, N. L., Cheung, W. W. L., Kairo, J. G., Arístegui, J., Guinder, V. A., Hallberg, R., et al. (2019). "Changing Ocean, Marine Ecosystems, and Dependent Communities," in IPCC Special Report on the Ocean and Cyrosphere in a Changing Climate, eds. H.-O. Pörtner, D. C. Roberts, V. Masson-Delmotte, P. Zhai, M. Tignor, E. Poloczanska, et al. (IPCC).

Canadell, J. G., Le Quéré, C., Raupach, M. R., Field, C. B., Buitenhuis, E. T., Ciais, P., et al. (2007). Contributions to accelerating atmospheric CO2 growth from economic activity, carbon intensity, and efficiency of natural sinks. Proc. Natl. Acad. Sci. 104, 18866–18870. doi:10.1073/pnas.0702737104.

Ciais, P., Gasser, T., Paris, J. D., Caldeira, K., Raupach, M. R., Canadell, J. G., et al. (2013). Attributing the increase in atmospheric CO2 to emitters and absorbers. Nat. Clim. Chang. 3, 926–930. doi:10.1038/nclimate1942.

Friedlingstein, P., Cox, P., Betts, R., Bopp, L., von Bloh, W., Brovkin, V., et al. (2006). Climate–Carbon Cycle Feedback Analysis: Results from the C4MIP Model Intercomparison. J. Clim. 19, 3337–3353. doi:10.1175/JCLI3800.1.

Friedlingstein, P., Jones, M. W., O'Sullivan, M., Andrew, R. M., Hauck, J., Peters, G. P., et al. (2019). Global Carbon Budget 2019. Earth Syst. Sci. Data 11, 1783–1838. doi:10.5194/essd-11-1783-2019.

Gregor, L., Lebehot, A. D., Kok, S., and Scheel Monteiro, P. M. (2019). A comparative assessment of the uncertainties of global surface ocean CO2 estimates using a machine-learning ensemble (CSIR-ML6 version 2019a) – have we hit the wall? Geosci. Model Dev. 12, 5113–5136. doi:10.5194/gmd-12-5113-2019.

Gruber, N., Landschützer, P., and Lovenduski, N. S. (2019). The Variable Southern Ocean Carbon Sink. Ann. Rev. Mar. Sci. 11, 159–186. doi:10.1146/annurev-marine-121916-063407.

Lohbeck, K. T., Riebesell, U., and Reusch, T. B. H. (2012). Adaptive evolution of a key phytoplankton species to ocean acidification. Nat. Geosci. 5, 346–351. doi:10.1038/ngeo1441.

Oppenheimer, M., Glavovic, B. C., Hinkel, J., van de Wal, R., Magnan, A. K., Abd-Elgawad, A., et al. (2019). "Sea Level Rise and Implications for Low-Lying Islands, Coasts and Communities," in IPCC Special Report on the Ocean and Cyrosphere in a Changing Climate, eds. H.-O. Pörtner, D. C. Roberts, V. Masson-Delmotte, P. Zhai, M. Tignor, E. Poloczanska, et al. (IPCC).

Sabine, C. L., and Feely, R. A. (2007). "The oceanic sink for carbon dioxide," in Greenhouse Gas Sinks, eds. D. Reay, N. Hewitt, J. Grace, and K. Smith (Oxfordshire, UK: CABI Publishing), 31–49.

Sarmiento, J. L., Gruber, N., Brzezinski, M. A., and Dunne, J. P. (2004). High-latitude controls of thermocline nutrients and low latitude biological productivity. Nature 427, 56–60. doi:10.1038/nature02127.

Sasse, T. P., McNeil, B. I., Matear, R. J., and Lenton, A. (2015). Quantifying the influence of CO2 seasonality on future aragonite undersaturation onset. Biogeosciences 12, 6017–6031. doi:10.5194/bg-12-6017-2015.

Schlitzer, R. (2002). Carbon export fluxes in the Southern Ocean: results from inverse modeling and comparison with satellite-based estimates. Deep Sea Res. Part II Top. Stud. Oceanogr. 49, 1623–1644. doi:10.1016/S0967-0645(02)00004-8.

Tortell, P. D., Payne, C. D., Li, Y., Trimborn, S., Rost, B., Smith, W. O., et al. (2008). CO2 sensitivity of Southern Ocean phytoplankton. Geophys. Res. Lett. 35. doi:10.1029/2007GL032583.

V.6 Nitrogen cycling across the southwest Indian Ocean

Principal investigators (on board): Thomas Ryan-Keogh SOCCO CSIR, thomasryankeogh@googlemail.com) & Heather Forrer (Florida State University & University of Cape Town, hforrer@fsu.edu),

Oher participants (on board): Millie Goddard-Dwyer (University of Liverpool), Isobel Turnbull (Plymouth University), David Santana-Gonzalez (LEMAR), Helene Planquette (LEMAR), Hugo Berthelot (LEMAR, station biologique de Roscoff), Stephane Blain (LOMIC), Audrey Gueneugues (LOMIC)

On shore: Sarah Fawcett (University of Cape Town, sarah.fawcett@uct.ac.za), Angela Knapp (Florida State University, anknapp@fsu.edu)

Abstract

Marine phytoplankton are recognized as a crucial link in the Earth's climate system. Phytoplankton convert atmospheric carbon dioxide (CO2) dissolved in surface waters into organic carbon (C) through the process of photosynthesis (primary production) and subsequently contribute towards the vertical export and sequestration of biological C (that originated as atmospheric CO2) in the deep ocean, termed the "biological C pump". In a mass balance sense, phytoplankton consumption of new nitrogen (N; e.g., allochthonous nitrate) is proportional to net C export, while growth fuelled by recycled N (e.g., ammonium) yields no net C flux. Iron limitation of phytoplankton is considered a primary cause of the Southern Ocean's inefficient biological C pump. However, the role of the phytoplankton community structure and response to N cycling remains poorly understood in this region. Therefore, the investigation into N cycling by phytoplankton across the southwest Indian Ocean is required to better understand the controls on biological nitrate utilization and how this is influenced by iron supply, informing us on this region's outsized role in setting atmospheric CO2 today and in the past, and potentially absorbing CO2 in the future.

V.6.1 Scientific context

Constraining the role biology plays in the Southern Ocean, remains a key uncertainty in our current understanding of the Earth's climate. Marine phytoplankton represent a crucial link in the Earth's climate system as they convert atmospheric CO_2 dissolved in surface waters into organic carbon (C) through photosynthesis (primary production), contributing towards the vertical export and sequestration of biological C that originated as atmospheric CO_2, termed the "biological C pump" (Volk & Hoffert, 1985; Berger et al., 1988; Sigman & Boyle, 2000; Ducklow et al., 2001; Karl et al., 2001). This has led to the oceans becoming one of the largest active natural and anthropogenic C reservoirs (Takahashi et al., 2002; Turner, 2015; Nayak & Twardowski, 2020).

Various factors affect the strength (i.e., the rate of organic C export) and efficiency (i.e., the degree to which primary productivity contributes to export from the available nutrients) of the global ocean's biological pump, including the availability of macronutrients such as nitrogen (N) as well as micronutrients such as iron (Fe) (Broecker, 1982a & b; Codispoti, 1989; Ridgwell, 2002; Salter et al., 2012 & 2014; Assmy et al., 2013). Biologically available N, including nitrite (NO_2^-), ammonium (NH_4^+), dissolved and particulate organic nitrogen (DON and PON, respectively) and the most common form, nitrate (NO_3^-), can be characterized as either "new" or "regenerated" (Dugdale & Goering, 1967). While the balance between biological N sources and sinks determine the availability of N in the global ocean (Zehr & Ward, 2002; Gruber, 2008), the form, speciation and distribution of N is directly linked to the internal processes of assimilation (uptake by phytoplankton), ammonification (remineralization of organic N to NH_4^+), nitrification (NH_4^+ oxidation NO_3^-) and organic N export (Gruber, 2008; Casciotti, 2016). "New production" refers to phytoplankton growth fuelled by new N (mainly allochthonous NO_3^- mixed up from the deep

ocean reservoir, augmented in the low latitude ocean by N fixation) whereas "regenerated production" refers to phytoplankton growth supported by N recycled in the surface ocean (largely NH_4^+, as well as forms of DON, and NO_2^- and NO_3^- produced in the euphotic zone) (Dugdale & Goering, 1967). Since new production must be balanced by the export of euphotic zone organic matter on an annual timescale ("export production"), the utilization of new N for primary production is quantitatively linked to C export. By contrast, regenerated production yields no net C export in a mass balance sense (Dugdale & Goering, 1967). Assuming parallel cycling of N and C (i.e., constrained by the Redfield ratio of C:N:P being 106:16:1; Redfield et al., 1934 & 1958), the strength of the biological pump can be inferred from the degree to which new N is utilized relative to total N. In this framework, high rates of new production are indicative of a strong biological pump that yields significant C export and vice versa (Dugdale & Goering, 1967; Eppley & Peterson, 1979).

Observations show that NO_3^- is never fully consumed by phytoplankton in Subantarctic and Antarctic surface waters, likely due to a combination of Fe and light limitation of phytoplankton (Martin et al. 1991; Sunda and Huntsman 1997). The high NO_3^- - low chlorophyll state of the present-day Southern Ocean represents a "leak" in the global ocean's biological pump since by consuming NO_3^- more completely, Antarctic phytoplankton could lower atmospheric CO_2. Indeed, a more efficient biological pump at high latitudes is a leading hypothesis for the decrease in atmospheric CO_2 that characterized the ice ages (Sigman and Boyle 2000; Sigman et al. 2010). Understanding the controls on biological NO_3^- utilization in the modern Southern Ocean and thus its interaction with Fe supply is central to our understanding of its significant role in setting atmospheric CO_2 today and in the past, and in absorbing CO_2 in the future (Sarmiento and Toggweiler, 1984).

V.6.2 Overview of the project and objectives

The major goal of the project is to describe and probe the cycling of N across the southwest Indian Ocean in order to better understand the controls on NO_3^- drawdown and export production (and thus CO_2 removal) in this region.

Experimental overview: Primary production is an indicator of the amount of energy available to an ecosystem, which is centrally important to ecological processes and biogeochemical cycling. To assess the summertime fertility of the southwest Indian Ocean and the relative importance of different phytoplankton groups for driving production, simulated *in situ* experiments (^{13}C and ^{15}N incorporation; Cullen 2001; Dugdale and Goering 1967) were conducted to measure rates of net primary production, and new and regenerated production by both the bulk and size-fractionated phytoplankton community. Rates of nitrification and NH_4^+ regeneration will also be quantified (Peng et al. 2018; Mdutyana et al. *in prep*). The rate data allows for the accurate calculation of the f-ratio (shorthand for "flux ratio"; Eppley and Peterson, 1979), which provides an indication of the strength of the region's biological C pump and thus its capacity for biological CO_2 removal.

In addition to the bulk and size-fractionated community N transformation experiments, a series of Fe addition + ^{15}N incubations (NO_3^- and NH_4^+ uptake) were undertaken. The resultant particle samples collected at the end of the incubations will be flow cytometrically-sorted and measured for N isotopes. These data will allow for the quantification of taxon-specific rates of NO_3^- and NH_4^+ uptake (e.g., by *Synechococcus*, eukaryotes, diatoms, heterotrophic bacteria) under ambient and fertilized Fe conditions. Using this approach, important biological populations can be isolated from mixed environmental samples and population-specific $\delta^{15}N$ can be measured. This yields an integrated (over the organism lifetime) view of the primary N source uptake supporting different phytoplankton groups, enhancing our understanding of the role of different phytoplankton groups in driving the biological pump under both ambient and

fertilized Fe condition. These findings will have implications for future Southern Ocean biogeochemistry given predictions that phytoplankton community composition and Fe supply is likely to change under a changing climate.

In addition to the experiments, components of the N pool including DON, NH_4^+ and NO_3^- isotopes were sampled for to assist with constraining the N cycle and mass balanced export production budget.

Due to the opportunity of access, dissolved organic phosphate (DOP) samples were collected in conjunction with DON samples for a collaborator. As a result of the lack of automated analysis techniques, very few marine DOP measurements exist globally. However, this parameter is important to investigate since it is a measure of primary productivity across this region.

V.6.3 Methodology and sampling strategy

Seawater samples: Seawater samples were collected from both the clean and standard casts as well as the ship's underway system (depth ~5 m) (Table 11). From each cast, water was collected at predetermined depths between the surface and bottom and immediately frozen at -20°C for the following parameters: NO_3^- isotopes (60 ml from full depth, clean cast), NH_4^+ (2x 60 ml from upper 300m, standard cast), nutrients (60 ml, full depth, only at hydrocast stations) and DON +DOP (2x 60 ml filtered though 0.2 um syringe filter from upper 300m standard cast, only at stations north of the Subtropical Front). Additionally, DON +DOP samples were collected via the ship's underway every ~6 hours along the subtropical transect. NH_4^+ was measured onboard (Holmes et al., 1999) while NO_3^- isotopes, nutrients, DON and DOP will be measured post-cruise at either the University of Cape Town or Florida State University.

Water column N isotopes of bulk particles and specific phytoplankton taxa: Water samples for bulk N isotopic analysis of particulate organic nitrogen biomass (PN) were collected from six euphotic zone depths at L stations. From each depth, 2L HDPE bottles were filled with seawater that was then filtered under gentle vacuum through pre-combusted GF/F filters with nominal pore sizes of 0.3 µm. After filtration, the filters were folded in half using ethanol-cleaned forceps and stored in ashed tinfoil envelopes at -80**°**C pending analysis at the Stable Light Isotope Laboratory at the University of Cape Town.

Primary productivity and nitrification incubation experiments: Tracer incubation experiments were conducted at 17 stations for primary productivity and 20 for nitrification to directly quantify rates of carbon fixation (i.e., primary production), NO_3^- and NH_4^+ uptake. Water samples were collected in 4 x 2 L PC bottles (uptake) and 2 x 500 mL PC bottles (nitrification) from three euphotic zone and a further 2 x 250 mL black HDPE bottles at three to sub-euphotic zone depths. Seawater was pre-screened through a 200 µm nylon mesh to remove large grazers. Duplicate 2 L bottles from each euphotic zone depth were amended with $^{15}NO_3^-$ or $^{15}NH_4^+$ and ^{13}C-bicarbonate (for N uptake and net carbon fixation) and duplicate 250 mL bottles from all depths are amended with $^{15}NH_4^+$ (for NH_4^+ oxidation). The isotope tracers were added at ~10% of the ambient nutrient concentration. Samples were also collected for flow cytometric counting of phytoplankton particles, which aid in the quantification of different phytoplankton groups.

Prior to incubation, 45 mL subsamples (T_0) were collected from all nitrification bottles and frozen at -20°C. All bottles (for uptake and nitrification) were then placed in a custom-built on-deck incubator equipped with neutral density screens to simulate *in situ* light levels and a supply of circulating seawater to maintain a constant temperature. Uptake experiments were incubated for 4-6 hrs and nitrification experiments for 20-30 hrs. A second 45 mL subsample (T_f) was collected from each nitrification bottle at the end of the incubation. The N uptake and carbon fixation incubations were terminated by size-

fractionated filtration (0.3 µm, 2.7 µm, 10 µm) onto ashed GF/Fs and stored in ashed tinfoil envelopes at -80°C pending analysis at the Stable Light Isotope Laboratory at the University of Cape Town.

Fe addition + N uptake experiments: 12 Fe + ^{15}N tracer incubation experiments were conducted across the subantarctic to directly quantify rates of NO_3^- and NH_4^+ uptake under varying Fe concentrations. 34 L of clean water was collected for each incubation either from the clean rosette cast (surface ~ 30 m) or from the FISH (~ 7 m depth) where 12 x 2 L PC bottles were filled and the remaining 10 L was used for T_0 sampling. T_0 sampling included the following parameters; nutrients, NO_3^- isotopes, NH_4^+, FRRf, chlorophyll, PN and florescence activated cell sorting (FACS) for two size classes 0.4 - 10.0 µm and >10 µm. Nutrients and NO_3^- isotope samples were immediately frozen at -20°C for further analysis at the University of Cape Town and Florida State University, respectively. NH_4^+, FRRf and chlorophyll was measured on-board while the PN samples (1 L) were filtered under a gentle vacuum through pre-combusted GF/F filters with nominal pore sizes of 0.3 µm. The filters were folded in half using ethanol-cleaned forceps and stored in ashed tinfoil envelopes at -80°C pending analysis at Florida State University. The FACS samples were firstly filtered onto a 10 µm mesh filter (4 L) and then the filtrate subsequently filtered onto 2 x 0.4 µm PC filters (2L each) under a gentle vacuum. Both the mesh and PC filter were then placed in 5 mL cryovials to which ~4 mL of filtered (0.2 µm) seawater and 50 µL glutaraldehyde were added in order to resuspend the cells from the filters and preserve them. The cryovials were subsequently stored in a 4°C fridge for 1-4 hours and thereafter frozen at -80°C pending flow cytometric sorting and further analysis at the University of Hawaii and Florida State University, respectively.

The 6 x 2 L PC bottles were then spiked with 1nM Fe while the remaining 6 x 2 L PC bottles were used as a 'control'. These bottles were then placed in a custom-built on-deck incubator equipped with neutral density screens to simulate *in situ* surface light levels and a supply of circulating seawater to maintain a constant temperature for 24 hours to acclimate to the new Fe concentrations. After which, the bottles were removed and half (3x control and 3x +Fe) were spiked with $^{15}NO_3^-$ and half with $^{15}NH_4^+$ and placed back into the on-deck incubator for a further 24 hours. The experiment was terminated after 48 hours (24 hours Fe acclimation, 24 hours N uptake) where the following parameters were collected for; nutrients, NH_4^+, FRRf, chlorophyll, PN and florescence activated cell sorting (FACS) for two size classes 0.4 - 10.0 µm and >10 µm. The treatment for each of these parameters is the same as the T_0 samples.

*Table 11: **Exhaustive** list of measured parameters*

Parameter	Code of operation (Station-cast)	Number of samples
1. NO_3^- isotopes	Clean CTD: all depths	850
2. NH_4^+	Standard CTD: upper 300 m	1000
3. DON	Standard CTD: upper 300 m Ship underway	200
4. PN	Standard CTD: upper 6 depths	80
5.Primary Productivity	Standard CTD: surface, 10% light, 1% light	17 incubations
6. Nitrification	Standard CTD: surface, 10% light, 1% light, 140 m, 200 m, 300 m	20 incubations
7. Fe addition experiments	FISH or GoFlo: surface	12 experiments

NH_4^+ data from onboard analyses will be available shortly after the cruise.

V.6.4 Post-cruise sampling analyses and envisioned timeline of working plan, people involved on shore

Silicate and nitrate analysis: Silicate and NO3- concentrations will be measured on a Lachat QuickChem Flow Analysis platform in MBL-UCT following published auto-analysis protocols (Diamond, 1994; Grasshoff, 1976). The configuration typically used gives the Lachat QuickChem Flow Analysis platform a detection limit of 0.1 µM. Timeline : 1 year

Nitrite analysis: Nitrite concentrations were determined shipboard using the benchtop colorimetric Greiss reaction (Bendschneider and Robinson, 1952; Parsons et al., 1984). Absorbance was measured using a Thermo Scientific Geneysis 30 Visible spectrophotometer at a wavelength of 543 nm. The method has a detection limit of 0.05 µM. Timeline : 1 year

Phosphate analysis: Phosphate concentrations were determined shipboard using the Strickland and Parsons colourimetric method (Strickland and Parsons, 1968). Samples and standards were measured using a Thermo Scientific Geneysis 30 Visible spectrophotometer at a wavelength of 880 nm. The method has a detection limit of 0.05 µM. Timeline : 1 year

Ammonium analysis: These measurements were conducted onboard however post cruise quality control will be done. Ammonium concentrations were determined using the Holmes fluorometric method (Holmes et al., 1999). Samples and standards were measured using a Turner Designs Trilogy Fluorometer 7500-000 equipped with a UV module. The method has a detection limit of 0.05 µM. Since NHx samples are easy to contaminate, precautions were taken to prevent contamination during sample collection and processing. Following the addition of the orthophthaldialdehyde (OPA) working reagent to frozen samples, a water bath was used to defrost the samples. Once at room temperature, the samples and standards were allowed to react for four hours. The matrix effect, from the comparison of seawater samples and standards made with type-1 ultrapure water, was calculated according to the standard addition method (Saxberg & Kowalski, 1979). Final concentrations were corrected for the matrix effect. Timeline : 3 months

Nitrate isotope analysis: The $\delta^{15}N$ of NO_3^- (and its $\delta^{18}O$, which offers additional constraints on NO_3^- cycling) will be measured in the MBL-UCT using the newly-installed "denitrifier-isotope ratio mass spectrometer (IRMS)". Briefly, denitrifying bacteria lacking a terminal nitrous oxide (N_2O) reductase quantitatively convert sample NO_3^- (and NO_2^-) to N_2O (Sigman et al. 2001; Casciotti et al. 2002) that is then measured using a Thermo Delta V Plus IRMS and purpose-built on-line N_2O extraction and purification system. Precision for $\delta^{15}N$ and $\delta^{18}O$ is ≤0.1‰ and ≤0.3‰, respectively, for NO_3^- concentrations ≥0.5 µM. NO_2^- removal, if necessary, will be undertaken via the method of Granger and Sigman (2009) prior to sample analysis. Timeline : 1 year

Primary Productivity: The $\delta^{15}N$ and $\delta^{13}C$ from the primary productivity experiments will be prepared and measured at the University of Cape Town. The The frozen ashed GF/Fs will be oven dried at 40°C and pelletized into tin cups for analysis at the Stable Light Isotope Laboratory at UCT. Timeline : 1 year

Water column bulk PN: The particulate $\delta^{15}N$ and $\delta^{13}C$ from the water column will be prepared and measured at the MBL-UCT. The frozen ashed GF/Fs will be oven dried at 40°C and pelletized into tin cups for analysis at the Stable Light Isotope Laboratory at UCT. Timeline : 6 months

FACS-N isotope analysis: Central to this project is the coupled flow cytometry-N isotope protocol (Fawcett et al. 2011; 2014; Treibergs et al. 2014). All sorting will take place either at the UCT Flow Cytometry Core Facility or the University of Hawaii. Vials are thawed in the dark and gently vortexed to dislodge cells from filters. Re-suspended cells are filtered through a 35 µm mesh; the >35 µm particles are archived for future analysis. All sorts will be conducted using a BD FACS Jazz Cell Sorter equipped with

a 488 nm blue laser. Samples will be sorted for *Synechococccus* and total eukaryotic phytoplankton according to Fawcett et al. (2011), as well as cryptophytes and heterotrophic bacteria (Marie et al., 2997). We also aim to optimize the flowcytometry protocol for sorting diatoms; we will begin with the approach of McNair et al. (2015) and Hansman and Sessions (2015).

Isotopic analysis of Fe experiment bulk PN and sorted cell population PN: These samples will be converted to NO3- at Florida State University using the persulfate oxidation method of Knapp et al. (2005) as modified by Fawcett et al. (2014), respectively. Briefly, PN sorted particles are filtered onto ashed 0.3 µm GF-75s. These GF/Fs along with the bulk PN GF/Fs are transferred to combusted 4 mL glass Wheaton vials to which 2 mL of persulfate oxidizing reagent (POR) is added. POR is also added to triplicate vials containing a GF-75 blank plus varying amounts of two L-glutamic acid isotope standards, USGS-40 and USGS-41 (Qi et al. 2003); this allows for quantification of the N content and δ15N of the blank. POR is made by dissolving 1-2 g of NaOH and 1-2 g of 4-times recrystallized, methanol-rinsed potassium persulfate in 100 mL of DI water. After POR addition, vials are autoclaved at 121°C for 55 mins on a slow-vent setting. Sample pH is lowered to 5-8 and vials are centrifuged at 3000 rpm for 10 mins to separate residual GF-75 from the liquid sample. The concentration of the resultant total dissolved N (TDN) is measured via chemiluminescent analysis (Garside 1982; Braman and Hendrix 1989) using a NOx analyzer (Teledyne T200) with custom-built front-end at Florida State University. The δ15N of the oxidized TDN is analysed using the aforementioned 'denitrifier method' at Florida State University. The precision of the full collection/cytometry/N isotope protocol is ~0.4‰ (Fawcett et al. 2011; 2014). Timeline: 1 year..

Isotopic analysis of DON: DON concentrations and isotopic compositions will be measured at Florida State University following the Knapp et al. (2005) method. This involves the POR oxidation of 12 mL of sample with 1.5 mL of POR. POR is made the same as discussed above. After POR addition, vials are autoclaved at 121°C for 55 mins on a slow-vent setting. The concentration of the resultant total TDN is measured via chemiluminescent analysis (Garside 1982; Braman and Hendrix 1989) using a NOx analyzer (Teledyne T200) with custom-built front-end. After the TDN concentration is measured, the sample pH is then lowered to 4-6 before the δ15N of the oxidized TDN is analysed using the 'denitrifier method'. Timeline: 1 year.

DOP analysis: DOP concentrations will be measured at Florida State University closely following the Monaghan and Ruttenberg (1999) ash/hydrolysis method (modified from Solórzano and Sharp, 1980). This involves the drying of seawater at 500˚C, after which magnesium sulfate is added and then dried again at 70˚C. Subsequential baking is then done including 3 hours at 130 ˚C and then 4.5 hours at 500 ˚C. HCl is lastly added to hydrolyze any remaining polyphosphate.

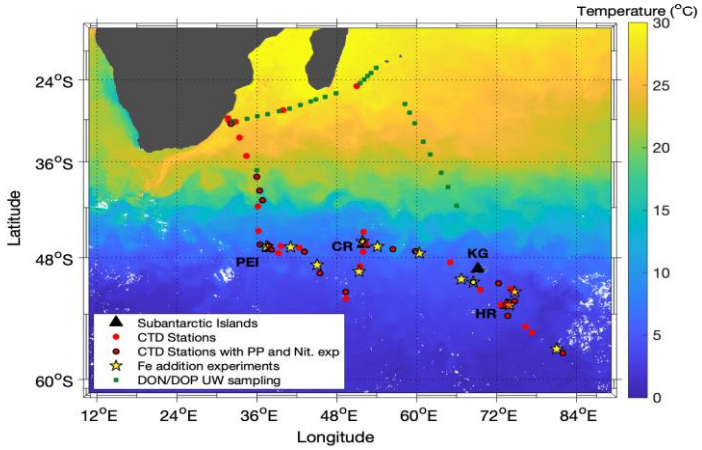

Figure V-3: overview of samples collected and experiments

References

Assmy, P., Smetacek, V., Montresor, M., Klaas, C., Henjes, J., Strass, V. H., ... & Cisewski, B. (2013). Thick-shelled, grazer-protected diatoms decouple ocean carbon and silicon cycles in the iron-limited Antarctic Circumpolar Current. *Proceedings of the National Academy of Sciences*, *110*(51), 20633-20638

Bendschneider K and Robinson RJ. 1952. A new spectrophotometric method for the determination of nitrite in sea water. Technical Report No. 8. University of Washington.

Berger, A. (1988). Milankovitch theory and climate. *Reviews of geophysics*, *26*(4), 624-657.

Broecker W. S. (1982b) Ocean chemistry during glacial time. *Geochimica et Cosmochimica Acta*, *46*, 1689 – 1706

Casciotti KL, Sigman DM, Hastings MG, Böhlke JK, and Hilkert A. 2002. Measurement of the oxygen isotopic composition of nitrate in seawater and freshwater using the denitrifier method, Anal. Chem. 74: 4905–4912. doi:10.1021/ac020113

Diamond D. 1994. QuikChem Method 10-114-21-1-B: Silicate by flow injection analysis. Lachat Instruments.

Ducklow, H. W., Steinberg, D. K., & Buesseler, K. O. (2001). Upper ocean carbon export and the biological pump. *OCEANOGRAPHY-WASHINGTON DC-OCEANOGRAPHY SOCIETY-*, *14*(4), 50-58.

Dugdale RC, Goering JJ. 1967. Uptake of new and regenerated forms of nitrogen in primary productivity. Limnology and Oceanography, 12: 196–206.

Eppley RW and Peterson BJ. 1979. Particulate organic matter flux and planktonic new production in the deep ocean. Nature, 282: 677-680.

Fawcett, S. E., Lomas, M.W., Casey, J.R., Ward, B.B., Sigman, D.M. (2011) Assimilation of upwelled nitrate by small eukaryotes in the Sargasso Sea. *Nature Geoscience* 4, 717-722.

Fawcett, S. E., Lomas, M.W., Ward, B.B., Sigman, D.M. (2014) The counterintuitive effect of summer-to-fall mixed layer deepening on eukaryotic new production in the Sargasso Sea. *Global Biogeochemical Cycles* 28, 86-102

Granger J and Sigman DM. 2009. Removal of nitrite with sulfamic acid for nitrate N and O isotope analysis with the denitrifier method. Rapid communication in mass spectrometry. 23: 3753-3762

Grasshoff K. 1976. Methods of seawater analysis. Verlag Chemie, Weinheim and New York.

Holmes R, Aminot I, Kërouel R, Hooker B and Peterson B. 1999. A simple and precise method for measuring ammonium in marine and freshwater ecosystems. Canadian Journal of Fisheries and Aquatic Sciences, 56(10): 1801-1808

Karl DM, Bidigare RR, Letelier RM (2001) Long-term changes in plankton community structure and productivity in the North Pacific Subtropical Gyre: the domain shift hypothesis. Deep-Sea Res II 48: 1449−1470

Knapp, A. N., Sigman, D. M., & Lipschultz, F. (2005). N isotopic composition of dissolved organic nitrogen and nitrate at the Bermuda Atlantic Time-series Study site. *Global Biogeochemical Cycles*, *19*(1).

Marie, D., Simon, N., Vaulot, D., 2005. Phytoplankton Cell Counting by Flow Cytometry, in: Algal Culturing Techniques. https://doi.org/10.1016/B978-012088426-1/50018-4

Martin, J.H., Gordon, R.M., Fitzwater, S.E. (1991) The case for iron. *Limnology and Oceanography* 36, 1793-1802.

McFarland MN, Rines J, Sullivan J, Donaghay P (2015) Impact of phytoplankton size and physiology on particulate optical properties determined with scanning flow cytometry. Mar Ecol Prog Ser 531: 43−61

Parsons TR, Maita Y and Lalli CM. 1984. A Manual of Chemical and Biological Methods for Seawater Analysis.

Peng X, Fawcett SE, van Oostende N, Wolf MJ, Marconi D, Sigman DM and Ward BB. 2018. Nitrogen uptake and nitrification in the subarctic North Atlantic Ocean. Limnology and Oceanography.

Sarmiento, J. L., Toggweiler, J.R. (1984) A new model for the role of the oceans in determining atmospheric pCO_2. *Nature* 308, 621-624.

Saxberg B and Kowalski W. 1979. Generalised standard edition method. Analytical Chemistry, 51(7): 1031-1038.

Sigman D, Casciotti KL, Andreani M, Barford C, Galanter M and Böhlke JK. 2001. A Bacterial Method for the Nitrogen Isotopic Analysis of Nitrate in Seawater and Freshwater. Analytical Chemistry, 73: 4145–4153.

Sigman, D.M., Boyle, E.A. (2000) Glacial/interglacial variations in atmospheric carbon dioxide. *Nature* 407, 859-869.

Sigman, D.M., Hain, M.P., Haug, G.H. (2010) The polar ocean and glacial cycles in atmospheric CO2 concentration. *Nature* 466, 47-55.

Strickland JD and Parsons TR. 1968. A practical handbook of seawater analysis. Bull. Fish. Res. Bd. Can. 167.

Sunda, W.G., Huntsman, S.A. (1997) Interrelated influence of iron, light and cell size on marine phytoplankton growth. *Nature* 390, 389-392.

Treibergs LA, and Granger J. (201). Enzyme level N and O isotope effects of assimilatory and dissimilatory nitrate reduction. Limnology and Oceanography, 62(1): 272-288.

Vaulot, D., Courties, C., Partensky, F., 1989. A simple method to preserve oceanic phytoplankton for flow cytometric analyses. Cytometry. https://doi.org/10.1002/cyto.990100519

Volk, T., & Hoffert, M. I. (1985). Ocean carbon pumps: Analysis of relative strengths and efficiencies in ocean-driven atmospheric CO2 changes. *The carbon cycle and atmospheric CO2: natural variations Archean to present*, *32*, 99-110.

V.7 Microbial diversity and activity, and the distribution of dissolved organic carbon and inorganic nutrients along the SWINGS transect

Principal investigator
On board : Ingrid Obernosterer
CNRS, Laboratoire d'Océanographie Microbienne (LOMIC), 1 ave Pierre Fabre, 66650 Banyuls sur mer, France
+ 33 (4) 68 88 73 53
ingrid.obernosterer@obs-banyuls.fr

Names of other participants
On board : Stéphane Blain, Sorbonne University, Laboratoire d'Océanographie Microbienne (LOMIC), Banyuls sur mer, France
Audrey Guéneugues, CNRS, Laboratoire d'Océanographie Microbienne (LOMIC), Banyuls sur mer, France
Rui Zhang, Sorbonne University, Laboratoire d'Océanographie Microbienne (LOMIC), Banyuls sur mer, France

Abstract

Our study aims to describe the taxonomic diversity of heterotrophic microbes, their metabolic potential, gene- and protein expression patterns under spatially varying environmental conditions. We have collected water samples in different oceanic provinces, covering Subtropical, Sub Antarctic and Antarctic waters. In each of these, we sampled specific water masses from surface to bottom, such as the wind mixed surface layer, oxygen and salinity minima and maxima, Upper and Lower Circumpolar Deep Water, and Antarctic Bottom Water. We have further collected samples for the enumeration of heterotrophic prokaryotes and small (up to 20 µm) autotrophic phytoplankton, the concentration of dissolved organic carbon (DOC) and major inorganic nutrients (nitrate and nitrite, phosphate and silicic acid). The concurrent detailed description of trace elemental distributions across ocean provinces and depth layers will provide the contextual data for the observations of the microbial functional and taxonomic diversity.

V.7.1 Scientific context

Marine microbial communities process the fluxes of all biologically important elements. Knowledge of the functions of individual taxa and their contribution to community performance is a key goal in microbial oceanography. The spatial distribution of microbial communities has illustrated the dynamics of distinct groups or taxa and linked to environmental factors, these patterns have informed on the ecological niches of microbes of interest. Contemporary environmental selection has widely been identified as one central mechanism for shaping the spatial distribution of heterotrophic microbes in the ocean (Hanson et al., 2012). Dispersal and drift are additional factors that were identified in biogeographic studies (Lindström and Langenheder, 2012; Wilkins et al., 2013). The potential influence of the community composition of microorganisms that can interact with heterotrophic microbes has only recently been taken into consideration in this context (Lima-Mendez et al., 2015; Zhou et al., 2018). Spatial and temporal patterns in the community structure of heterotrophic microbes in surface waters of the Southern Ocean were tightly associated with changes in the diatom assemblages, while they were

not related to geographic distance and environmental conditions (Liu et al. 2019, 2020). Identifying the factors that shape microbial community composition and their functional potential, and how in turn this could affect the cycling of elements remains a challenge, in particular in the poorly studies Southern Ocean.

V.7.2 Overview of the project and objectives

Our overall objective is to describe the taxonomic diversity of heterotrophic microbes, their metabolic potential, gene- and protein expression patterns under spatially varying environmental conditions.

Objective 1) is to describe the composition of prokaryotic communities (*Bacteria* and *Archaea*) in different oceanic provinces, covering Subtropical, Sub Antarctic and Antarctic waters. In each of these, we sampled specific water masses from surface to bottom, such as the wind mixed surface layer, oxygen and salinity minima and maxima, Upper and Lower Circumpolar Deep Water, and Antarctic Bottom Water.

Objective 2) is to explore the gene inventories of prokaryotic communities (*Bacteria* and *Archaea*) at sites and water masses characterized by contrasting environmental conditions. We aim to focus in particular on the content of trace elements and to identify potential links between gene inventories and trace element concentrations.

Objective 3) is to determine the gene- and protein expression patterns of prokaryotic communities (*Bacteria* and *Archaea*) in surface waters across the SWINGS transect to investigate limiting factors of the prokaryotic communities.

V.7.3 Methodology and sampling strategy

Inorganic nutrients

Seawater samples were collected using trace metal clean GoFlo bottles and standard Niskin bottles (Table 12). For samples collected by GoFlo bottles, seawater was filtered (0.45 µm) in the trace metal clean van. For samples collected with standard Niskin bottles, 125 mL of raw seawater was collected in HDPE flask, and 60 mL were filtered (0.45 µm Acetate Cellulose filters). All samples were preserved with $HgCl_2$ (4g/l; 300 µL in 20mL) in 60 mL LDPE bottles. They are stored in the dark and at room temperature until analysis back in the laboratory 5 months later. The analyses of nitrate (NO_3^-), nitrite (NO_2^-), phosphate (PO_4^{3-}) and silicic acid $Si(OH)_4$ will be carried out in the laboratory with a segmented flow analyzer (Skalar) equipped with colorimetric detection using methods described in (Aminot and Kérouel, 2007; Blain et al. 2018). The accuracy of the methods is assessed using reference material (Certipur, Merck).

Dissolved organic carbon (DOC)

Samples for DOC were taken at 10-12 depths covering the entire water column. Raw seawater samples were collected by trace metal clean GoFlo bottles into acid cleaned Schott Glass bottles (250 mL) with a Teflon-lined lid. Samples were filtered through two pre-combusted (24 h, 450°C) glass fiber filters (Whatman GF/F, 25 mm) using a custom-made all-glass/Teflon filtration syringe system. Samples (10 mL in duplicates) were collected into pre-combusted glass ampoules and acidified to pH 2 with phosphoric

acid (H_3PO_4). Ampoules were immediately sealed and stored in the dark at room temperature until analyses by high temperature catalytic oxidation (HTCO) on a Shimadzu TOC-V-CSH analyzer (Benner and Strom 1993). Prior to injection, DOC samples are sparged with CO_2 -free air for 6 min to remove inorganic carbon. Hundred µL of sample are injected in triplicate and the analytical precision is generally 2%. Consensus reference materials provided in sealed glass ampoules (http://www.rsmas.miami.edu/groups/biogeochem/CRM.html) is injected every 12 to 17 samples to insure stable operating conditions.

Enumeration of heterotrophic prokaryotes and autotrophic picoplankton

Samples were taken as for DOC (see above). Sub-samples of raw seawater (1.8-mL for heterotrophic prokaryotes and 4.5 mL for autotrophic picoplankton) were fixed with 1% glutaraldehyde (final concentration), stored in the dark at 4°C for 30 min, and quick frozen in liquid nitrogen. Samples were stored at -80 °C until analysis in the home lab. The abundance of heterotrophic and autotrophic prokaryotes and pico- and nano-eukaryotes will be done by flow cytometric analyses on a BD FACS Canto as described in Obernosterer et al. (2008).

Prokaryotic community composition and metagenomic analysis

Two 6 L biological replicates were collected at 5 depths. Seawater was filtered onto 0.8 µm polycarbonate filters (47-mm diameter, Nuclepore, Whatman, Sigma Aldrich, St Louis, MO) and the cells in the < 0.8 µm fraction were then concentrated on 0.2 µm Sterivex filter units (Sterivex, Millipore, EMD, Billerica, MA) using a peristaltic pumping system (Masterflex L/S Easy-Load II). The Sterivex filter units are kept at −80°C until DNA extraction in the LOMIC and sequencing at a platform following previously published protocols (Liu et al. 2019).

Metatranscriptomics

About 15L of surface seawater (in triplicates, collected by the FISH) were prefiltered through a 0.8 µm Polycarbonate filter (142 mm) and cells were then concentrated on a 0.2 µm Supor plus membrane (142 mm). The Supor filters were stored in RNA-later at -80°C. RNA extraction will be performed in the molecular laboratory in Banyuls sur Mer following previously published protocols (Debeljak et al. 2019) and samples will be sent to a sequencing platform.

Metaproteomics

About 20L of seawater (in triplicates, collected by the FISH) were prefiltered through a 0.8 µm Polycarbonate filter (142 mm), cells were then concentrated on a 0.2 µm Supor plus membrane (142 mm). The Supor filters were flash frozen in liquid nitrogen and stored in falcon tubes at -80°C. Protein extraction will be performed in the laboratory in Banyuls sur Mer following previously established protocols (Debeljak et al., in preparation) and samples will be measured on a MS Orbitrap.

Table 12: Samples collected for microbial diversity and activity, and the distribution of dissolved organic carbon and inorganic nutrients

Parameter	Code of operation (Station-cast)	Number of samples
1. Inorganic nutrients	SWG_S_002_006	19
	SWG_C_002_007	21
	SWG_C_003_011	23
	SWG_C_004_014	12
	SWG_C_005_018	11
	SWG_S_007_021	21
	SWG_C_008_023	17
	SWG_S_009_025	9
	SWG_C_010_027	23
	SWG_S_010_028	20
	SWG_C_011_034	24
	SWG_C_014_040	6
	SWG_C_014_041	21
	SWG_S_015_044	7
	SWG_C_016_047	21
	SWG_S_017_048	11
	SWG_C_018_049	22
	SWG_C_019_051	12
	SWG_C_020_053	5
	SWG_C_021_058	12
	SWG_C_025_068	21
	SWG_S_026_073	10
	SWG_C_027_074	24
	SWG_C_029_077	23
	SWG_S_030_079	11
	SWG_C_031_082	23
	SWG_C_032_084	23

	SWG_C_033_087	17
	SWG_S_034_091	21
	SWG_C_035_093	15
	SWG_C_036_098	23
	SWG_S_037_101	21
	SWG_C_038_102	23
	SWG_S_039_107	21
	SWG_S_040_108	18
	SWG_C_040_109	20
	SWG_S_042_111	22
	SWG_C_042_112	19
	SWG_S_043_115	10
	SWG_C_044_117	6
	SWG_C_045_122	2
	SWG_C_046_125	3
	SWG_C_047_130	18
	SWG_C_048_134	23
	SWG_S_053_139	13
	SWG_C_058_144	16
	SWG_S_062_154	11
	SWG_C_063_156	22
	SWG_C_065_159	3
	SWG_C_066_163	11
	SWG_C_067_167	11
	SWG_S_068_168	21
	SWG_C_068_169	10
2. Dissolved Organic Carbon (DOC)	SWG_C_002_007	12
	SWG_C_003_011	12
	SWG_C_004_014	12
	SWG_C_005_018	10

	SWG_C_008_023	12
	SWG_C_010_027	11
	SWG_C_011_034	12
	SWG_C_014_041	10
	SWG_C_016_047	12
	SWG_C_021_058	11
	SWG_C_025_068	12
	SWG_C_027_074	12
	SWG_C_029_077	12
	SWG_C_031_082	12
	SWG_C_033_087	11
	SWG_C_036_098	12
	SWG_C_040_109	12
	SWG_C_042_112	12
	SWG_C_044_117	7
	SWG_C_047_130	12
	SWG_C_058_144	12
	SWG_C_063_156	12
	SWG_C_066_163	10
	SWG_C_068_169	9
2. Abundance of heterotrophic prokaryotes	SWG_C_002_007	12
	SWG_S_003_010	12
	SWG_C_005_018	10
	SWG_C_008_023	12
	SWG_C_011_034	12
	SWG_C_014_041	10
	SWG_C_016_047	12
	SWG_C_021_058	11
	SWG_C_025_068	12
	SWG_C_029_077	12

	SWG_C_031_082	12
	SWG_C_033_087	11
	SWG_C_036_098	12
	SWG_C_042_112	12
	SWG_C_044_117	7
	SWG_C_047_130	12
	SWG_C_058_144	12
	SWG_C_063_156	12
	SWG_C_068_169	9
3. Abundance of autotrophic microplankton	SWG_C_002_007	7
	SWG_S_003_010	7
	SWG_C_005_018	7
	SWG_C_008_023	6
	SWG_C_011_034	6
	SWG_C_016_047	6
	SWG_C_021_058	5
	SWG_C_025_068	6
	SWG_C_029_077	6
	SWG_C_031_082	7
	SWG_C_033_087	5
	SWG_C_036_098	7
	SWG_C_042_112	6
	SWG_C_044_117	3
	SWG_C_047_130	6
	SWG_C_058_144	5
	SWG_C_063_156	5
	SWG_C_068_169	6
4. DNA/RNA extraction (metabarcoding, metagenomics)	SWG_C_002_007	4
	SWG_S_003_010	1
	SWG_C_003_011	1

	SWG_S_003_012	3
	SWG_S_005_017	2
	SWG_S_005_019	2
	SWG_C_008_023	4
	SWG_S_011_029	2
	SWG_S_011_032	1
	SWG_S_011_033	3
	SWG_S_014_042	4
	SWG_S_015_044	4
	SWG_S_016_046	4
	SWG_S_021_059	4
	SWG_S_025_067	3
	SWG_S_025_069	2
	SWG_S_025_071	1
	SWG_S_029_078	4
	SWG_S_031_083	1
	SWG_S_036_097	2
	SWG_S_036_100	3
	SWG_S_038_103	1
	SWG_C_042_112	4
	SWG_C_044_117	3
	SWG_C_045_122	1
	SWG_C_046_125	1
	SWG_C_058_144	4
	SWG_C_063_155	5
	SWG_C_068_169	4
	SWG_S_068_170	1
5.Metatranscriptomics	FISH_SWG_8_22/01/21_23:16-23/01021_00:23UTC	3
	FISH_SWG_16_30/01/21_19:47-20:17UTC	3
	FISH_SWG_30_07/02/2021_04:02-04:31UTC	3

	FISH_SWG_31_08/02/2021_12:00-12:45LTC	3
	FISH_SWG_33_10/02/2021_01:25-02:16UTC	3
	FISH_SWG_42_15/02/2021_12:26-13:15UTC	3
	FISH_SWG_58_21/02/2021_12:29-13:00UTC	3
	FISH_SWG_68_27/02/2021_03:01-03:47UTC	1
6. Metaproteomics	FISH_SWG_8_22/01/21_12:55-13:20UTC	3
	FISH_SWG_16_30/01/21_18:26-19:16UTC	3
	FISH_SWG_21_01/02/21_10:20-10:45UTC	1
	FISH_SWG_30_07/02/2021_03:02-03:32UTC	3
	FISH_SWG_31_08/02/2021_12:45-13:30LTC	3
	FISH_SWG_33_10/02/2021_02:31-03:01UTC	3
	FISH_SWG_42_15/02/2021_13:15-14:00UTC	3
	FISH_SWG_58_21/02/2021_13:19-13:55UTC	3
	FISH_SWG_68_27/02/2021_04:12-04:30UTC	1

No results are yet available onboard.

V.7.4 Post-cruise sampling analyses and envisioned timeline of working plan, people involved on shore

Inorganic nutrients. All inorganic nutrient analyses will be performed at the LOMIC by Olivier Crispi and Audrey Guéneugues. Results should be available in October 2021.

Dissolved organic carbon (DOC). All dissolved organic carbon analyses will be performed at the LOMIC by Barbara Marie. Results should be available in October 2021.

Enumeration of heterotrophic prokaryotes and autotrophic picoplankton. All flow cytometric analyses will be performed at the LOMIC by Philippe Catala. Results should be available in May 2021.

Prokaryotic community composition and metagenomic analysis. DNA extractions will be done at the LOMIC by Rui Zhang and sequencing will be performed at an appropriate platform. Results of the prokaryotic community composition should be available by December 2021. Results of metagenomic analyses should in part be available in the course of 2022 or in 2023.

Metatranscriptomics and metaproteomics. mRNA and protein extractions will be carried at the LOMIC by Rui Zhang and student to be hired, and sequencing will be performed at an appropriate platform. Results of metatranscriptomics analyses should in part be available in the course of 2022 or in 2023.

References

Aminot, A. and Kérouel, R. (2007) Dosage automatique des nutrimentsdans les eaux marines, méthodes en flux continu, Ifremer.

Blain S., Capparos J., Guéneuguès A., Obernosterer I., Oriol L. (2015). Distributions and stoichiometry of dissolved nitrogen and phosphorus in the iron-fertilized region near Kerguelen (Southern Ocean). Biogeosciences, 12, 623-635, doi:10.5194/bg-12-623-2015.

Benner, R., and Strom, M. (1993) A critical evaluation of the analytical blank associated with DOC measurements by high-temperature catalytic oxidation. Marine Chemistry 41: 153–160.

Debeljak P., E. Toulza, S. Beier, S. Blain, I. Obernosterer (2019) Microbial iron metabolism as revealed by gene expression profiles in contrasted Southern Ocean regimes Environ. Microbiol. 21: 2360-2374. doi:10.1111/1462-2920.14621

Hanson, C.A., Fuhrman, J.A., Horner-Devine, M.C., and Martiny, J.B.H. (2012) Beyond biogeographic patterns: processes shaping the microbial landscape. Nat Rev Microbiol 10: 497–506.

Lindström, E.S., and Langenheder, S. (2012) Local and regional factors influencing bacterial community assem-bly: bacterial community assembly. Environ Microbiol Rep 4:1–9.

Wilkins, D., van Sebille, E., Rintoul, S.R., Lauro, F.M., and Cavicchioli, R. (2013) Advection shapes Southern Ocean microbial assemblages independent of distance and environment effects. Nat Commun 4: 2457.

Lima-Mendez, G., Faust, K., Henry, N., Decelle, J., Colin, S., Carcillo, F., et al. (2015) Determinants of community structure in the global plankton interactome. Science 348: 1262073.

Zhou, J., Song, X., Zhang, C.-Y., Chen, G.-F., Lao, Y.-M., Jin, H., and Cai, Z.-H. (2018) Distribution patterns of microbial community structure along a 7000-mile latitudinal transect from the Mediterranean Sea across the Atlantic Ocean to the Brazilian Coastal Sea. Microbial Ecology 76:592–609.

Liu Y., P. Debeljak, M. Rembauville, S. Blain, I. Obernosterer (2019) Diatoms shape the biogeography of heterotrophic prokaryotes in early spring in the Southern Ocean. Environ. Microbiol. 21 : 1452-1465. doi:10.1111/1462-2920.14579

Liu Y., S. Blain, O. Crispi, M. Rembauville, I. Obernosterer (2020). Seasonal dynamics of prokaryotes and their associations with diatoms in the Southern Ocean as revealed by an autonomous sampler. Environ. Microbiol. Doi. 10.1111/1462-2920.15184

Obernosterer I., U. Christaki, D. Lefèvre, P. Catala, F. Van Wambeke and P. Lebaron (2008) Rapid Mineralization Of Organic Carbon Produced During A Phytoplankton Bloom Induced By Natural Iron Fertilization. Deep Sea Res Part II 55: 777-789

V.8 Biological Understanding of the CO_2 and O_2 LeveL in the ocEan (BULLE project)

Principal investigator

On board : FOURQUEZ MARION, MIO Luminy Marseille, +33(0)7 67 32 42 31, marion.fourquez@gmail.com. Aix Marseille Université, CNRS, Université de Toulon, IRD, OSU Pythéas, Mediterranean Institute of Oceanography (MIO), UM 110, 13288, Marseille, France.

Marion Fourquez is funded from the European Union H2020-MSCA-IF-2019 program under grant agreement n°894264 (BULLE project)

Names of other participants

On board : Hugo Berthelot Laboratoire des sciences de l'environnement marin, IUEM, Université de Brest-UMR 6539 CNRS/UBO/IRD. Sorbonne Université, CNRS - UMR7144, FR Tara GOSEE, station biologique de Roscoff, France

Ingrid Obernosterer Laboratoire d'Océanographie Microbienne UMR 7621, Observatoire Océanologique de Banyuls sur mer, France

Claire Lo Monaco (+ OISO team) LOCEAN-IPSL, Sorbonne Université, CNRS/IRD/MNHN Paris, Paris, France

Stéphane Blain Laboratoire d'Océanographie Microbienne UMR 7621, Observatoire Océanologique de Banyuls sur mer, France

On shore : Dominique Lefèvre Aix Marseille Université, CNRS, Université de Toulon, IRD, OSU Pythéas, Mediterranean Institute of Oceanography (MIO), UM 110, 13288, Marseille, France

Gérald Grégori Aix Marseille Université, CNRS, Université de Toulon, IRD, OSU Pythéas, Mediterranean Institute of Oceanography (MIO), UM 110, 13288, Marseille, France

Abstract

There is often a disconnect between scales in oceanography. Major biological processes occur at microscopic scales but have global consequences. As microbial life is the support system of the biosphere, there is an unquestionable need to include microorganisms in mainstream climate change research, particularly research addressing carbon dioxide (CO_2) and dioxygen (O_2) fluxes. Phytoplankton acts for half of the Earth's photosynthesis, allowing oceans to supply major living resources and O_2. Bacterial respiration is the other fundamental biological process that counterbalances photosynthesis and returns organic carbon back as CO_2. Yet, despite ocean's pivotal role in global climate, microbial respiration remains one of the least explored metabolic processes; so that, whether oligotrophic ocean is a net sink or source of CO_2, is highly debated for the last 20 years. The BULLE project aims to evaluate the ocean's metabolic balance between photosynthesis and respiration by looking at the production of CO_2 evolved to that O_2 consumed by marine bacteria, the so-called "respiratory quotient" (RQ). The BULLE project is funded by the European Union H2020 program and it partly relies on experimental approaches that took place during the SWINGS expedition.

V.8.1 Scientific context

Oceans are home to some of the most climatically important microorganisms on Earth. Billions of tiny marine plants, the phytoplankton, inhabit the ocean surface to capture the sun's energy by photosynthesis. Through this biological process the carbon dioxide (CO_2) is taken up from surface waters, and as they grow phytoplankton convert it to particulate organic matter containing carbon. A fraction of this carbon can be sequestrated on timescales of months to centuries, it is the so-called "biological pump of carbon". Through an ensemble of mechanisms (passive sinking of particles, active transport by animals, or mixing of dissolved organic matter), about 10 billion tons of carbon per year is thus exported from the surface layer, which is in the same magnitude as the global CO_2 emissions by humans' activities (Le Quéré et al. 2018; Friedlingstein et al. 2020). This research largely focuses on the other side of the coin: the microbial respiration that returns organic carbon back as CO_2 to the atmosphere. Indeed, the fate of the carbon produced by photosynthesis is rather uncertain, as instead of being isolated in the deep ocean it could be respired. Consequently, the balance between the rate of CO_2 sequestration by photosynthesis and the rate of CO_2 discharge into the atmosphere by respiration has important consequences. Organisms of all trophic levels contribute to ecosystem respiration, but respiration by bacteria (BR) is known to act as the quantitatively most important pathway accounting for about 50-90% of the total respiration in the oceans (Robinson 2008). Yet, despite its pivotal role in oceanic CO_2 sequestration, microbial respiration remains the major area of ignorance in our understanding of the global carbon cycle. The world's ocean provides another crucial service for the maintenance of Life on Earth: it is the supplier of half of the world's dioxygen (O_2), playing an equally important role as the land forests. In aerobic respiring bacteria, O_2 is used as terminal electron acceptor. Since carbon is used as the currency for large scale model, respiration measured as O_2 consumption rates must be converted to units of CO_2. The respiratory quotient (RQ) is the ratio of the volume of CO_2 evolved to that of O_2 consumed in the respiration process. RQ is dimensionless, but it is not a fixed value. Depending on the composition of the pool of organic matter, preferential organic substrates are utilized in BR which directly affect the value of RQ. Theoretically, the RQ can range from as low as 0.5 to 4. However, a complete understanding of microbial respiration is still precluded by the fact that most studies have assumed a fixed RQ of 1. RQ

is not only a practical aspect of bacterial respiration determination, it is a major variable for the biological pump of carbon. Arbitrary values of RQ contribute to mismatch between measurements of microbial activities and the carbon budget. In this way, RQ greatly influences calculations of carbon fluxes from marine microorganisms and becomes an intrinsic factor of uncertainty in oceanic carbon cycling studies. Global climate change, and its impact on oceanic processes, is a major issue for the coming decades. Hence, understanding how much CO_2 is being absorbed by the oceans is an active area of research. Although the microbial RQ has profound conceptual importance and significant practical implications, only few empirical determinations exist. It is thus critical to shed new lights on factors controlling the RQ and to reconsider the ocean's metabolic balance considering its true variability. The project presented herein aims to bring about a step change in our understanding of microbial respiration and RQ and its impact on carbon cycle, both at the cellular and the community level.

V.8.2 Overview of the project and objectives

Both physical and biological mechanisms contribute to the absorption and storage of oceanic carbon, the planktonic ecosystem being the main contributor to the biological pump. Although this biological carbon pump has been clearly identified, the scope of its action remains to be determined as the microbial respiration (mainly driven by heterotrophic bacteria) may also represent the largest driver of CO_2 emissions. In oceanography, bacterial respiration (BR) measurements only represents two to three orders of magnitude less than the number of measurements for primary production by phytoplankton and there are only few attempts for concurrent measurements of O_2 consumption and CO_2 production during BR process, thus "prompting the urgent need to assess bacterial respiratory quotient (RQ) in marine environment" (Robinson 2019).

In the context of the SWINGS expedition, the BULLE project (H2020-MSCA-IF-2019, grant project number 894264) aims to (1) decipher the bacterial respiration to that of photorespiration by phytoplankton and (2) quantify the respiratory quotient (ratio of the volume of CO_2 evolved to that of O_2 consumed in the respiration process) at both community and cellular levels. The corresponding objectives are to determine (1) the respiratory quotient (RQ) in different bacterial communities, (2) the activity of uncultured cells directly in their habitat and (3) the RQ at the single cell level.

V.8.3 Methodology and sampling strategy

Sampling strategy

Changes in temperature may affect different types of metabolism including the respiration process. This temperature dependence is, by simplification, often characterized through the Q10 factor which is the relative process rate increase following a temperature raise of 10°C. In this study, the positioning of the sampling sites (Figure V-4) was chosen to determine whether a change in temperature affects BR and QR, and whether it changes between sites due to varying resource controlling factors and/or because of the composition of the active fraction of the bacterial community.

The Q10 factor will be determined by analysing bivariate correlations between experimental temperature and the logarithms of metabolic activities measured (BR, QR, glucose consumption rate

etc.). Finally, multivariable analyses will be performed including other physico-chemical parameters such as DFe, Chla, macronutrients, DOM etc. when they will be available. Together, we hope that this exhaustive set of data will provide a comprehensive view of parameters influencing RQ, BR and bacterial activity in natural oceanic environments.

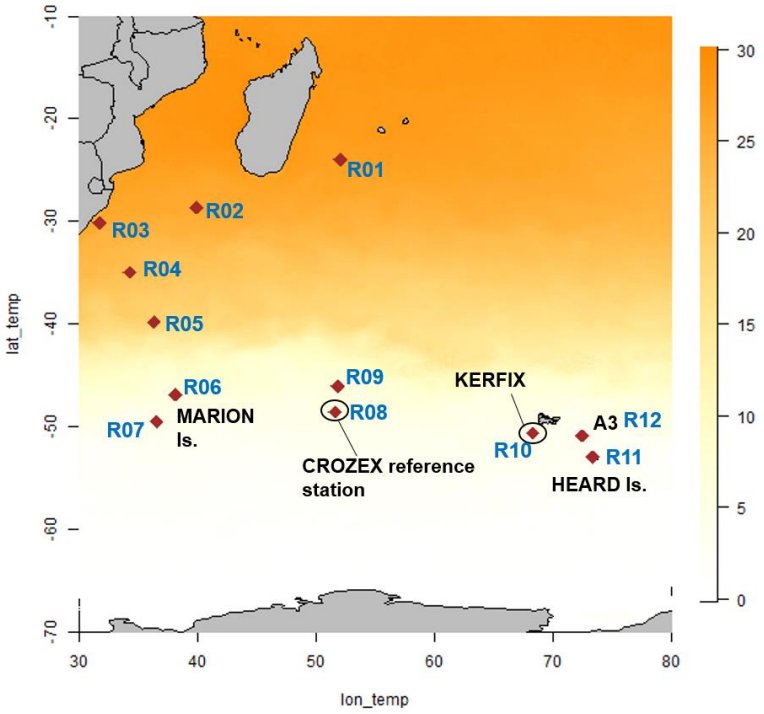

Figure V-4: Map of SWINGS study area showing the stations sampled for the BULLE's project. Seawater samples were collected at contrasted sites located within tropical waters, in the vicinity of the sub Antarctic islands Marion, Crozet, Heard and Kerguelen archipelago, and at reference stations from previous oceanographic expeditions (CROZEX and KEOPS)

V.8.4 Overview of the methods

Seawater samples for incubation experiments were collected at 12 different sites (R01 to R12) from 23.9° to 52°S along temperature gradient and front crossing in the Indian sector of the Southern Ocean (Fig. V-4). Surface (5m) or subsurface (max 30m) seawater was collected either using a towed *in situ* sampler, drawn onboard using an air driven Teflon diaphragm pump (FISH), the underway system, the standard CTD or the clean CTD. Details for each sampling site are given in Table 13 and a simplified view of the experimental set up is presented in Figure V-5.

Objective 1: Determining the respiratory quotient (RQ) in different bacterial communities.

To investigate the RQ in the sector of the Indian Ocean (North and South of the ACC), short (30h) and long-term experiments (up to 7 days) were run on batch at *in situ* temperature. Seawater samples were transferred into cleaned and acid-washed glass biological oxygen demand stoppered bottle equipped with an optode and maintained in a thermoregulated water bath. The consumption of O_2 by microbes was monitored in the dark for the total community (unfiltered seawater, dark community respiration or DCR) and the bacterial respiration only (fraction-size <0,8µm, BR) with non-invasive O_2 sensors (Presens). For continuous measurements, O_2 concentration was recorded every 4 min for up to 7 days. Additional incubations were performed on the fraction-size <0,8µm with glucose addition (10µm). Besides

continuous measurements using optodes, BR was also determined from incubation amended with glucose using the Winkler method plus modifications (Carpenter 1965; Culberson 1991). To do so, replicates of 125 cm^3 borosilicate glass bottles were filled with 0.8µm prefiltered seawater and three other replicates were immediately fixed with Winkler reagents (manganese chloride followed by alkaline iodide) to determine the initial O_2 concentration. Bottles were maintained in the dark at *in situ* temperature for 1–7 days. Dissolved O_2 measurements were made using an automatic colorimetric endpoint detector and the BR rate was determined by dividing the O_2 concentration difference (initial – final) by the incubation time for each time point. The linear consumption of O_2 over time was very verified with continuous measurements run in parallel (optodes). Every time a discrete sampling in biological triplicates was taken, a parallel measurement for dissolved inorganic carbon (DIC) was also performed in duplicate by potentiometry (Edmond 1970). Analyses for BR (Winkler's method) and DIC were directly performed onboard the R/V Marion Dufresne by Coraline Leseurre, Claude Mignon, Jonathan Fin, Guillaume Barut and Claire Lo Monaco (OISO team). BR rates as O_2 consumption and CO_2 released will be normalized to C biomass by considering the bacterial cell abundance (CYTO) and activity (BONCAT) in incubation bottles when analyses will be processed. See below for details.

Objective 2: Determining the activity of uncultured cells directly in their habitat.

To understand the biogeochemical roles of marine bacteria in their environment, it is important to determine when and under which conditions they are metabolically active. Here, I used the bio-orthogonal noncanonical amino acid tagging (BONCAT) method that can reveal active cells by tracking the incorporation of synthetic amino acids into newly synthesized proteins. For BONCAT, seawater samples were incubated with 1µM of substrate (HPG) for 6 hours before being fixed by the addition of 0.25% (final concentration) of glutaraldehyde. Samples for cell abundance determination were taken simultaneously at the start of the incubation and stored in separated cryotubes. Cell abundances will be determined in the home lab (MIO) by flow cytometry as described in Fourquez et al. (2020). For each measure (CYTO and BONCAT) 4.5 mL subsamples were fixed with glutaraldehyde (0.25% final concentration), stored in the dark at 4°C for up to 12 hours, shock-frozen in liquid nitrogen, and stored at -80°C. In theory, BONCAT-labelled cells could be isolated with fluorescence-activated cell sorting (BONCAT-FACS) for subsequent genetic analyses. Additional samples were additionally taken to apply this method back to the lab (MIO). If successful, sorting of individual BONCAT-labelled bacterial cells followed by 16S rRNA gene sequencing will allow active-cells to be identified at the single cell level on their genetic basis.

Objective 3: Determining the respiratory quotient at the single cell level.

Additional incubation with glucose labeled with ^{13}C were conducted in parallel and run simultaneously to other microbial parameters. This will allow to measure accurately the passage of organic carbon trough heterotrophic respiration process and its losses as CO_2. Incubations consisted in 1L of 0.8µm prefiltered seawater spiked with 13C-glucose (100% of carbon labelled with 13C) at10µM final concentration. Independent replicates were prepared and placed in the dark at *in situ* temperature. One replicate was taken at each time point (usually 24h, 72h and 7 days of incubation time). The incorporation of ^{13}C into biomass will be determined at the cellular scale using NanoSIMS technique in collaboration with Hugo Berthelot. The release of ^{13}C as CO_2 through the respiration process will be analyzed back in the lab by mass spectrometry. In addition to sample for NanoSIMS and 13C-DIC analyses, one sample for

cell abundance, BONCAT, and glucose concentration determination by spectrophotometric method (Myklestad et al. 1997) from each replicate.

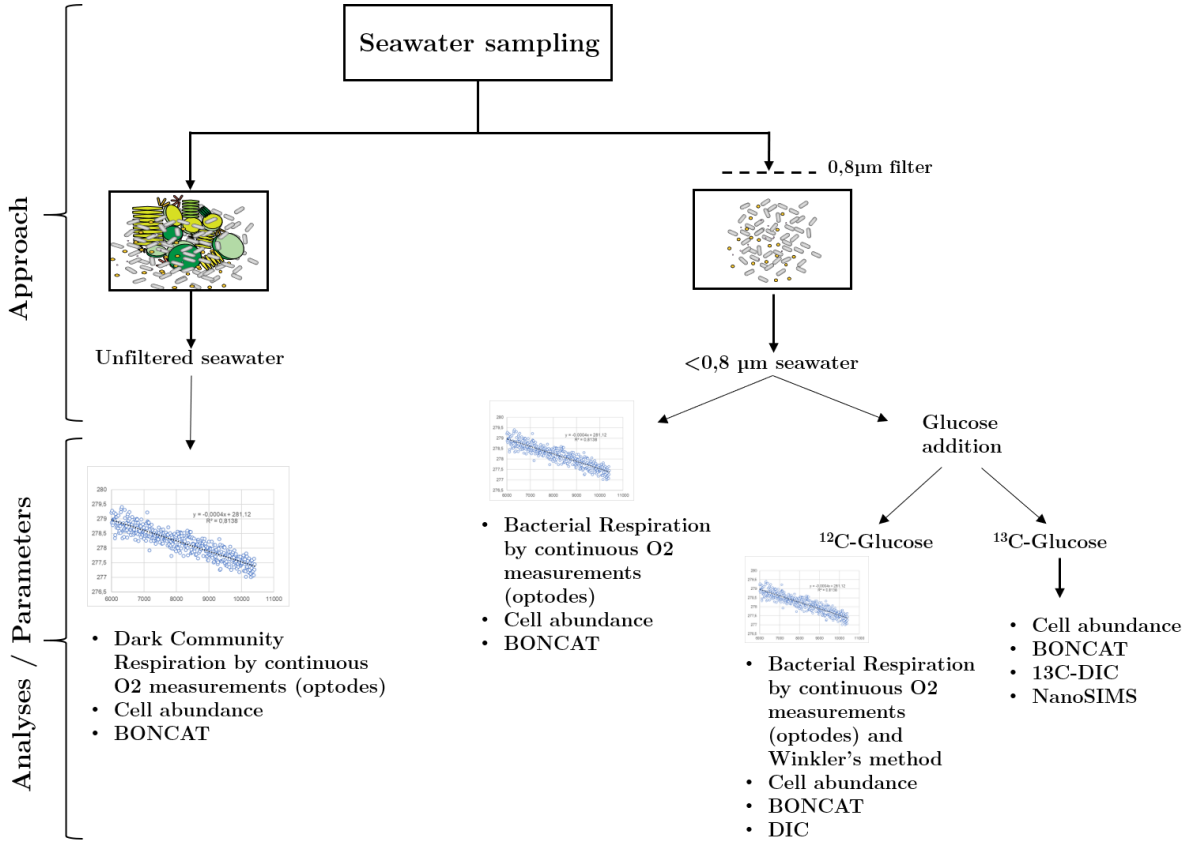

Figure V-5: Schematic representation of the experimental set-up to answer the objectives of the project.

V.8.5 Perspectives and future work

The direct effect of temperature on BR is difficult to separate from indirect effects such as changes in resource availability or community composition. For this project, an on-going collaboration with Ingrid Obernosterer and Stéphane Blain at LOMIC will help to address this question. Indeed, samples for microbial taxonomy and diversity were taken for experiment. The composition of the prokaryotic community will be established in combination with functional profiling (metagenomics) and expression patterns (metatranscriptomics). These data will further serve the project to get new insights into the ability of bacterial communities to influence the O_2 and CO_2 pool by their metabolic activities. Moreover, dissolved organic carbon and macronutrients concentration were also collected on sampling site and will be analysed at the LOMIC. These data will be later used for multivariable analyses.

Table 13: Parameters sampled. Cell abundances (CYTO) for heterotrophic bacteria, heterotrophic nanoflagellates, photopico- and nanoplankton, bacterial respiration using optodes (BR) and traditional method (WINKLER), dark community respiration (DCR), bacterial production of CO_2 within the dissolved inorganic pool (DIC) bacterial activity (BONCAT), bacterial diversity (BD), and single-cell analysis of bacterial growth efficiency using 13C glucose amended experiments (^{13}C). Overall, all parameters described here below were tested over a range of experimental temperatures from 3 to 26°C corresponding to in situ conditions.

#ID	Closest station	Latitude N	Longitude E	T°C	Date (jj/mm/yyy)	Sampling procedure	Parameter
R01	SWG 01	-23,9652	52,0949	25,9	14/01/2021	FISH	BR, DCR, CYTO, BONCAT
R02	SWG 02	-28,6375	39,9875	26	17/01/2021	UNDERWAY	BR, DCR, CYTO, 13C, BONCAT
R03	SWG 05	-30,1319	31,7821	25,2	21/01/2021	CTD 15m	BR, DCR, CYTO, WINKLER, DIC, 13C, BONCAT
R04	SWG 08	-34,9614	34,3653	22,7	22/01/2021	FISH	BR, DCR, CYTO, WINKLER, DIC, 13C, BONCAT
R05	SWG 11	-39,8117	36,3880	20,3	24/01/2021	CTD 15m	BR, DCR, CYTO, WINKLER, DIC, 13C, BONCAT
R06	SWG 16	-49,4997	36,6003	8,1	30/01/2021	CTD 15m	BR, DCR, CYTO, WINKLER, DIC, 13C, BONCAT, BD
R07	SWG 22	-46,8581	38,2007	6,3	01/02/2021	FISH	BR, DCR, CYTO, 13C, BONCAT
R08	SWG 31	-48,5692	51,6525	5,1	08/02/2021	FISH	BR, DCR, CYTO, WINKLER, DIC, 13C, BONCAT
R09	SWG 33	-46,0432	51,8930	6,3	10/02/2021	FISH	BR, DCR, CYTO, WINKLER, DIC, 13C, BONCAT, BD
R10	SWG 42	-50,6091	68,3622	4,3	15/02/2021	FISH	BR, DCR, CYTO, WINKLER, DIC, 13C, BONCAT
R11	SWG 46	-52,9753	73,4111	3,1	18/02/2021	TMR cast 125 30m	BR, DCR, CYTO, 13C, BONCAT
R12	SWG 68	-50,8809	72,5225	3,9	27/02/2021	FISH	BR, DCR, CYTO, WINKLER, DIC, 13C, BONCAT, BD

V.8.6 Preliminary results

Across all sampling sites, rates of dark community respiration (DCR), bacterial respiration (BR <0.8 µm) and bacterial respiration with glucose amendment (BR <0.8µm + Glc) varied from 0.55±0.11 to 37.1±8.14 µmol O_2 L^{-1} d^{-1}, from 0.19±0.05 to 9.17±2.22, and from 0.55±0.08 to 16.7±13.1 µmol O_2 L^{-1} d^{-1}, respectively. Overall, the contribution of bacteria to the community respiration varied between 4 to up to 77% on surface seawater Figure V-6).

The preliminary results of the experiments also show values of RQ relatively small (0.3) to what was estimated before by Lefevre et al. (2008).

Moreover, it seems that over the natural range of temperatures encountered in this study, the raw data show that the temperature dependence of the bacterial respiration cannot be defined solely according to the Arrhenius law (Figure V-6: Preliminary results showing respiration rates for the entire community (DCR) and bacterial respiration (BR) for various temperature corresponding to different sampling sites.

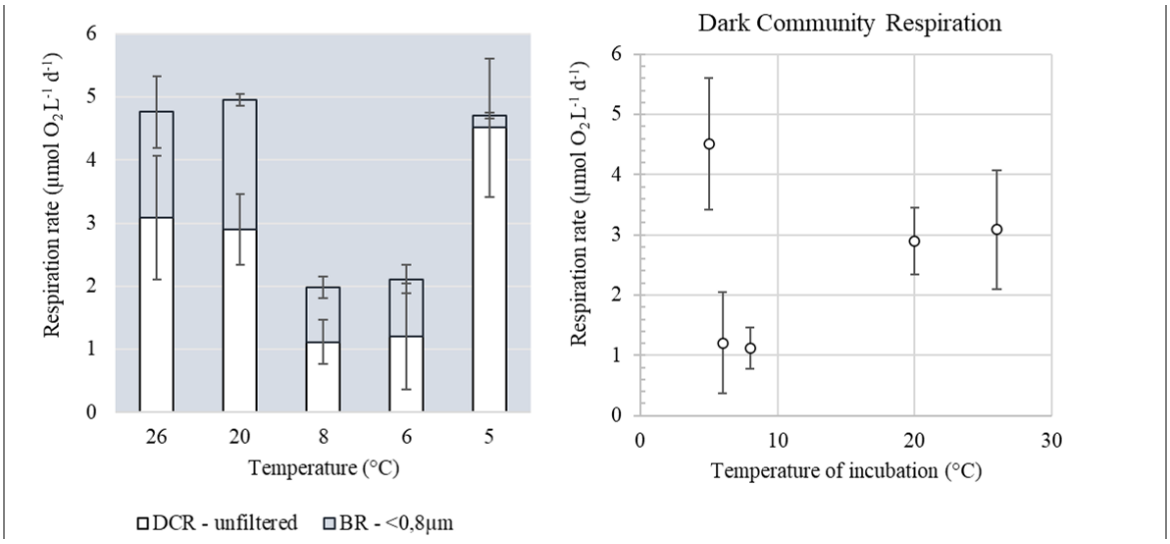

Figure V-6: Preliminary results showing respiration rates for the entire community (DCR) and bacterial respiration (BR) for various temperature corresponding to different sampling sites.

Further investigations need to be conducted to confirm these results. Interestingly, a similar trend in O_2 over the time course of experiments was also observed at all stations (Figure V-7). Distinct phases of consumption rate of O_2 were recorded that can be denoted as "low", "medium" and "high". Analyses of cell abundances by flow cytometry will help to understand this result.

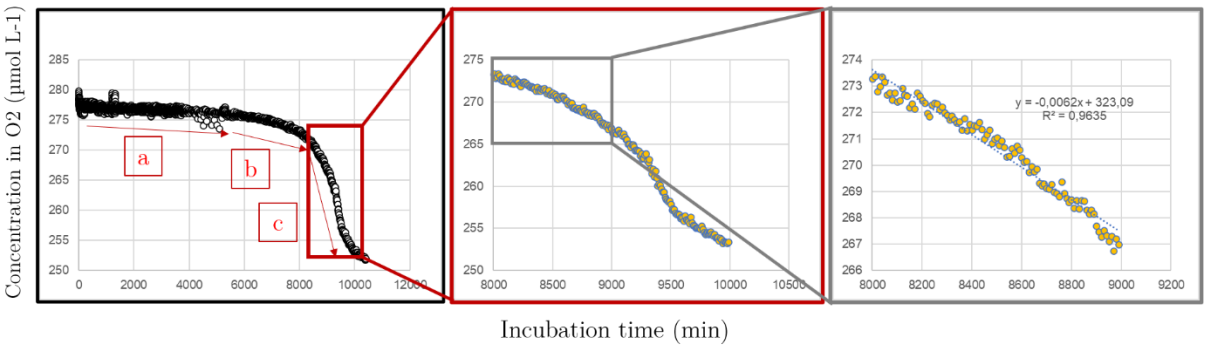

Figure V-7: Example of continuous measurement using optodes (recorded at R06). Three distinct phases were systematically recorded over the time course of the experiment. Phase a: "slow" rate of O_2 consumption, b: "medium" rate of O_2 consumption and c: "high" rate of O_2 consumption.

V.8.7 Post-cruise sampling analyses and envisioned timeline of working plan, people involved on shore

Samples for BONCAT and CYTO will be processed at the MIO by May 2021 by Marion Fourquez in collaboration with Gérald Gregori (MIO). Data processing of O_2 continuous measurements will be done in collaboration with Dominique Lefevre (MIO). Samples for 13C (DIC, NanoSIMS) will be processed by the end of the year 2021 in collaboration with Hugo Berthelot (LEMAR, Station Biologique de Roscoff). Bacterial diversity and "OMICS" analyses will be done in collaboration with Ingrid Obernosterer (LOMIC).

References

Carpenter, J. I. 1965. The accuracy of the Winkler method for dissolved oxygen analysis. Limnol. Oceanogr. 10: 135–140. doi:10.4319/lo.1965.10.1.0135

Culberson, C. 1991. Dissolved Oxygen. WHPO Publ. 91.

Edmond, J. M. 1970. High precision determination of titration of alkalinity and total CO2 of seawater by potentiometric titration. Deep Sea Res. 17: 737–750.

Fourquez, M., M. Bressac, S. L. Deppeler, M. Ellwood, I. Obernosterer, T. W. Trull, P. W. Boyd, and M. N. Müller. 2020. Microbial Competition in the Subpolar Southern Ocean : An Fe – C Co-limitation Experiment. Front. Mar. Sci. 6: 776. doi:10.3389/fmars.2019.00776

Friedlingstein, P., M. O'Sullivan, M. W. Jones, and others. 2020. Global Carbon Budget 2020. Earth Syst. Sci. Data 12: 3269–3340. doi:10.5194/essd-12-3269-2020

Lefevre, D., C. Guigue, and I. Obernosterer. 2008. The metabolic balance at two contrasting sites in the Southern Ocean: The iron-fertilized Kerguelen area and HNLC waters. Deep Sea Res. Part II Top. Stud. Oceanogr. 55: 766–776. doi:10.1016/j.dsr2.2007.12.006

Myklestad, S. M., E. Skanoy, and S. Hestmann. 1997. A sensitive and rapid method for analysis of dissolved mono- and polysaccharides in seawater. Mar. Chem. 56: 279–286.

Le Quéré, C., R. M. Andrew, P. Friedlingstein, and others. 2018. Global Carbon Budget 2018. Earth Syst. Sci. Data 10: 2141–2194. doi:10.5194/essd-10-2141-2018

Robinson, C. 2008. Heterotrophic bacterial respiration, p. 299–334. In D.L. Kirchman [ed.], Microbial Ecology of the Oceans. John Wiley & Sons, Incorporated.

Robinson, C. 2019. Microbial Respiration, the Engine of Ocean Deoxygenation. Front. Mar. Sci. 5: 1–13. doi:10.3389/fmars.2018.00533

V.9 Mapping diazotrophy in the Southern Indian Ocean and Southern Ocean

Principal investigators

On shore: Nicolas CASSAR (Division of Earth and Ocean Sciences, Nicholas School of the Environment, Duke University (USA), Laboratoire des sciences de l'environnement marin, IUEM, Université de Brest-UMR 6539 CNRS/UBO/IRD**,** nicolas.cassar@duke.edu)

On board: Hugo BERTHELOT (Laboratoire des sciences de l'environnement marin, IUEM, Université de Brest-UMR 6539 CNRS/UBO/IRD, hugo.berthelot@gmail.com)

Names of other participants (on shore) : Colomban de Vargas, Sorbonne Université, CNRS - UMR7144, FR Tara GOSEE, station biologique de Roscoff **; Stéphane L'Helguen,** Laboratoire des sciences de l'environnement marin, IUEM, Université de Brest-UMR 6539 CNRS/UBO/IRD**,** Ifremer, Plouzané, France **; Sophie Bonnet,** Aix Marseille Université, CNRS, Université de Toulon, IRD, OSU Pythéas, Mediterranean Institute of Oceanography (MIO), UM 110, 13288, Marseille, France

Abstract

N_2 fixation (or diazotrophy) is the main exogeneous source of nitrogen (N) to the ocean. Most of the sampling effort has been focused in oligotrophic regions where N is limiting. Nevertheless, recent studies report high N_2 fixation rates in mesotrophic waters, in particular in coastal margins and polar regions. Here, we investigated the magnitude N_2 fixation in surface waters of the contrasting oceanic regions sampled during the SWINGS cruise and its relation to net primary production (NPP) and planktonic community structure. For this purpose, we performed stable isotope labelling experiments (^{15}N and ^{13}C) at 46 stations. Planktonic abundances and community structure will be characterized by microscopy, cytometry, DNA metabarcoding and metagenomic/metatranscriptomic. In addition, NPP and N_2 fixation will be measured at the single cell level to measure the contribution of the different plankton groups to the community N_2 fixation and NPP.

V.9.1 Scientific context

Nitrogen (N_2) fixation, conducted by a group of specialized microorganisms called diazotrophs, provides the largest external nitrogen input into the ocean (Gruber and Galloway, 2008; Sohm *et al.*, 2011). Alleviating nitrogen limitation over a large portion of the global surface oceans, N_2 fixation supports new production and net oceanic carbon uptake (Casey *et al.*, 2019). Over geological time scales, N_2 fixation is believed to compensate for nitrogen removal from denitrification and anammox (Deutsch, 2004). The balance between these microbial processes influences oceanic productivity, export of carbon to the deep ocean and ultimately atmospheric CO_2 concentrations (Falkowski, 1997). Therefore, understanding the factors regulating N_2 fixation and diazotrophs is important for evaluating and predicting changes to nitrogen and carbon cycling in the global ocean.

The dominant environmental controls on N_2 fixation rates and diazotrophs in the global ocean remain elusive. Various factors have been proposed as controls, including temperature, phosphorus, iron, nutrient supply ratios, zooplankton grazing and a combination of multiple factors (Sañudo-Wilhelmy *et al.*, 2001; Mills *et al.*, 2004; Moisander *et al.*, 2010; Dutkiewicz *et al.*, 2012; Weber and Deutsch, 2014). Specifically, warm and oligotrophic subtropical waters enriched in iron while depleted in nitrogen are traditionally recognized as hot spots of N_2 fixation performed by diazotrophs belonging to the *Trichodesmium*, *Crocosphaera* and *Richelia* groups (Luo *et al.*, 2014). However, recent investigations revealed new niches for marine diazotrophy including midlatitude continental margins and polar waters (Tang *et al.*, 2019). In these regions, it is postulated that diazotrophy is mostly mediated by small unicellular cyanobacterial (e.g. UCYN-A) and non-cyanobacterial diazotrophs. In the southern sector of the Indian Ocean, the magnitude of N_2 fixation and the diazotrophic community remains uncharacterized. Thus, it is of primary importance to better map this process together with the understanding of the factors controlling it distribution.

V.9.2 Overview of the project and objectives

The overreaching goal of this project is to investigate the distribution of diazotrophs, their activity and their interactions with the planktonic community in surface waters of the contrasting regions crossed during the SWINGS cruise. For this purpose, we combine tools to acquire data in order to: (i) describe and measure the organismal, ultrastructural, and molecular complexity of the most dominant diazotrophs, (ii) assess the genomic and metabolic roles and interactions of the partners, and (iii) quantify the biogeochemical importance of this process in the regions sampled.

V.9.3 Methodology and sampling strategy

Discrete samples were taken from Niskin bottles or from the underway system at 5-10 meter deep. N_2 fixation and NPP were measured in triplicate by stable isotope probing ($^{15}N/^{13}C$). Incubations were performed in polycarbonate bottles amended with bicarbonate $H^{13}CO_3^-$ and $^{15}N_2$ and bottles were placed in on-deck incubators continuously cooled with sea surface water reproducing temperature and light characteristics at the sampling depth. Incubation lasted for 24h. The incubations where terminated by filtration of the particulate matter on GF/F filters for the determination of the rates at the planktonic community level. $^{15}N/^{14}N$ and $^{13}C/^{12}C$ ratios in the particulate matter will be analyzed by an elemental analyzer coupled to an isotope ratio mass spectrometer (EA-IRMS). Samples were collected for determination of the $^{13}C/^{12}C$ ratio in the dissolved inorganic C and $^{15}N/^{14}N$ ratio in dissolved N_2 in 12 ml borosilicate exetainers poisoned with $HgCl_2$. Additional samples were taken for determination of N_2

fixation and NPP rates at the single cell level. For this purpose, incubations were terminated by fixation with paraformaldehyde and gentle filtration on polycarbonate membranes (0.2 µm, 1.0 µm or 8 µm pore size). Planktonic cells will be identified and sorted by electron and light microscopy for the largest cells (>8 µm) and by flow cytometry cell sorting for the smallest cells (<8 µm). $^{13}C/^{12}C$ and $^{15}N/^{14}N$ isotopic ratios of the sorted cells will be analyzed at the single cell level on secondary ion mass spectrometers (nanoSIMS/IMS1280, Cameca, France).

Samples for determination of planktonic diversity and community structure were collected for further identification by microscopy (light, confocal and electron microscopy), cytometry, DNA barcoding (16S, 18S and nifH) and metagenomic/metatranscriptomic. For determination of micro-phytoplankton by light microscopy, samples were collected in 50 mL falcon tubes fixed with acidified Lugol solution. Samples will be analyzed according to the Utermöhl methodology. Additional samples were also collected for High Content Fluorescent Microscopy (eHCFM) to resolve 3D fine scale cellular structure (Colin *et al.*, 2017). For this purpose, large volumes of water (20-50 L) were concentrated on 20 µm mesh size sieve then on 3µm pore size filter resulting in a concentration factor of 100 to 500x. Samples were fixed with paraformaldehyde (1%) and Glutaraldehyde (0.25%) and stored at 4°C. They will be analyzed on a confocal microscope and taxonomic assignation will be made on detected particles by random forest automatic classification. For the determination of nano- and pico-plankton, samples were taken in 2 ml cryovials and fixed with paraformaldehyde. They will be analyzed by cytometry according to Marie et al. (1999). DNA based planktonic composition and diversity will be assessed by metabarcoding using high-throughput sequencing of 16S and 18S genes. Two size fractions were collected at each time point: >3 µm and 0.2-3.0 µm on polycarbonate membrane filter. Additional samples were collected for the quantification of diazotrophs based on the abundance of nifH genes on 0.2 µm pore size polycarbonate membrane. Samples for metagenomic and metatranscriptomic were collected in duplicate on 3µm and 0.2µm pore size polycarbonate membrane and processed within 10 minutes after collection. All DNA/RNA based samples were flash frozen in liquid dinitrogen and conserved at -80°C.

Samples for macronutrients were collected at the stations which were not otherwise sampled for these parameters. Nitrate, ammonium and phosphate samples are stored at -20°C and will be analyzed according to the colorimetric methods described in Raimbault et al. (1990), Chen et al (2015), Holmes et al. (1999) and Strickland and Pearson (1974).

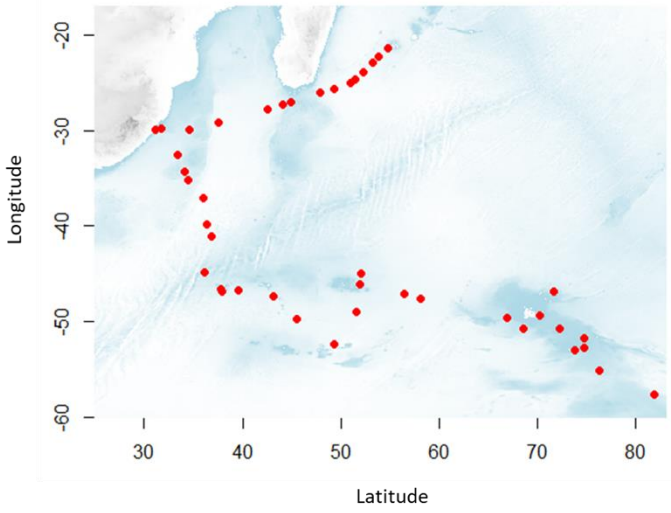

Figure V-8: Location of the stations sampled for investigating diazotrophy

In total 46 stations were sampled (Figure V-8). 46 triplicate samples were collected for PP and/or N_2 fixation, 20 samples for cell sorting and nanoSIMS, 30 samples for light microscopy, 47 samples for DNA metabarcoding, 9 samples for metagenomic and metatranscriptomic and 18 samples for nutrient concentration determination (Table 14).

V.9.4. Preliminary results

Preliminary observations with light and epifluorescent microscopy confirmed the presence of diazotrophs (mostly *Trichodesmium* and *Crocosphaera*) between la Réunion and Durban. In particular, large *Trichodesmium* blooms were spotted on January 16th, with formation of long filaments at the water surface (Fig. 1). After Durban, abundances of *Trichodesmium* and *Crocosphaera* abundances decreased as the ship was steaming South.

V.9.5. Post-cruise sampling analyses and envisioned timeline of working plan, people involved on shore

N_2 fixation and NPP rates and nutrients will be analyzed at LEMAR by Stephane L'Helguen in spring 2021. nifH gene will be analyzed at the MIO by Sophie Bonnet in spring 2021. Microscopy, metabarcoding and metagenomic/metatranscriptomic samples will be analyzed during summer 2021 at Roscoff by Hugo Berthelot and Colomban de Vargas.

References

Casey, J.R., Björkman, K.M., Ferrón, S., and Karl, D.M. (2019) Size dependence of metabolism within marine picoplankton populations. Limnol. Oceanogr. 64: 1819–1827.

Colin, S., Coelho, L.P., Sunagawa, S., Bowler, C., Karsenti, E., Bork, P., et al. (2017) Quantitative 3D-imaging for cell biology and ecology of environmental microbial eukaryotes. Elife 6:.

Deutsch, C. (2004) Isotopic constraints on glacial/interglacial changes in the oceanic nitrogen budget. Global Biogeochem. Cycles 18:.

Dutkiewicz, S., Ward, B. a., Monteiro, F., and Follows, M.J. (2012) Interconnection of nitrogen fixers and iron in the Pacific Ocean: Theory and numerical simulations. Global Biogeochem. Cycles 26: 1–16.

Falkowski, P.G. (1997) Evolution of the nitrogen cycle and its influence on the biological sequestration of CO2 in the ocean. Nature 387: 272–275.

Gruber, N. and Galloway, J.N. (2008) An Earth-system perspective of the global nitrogen cycle. Nature 451: 293–6.

Luo, Y.W., Lima, I.D., Karl, D.M., Deutsch, C.A., and Doney, S.C. (2014) Data-based assessment of environmental controls on global marine nitrogen fixation. Biogeosciences 11: 691–708.

Marie, D., Partensky, F., Vaulot, D., and Brussard, C. (1999) Enumeration of phytoplankton, bacteria and viruses in marine samples. In, Robinson,J.P. (ed), Current Protocols in Cytometry. John Wiley & Sons, pp. 11–15.

Mills, M.M., Ridame, C., Davey, M., La Roche, J., and Geider, R.J. (2004) Iron and phosphorus co-limit nitrogen fixation in the eastern tropical North Atlantic. Nature 429: 292–4.

Moisander, P.H., Beinart, R.A., Hewson, I., White, A.E., Johnson, K.S., Carlson, C.A., et al. (2010) Unicellular cyanobacterial distributions broaden the oceanic N2 fixation domain. Science 327: 1512–4.

Sañudo-Wilhelmy, S. a, Kustka, a B., Gobler, C.J., Hutchins, D. a, Yang, M., Lwiza, K., et al. (2001) Phosphorus limitation of nitrogen fixation by Trichodesmium in the central Atlantic Ocean. Nature 411: 66–9.

Sohm, J.A., Webb, E.A., and Capone, D.G. (2011) Emerging patterns of marine nitrogen fixation. Nat. Rev. Microbiol. 9: 499–508.

Tang, W., Wang, S., Fonseca-Batista, D., Dehairs, F., Gifford, S., Gonzalez, A.G., et al. (2019) Revisiting the distribution of oceanic N 2 fixation and estimating diazotrophic contribution to marine production. Nat. Commun.

Weber, T. and Deutsch, C. (2014) Local versus basin-scale limitation of marine nitrogen fixation. Proc. Natl. Acad. Sci. 111: 8741–6.

Table 14: List of samples collected for investigating diazotrophy along the SWINGS transect

Event #	Date (dd/mm/yy)	Sampling Time (UTC)	longitude	latitude	Cast type	N2fix/NPP	Cytometry	nifH gene	Metabarcoding (16S/18S)	Metagenomic/ Metatranscriptomic	nanoSIMS	eHCFM	Macro nutrient
SWG_Fix_001	13/01/21	06:40	54.85	-21.34	Underway	•	•	•	•				•
SWG_Fix_002	13/01/21	14:20	53.89	-22.25	Underway	•	•	•	•				•
SWG_Fix_003	13/01/21	19:40	53.19	-22.92	Underway	•		•					
SWG_Fix_004	14/01/21	03:00	52.25	-23.82	Underway	•		•					•
SWG_Fix_005	14/01/21	08:00	51.45	-24.58	Underway	•		•					•
SWG_Fix_006	15/01/21	14:00	51.00	-25.00	Underway	•		•					•
SWG_Fix_007	15/01/21	20:00	49.27	-25.58	Underway	•		•	•				•
SWG_Ph_001	15/01/21	06:00	49.73	-25.42	CTD	•	•	•	•	•	•	•	•
SWG_Fix_008	15/01/21	03:00	47.88	-26.04	Underway	•		•					
SWG_Fix_009	16/01/21	09:00	44.87	-27.04	Underway	•		•	•	•	•		•
SWG_Fix_010	16/01/21	15:00	44.12	-27.29	Underway	•		•					•
SWG_Fix_011	16/01/21	21:00	42.51	-27.81	Underway	•		•					•
SWG_Ph_002	17/01/21	12:00	39.99	-28.64	CTD	•	•	•	•	•	•	•	•
SWG_Fix_012	18/01/21	04:10	37.62	-29.19	Underway	•	•	•	•		•		
SWG_Fix_013	18/01/21	16:00	34.55	-29.90	Underway	•		•	•		•		
SWG_Ph_003	19/01/21	12:00	32.80	-30.30	CTD	•	•	•	•	•	•	•	•
SWG_Fix_014	20/01/21	04:10	31.12	-29.87	Underway	•		•	•		•		•
SWG_Fix_015	20/01/21	12:00	31.70	-29.81	ctd	•		•	•				
SWG_Fix_016	21/01/21	21:15	33.44	-32.60	ctd	•	•	•	•		•	•	•
SWG_Fix_017	22/01/21	10:00	34.09	-34.30	Underway	•		•					
SWG_Fix_018	22/01/21	17:10	34.47	-35.22	Underway	•		•	•				•
SWG_Fix_019	23/01/21	11:15	36.02	-37.10	Underway	•		•	•		•		
SWG_Fix_020	25/01/21	13:30	36.39	-39.81	ctd	•	•	•	•	•	•	•	•

SWG_Fix_021	27/01/21	03:00	36.87	-41.04	Underway	•	•	•	•		•		
SWG_Fix_022	29/01/21	03:10	36.17	-44.86	Underway	•		•	•		•	•	•
SWG_Fix_023	31/01/21	17:45	37.94	-46.87	ctd cast 52	•	•	•	•				
SWG_Fix_024	01/02/21	08:00	37.78	-46.60	Underway	•		•	•			•	•
SWG_Fix_025	02/02/21	08:00	39.61	-46.68	Underway	•	•	•	•		•	•	•
SWG_Fix_026	04/02/21	09:00	43.11	-47.31	Underway	•	•	•	•		•		•
SWG_Fix_027	05/02/21	11:35	45.54	-49.72	Underway	•		•	•				
SWG_Fix_028	06/02/21	13:45	49.38	-52.40	Underway	•	•	•	•			•	•
SWG_Fix_029	08/02/21	11:30	51.55	-48.96	Underway	•		•	•				
SWG_Fix_030	09/02/21	11:30	51.89	-46.12	Underway	•	•	•	•			•	•
SWG_Fix_031	10/02/21	09:15	52.00	-45.01	Underway	•		•	•				•
SWG_Fix_032	12/02/21	05:00	56.42	-47.08	Underway	•		•	•			•	•
SWG_Fix_033	12/02/21	18:00	58.12	-47.67	Underway	•		•	•				
SWG_Fix_034	15/02/21	07:00	66.88	-49.63	Underway	•		•	•				
SWG_Fix_035	16/02/21	03:00	68.51	-50.72	Underway	•	•	•	•			•	•
SWG_Fix_036	17/02/21	08:00	74.72	-52.71	Underway	•	•	•	•				
SWG_Fix_037	18/02/21	05:15	73.73	-53.02	Underway	•	•	•	•				
SWG_Fix_038	20/02/21	02:40	76.31	-55.20	Underway	•	•	•	•			•	•
SWG_Fix_039	22/02/21	03:30	81.92	-57.69	Underway	•	•	•	•	•	•	•	•
SWG_Fix_040	26/02/21	16:20	74.72	-51.75	Underway	•	•	•	•				
SWG_Fix_041	27/02/21	05:35	72.30	-50.80	Underway	•	•	•	•				
SWG_Fix_042	28/02/21	08:05	70.21	-49.36	Underway	•	•	•	•				
SWG_Fix_043	01/03/21	10:20	71.69	-46.85	Underway	•	•	•	•				
SWG_Fix_044	02/03/21	Pending			Underway	•	•	•	•	•	•	•	•
SWG_Fix_045	03/03/21	Pending			Underway	•	•	•	•	•	•	•	•
SWG_Fix_046	04/03/21	Pending			Underway	•	•	•	•				

V.10 Short-term phytoplankton photophysiological response to iron addition

Principal investigator
On board: Thomas Ryan-Keogh
SOCCO, CSIR, 15 Lower Hope Road, Rosebank, Cape Town, 7700, South Africa
+27 679 016 532
tjryankeogh@gmail.com

Names of other participants

On board: Heather Forrer (Florida State university), Isobel Turnbull (Plymouth Univ.), Goddard-Dwyer Millie (Liverpool Univ.)

Abstract

Measurements of rapid photo physiological changes (~24 h) following deliberate experimental manipulations avoids potential problems in the interpretation of, for example, the absolute value of F_v/F_m in situ, where any physiological signal will be superimposed over taxonomic variability. As these physiological changes precede resultant changes in biomass accumulation (>24 h), the ability to restrict experimental time when monitoring sensitive changes to the photosynthetic apparatus minimizes the influence of bottle effects on biomass accumulation and the potential confounding influence of shifts in community structure on physiological measurements. Linking these photo physiological responses to the iron pool speciation, i.e., the soluble and colloidal fractions, will begin to enhance our understanding of the bioavailability of iron.

V.10.1 Scientific context

An estimated 40% of photosynthesis on earth occurs in the marine environment and the turnover time for marine plant biomass is nearly three orders of magnitude faster than that of terrestrial biomass (Field et al., 1998). Hence, nutrients that regulate primary production in the ocean have a significant effect on the global carbon cycle and consequently play a key role in regulating climate. In many oceanic regions, primary productivity, species composition, and the trophic structure of planktonic communities is controlled by light and nutrients i.e. N, P, Si (Graziano et al., 1996; Wu et al., 2000; Nelson et al., 2001). However, there is evidence that the availability of the micronutrient Fe plays a critical role in regulating phytoplankton primary productivity and microbial diversity in the major High Nutrient Low Chlorophyll (HNLC) regions of the subarctic and equatorial Pacific (Martin & Fitzwater, 1988; Coale et al., 1996) and Southern Ocean (Boyd et al., 2000). These regions account for 40% of the world's oceans and are replete with nutrients but have low productivity as a result of a limited supply of Fe, intensified by the low solubility of Fe under oxidizing conditions (Ussher et al., 2004). The important role of Fe for microbial organisms is linked to its obligatory requirement in enzymes involved in photosynthesis, respiration, nitrate reduction and nitrogen fixation (Falkowski et al., 1998; Morel & Price 2003; Geider & LaRoche, 1994).

V.10.2 Overview of the project and objectives

Objective 1: Measure the photo physiological response to iron addition upstream and downstream of the sub Antarctic islands along the GS02 transect line.

Objective 2: Link the responses to measurements of dissolved iron, including the speciation between colloidal and soluble fractions.

V.10.3 Methodology and sampling strategy

Incubations of the collected trace metal clean seawater were performed in 500mL and 1L polycarbonate bottles. All bottles used for the incubations were passed through a rigorous cleaning process involving a Decon wash and a soak in 50% HCl for 1 week, followed by rinsing then storage with acidified Milli-Q prior to sailing.

Trace metal clean seawater for the incubations were collected using two methods: 1) a trace metal clean FISH towed alongside the ship, submerged at approximately 2 – 5 m depth and 2) GoFlo bottles from the clean CTD rosette equipped with clean 24 x 12L GoFlo bottles, deployed on a conducting Kevlar cable (General Oceanics, USA) with TMC seawater collected at ~30 m depth. Each of the polycarbonate bottles used for the incubations were rinsed three times and filled for triplicate control and triplicate $FeCl_3$-spiked samples, to a concentration of 2.0 nM. Each bottle top was sealed with Parafilm, and placed inside an on-deck incubator, with flowing seawater, shaded with blue screen to a 55% light level. All incubations were terminated and subsamples after approximately 24 hours.

Prior to the commencement of each incubation, samples were collected for the initial conditions including chlorophyll-a concentrations, nutrients and photophysiology. After each 24-hour experiment was terminated samples were collected for chlorophyll-a concentrations and photophysiology. Between 250-500 mL were filtered for chlorophyll-a concentrations onto 25mm Whatman (Glass Fibre Filter) GF/F filter (nominal pore size 0.7 µm), extracted into 90% acetone, stored at -20°C and read on a Turner Trilogy Fluorometer after 24 hours. Samples for photophysiology were performed using Fast Repetition Rate fluorometry (FRRf) run on a Chelsea Scientific Instruments FastOcean™ FRRf incorporating a FastAct™ laboratory system for each sample, along with a blank correction (carefully prepared using syringe filtering of the sample through a 0.2 µm syringe filter) for determining the photochemical efficiency (F_v/F_m) of the phytoplankton.

Bottle filling and all manipulation steps including spiking and sub-sampling were performed within the dedicated Class-100 filtered air and under clean laminar flow, inside a trace metal clean certified container. A complete list of sampling locations and relevant information is provided in Table 15 below. The FRRf data was analyzed with the "Phytoplankton Photophysiology Utilities" package in Python.

Table 15: Exhaustive list of measured parameters dedicated to the understanding of the photo physiological response of the phytoplankton to iron addition.

Parameter	Code of operation (Station-cast)	Number of samples
1. FRRf	FISH/Clean CTD	33 Experiments
2. Chlorophyll-a	FISH/Clean CTD	
3. Nutrients	FISH	

V.10.4 Preliminary results

There is a high degree of variability in the results that will need to undergo quality control before further analysis with ancillary information such as dFe concentrations. For now, the first version of the results is presented in the map below showing areas with potentially higher iron limitation found upstream of the islands and areas with none to low iron limitation downstream of the islands (Figure 5-9).

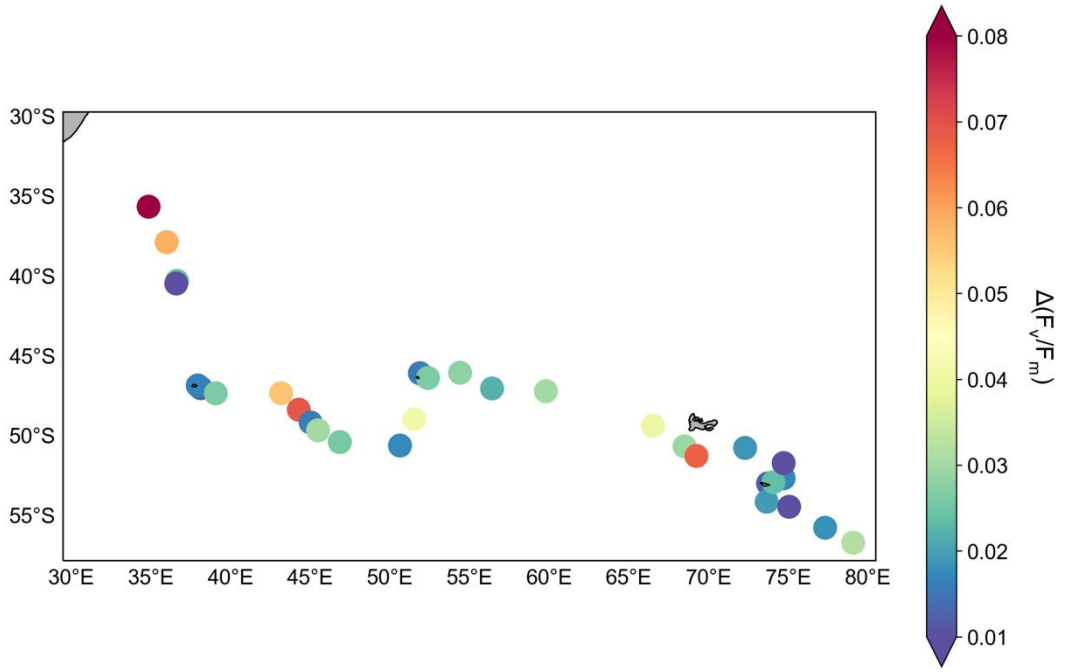

Figure V-9: Iron addition incubation experiment results from SWINGS GS02.

V.10.5 Post-cruise sampling analyses and envisioned timeline of working plan, people involved on shore

All FRRf data is analyzed on board, with quality control applied at time of analysis. The chlorophyll data will be updated following the post cruise calibration of the fluorometer (within ~1-2 months). Nutrient samples will be analyzed within 3 months of the end of the cruise. Further analysis of the data will begin once additional parameter data is available, i.e. dFe, sFe and community structure.

References

Boyd, P.W.; Watson, A.J.; Law, C.S.; et al. Nature 2000, 407, 695-702.
Coale, K.H.; Johnson, K.S.; Fitzwater, S.E.; et al. Nature 1996, 383, 495-501.
Falkowski, P.G.; Barber, R.T.; Smetacek, V. Science 1998, 281, 200-206.
Field, C.B.; Behrenfeld, M.J.; Randerson, J.T.; Falkowski, P. Science 1998, 281, 237-240.
Geider, R.J.; LaRoche, J. Photosynth. Res. 1994, 39, 275-301
Graziano, L.M.; Geider, R.J.; Li, W.K. W.; Olaizola,M. Aquat. Microb. Ecol. 1996, 11, 53-64.
Martin, J.H.; Fitzwater, S. E. Nature 1988, 331, 341-343.
Morel, F.M.M.; Price, N.M. Science 2003, 300, 944-947.
Nelson, D.M.; Brzezinski, M.A.; Sigmon, D.E.; Franck, V.M. Deep-Sea Res. Part II 2001, 48, 3973-3995.
Ussher, S.J.; Achterberg, E.P.; Worsfold, P.J. Env. Chem. 2004, 1, 67-80.
Wu, J.F.; Sunda, W.; Boyle, E.A.; Karl, D.M. Science 2000, 289, 759-762.

V.11Investigating the bioavailability of dissolved iron along the South West Indian Geotraces Section

Principal investigators
On shore: Angela Milne
Davy Building, University of Plymouth, Plymouth, Devon, PL4 8AA
+447779667080
angela.milne@plymouth.ac.uk

On board: Isobel Grace Turnbull
Davy Building, University of Plymouth, Plymouth, Devon, PL4 8AA
+447594959190
isobel.turnbull@plymouth.ac.uk

Names of other participants

Angela Milne, University of Plymouth, UK; Simon Ussher, University of Plymouth, UK; Joanna Dixon, Plymouth Marine Laboratory, UK; Martha Gledhill, GEOMAR, Kiel, Germany ; Hannah Whitby, University of Liverpool, UK; Maite Maldonado, University of British Columbia, Canada ; Millie Goddard-Dwyer, University of Liverpool, University of Southampton, UK ; Ingrid Obernosterer, LOMIC, Banyuls sur mer, France; Marion Fourquez, LOMIC, Banyuls sur mer, France; Stephane Blain, LOMIC, Banyuls sur mer, France; Thomas James Ryan-Keogh, Southern Ocean Carbon and Climate Observatory (SOCCO) CSIR, South Africa ; Hélène Planquette, LEMAR, Brest, France; Heather Forrer, Florida State University, University of Cape Town, South Africa ; Claire Evans, National Oceanography Centre Southampton (NOCS), UK; David Gonzalez- Santana, LEMAR, Brest, France

Abstract

Iron (Fe) in the oceans is maintained in the dissolved phase (dFe) through complexation by organic ligands. Since phytoplankton and other microbes primarily acquire iron from the dissolved phase, these ligands exert significant control over how available iron is for growth, so-called 'bioavailability'. Understanding the bioavailability of dFe is of paramount importance in understanding the efficiency of the biological carbon pump in regions where iron limits primary production, such as the Southern Ocean. Here, we investigate the bioavailability of iron to both bacteria and phytoplankton along the South West Indian Geotraces Section. Characterization of siderophores (ligands actively produced by marine bacteria during iron stress as a specific iron uptake strategy) in the water column, as well as those produced during incubation experiments will give insights into the bioavailability of dFe to bacteria. Water was also collected to conduct dFe uptake experiments with Fe-limited phytoplankton cultures back on shore, to obtain an uptake rate constant. This will be compared to *in-situ* speciation parameters such as concentrations of humic substances and ligands, allowing assessment of how bioavailable the dissolved pool is to phytoplankton. Together, these measurements will enable a deeper understanding of how iron speciation and uptake interact to control bioavailability.

V.11.1 Scientific context

The oceans are responsible for the uptake of ~25-30% of anthropogenically produced carbon dioxide (Sabine et al., 2004), ~40% of which occurs in the Southern Ocean (Frölicher et al., 2015). A portion of this uptake is carried out by phytoplankton photosynthesizing in the ocean surface, converting carbon dioxide into organic matter. This organic matter then sinks out of the surface, transporting carbon to be stored in the deep ocean, known as the 'biological carbon pump'. The efficiency of this pump in the Southern Ocean is limited by sub nanomolar concentrations of dissolved iron (dFe) (Boyd et al., 2007) needed by phytoplankton for multiple cellular processes (Geider and La Roche, 1994). Exceptions to this are regions surrounding sub Antarctic Islands, such as Crozet Island, Kerguelen Island and Heard Island, where iron supply from land masses and sediments fuels annual phytoplankton blooms (Blain et al., 2001). Understanding mechanisms which impact the supply and availability of dFe in the Southern Ocean are crucial in predicting changes to the future of the Earth system under future climate change scenarios. The majority of dFe in the oceans is complexed by organic compounds which act as iron-binding ligands (Gledhill and Buck, 2012), maintaining iron in the dissolved phase by preventing scavenging onto particles. The exact origin and identity of the total ligand pool (L) is still poorly understood, though it is known to consist of siderophores (compounds actively produced by marine bacteria during iron stress as a specific iron uptake strategy), saccharides, humic acids and other cellular breakdown products (Gledhill and Buck, 2012). Since phytoplankton and other microbes acquire iron from the dissolved phase (Shaked et al., 2005) L exerts control on how much iron is available for microbial growth, or how 'bioavailable' it is (Shaked and Lis, 2012, Lis et al., 2015). The impact of specific model ligands to phytoplankton growth has been examined through use of the radiotracer ^{55}Fe to obtain iron uptake rates in both phytoplankton cultures (Chen and Wang, 2008, Hassler and Schoemann, 2009, Strzepek et al., 2011) and natural seawater communities (Hassler et al., 2011, Hutchins et al., 1999, Maldonado et al., 1999, Maldonado et al., 2001, Maldonado et al., 2005). A synthesis of these studies demonstrated that the model siderophore desferrioxamine B is the least available ligand-iron complex to phytoplankton, whereas free inorganic iron is the most accessible, with other ligands investigated (e.g. saccharides, humic acids) falling between these two extremes (Lis et al., 2015). This 'bioavailability envelope' provided a framework to investigate the relative bioavailability of different dFe substrates to phytoplankton. However, due to a lack of understanding of the relative contribution of each model ligand to the total *in-situ* ligand pool, it remains difficult to extrapolate these findings to define the bioavailability of dFe in natural seawater.

V.11.2 Overview of the project and objectives

This project aims to examine the bioavailability of dissolved iron to both bacteria and phytoplankton along the South West Indian Geotraces Section, using two different approaches. The first is through characterization of the types of siderophores which may be produced by the in situ bacterial community, which will inform about bacterial iron stress and also may form part of the dissolved iron-binding ligand pool, impacting on bioavailability of iron to phytoplankton. Samples were taken from the water column for analysis of siderophores which may be part of the dissolved ligand pool as well as in the particle attached fraction. Additionally, incubation experiments were conducted to try to stimulate siderophore production by surface bacteria.

The second approach is through collection of filtered seawater, to conduct short term dFe-uptake experiments back on shore using the radiotracer ^{55}Fe to and Fe-limited phytoplankton cultures examine the bioavailability of dFe to phytoplankton (Shaked et al., 2020).

Finally, a remineralization particle experiment was conducted to examine the speciation and bioavailability of iron released during particle remineralization in collaboration with Millie Goddard-Dwyer (see section 95).

Objective 1: Characterize siderophores which are present in the water column using HPLC-MS/ICP-MS.

Objective 2: Characterize siderophores produced by the bacterial community in incubation experiments after the addition of glucose using HPLC-MS/ICP-MS.

Objective 3: Characterize siderophores produced by the bacterial community in incubation experiments after the addition of Fe to stimulate a phytoplankton bloom.

Objective 4: Conduct short term dFe-uptake experiments using dFe-limited phytoplankton cultures and the radiotracer ^{55}Fe, to calculate a surface-area normalized dFe-uptake rate for each water sample to use as a proxy for the bioavailability of iron in that sample.

Objective 5: Determine the speciation and bioavailability of dissolved iron released during particle remineralization.

V.11.3 Methodology and sampling strategy

Objective 1: Characterize siderophores which are present in the water column using HPLC-MS/ICP-MS

~2L of seawater from 3-5 depths was collected from GoFlo bottles deployed on a trace-metal free CTD rosette, into HDPE bottles. This was then sequentially vacuum filtered over a 0.22µm Sterivex PVDF membrane filter (Merck Millipore), connected to a 1g 6ml Bond Elut Env+ solid phase extraction (SPE) cartridge (Agilent Technologies) precleaned with 15ml LC-MS grade methanol, followed by 15ml 0.1M HCl and 15ml ultra high purity water. The particulate filters were frozen at -80 ˚C and SPE cartridge at -20 ˚C until on shore analysis (see section V.II.4).

Objective 2: characterize siderophores produced by the bacterial community in incubation experiments after the addition of glucose using HPLC-MS/ICP-MS

Unfiltered seawater was collected into 12 x 2L trace metal clean polycarbonate bottles, either from the GoFlo bottles deployed on a trace-metal free CTD rosette, or from the trace metal free towed-fish. 12 bottles had 100µM glucose added and 12 were left unamended as controls. 6 were then incubated at in situ ambient temperature in the dark in a temperature-controlled room (~4˚C) for two weeks, and 6 were kept at room temperature (~15˚C) for 5 days. This was to investigate the effect of both increasing temperature and alleviating carbon limitation on bacterial metabolites and production of siderophores. 2 experiments were carried out, one before Crozet Island (station 33) 'Bac exp 1' and the second in the iron fertilized plume downstream of the island. Experiments were subsampled for parameters displayed in Figure V-10**.** Bacterial respiration was measured on board by Dr. Fourquez (see Fourquez cruise report),

all other parameters will be analyzed on shore. DFe was filtered over a 0.2µM polyethylene sulfate (PES) membrane using an in-line filtration system into clean 60ml bottles to be analyzed by David Gonzalez-Santana. Bacterial abundance was subsampled for flow cytometry by fixing 1.96ml of sample with glutaraldehyde (final concentration 0.5%) for 30 mins before flash freezing and storage at -80 ˚C. Bioorthogonal non-canonical amino acid tagging (BONCAT) phase 1, the incubation step (Leizeaga et al., 2017) was carried out on board with the remainder of the analysis being carried out at National Oceanography Centre Southampton. Briefly, at each bac exp timepoint where BONCAT was conducted, L-Homopropargylglycine was added to 15ml of subsample to a final concentration of 1µM. This was incubated for 12h in the dark at the same temperature the incubation was conducted at. 5mL of the sample was then fixed with glutaraldehyde (final concentration 0.5% ([v/v]) for 30 mins at 4˚C before flash freezing and storage at -80˚C. The remaining volume was gently filtered over a 0.2µM polycarbonate filter, which was placed on top of a GF/F filter that had been soaked in 0.5% glutaraldehyde, left to fix at 4˚C overnight before storage at -80˚C. This method allows identification of the abundance of translationally active bacterial cells through use of flow cytometry and CARD-FISH (see Fourquez cruise report) (Leizeaga et al., 2017) and will be conducted at NOCS in collaboration with Millie Goddard-Dwyer. At Tfinal, 500ml from each replicate incubation bottle was filtered over a 0.2µM polycarbonate filter, and frozen at -80˚C for on shore analysis of bacterial community composition (see Obernosterer cruise report). The remaining volume from the incubation bottles was filtered as in Objective 1 for siderophores.

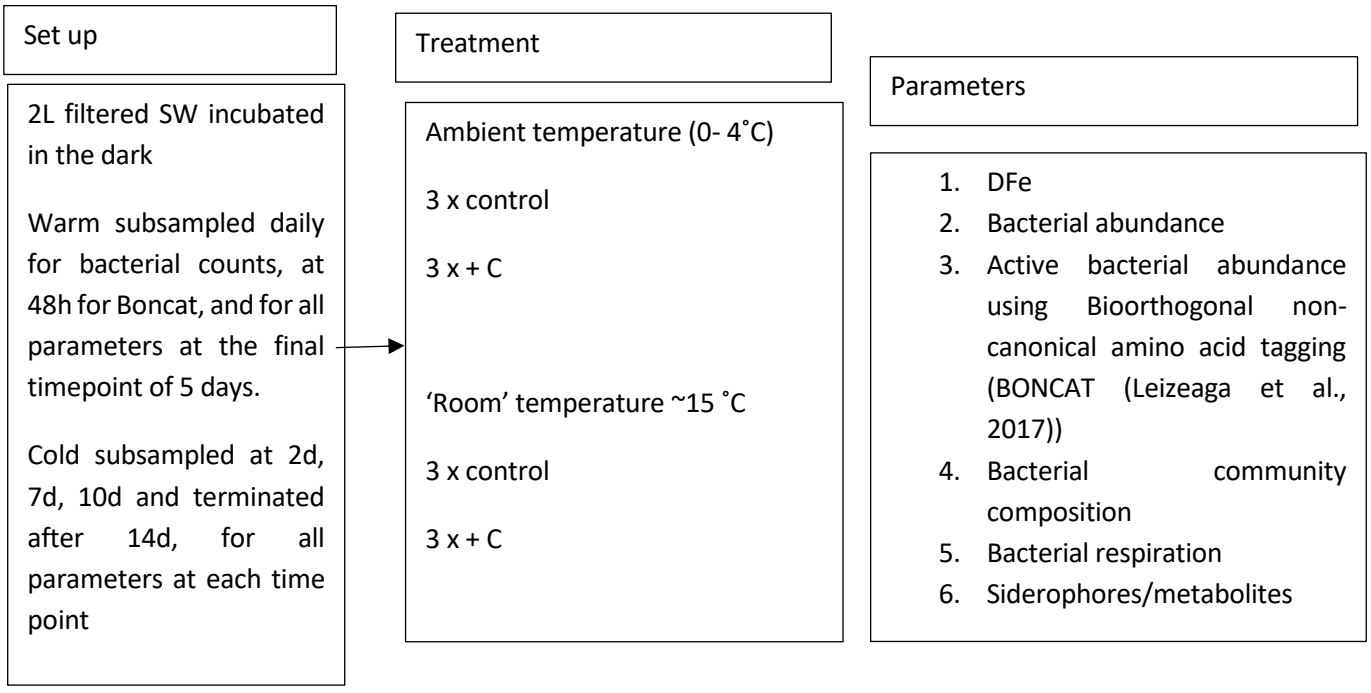

Figure V-10: experimental set up and parameters measured for bacterial experiments carried out on SWINGS cruise.

Objective 3: characterize siderophores produced by the bacterial community in incubation experiments after the addition of Fe to stimulate a phytoplankton bloom

Unfiltered seawater was collected into 6 x 4L trace metal clean polycarbonate bottles, either from the GoFlo bottles deployed on a trace-metal free CTD rosette, or from the trace metal free towed-fish. 3 bottles had FeCl added to a final concentration of 2nm, 3 bottles had no amendments to act as controls.

The bottles were then place in on deck incubators for 15 days. This experiment was to investigate the question: Does production of labile dissolved organic matter from phytoplankton blooms in the Southern Indian Ocean stimulate siderophore production through alleviation of bacterial carbon limitation? 3 experiments were carried out, Fe exp 1 upstream of Marion island after fish 31 before station 18, Fe exp 2 upstream of Crozet island after Fish 53 before station 33 and Fe exp 3 set up at station 33 from clean cast 85 (Table 16). Experiments were subsampled for parameters displayed in Figure V-11. Subsamples for chlorophyll (250ml) and Fv/Fm (50ml) were measured on board by Dr. Ryan-Keogh (see Ryan-Keogh cruise report), all other parameters are to be measured back on shore. DFe, bacterial abundance and bacterial community composition were subsampled for as above. 50ml of subsample was filtered over a 0.2µM PES membrane filter into a centrifuge tube for macronutrients to be analysed by Stephane Blain (see Blain cruise report). Humic ligands were filtered as for dFe (see above), and the remaining incubation volume was filtered as above for siderophores/metabolites.

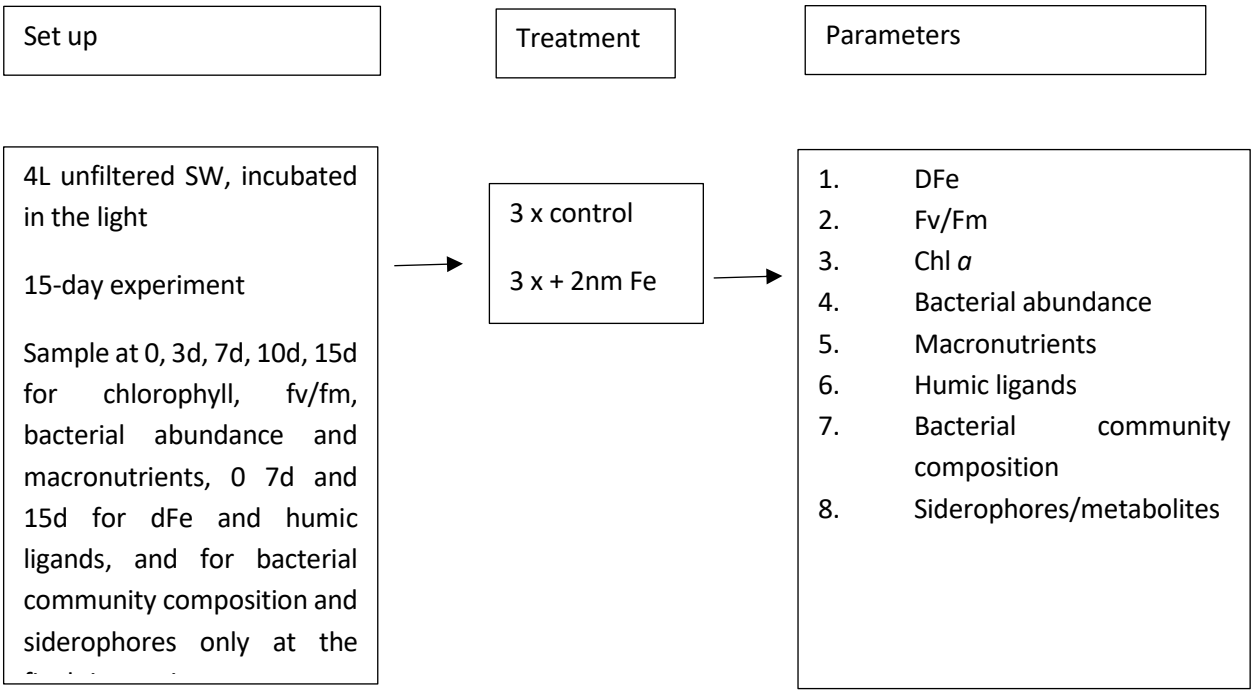

Figure V-11: Experimental set up and parameters measured for iron addition experiments carried out on SWINGS cruise.

Objective 4: Conduct short term dFe-uptake experiments using dFe-limited phytoplankton cultures and the radiotracer ^{55}Fe, to calculate a surface-area normalised dFe-uptake rate for each water sample to use as a proxy for the bioavailability of iron in that sample

Duplicate or triplicate 125ml seawater samples were collected from 12L GoFlo bottles deployed on a trace-metal free CTD. Samples were filtered through a 0.45µM PES filter from (see trace-metal sampling cruise report) into fluorinated high-density polyethylene (FPE) bottles and frozen at -20˚C. Between 3 and 5 depths were chosen at each station dependent on the depth of the site, targeting one depth within the mixed layer, the base of the mixed layer, and 2-3 in the mesopelagic layer. This water will be used to conduct short term iron uptake experiments using iron limited phytoplankton cultures and the radionuclide ^{55}Fe back on shore.

Objective 5: Determine the speciation and bioavailability of iron released during particle remineralization.

Trace-metal clean seawater was collected from GoFlo bottles deployed on a trace-metal free CTD rosette. 36L was filtered through a 0.45µM PES filter, 24L of this filtrate was kept for the incubations in acid washed polycarbonate carboys. The particles collected on the filters were resuspended in filtered seawater, and this suspension added to 12L as the particle addition treatment. The other 12L filtrate was left unamended as a negative control. Each of the treatments were then divided into 3 x 4L polycarbonate bottles and incubated for 3 days in the dark in a temperature-controlled room (~4˚C). Parameters were subsampled for at T0 and when the experiment was terminated. Parameters subsampled for: dFe, humic ligands, ligand classes, siderophores, macronutrients, dissolved organic carbon (DOC) (see Blain cruise report), dissolved organic matter (DOM) (see Goddard-Dwyer cruise report), bacterial community composition, bacterial respiration, BONCAT, ammonium, bacterial abundance, water for Fe uptake, dissolved trace metals dTM. Particulate Fe for the start of the experiment will also be determined by Dr. Planquette, however due to limited sample volume this was not able for the end of the experiment. All parameters were subsampled for as above.

V.11.4 Post-cruise sampling analyses and envisioned timeline of working plan.

Siderophore analysis:

Back on shore, particulate samples will be analysed using a targeted metabolomics liquid chromatography-mass spectrometry (HPLC-MS) method adapted by Dr. Martha Gledhill from (Kido Soule et al., 2015). As well as siderophores produced by particle attached bacteria, other intracellular metabolites such as B vitamins are included in the analysis. The dissolved phase is analysed using high performance liquid chromatography coupled to inductively-coupled mass spectrometry (Boiteau and Repeta, 2015). The chemical structure of the siderophore as well as the concentration of iron bound to the ligand will be determined this way. This analysis will take place at GEOMAR, Kiel, Germany, in collaboration with Martha Gledhill.

Parameters subsampled from experiments:

DFe and dTM is to be analysed using SF-ICP-MS at LEMAR. Bacterial abundance will be measured by flow cytometry at NOCS by Millie Goddard-Dwyer (see Goddard-Dwyer cruise report) and bacterial community composition through analysis of 16S gene amplicon sequencing by Ingrid Obernosterer (See Obernosterer cruise report). Bacterial respiration was measured on board by Marion Fourquez (See Fourquez cruise report)

Determination of electroactive humic substances and ligand classes will be carried out by Dr. Hannah Whitby and Millie Goddard Dwyer using catalytic cathodic stripping voltammetry at University of Liverpool (see Goddard-Dwyer cruise report, Sukekava et al., 2018). Macronutrients (silicate, nitrate, phosphate) concentrations will be analysed by Dr. Stephane Blain at LOMIC (see Blain cruise report). The second phase of BONCAT analysis is to be carried out using a method adapted by Dr. Fourqez in collaboration with Millie Goddard-Dwyer at NOCS (see Fourquez cruise report). Dissolved organic carbon analysis is to be carried out by Dr. Stephane Blain at LOMIC (see Blain cruise report),and dissolved organic matter by Millie Goddard-Dwyer and Dr. Claire Evans (see Goddard-Dwyer cruise report). Analysis for ammonium is to be carried out by Heather Forrer (see Forrer cruise report).

Table 16: investigated parameters for the bioavailability of iron

Parameter	Code of operation (Station-cast)	Number of samples
1. Siderophores	SWG_14_41 c	5
	SWG_21_58 c	5
	SWG_33_87 c	5
2. Iron uptake water	SWG_14_41 c	6
	SWG_21_58 c	15
	SWG_33_87 c	15
	SWG_46_125 c	6
	SWG_48_134 c	15
	SWG_58_144 c	15
	SWG_65_159 c	15
	SWG_66_163 c	15
	SWG_67_167 c	15
	SWG_68_169 c	15
Parameters subsampled from experiments		
3. Chlorophyll	Fe Exp 1 set up using FISH, after FISH 31 before station 18 Fe exp 2 set up after FISH 53 before station 33 Fe exp 3 set up station 33_85 c	75
4. Fv/Fm	Fe Exp 1 set up using FISH, after FISH 31 before station 18 Fe exp 2 set up after FISH 53 before station 33 Fe exp 3 set up station 33_85 c	75
5. Nutrients	Fe Exp 1 set up using FISH, after FISH 31 before station 18 Fe exp 2 set up after FISH 53 before station 33 Fe exp 3 set up station 33_85 c	75
6. Flow cytometry	Fe Exp 1 set up using FISH, after FISH 31 before station 18 Fe exp 2 set up after FISH 53 before station 33 Fe exp 3 set up station 33_85 c Bac exp 1 set up after FISH 53 before station 33 Bac exp 2 set up station 33_85 and cast 87 c	185
7. Dissolved iron	Fe Exp 1 set up using FISH, after FISH 31 before station 18 Exp 2 Fe exp 2 set up after FISH 53 before station 33 Fe exp 3 set up station 33_85 c Bac exp 1 set up after FISH 53 before station 33 Bac exp 2 set up station 33_85 and cast 87 c	84
8. Humic ligands	Fe Exp 1 set up using FISH, after FISH 31 before station 18 Exp 2 Fe exp 2 set up after FISH 53 before station 33	45

Iron bioavailability:

Bioavailability of dissolved iron to phytoplankton will be assessed using a recent approach developed at the University of British Columbia (Shaked et al., 2020). Briefly, 125ml water samples will be thawed and spiked with ^{55}Fe 24h prior to uptake experiments to allow sufficient time for equilibration with the ambient organic ligands. Fe-limited cultured phytoplankton species are then resuspended into the ^{55}Fe spiked water sample and incubated for 4-6h. The ^{55}Fe activity accumulated by the cells will be measured

in a scintillation counter (Beckman-Coulter LS 6500; Beckman Counter Inc.) using Ecolite + scintillation cocktail (Fisher). Fe uptake rates (mol Fe $cell^{-1}$ d^{-1}) will be calculated from the linear regression of the accumulated cellular Fe as a function of incubation time, and will be converted to per cell uptake rates constants ($k_{in\text{-}app}$) based on the measured dFe in the sample (ambient+ added ^{55}Fe) and cell numbers, before normalizing to the cell-surface area, yielding the measure of dFe availability—$k_{in\text{-}app/S.A.}$ This will then be compared to the in-situ dFe speciation parameters, such as the stability constants and concentrations of naturally occurring organic Fe ligand classes, as well as the siderophore type/concentrations and concentration of humic ligands measured by collaborators in Liverpool. These findings will help us establish how iron speciation controls Fe bioavailability.

V.11.5 Envisioned timeline

HPLC and MS/ICP-MS analyses will be performed before the end of Summer 2021, while ^{55}Fe uptake experiments outcomes will be investigated in the second half of 2021.

References

BLAIN, S., TRÉGUER, P., BELVISO, S., BUCCIARELLI, E., DENIS, M., DESABRE, S., FIALA, M., JÉZÉQUEL, V. M., LE FÈVRE, J. & MAYZAUD, P. 2001. A biogeochemical study of the island mass effect in the context of the iron hypothesis: Kerguelen Islands, Southern Ocean. Deep Sea Research Part I: Oceanographic Research Papers, 48, 163-187.

BOITEAU, R. M. & REPETA, D. J. 2015. An extended siderophore suite from Synechococcus sp. PCC 7002 revealed by LC-ICPMS-ESIMS. Metallomics, 7, 877-884.

BOYD, P. W., JICKELLS, T., LAW, C., BLAIN, S., BOYLE, E., BUESSELER, K., COALE, K., CULLEN, J., DE BAAR, H. J. & FOLLOWS, M. 2007. Mesoscale iron enrichment experiments 1993-2005: synthesis and future directions. science, 315, 612-617.

CHEN, M. & WANG, W.-X. 2008. Accelerated uptake by phytoplankton of iron bound to humic acids. Aquatic Biology, 3, 155-166.

FRÖLICHER, T. L., SARMIENTO, J. L., PAYNTER, D. J., DUNNE, J. P., KRASTING, J. P. & WINTON, M. 2015. Dominance of the Southern Ocean in anthropogenic carbon and heat uptake in CMIP5 models. Journal of Climate, 28, 862-886.

GEIDER, R. J. & LA ROCHE, J. 1994. The role of iron in phytoplankton photosynthesis, and the potential for iron-limitation of primary productivity in the sea. Photosynthesis research, 39, 275-301.

GLEDHILL, M. & BUCK, K. N. 2012. The organic complexation of iron in the marine environment: a review. Frontiers in microbiology, 3, 69.

HASSLER, C. & SCHOEMANN, V. 2009. Bioavailability of organically bound Fe to model phytoplankton of the Southern Ocean. Biogeosciences, 6, 2281-2296.

HASSLER, C. S., SCHOEMANN, V., NICHOLS, C. M., BUTLER, E. C. & BOYD, P. W. 2011. Saccharides enhance iron bioavailability to Southern Ocean phytoplankton. Proceedings of the National Academy of Sciences, 108, 1076-1081.

HUTCHINS, D. A., WITTER, A. E., BUTLER, A. & LUTHER, G. W. 1999. Competition among marine phytoplankton for different chelated iron species. Nature, 400, 858-861.

KIDO SOULE, M. C., LONGNECKER, K., JOHNSON, W. M. & KUJAWINSKI, E. B. 2015. Environmental metabolomics: Analytical strategies. Marine Chemistry, 177, 374-387.

LEIZEAGA, A., ESTRANY, M., FORN, I. & SEBASTIÁN, M. 2017. Using click-chemistry for visualizing in situ changes of translational activity in planktonic marine bacteria. Frontiers in microbiology, 8, 2360.

LIS, H., SHAKED, Y., KRANZLER, C., KEREN, N. & MOREL, F. M. 2015. Iron bioavailability to phytoplankton: an empirical approach. The ISME journal, 9, 1003-1013.

MALDONADO, M. T., BOYD, P. W., HARRISON, P. J. & PRICE, N. M. 1999. Co-limitation of phytoplankton growth by light and Fe during winter in the NE subarctic Pacific Ocean. Deep Sea Research Part II: Topical Studies in Oceanography, 46, 2475-2485.

MALDONADO, M. T., BOYD, P. W., LAROCHE, J., STRZEPEK, R., WAITE, A., BOWIE, A. R., CROOT, P. L., FREW, R. D. & PRICE, N. M. 2001. Iron uptake and physiological response of phytoplankton during a mesoscale Southern Ocean iron enrichment. Limnology and oceanography, 46, 1802-1808.

MALDONADO, M. T., STRZEPEK, R. F., SANDER, S. & BOYD, P. W. 2005. Acquisition of iron bound to strong organic complexes, with different Fe binding groups and photochemical reactivities, by plankton communities in Fe-limited subantarctic waters. Global Biogeochemical Cycles, 19.

SABINE, C. L., FEELY, R. A., GRUBER, N., KEY, R. M., LEE, K., BULLISTER, J. L., WANNINKHOF, R., WONG, C., WALLACE, D. W. & TILBROOK, B. 2004. The oceanic sink for anthropogenic CO2. science, 305, 367-371.

SHAKED, Y., BUCK, K. N., MELLETT, T. & MALDONADO, M. T. 2020. Insights into the bioavailability of oceanic dissolved Fe from phytoplankton uptake kinetics. The ISME Journal, 14, 1182-1193.

SHAKED, Y., KUSTKA, A. B. & MOREL, F. M. 2005. A general kinetic model for iron acquisition by eukaryotic phytoplankton. Limnology and Oceanography, 50, 872-882.

SHAKED, Y. & LIS, H. 2012. Disassembling iron availability to phytoplankton. Frontiers in Microbiology, 3, 123.

STRZEPEK, R. F., MALDONADO, M. T., HUNTER, K. A., FREW, R. D. & BOYD, P. W. 2011. Adaptive strategies by Southern Ocean phytoplankton to lessen iron limitation: Uptake of organically complexed iron and reduced cellular iron requirements. Limnology and Oceanography, 56, 1983-2002.

V.12 Iron binding ligand cycling during dissolved organic matter processing by bacterioplankton in the Southern Ocean

On shore: Principal investigator
Hannah Whitby
University of Liverpool
+44 (0)151 795 1353
Hannah.Whitby@liverpool.ac.uk
On board: Millie Goddard-Dwyer (University of Liverpool, UK), Ingrid Obernosterer (LOMIC, Banyuls-sur-mer, France), Stephane Blain (LOMIC, Banyuls-sur-mer, France), Audrey Gueneugues (LOMIC, Banyuls-sur-mer, France), Heather Forrer (Florida State University, FL, USA), Hélène Planquette (LEMAR, Brest, France), David Gonzalez-Santana (LEMAR, Brest, France), Marion Fourquez (LOMIC, Banyuls-sur-mer, France), Izzy Turnbull (University of Plymouth, UK), Corentin Baudet (LEMAR, Brest, France), Wen-Hsuan Liao (LEMAR, Brest, France)

Abstract:

Iron binding ligands (FeL) play a key role in regulating the bioavailability of iron to micro-organisms, however very little is known about the cycling of these organic molecules. We aim to decipher FeL and humic ligand cycling during dissolved organic matter (DOM) processing by bacterioplankton in the Southern Ocean. More specifically, how does DOM composition and biogeochemical setting, i.e. low iron high nitrate low chlorophyll site v. island mass fertilized high iron site, mediate FeL cycling? These data will give insights into bacterial iron cycling and how this affects primary production in the Southern Ocean.

V.12.1 Scientific context

Primary production in the Southern Ocean plays a key role in regulating global climate via carbon fixation and subsequent storage (Sabine et al. 2004). However, primary production in the Southern Ocean is largely limited by the supply and bioavailability of iron - an essential micronutrient. The amount of iron in seawater is regulated by organic molecules called ligands (FeL; Gledhill and van den Berg, 1994), which control how much iron can be taken up by microorganisms. The FeL pool is comprised of a complex suite of organic molecules including siderophores, humic ligands, and exopolymeric substances (Gledhill and Buck, 2012). Due to this molecular diversity, with each group of ligands presenting distinct production and degradation pathways, biogeochemical cycling of the FeL pool as a whole is unresolved. In particular, the cycling of humic ligands is poorly known, although they are thought to be produced by microbial degradation of organic matter. Recent work has shown microbial remineralization of particulate organic matter to be key production pathway of humic ligands (Bressac et al. 2019; Whitby et al. 2020). However, little is known of ligand pool cycling within the dissolved organic matter (DOM) pool, of which ligands are themselves a part of. Without this knowledge, the potential for change in the concentration and composition of the FeL pool and the resultant impact on primary productivity through changes in iron

bioavailability are unknown. When considering the key role of this poorly defined pool in supporting carbon storage in the Southern Ocean, process-based understanding of FeL cycling is essential to understand and predict future climate change.

V.12.2 Overview of the project and objectives

This project aims to investigate the cycling of the FeL pool by bacterioplankton during DOM processing within the Sub-Antarctic zone of the Southern Ocean. In particular, we will probe the influence of DOM composition and biogeochemical setting. This experiment will dissect the links between iron speciation, dissolved organic matter composition, bacterioplankton community composition and metabolic activity.

Objective 1: Determine FeL cycling during DOM processing by bacterioplankton.

To decipher the influence of DOM composition on FeL pool cycling during DOM processing by bacterioplankton, DOM was harvested from different depths (deep, mesopelagic, and surface) within the Southern Ocean and were incubated with a surface bacterioplankton community from a low iron high nitrate (HNLC) site. To probe the role of biogeochemical setting on FeL pool cycling, an additional treatment comprising of surface DOM harvested from a phytoplankton bloom at a high iron island mass fertilized site (Crozet islands) was incubated with the surface bacterioplankton community from the same site. Comparison of FeL cycling between the HNLC surface DOM incubation with the island mass fertilized surface DOM incubation will probe the role of the island mass effect (IME) in mediating FeL cycling via changes in bacterioplankton carbon processing.

V.12.3 Methodology and sampling strategy

Sampling and experimental set-up.

Sampling was conducted around Crozet Island. Upstream of Crozet, filtered (Acropak 0.2 µm capsule filter) water samples were collected at 2500 m and 700 m depth using Go-Flo's on a TM clean rosette and at 30 m depth downstream of Crozet (Station 25) and from upstream of Crozet at 5 m depth using a TM-clean TOWFISH (47˚24.821'S, 43˚13.490'E) (Table 17). These water samples are hereafter termed the 'deep-', 'mesopelagic-', 'surface IME-' and 'surface HNLC-DOM' water, respectively. Unfiltered water samples were collected from upstream of Crozet at 5 m depth using TOWFISH line (47˚27.200'S, 43˚16.235'E) and downstream of Crozet at 30 m depth using Go-Flo rosette (Station 33) and subsequently filtered through a 0.8 µm polycarbonate filter to isolate the bacterioplankton community. These 0.8 µm filtered samples are hereafter termed the 'HNLC-' (upstream sample) and 'IME-bacterioplankton inoculum' (downstream sample).

HNLC-bacterioplankton inoculum was added in a 1:3 ratio to deep-, mesopelagic-, and surface HNLC-DOM water, and IME-bacterioplankton inoculum was added to surface IME-DOM water, all added to a ratio of 1:3. These were allowed to incubate for ~28 days at ~5˚C in the dark and subsampled every 3 days for bacterioplankton abundance to monitor the progress of DOM remineralization by bacterioplankton and at t=initial, t=2 weeks, and, t=end for other parameters.

dFe, electroactive humic substances (eHS), and FeL concentration.

Water samples were filtered through 0.22 µm PES filter units (Millex)using using a peristaltic pump set to ~225 mL/h. Samples were collected in TM clean 60 mL (dFe and humic ligands) and 125 mL (FeL) LPDE bottles. eHS and FeL samples were stored at -20˚C prior to analysis.

Inorganic nutrients

Samples for determination of nitrate, nitrite, phosphate, and silicate concentration were syringe filtered through 0.22 µm PES filter units (Millex), for sample handling see Blain's cruise report. For collection procedure for ammonium samples see Forrer's cruise report.

DOM

Samples for dissolved organic carbon (DOC) were collected and processed as described in Blain's report. Samples for DOM composition were filtered using a HCl clean glass filtration rig through an ashed GF/F filter. Filtrate was collected in a HCl clean glass bottle with a teflon lid, acidified to pH 2.0 using Suprapure HCl (30 %, Supelco), and stored at ~5 ˚C in the dark until sample extraction onshore.

Bacterioplankton abundance, community composition, and metabolism

Bacterioplankton abundance samples were fixed with glutaraldehyde (final concentration of 0.5 %) for ~1 h at 5˚C prior to flash freezing in liquid nitrogen and storage at -80 ˚C. Samples for bacterioplankton community composition analysis were collected and stored as described in Obernosterer's report. Bacterioplankton respiration was measured by incubating samples in HCl clean glass vials with septa lids containing an oxygen sensor spot (Presens) and monitoring changes in oxygen concentration over the course of the incubation. The percentage of active bacterioplankton cells was determined by the BONCAT protocol, samples were either filtered and subsequently fixed by glutaraldehyde (for samples to be analyzed by epifluorescence microscopy; Leizeaga et al. 2017) or only fixed by glutaraldehyde (final concentration 0.5 %; samples to be analyzed by Flow Cytometry ; Couradeau et al. 2019) prior to flash freezing in liquid nitrogen and storage at -80 ˚C.

Table 17: list of measured parameters

Parameter	Code of operation (Station-cast)	Number of samples
dFe	Clean CTD Station 25-068, FISH 47˚27.200'S, 43˚16.235'E, Clean CTD Station 33-085, Clean CTD Station 33-087, within incubations	30
Electroactive humic substances	Clean CTD Station 25-068, FISH 47˚27.200'S, 43˚16.235'E, Clean CTD Station 33-085, Clean CTD Station 33-087, within incubations	30
Iron binding ligands	Clean CTD Station 25-068, FISH 47˚27.200'S, 43˚16.235'E, Clean	30

	CTD Station 33-085, Clean CTD Station 33-087, within incubations	
Nitrate, phosphate, silicate	Clean CTD Station 25-068, FISH 47˚27.200'S, 43˚16.235'E, Clean CTD Station 33-085, Clean CTD Station 33-087, within incubations	30
Ammonium	Clean CTD Station 25-068, FISH 47˚27.200'S, 43˚16.235'E, Clean CTD Station 33-085, Clean CTD Station 33-087, within incubations	30
DOC	Clean CTD Station 25-068, FISH 47˚27.200'S, 43˚16.235'E, Clean CTD Station 33-085, Clean CTD Station 33-087, within incubations	30
DOM composition	Clean CTD Station 25-068, FISH 47˚27.200'S, 43˚16.235'E, Clean CTD Station 33-085, Clean CTD Station 33-087, within incubations	8
Bacterioplankton abundance	Clean CTD Station 25-068, FISH 47˚27.200'S, 43˚16.235'E, Clean CTD Station 33-085, Clean CTD Station 33-087, within incubations	200
Bacterioplankton community composition	Clean CTD Station 25-068, FISH 47˚27.200'S, 43˚16.235'E, Clean CTD Station 33-085, Clean CTD Station 33-087, within incubations	14
BONCAT	Clean CTD Station 25-068, FISH 47˚27.200'S, 43˚16.235'E, Clean CTD Station 33-085, Clean CTD Station 33-087, within incubations	120

V.12.4 Post-cruise sampling analyses and envisioned timeline of working plan, people involved on shore

dFe, eHS, and FeL concentration

For dFe sample analysis, see Gonzalez-Santana's cruise report. FeL and eHS will be analyzed using cathodic stripping volammetry (Abualhaija and van den Berg, 2014 ; Sukekava et al. 2018) and will be analyzed within the next 18 – 24 months. Analysis will be conducted by Millie Goddard-Dwyer and Hannah Whitby.

Inorganic nutrients

For sample analysis of nitrate, nitrite, phosphate, and silicate concentration see Blain's cruise report. For sample analysis of ammonium concentration see Forrer's report.

DOC and DOM

For sample analysis of DOC see Blain's cruise report. Samples for DOM composition will be extracted using 200 mg Bond Elut columns (Agilent), eluted with methanol, before drying with nitrogen gas. The resultant DOM extracts will be stored at -80 ˚C prior to analysis by Fourier Transform Ion Cyclotron Resonance Mass Spectrometry. DOM samples will be analysed by Millie Goddard-Dwyer and Claire Evans within the next 6 months.

Bacterioplankton abundance, community composition, and metabolism

Onshore, samples for bacterioplankton abundance will be stained for 1 h in the dark at room temperature with the DNA stain SYBR Green I prior to enumeration using a Becton Dickinson FACScalibur flow cytometer. Different bacterioplankton groups will be discriminated based on DNA content and light scattering properties. For bacterioplankton community composition analysis, see Obernosterer's report.

The percentage of active bacterioplankton cells will be determined by the BONCAT protocol. Briefly, a click reaction will be performed prior to analysis by both epifluorescence microscopy (Leizeaga et al. 2017) and flow cytometry (Couradeau et al. 2019).

Samples for bacterioplankton abundance and metabolism will be analysed within the next 6 months by Millie Goddard-Dwyer, Isobel Turnbull, and Claire Evans.

References

Abualhaija, M.M. and van den Berg, C.M., 2014. Chemical speciation of iron in seawater using catalytic cathodic stripping voltammetry with ligand competition against salicylaldoxime. Marine Chemistry, 164, pp.60-74.

Bressac, M., Guieu, C., Ellwood, M.J., Tagliabue, A., Wagener, T., Laurenceau-Cornec, E.C., Whitby, H., Sarthou, G. and Boyd, P.W., 2019. Resupply of mesopelagic dissolved iron controlled by particulate iron composition. Nature Geoscience, 12(12), pp.995-1000.

Couradeau, E., Sasse, J., Goudeau, D., Nath, N., Hazen, T.C., Bowen, B.P., Chakraborty, R., Malmstrom, R.R. and Northen, T.R., 2019. Probing the active fraction of soil microbiomes using BONCAT-FACS. Nature communications, 10(1), pp.1-10.

Gledhill, M. and Buck, K.N., 2012. The organic complexation of iron in the marine environment: a review. Frontiers in microbiology, 3, p.69.

Gledhill, M. and van den Berg, C.M., 1994. Determination of complexation of iron (III) with natural organic complexing ligands in seawater using cathodic stripping voltammetry. Marine Chemistry, 47(1), pp.41-54.

Leizeaga, A., Estrany, M., Forn, I. and Sebastián, M., 2017. Using click-chemistry for visualizing in situ changes of translational activity in planktonic marine bacteria. Frontiers in microbiology, 8, p.2360.

Sabine, C.L., Feely, R.A., Gruber, N., Key, R.M., Lee, K., Bullister, J.L., Wanninkhof, R., Wong, C.S.L., Wallace, D.W., Tilbrook, B. and Millero, F.J., 2004. The oceanic sink for anthropogenic CO2. science, 305(5682), pp.367-371.

Sukekava, C., Downes, J., Slagter, H.A., Gerringa, L.J. and Laglera, L.M., 2018. Determination of the contribution of humic substances to iron complexation in seawater by catalytic cathodic stripping voltammetry. Talanta, 189, pp.359-364.

Whitby, H., Bressac, M., Sarthou, G., Ellwood, M.J., Guieu, C. and Boyd, P.W., 2020. Contribution of electroactive humic substances to the iron-binding ligands released during microbial remineralization of sinking particles. Geophysical Research Letters, 47(7), p.e2019GL086685.

VI. DISSOLVED AND PARTICULATE TRACE METALS DISTRIBUTION, SPECIATION, AND THEIR ISOTOPE COMPOSITION

Principal investigator:
On board : Hélène Planquette
Univ Brest, CNRS, IRD, Ifremer, LEMAR, F-29280 Plouzane, France
helene.planquette@univ-brest.fr

Other participants (on board): Bruno Hamelin (CEREGE, hamelin@cerege.fr), Wen-Hsuan Liao (LEMAR, liao.wenhsuan@univ-brest.fr), David González-Santana (LEMAR, david.gonzalezsantana@univ-brest.fr), Corentin Baudet (LEMAR, corentin.baudet@univ-brest.fr), Maria-Elena Vorrath (LEMAR, mariaelena.vorrath@univ-brest.fr), Catherine Jeandel (Co-chief Scientist, LEGOS, Catherine.jeandel@legos.obs-mip.fr), Moustafa Belhadj (LEGOS, moustafa.belhadj@legos.obs-mip.fr), Nolwenn Lemaitre (ETH Zürich, nolwenn.lemaitre@erdw.ethz.ch), Natalia Torres-Rodriguez (Mediterranean Institute of Oceanography, natalia.torres-rodriguez@mio.osupytheas.fr, Millie Goddard-Myer (University of Liverpool, UK, milliard@noc.ac.uk), Ingrid Obernosterer (LOMIC, ingrid.obernosterer@obs-banyuls.fr)

Other participants (on shore): Derek Vance (ETH Zürich, derek.vance@erdw.ethz.ch), Lars-Eric Heimburger (Mediterranean Institute of Oceanography, lars-eric.heimburger@mio.osupytheas.fr), Hannah Whitby (University of Liverpool, UK, Hannah.Whitby@liverpool.ac.uk), Joe Resing (PMEL/NOAA, USA, resing@uw.edu), Alan M. Shiller (University of Southern Mississippi, USA, Alan.Shiller@usm.edu), Zvika Steiner (GEOMAR, Germany, zsteiner@geomar.de), G. Gonzalez Aridane (Instituto de Oceanografía y Cambio Global (IOCAG), Las Palmas, aridaneglez@gmail.com), G. Sarthou (LEMAR; Geraldine.sarthou@univ-brest.fr), M. Gallinari (LEMAR, morgane.gallinari@univ-brest.fr), Eva Bucciarelli (LEMAR, eva.bucciarelli@univ-brest.fr)

Abstract:

Trace metals, such as Fe, play a crucial role in regulating primary production in the ocean, especially in the Southern Ocean, a HNLC region. In order to better understand and quantify their biogeochemical cycle and their sources in the Southern Ocean, we study their distributions in the dissolved and particulate phases (Fe, Mn, Cu, Co, Ni, Zn, Cd, Al, and Pb), their organic speciation (Fe and Cu), and their isotopic composition (Fe, Zn, Pb, and Ni). We anticipate that we can decipher the relative importance of sedimentary, atmospheric and hydrothermal sources of TEI in the Indian sector of the SO.

Measurements will be carried out back to the different home laboratories: LEMAR (Brest, France), LEGOS (Toulouse, France), MIO and CEREGE (Marseille, France), University of Liverpool (UK), Universidad de Las Palmas de Gran Canaria (Spain) and ETH, Zurich (Switzerland).

VI.1 Samples collected with the trace metal clean rosette

VI.1.1 Scientific context

Trace elements and isotopes (TEIs) play a crucial role in regulating primary production in the ocean. Some of them (e.g., Fe, Cu, Mn, Co, Zn) serve as essential micronutrients, being involved in many metabolic processes of marine organisms (e.g., Sunda, 1994; Morel and Price, 2003; Sarthou et al., 2005). Some of these elements are also contaminants of the environment. They are either toxic at high concentration but essential at low concentration, or only toxic (e.g., Pb, Zn, Cu, Cd, Ag).

Trace metals are present in operationally defined colloidal (5 kDa–0.2 µm), dissolved (< 0.2-0.45 µm) and particulate (>0.2-0.45 µm) phases and for some of them, more than 90% of their dissolved fraction is complexed by organic ligands (Rue and Bruland, 1995, Buck et al., 2012), preventing precipitation and removal by scavenging or regulating their bioavailability. Among the known organic ligands of Fe and Cu, humic-like substances play a crucial role, although very little is known about their oceanic cycle (Hioki et al., 2014). The poor knowledge of their cycles is a major drawback for the understanding of their biogeochemical impact on the food web. Their sources remain poorly constrained, and Fe isotopes in particular emerged as a new very promising tool to better constrain the Fe sources (Labatut et al. 2014). Thanks to the GEOTRACES programme and its global survey, hydrothermal vents have been recently discovered as important sources of Fe to the global ocean (Resing et al., 2015) or more locally, even up to the surface, when shallow hydrothermal vents are present (Guieu et al., 2018).

VI.1.2 Overview of the project and objectives

Three major objectives within the SWINGS cruise were listed below. In this cruise, we aim to 1) decipher the relative importance of sedimentary, atmospheric and hydrothermal sources of trace elements and isotopes (TEIs) in the Indian sector of the SO, 2) investigate the drivers of the internal trace element cycles: biogenic uptake, remineralization, particle fate, and export, and 3) try to quantify TEI transport by the Antarctic Circumpolar Current and the complex frontal areas at the confluence between Indian and Atlantic Oceans.

Specifically, for ligands and humic ligands, samples were collected from Go-Flo casts across a broad range of biogeochemical settings across the Sub-Antarctic Frontal Zone. Changes in iron ligand concentration and composition across these different biogeochemical settings will give insights into the potential roles of processes such as frontal upwelling or the island mass effect in mediating ligand cycling. Further, relative changes in ligand concentration and composition with depth may give further insights into the biological cycling of these molecules. For example, the importance of microbial remineralisation in ligand production or degradation. The extensive profiles of ligand concentration and composition provides the opportunity to assimilate these data into a biogeochemical model to further reveal the sources and sinks of these ligands and probe the role of ligands in supporting primary production in the Southern Ocean.

VI.1.3 Methodology and sampling strategy

Seawater and particle samples were collected using a Trace Metal Clean Rosette (TMR, General Oceanics Inc. Model 1018 Intelligent Rosette), attached to a 6 mm Kevlar line. After recovery, the whole trace metal rosette was transferred into a clean container for sampling. On each TMR cast, nutrient samples were taken to check potential leakage of the Go-Flo bottles. Analyses will be performed back to the shore-based laboratory. Salinity samples were taken and measured onboard for several stations (Table 18 & 19).

VI.1.4 Dissolved and particulate trace metal concentrations (dTM and pTM)

Dissolved trace metal (Mn, Co, Ni, Cu, Zn, Cd and Pb)

Samples were filtered on-line through 0.45 µm using a polyethersulfone filter (Supor®). All samples were acidified within 24 h of collection with ultrapure hydrochloric acid (HCl, Merck, 0.2%, final pH 1.7).

Dissolved trace metals will be analyzed using a preconcentration system SeaFAST coupled to a high-resolution magnetic sector field inductively coupled mass spectrometer (HR-ICP-MS, Element XR) method following Tonnard et al. (2019), in the shore-based LEMAR laboratory.

On board dissolved iron (dFe) measurements

Dissolved Fe samples were filtered on-line through 0.45 µm using a polyethersulfone filter (Supor®). All samples were acidified within 24 h of collection with ultrapure hydrochloric acid (HCl, Merck, 0.2%, final pH 1.7). Initial dFe samples were analyzed on board to check for any possible contamination issues (no issues were found) using FIA with chemiluminescence detection (Obata et al., 1993). Samples were pre-concentrated in a Toyopearl column instead of the original 8-hydroxyquinoline resin.

The general principle of FIA is that a trace metal analyte (e.g. Fe (III)), present at a low concentration in a sample solution, is pre-concentrated onto a chelating resin over time and eluted off using acid. Through pre-concentration the trace metal analyte is now present in a larger concentration for analysis, whilst removing the seawater matrix. In this Fe(III) luminol/peroxide system, Fe(III) is selectively pre-concentrated onto a Toyopearl 650 M chelating resin at ~pH 3.5. Following elution with hydrochloric acid solution, Fe(III) initiates the three-step oxidation reaction of luminol with hydrogen peroxide; chemiluminescence from the reaction is detected using a photomultiplier tube (PMT).

Soluble trace metals (sTM)

The on-line filtration system was set up by David González-Santana based on a system described in Wu et al. (2001) using Whatman Anotop syringe filters, but a peristaltic pump forward pressure is used to filter the samples in multiple channels rather than processing the samples manually (information given by Dr Simon Ussher). Flow rates did not exceed 1.5 mL min^{-1}.

Fe oxidation kinetics

In order to measure the Fe(II) oxidation rate constants, continuous Fe(II) concentrations were determined using the FeLume System (Waterville Analytical), with a data point acquisition every 1 s. This direct FIA system uses luminol (5-amino-2,3-dihydro-1,4-phthalazine dione, Sigma-Aldrich) as the

reagent (King et al., 1995) which reacts with Fe(II). The sample was continuously aerated with pure air (Carburos Metalicos S.A.). A 0.8 nmol L-1 addition of Fe(II) (ammonium iron(II) sulfate hexahydrate, Sigma-Aldrich) was introduced into each sample and the Fe(II) concentration was continuously monitored until the signal had reduced by 70%. This method produces apparent rate constants (kapp) because the oxidation rate constant is measured on a Fe(II) spike rather than on the ambient Fe(II). For further information please check González-Santana et al. (2021).

Organic speciation of Cu and Fe (Fe org sp and Cu org sp)

Samples for organic speciation of Fe were filtered on- line through 0.45 µm using a polyethersulfone filter (Supor®) and immediately frozen at -20°C. They will be analyzed in the shore-based laboratory (Univ. Liverpool, UK) by a newly developed method of cathodic stripping voltammetry (Mahieu et al., in prep.).

Samples for organic speciation of Cu were filtered on- line through 0.45 µm using a polysulfone filter (Supor®) and immediately frozen at -20°C. They will be analyzed in the shore-based laboratory (Univ. de Las Palmas de Gran Canaria) by cathodic stripping voltammetry (Campos and van den Berg, 1994).

Humic substances and thiols (Humics A&B, thiols, Fe binding)

Samples for humic substances and thiols were filtered on-line through 0.45 µm using a polyethersulfone filter (Supor®) and immediately frozen at -20°C. The formers will be analyzed in the shore-based laboratory (Univ. Liverpool, UK) by cathodic stripping voltammetry of their complexes with copper, as described by Whitby and van den Berg (2015). Voltammetric detection of iron-humic complexes directly will also be performed following Abualhaija et al. (2015). Thiols concentrations will be analyzed following Leal et al. (1999).

Zn and Ni isotopes

Sample for Zn isotopic composition were filtered on-line through 0.45 µm filter (Planquette and Sherrell 2012). Both isotopic compositions will be measured back to the shore-based laboratory (ETH, Switerland) as described in Lemaitre et al. (2020). Basically, after preconcentration and purification, Zn and Ni isotopic composition will be measured by a multi-collector ICPMS (Neptune).

Pb isotopes

Samples for Pb stable isotopes measurements were collected unfiltered in 1 l pre-cleaned HDPE bottles, except for the last three stations on the Kerguelen-Heard plateau, where samples were also filtered at the same depths. The analyses will be carried out at CEREGE in Aix-en-Provence, following the protocol recently published by Griffiths et al. (2020), and the isotopic measurements performed on the NEPTUNE+ of the lab. Pb concentrations will be obtained along with the isotopic composition, through isotope dilution with a 205Pb spike available in the lab. Additional analyses will also be performed on a selection of aliquotes of the leachates prepared at LEMAR from the filters.

Total mercury and dissolve gaseous mercury

Unfiltered samples for total mercury and dissolve gaseous mercury were collected and analyzed on board by means of cold vapor atomic fluorescence spectrometry. For further details regarding the method and the collected samples see mercury cruise report.

Table 18: List of samples collected at each station using the trace metal clean rosette

Station #	Cast #	THg	DGM	MeHg	Salinity	DOC	N isotopes	Fe kinetics	Nutrient	dTM	dFe	sTM	pTM	dAl	dGa	Ligands	Humics	Fluorine	Cation	REE	Zn Isotopes	Pb isotopes
1	2	x	x		x				x	x	x		x							x		
3	11	x	x	x	x	x	x	x	x	x	x	x	x	x		x	x			x	x	x
4	14	x	x	x	x	x	x	x	x	x	x	x	x	x		x	x	x	x	x	x	x
5	18	x	x	x	x	x	x	x	x	x	x	x	x	x		x	x	x	x	x		x
8	23	x	x	x	x	x	x		x	x	x		x	x		x	x				x	x
10	27	x	x	x	x	x	x	x	x	x	x	x	x	x		x	x					x
11	34	x	x	x		x	x		x	x	x		x	x		x	x	x	x	x	x	x
14	41	x	x	x	x		x	x	x	x	x	x	x	x		x	x			x	x	x
16	47	x	x	x		x	x		x	x	x		x	x		x	x	x	x	x		x
18	49	x	x	x		x	x		x	x	x	x	x	x		x	x			x	x	x
19	51	x	x	x			x	x	x	x	x	x	x			x	x			x	x	x
20	53	x	x	x			x	x	x	x	x	x	x	x		x	x			x	x	x
21	58	x	x	x		x	x	x	x	x	x		x	x		x	x	x	x	x	x	x
25	68	x	x	x		x	x	x	x	x	x	x	x	x		x	x	x	x	x	x	x
27	74	x	x	x		x	x	x	x	x	x	x	x	x		x	x	x	x	x		x
29	77	x	x	x		x	x	x	x	x	x		x	x	x	x	x	x	x	x	x	x
31	82	x	x	x		x	x		x	x	x		x	x		x	x	x	x			x
32	84					x	x		x	x	x		x	x		x	x	x	x			
33	87	x	x	x		x	x	x	x	x	x	x	x	x		x	x			x	x	x
35	93	x	x	x			x		x	x	x	x	x	x		x	x	x	x	x		x
36	98	x	x	x		x	x	x	x	x	x	x	x	x		x	x	x	x	x	x	x
38	102	x	x	x			x		x	x	x	x	x	x		x	x	x	x		x	x
40	109	x	x	x	x	x	x		x	x	x		x	x		x	x	x	x			
42	112	x	x	x		x	x	x	x	x	x	x	x	x		x	x	x	x	x	x	x
44	117	x	x	x		x	x	x	x	x	x	x	x	x		x	x	x	x	x	x	x
45	122	x	x	x			x	x	x	x	x	x	x	x	x	x	x	x	x	x	x	x
46	125	x	x	x		x	x		x	x	x	x	x	x		x	x	x	x	x	x	x
47	130	x	x	x		x	x		x	x	x	x	x	x		x	x	x	x	x	x	x
48	134				x	x	x		x	x	x	x	x	x		x	x	x	x		x	x
58	144	x	x	x		x	x	x	x	x	x	x	x	x	x	x	x	x	x		x	x
63	156	x	x	x		x	x	x	x	x	x	x	x	x		x	x	x	x		x	x
65	159	x	x	x			x	x	x	x	x	x	x	x		x	x	x	x	x	x	x
66	163	x	x	x		x	x		x	x	x	x	x	x		x	x	x	x	x	x	x
67	167	x	x	x			x		x	x	x	x	x	x		x	x			x	x	x
68	169	x	x	x		x	x	x	x	x	x	x	x	x		x	x	x	x	x	x	x

Dissolved Ga analysis

Dissolved Ga will be determined using isotope dilution ICP-MS. Acidified samples are spiked with enriched Ga-71 and extracted using a SeaFAST pico system operated offline. The method provides a 66-fold concentration of Ga from 20 mL of sample, allowing the use of medium resolution to avoid residual doubly charged Ba interference. The method also uses a rinse of dilute HF to minimize carry-over of Ga. The method detection limit is ~0.1 pM with an uncertainty of <3% at 20 pM Ga.

Dissolved Rare earth elements (REE) analysis

For dissolved REE concentration analyses, 500 mL were immediately filtered onboard (PES membrane, 25mm 0.45 µm) in the clean container. This strategy allowed us to collect exactly at the same depths the dissolved and particulate REE, essential when tracing the exchanges between these 2 phases. The 500 ml aliquots were acidified to pH = 1.5 with twice-distilled HCl. The samples were stored at room temperature and then transferred to the laboratory on land (LEGOS, Toulouse, France).

The purification and preconcentration of REE will be performed following the method developed in LEGOS by Viet Pham as part of his PhD thesis (Pham, 2020). Briefly, the acidified seawater samples will be spiked with ^{150}Nd and ^{172}Yb and brought o pH ca 5-6 using and ammonium acetate buffer. DREE will be then passed on Nobias resin cartridges using an online manifold. After elution, dissolved Rare Earth Element concentrations will be then measured by High Resolution Inductively Coupled Plasma Mass Spectrometers (ICP-MS) using an Element-XR (using Aridus desolvation introduction system). All the REEs

will be determined by the external standard method, whereas Nd and Yb are additionally determined by isotopic dilution. The values obtained for Nd and Yb concentrations by both methods enable us to determine the analytical recovery yields of these two elements in each sample, which ranges are: 88-96% and 83-94% for Nd and Yb, respectively. Efficiencies of the chemical protocol for the other REE are calculated by linear interpolation. Potential sensibility variations during the measurement session are monitored by In/Re internal standard method so that the final REE concentrations are corrected accordingly.

Particulate Rare earth elements (REE) analysis

The full filters will be digested in LEMAR (together with the other pTM, see the following section) in the framework of Corentin Baudet's thesis and an aliquot of each leachate will be sent to Toulouse (LEGOS) in order to proceed to the PREE analyses.

Particulate Rare Earth Element concentrations will be measured by High Resolution Inductively Coupled Plasma Mass Spectrometers (ICP-MS) using an Element-XR (using Aridus desolvation introduction system). All the REEs will be determined by the external standard method. Potential sensibility variations during the measurement session are monitored by In/Re internal standard method so that the final REE concentrations are corrected accordingly.

Particulate trace metals (pTM)

Particulate trace metal samples were taken from the filtration through 0.45 µm using a polyethersulfone filter (Supor®). All filters will be digested and analyzed back in LEMAR by SF-ICP-MS following Planquette and Sherrell (2012) method. Acetic acid leaches (Berger et al., 2008) will also be undertaken in order to assess the bioavailable fraction. A subset of samples will also be dedicated for SEM imaging.

Dissolved fluorine

Samples for fluorine (F) were collected from the standard CTD casts (stainless steel rosette frame), filtered, and stored unacidified with no head space in acid cleaned low density polyethylene (LDPE) bottles. Determination of F concentrations in the seawater samples will be done by a potentiometric method, using a F^- ion specific electrode (Rude and Aller, 1991; Warner, 1971), and a spectrophotometric method (Greenhalgh and Riley, 1961; Kremling, 1999). The spectrophotometric and potentiometric methods for F determination provide slightly different information, the spectrophotometric method analyses the soluble reactive F whereas the potentiometric method analyses the activity of the F^- ion. Past studies suggested that oceanographic data obtained by the potentiometric and spectrophotometric methods are internally consistent for each method, but there were very large differences in F concentration profiles obtained by analysis of filtered samples from similar regions using the different methods (Wilson, 1975).

Dissolved cations

Samples for major cations (Ca, Sr, Li) were filtered into acid cleaned LDPE bottles, and acidified using hydrochloric acid. The concentrations of Ca, Sr and Li will be analyzed with inductively coupled plasma

optical emission spectroscopy (ICP-OES) by sample standard bracketing using the method developed by Schrag (1999) and de Villiers et al. (2002), and modified for analyses of major elements in seawater by Steiner et al. (2018; 2020). The ICP-OES measures the concentrations of all elements simultaneously. Thanks to the simultaneous analyses, plasma and flow rates instability affect the readings of all intensity data in the same manner, and element to sodium ratios correct for these instrumental errors.

Intercalibration

Samples for intercalibration (dFe, dTM, dREE, pTM, pREE, Fe and Cu organic speciation, DGM, MMHg, TMeHg, and Pb isotopes) were taken at the crossover station (station 47, cast 130) following the GEOTRACES protocols.

Other parameters

The details of nitrogen isotope analysis can be found in the report of Heather Forrer. The ones linked to mercury (tHg, DGM, TMeHg, and Hg isotopes,) in the report of Natalia Torres-Rodriguez. For DOC analysis, the details can be found in the report of Ingrid Obernosterer.

Table 19: List of measured parameters (all the samples listed below were collected by clean CTD casts).

Parameters	Number of samples
THg	518
DGM	308
MeHg	499
Salinity	197
DOC	289
N isotopes	565
Fe oxidation kinetics	84
Pb isotopes	181
Particulate trace elements	662
Nutrients	593
dFe	605
dTM	605
dAl	249
ligands	290
Humics	478
Fluorine	128
Cation	66
REES	205
Zn and Ni isotopes	200
Soluble TM	223
dGa	41

VI.1.5 Preliminary results

All samples will be analyzed back to the different laboratories. Below are examples of filters collected at station 1 and 66 (Figure VI-1). Two dissolved Fe profiles were also shown below, the samples were measured by David Gonzalez-Santana by using onboard FIA analysis (Figure 0-).

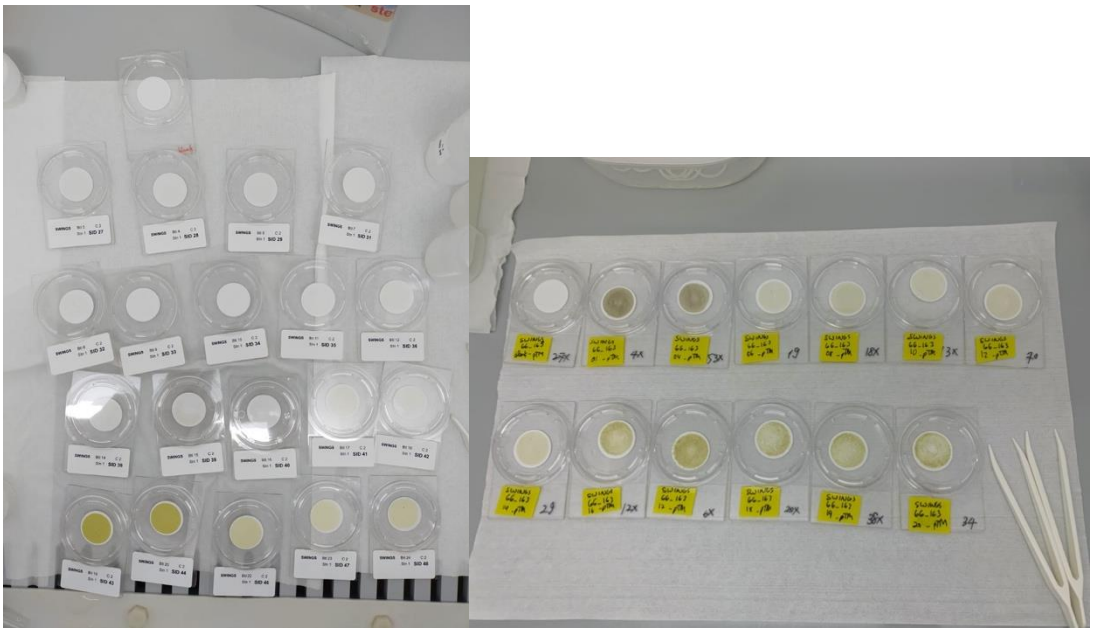

Figure VI-1: Particle samples collected at station 1 (cast 2) and 66 (cast 163).

VI.1.6 Post-cruise sampling analyses and envisioned timeline of working plan, people involved on shore

The cycling processes of trace metals involve interactions between dissolved and particulate phases. However, these mechanisms are complex and poorly understood and need to be further studied. To study the cycling processes of trace metals in the ocean, particularly with a focus on iron, all traces metals samples (soluble (sTM), dTM and pTM) collected in the SWINGS cruise will be analyzed by Corentin Baudet during his PhD. The distribution of iron, impacted by sources/sinks and physical, biological and chemical processes, in different forms, soluble, colloidal, particulate phases, will be studied using a multi-elemental approach (using other tracers sampling during the SWINGS cruise). The envisioned timeline to analyse sTM, dTM and pTM should be take about one year.

Analyses of dissolved and particulate REE require on land based clean laboratory. They cannot be done on board. This protocol is relatively long. We will make all what's possible to perform these analyses within the next 2 years at LEGOS.

References

Abualhaija, M. M., Whitby, H. and van den Berg, C. M. G.: Competition between copper and iron for humic ligands in estuarine waters, Marine Chemistry, 172, 46–56, doi:10.1016/j.marchem.2015.03.010, 2015.

Buck, K. N., Moffett, J., Barbeau, K. A., Bundy, R. M., Kondo, Y. and Wu, J.: The organic complexation of iron and copper: an intercomparison of competitive ligand exchange-adsorptive cathodic stripping voltammetry (CLE-ACSV) techniques, Limnology and Oceanography: Methods, 10(7), 496–515, doi:10.4319/lom.2012.10.496, 2012.

Campos, M., van den Berg, C.M.G.: Determination of copper complexation in seawater by cathodic stripping voltammetry and ligand competition with salicylaldoxime. Analitica Chimica Acta 284 (3), 481–496, 1994.

de Villiers, S., Greaves, M. and Elderfield, H. (2002) An intensity ratio calibration method for the accurate determination of Mg/Ca and Sr/Ca of marine carbonates by ICP-AES. Geochemistry, Geophysics, Geosystems 3.

González-Santana, D., González-Dávila, M., Lohan, M. C., Artigue, L., Planquette, H., Sarthou, G., & Santana-Casiano, J. M. (2021). Variability in iron (II) oxidation kinetics across diverse hydrothermal sites on the northern Mid Atlantic Ridge. Geochimica et Cosmochimica Acta. https://doi.org/10.1016/j.gca.2021.01.013

Greenhalgh, R. and Riley, J.P. (1961) The determination of fluorides in natural waters, with particular reference to sea water. Analytica Chimica Acta 25, 179-188.

Griffiths, A., Packman, H., Leung, Y.L., Coles, B.J., Kreissig, K., Little, S.H., van der Fliert, T and Rehkämper, M.: Evaluation of optimized procedures for high precision Pb isotope analyses of sea water by MC-ICP-MS, Anal. Chem., doi: 10.1021/acs.analchem.0c01780, 2020.

Hioki, N., Kuma, K., Morita, Y., Sasayama, R., Ooki, A., Kondo, Y., Obata, H., Nishioka, J., Yamashita, Y., Nishino, S., Kikuchi, T. and Aoyama, M.: Laterally spreading iron, humic-like dissolved organic matter and nutrients in cold, dense subsurface water of the Arctic Ocean, Sci Rep, 4(1), 1–9, doi:10.1038/srep06775, 2014.

King D. W., Lounsbury H. A. and Millero F. J. (1995) Rates and mechanism of Fe(II) oxidation at nanomolar total iron concentrations. Environ. Sci. Technol. 29(3), 818–824.

Kremling, K. (1999) Determination of the major constituents, in: K. Grasshoff, K.K.a.M.E. (Ed.), Methods of Seawater Analysis. WILEY-VCH Verlag GmbH, Weinheim, pp. 229-251.

Labatut, M., Lacan, F., Pradoux, C., Chmeleff, J., Radic, A., Murray, J. W., Poitrasson, F., Johansen, A. M. and Thil, F.: Iron sources and dissolved-particulate interactions in the seawater of the western Equatorial Pacific, iron isotope perspectives, Global Biogeochemical Cycles, 28, 1044–1065, doi:10.1002/2014GB004928, 2014.

Leal, M. F. C., Vasconcelos, M. T. S. D. and van den Berg, C. M. G.: Copper-induced release of complexing ligands similar to thiols by Emiliania huxleyi in seawater culutres, Limnology and Oceanography, 44(7), 1750–1762, 1999.

Lemaitre et al., 2020. Pervasive sources of isotopically light zinc in the North Atlantic Ocean. EPSL, 539, 116216.

Morel, F. M. M. and Price, N. M.: The biogeochemical cycles of trace metals in the Oceans, Science, 300(5621), 944–947, DOI: 10.1126/science.1083545, 2003.

Obata, H., Karatani, H. and Nakayama, E.: Automated determination of iron in seawater by chelating resin concentration and chemiluminescence, Analytical Chemistry, 65, 1524–1528, 1993.

Pham,V. (2021) Tracing the lithogenic imprint in the Coral and Solomon seas using the rare earth concentrations and neodymium isotopic compositions PhD thesis, Paul Sabatier University.

Planquette, H. and Sherrell, R. M.: Sampling for particulate trace element determination using water sampling bottles: methodology and comparison to in situ pumps, Limnology and Oceanography: Methods, 10(5), 367–388, doi:10.4319/lom.2012.10.367, 2012.

Resing, J. A., Sedwick, P. N., German, C. R., Jenkins, W. J., Moffett, J. W., Sohst, B. M. and Tagliabue, A.: Basin-scale transport of hydrothermal dissolved metals across the South Pacific Ocean, Nature, 523(7559), 200–203, doi:10.1038/nature14577, 2015.

Rue, E. L. and Bruland, K. W.: Complexation of iron(III) by natural organic ligands in the Central North Pacific as determined by a new competitive ligand equilibration/adsorptive cathodic stripping voltammetric method, Marine Chemistry, 50(1–4), 117–138, 1995.

Sarthou, G., Timmermans, K. R., Blain, S. and Tréguer, P.: Growth physiology and fate of diatoms in the ocean: a review, Journal of Sea Research, 53(1), 25–42, doi:10.1016/j.seares.2004.01.007, 2005.

Schrag, D.P. (1999) Rapid analysis of high-precision Sr/Ca ratios in corals and other marine carbonates. Paleoceanography 14, 97-102.

Steiner, Z., Turchyn, A.V., Harpaz, E. and Silverman, J. (2018) Water chemistry reveals a significant decline in coral calcification rates in the southern Red Sea. Nature Communications 9, 3615.

Steiner Z., Sarkar A., Prakash S., Vinayachandran P.N., Turchyn A.V. (2020). Dissolved strontium, Sr/Ca ratios, and the abundance of Acantharia in the Indian and Southern Oceans. ACS Earth and Space Chemistry.

Sunda, W. G.: Trace metal/phytoplankton interactions in the sea, in Chemistry of Aquatic systems: Local and Global Perspectives, edited by G. B. and W. Stumm, pp. 213–247, ECSC, EEC, EAEC, Brussels and Luxembourg., 1994.

Tonnard, M., Planquette, H., Bowie, A. R., van der Merwe, P., Gallinari, M., Desprez de Gésincourt, F., Germain, Y., Gourain, A., Benetti, M., Reverdin, G., Tréguer, P., Boutorh, J., Cheize, M., Menzel Barraqueta, J.-L., Pereira-Contreira, L., Shelley, R., Lherminier, P. and Sarthou, G.: Dissolved iron in the North Atlantic Ocean and Labrador Sea along the GEOVIDE section (GEOTRACES section GA01), Biogeosciences Discuss., 1–53, doi:10.5194/bg-2018-147, 2018.

Warner, T.B. (1971) Normal fluoride content of seawater. Deep Sea Research and Oceanographic Abstracts 18, 1255-1263.

Whitby, H. and Van den Berg, C. M. G.: Evidence for copper-binding humic substances in seawater - https://www.sciencedirect.com/science/article/pii/S0304420314001595, 2015.

Wilson, T.R.S. (1975) Salinity and the major elements of seawater, in: Riley, J.P., Skirrow, G. (Eds.), Chemical Oceanography, 2nd edition ed. Academic Press, Norwich, pp. 365-414.

VI.2 Surface trace metal clean sampling using the GeoFISH

Partipants: same as section VI.1 plus Hugo Berthelot (Latitude and longitude determination, LEMAR, hugo.berthelot@univ-brest.fr) **and**

On shore: Jeroen E. Sonke (Microplastics, Géosciences Environnement Toulouse (GET), jeroen.sonke@get.omp.eu),

Abstract:

The ocean surface is highly variable requiring high resolution sampling to determine processes which are spatially constrained. Trace metals, such as Fe, play a crucial role in regulating primary production in the ocean, especially in the Southern Ocean, a HNLC region. In order to better understand and quantify their biogeochemical cycle and their sources in the Southern Ocean, we studied their distributions. By deploying a trace metal clean surface sampler (GeoFISH), filtered and unfiltered samples were collected while in transit between station at a resolution of 2-4 hours with seawater flow rates of 1.5 L min^{-1}. High resolution sampling was performed after departing from Crozet and Kerguelen to characterize the island input of different trace metals.

VI.2.1 Scientific context

The GeoFISH sampling was performed to obtain high spatial resolution sampling (and high-volume samples) on the atmosphere-ocean interface along the whole cruise transect (Figure VI-2).

VI.2.2 Methodology and sampling strategy

The GeoFISH towed sampler is a custom designed near surface (<2m) sampling system for the collection of trace metal clean seawater. It consists of a PVC encapsulated lead weighted torpedo and separate PVC depressor vane supporting the intake utilizing all PFA Teflon tubing connected to a deck mounted, air-driven, PFA Teflon dual-diaphragm pump which provides trace-metal clean seawater. The GeoFISH is towed at up to 13 knots off to the side of the vessel outside of the ship's wake to avoid possible contamination from the ship's hull.

Surface samples were collected with a clean surface pump “sipper” system using an all-PTFE Teflon diaphragm pump (Almatec Serie E) and PFA Teflon tubing mounted to a PVC depressor vane 1 m above a 20-kg PVC fish (Bruland et al., 2005) with the outflow directly inside the clean sampling van. After leaving a station, the GeoFISH was deployed with the water intake situated at an approximate depth of 2 m (wave and speed dependent). The flow rate of the GeoFISH into the sampling van was on average 1.5 L min^{-1}. The GeoFISH was allowed to flush for at least 30 minutes before the first sample was collected. Before collecting the samples, a cartridge filter (Acropak) was allowed to flush for at least 5 minutes (cartridge filters were swapped every 5 days depending on filtered volume). During this time, sample bottles were prepared and labelled. Filtered samples were collected first followed by unfiltered samples. The FISH ID, starting time, end time, and samples collected were written down. The latitude and longitude were obtained from the Marion Dufresne GPS. Dissolved iron and mercury samples were collected every two hours, dissolved aluminium, fluorine and cation samples were collected every four hours. Samples for microplastics were collected every 12 hours. Dissolved gallium samples were collected

every four hours once we started the W-E transect. Further information about the sampling sites and samples collected can be obtained in Table 20.

Breaks in sampling were caused by: broken Kevlar cable (FISH006 - FISH007), ship speeds greater than 14 knots (e.g. FISH021 - FISH022) or due to extreme weather conditions (e.g. FISH079 - FISH080).

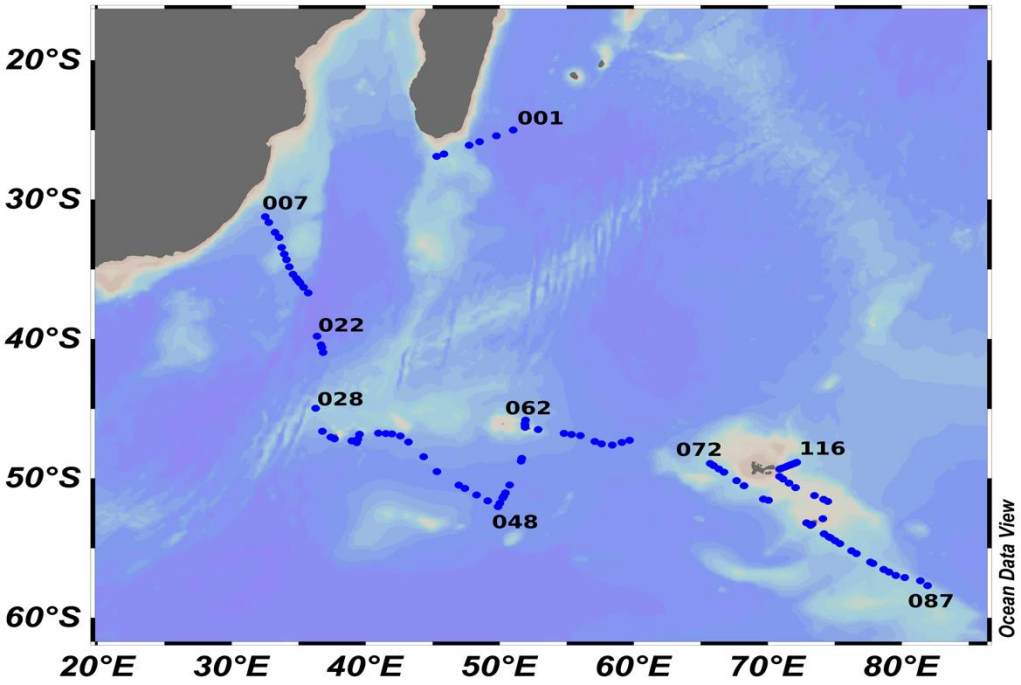

Figure VI-2: Map of GeoFISH sampling sites. Blue dots indicate locations were fish samples were collected. Some GeoFISH ID have been included to locate sites.

All analyses will be performed in the various home laboratories and have already been detailed in VI.1.6 hence are not repeated here. Samples for microplastics will be filtered, digested, density-separated and then quantified for MP size and chemical composition using Raman and Infrared microscopy. By analyzing both atmospheric and surface Ocean MP we can determine MP deposition fluxes and marine MP emission fluxes, similar to sea salt aerosol production.

VI.2.3 Post-cruise sampling analyses and envisioned timeline of working plan, people involved on shore

Dissolved trace metal samples will be analyzed by Corentin Baudet during his PhD. Samples will be analyzed by summer 2022. Mercury samples were analyzed by Natalia Torres-Rodriguez. Some samples will be re-analyzed by winter 2021. Dissolved aluminium samples will be shipped to Resing's lab. They will arrive early June 2021 and analysis will be performed by summer 2021. Gallium samples will be shipped to Shiller's lab. They will arrive early June 2021 and analysis will be performed by summer 2021. Fluorine and cation samples will be shipped to Steiner's lab. They will arrive in early June 2021 and analysis will be performed by winter 2021. Microplastic samples will be shipped to Sonke's lab. They will arrive early June 2021 and analysis will be performed by summer 2022.

Table 20: Exhaustive list of collected parameters from the GEOFISH. "x" are used to identify the number of samples collected for each parameter

FISH ID	Date	Time start	Time end	Long.	Lat.	dFe	Hg	dAl	Fluorine	Cation	Micro-plastics	dGa	dTM	HS	Other
001	15/01/2021	11:55	12:19	49.750	-25.418	x	xx								
002	15/01/2021	17:20	17:30	48.496	-25.837	x	xx								
003	15/01/2021	20:40	20:59	47.723	-26.097	x	xx								
004	16/01/2021	00:00	00:13	51.000	-25.000	x	xx								
005	16/01/2021	04:45	04:47	45.830	-26.722	x									
006	16/01/2021	07:10	07:10	45.293	-26.900	x									
007	21/01/2021	10:20	10:22	32.513	-31.232	x	xx								
008	21/01/2021	12:20	12:27	32.770	-31.625	x	xx	x	xx	x	x				
009	21/01/2021	16:00	16:21	33.239	-32.349	x	xx								2x25L Hg isotopes
010	22/01/2021	02:30	02:55	33.531	-32.712	x	xx								
011	22/01/2021	05:50	06:02	33.734	-33.425	x	xx								
012	22/01/2021	08:05	08:14	33.927	-33.900	x	xx								
013	22/01/2021	10:00	10:05	34.093	-34.304	x	xx								
014	22/01/2021	12:27	12:32	34.308	-34.824	x	xx	x	xx	x	x				
015	22/01/2021	22:50	23:05	34.582	-35.353	x	xx	x	xx	x	x				
016															
017	23/01/2021	00:20	00:25	34.836	-35.656	x									
018	23/01/2021	01:20	01:38	35.004	-35.855	x	xx	x	xx	x					
019	23/01/2021	01:53	01:59	35.097	-35.966						x				
020	23/01/2021	03:25	03:37	35.368	-36.289	x	xx	x	xx	x					
021	23/01/2021	05:13	05:22	35.702	-36.685	x	xx								
022	24/01/2021	21:20	21:40	36.379	-39.801	x			xx	x					

023	24/01/2021	21:40	22:44	36.379	-39.801		xx								2x25L Hg isotopes
024	24/01/2021	22:58	23:05	36.380	-39.801	x									
025	26/01/2021	18:58	19:10	36.673	-40.418	x	xx	x	xx	x	x				
026	26/01/2021	19:58	20:07	36.734	-40.613	x	xx		xx	x					
027	26/01/2021	21:45	22:06	36.830	-40.961	x	xx	x	xx	x					
028	30/01/2021	01:11	02:26	36.269	-44.958	x	xx		xx	x	x				2x25L Hg isotopes
029	30/01/2021	17:14	17:31	36.770	-46.614	x	xx	x	xx	x					
030	30/01/2021	20:57	21:29	37.391	-47.030	x	xx	x	xx	x	x				
031	31/01/2021	02:08	02:25	37.671	-47.157	x	xx	x	xx	x					
032	01/02/2021	15:00	15:13	38.966	-47.307	x	xx	x	xx	x	x				
033	02/02/2021	01:32	01:48	39.328	-47.428	x	xx	x	xx	x					
034	02/02/2021	03:03	03:24	39.415	-47.188	x	xx	x	xx	x	x				1L dFe for calibrations
035	02/02/2021	05:17	05:28	39.539	-46.837	x	xx								
036	02/02/2021	13:25	13:35	40.942	-46.747	x	xx	x	xx	x					
037	02/02/2021	15:15	15:20	41.497	-46.774	x	xx								
038	02/02/2021	16:50	17:00	41.963	-46.802	x	xx	x	xx	x	x				
039	03/02/2021	01:15	01:32	42.581	-46.954	x	xx	x	xx	x					
040	04/02/2021	12:21	12:24	43.196	-47.387	x									
041	04/02/2021	21:30	21:43	44.324	-48.442	x		x	xx	x	x				
042	05/02/2021														
043	05/02/2021	04:20	04:25	45.313	-49.504	x		x	xx	x					
044	05/02/2021	18:35	18:46	46.951	-50.478	x	xx	x	xx	x	x				
045	05/02/2021	20:34	20:46	47.399	-50.716	x	xx	x	xx	x					
046	06/02/2021	00:26	00:36	48.278	-51.182	x	xx	x	xx	x					

047	06/02/2021	03:55	04:11	49.102	-51.610	x	xx	x	xx	x	x				
048	07/02/2021	06:17	06:28	49.871	-52.028	x	xx	x	xx	x					
049	07/02/2021	08:08	08:19	50.011	-51.774	x	xx								
050	07/02/2021	11:00	11:13	50.225	-51.404	x	xx	x	xx	x		x			
051	07/02/2021	12:15	12:20	50.305	-51.258	x	xx								
052	07/02/2021	14:15	14:29	50.434	-51.031	x	xx	x	xx	x	x	x			
053	07/02/2021	18:15	18:21	50.741	-50.471	x		x	xx	x		x			
054	08/02/2021	12:50	12:55	51.606	-48.750	x		x	xx	x		x			
055	08/02/2021	13:51	14:30	51.654	-48.562		xx								2x25L Hg isotopes
056	09/02/2021	05:12	05:22	51.888	-46.333	x		x	xx	x	x	x			
057	09/02/2021	05:35	05:38	51.889	-46.252	x							x	x	
058	09/02/2021	05:45	05:45	51.891	-46.218	x							x	x	
059	09/02/2021	05:55	05:55	51.893	-46.185	x		x					x	x	
060	09/02/2021	06:05	06:05	51.893	-46.152	x		x					x	x	
061	10/02/2021	01:24	01:25	51.884	-46.091	x									
062	10/02/2021	03:00	03:03	51.920	-45.822	x							x		
063	11/02/2021	00:17	00:26	52.875	-46.488	x		x	xx	x			x		
064	11/02/2021	06:05	06:11	54.798	-46.761	x			xx	x					
065	11/02/2021	08:05	08:07	55.358	-46.839	x		x			x				
066	11/02/2021	10:30	10:40	56.010	-46.931	x	xx	x	xx	x		x			
067	12/02/2021	12:20	12:32	57.103	-47.341	x	xx	x	xx	x	x	x			
068	12/02/2021	14:10	14:12	57.598	-47.524	x	xx								
069	12/02/2021	19:01	19:14	58.408	-47.597	x	xx	x	xx	x	x				
070	12/02/2021	21:41	21:47	59.122	-47.413	x	xx								

071	12/02/2021	23:56	23:59	59.690	-47.266	x	xx								
072	14/02/2021	23:58	00:16	65.706	-48.930	x	xx	x	xx	x	x				
073	15/02/2021	01:14	01:18	65.948	-49.074	x	xx								
074	15/02/2021	03:14	03:26	66.352	-49.315	x	xx	x	xx	x					
075	15/02/2021	05:12	05:19	66.738	-49.544	x	xx								
076	15/02/2021	11:15	11:25	67.672	-50.155	x	xx	x	xx	x	x	x			
077	15/02/2021	13:40	13:50	68.230	-50.520	x			xx	x		x			
078	16/02/2021	11:34	12:50	69.682	-51.478										Carboys Helene (2x20L+2 x25L)
079	16/02/2021	12:57	13:10	70.059	-51.559	x	xx	x	xx	x	x	x			
080	20/02/2021	19:10	19:25	77.666	-56.000	x	xx	x	xx	x					
081	20/02/2021	21:10	21:14	77.850	-56.100	x	xx								
082	21/02/2021	22:55	23:05	78.656	-56.532	x	xx	x	xx	x	x				
083	21/02/2021	05:45	05:52	79.049	-56.718	x	xx	x	xx	x	x	x			
084	21/02/2021	07:15	07:15	79.567	-56.962	x									
085	21/02/2021	09:10	09:15	80.227	-57.112	x		x	xx	x					
086	21/02/2021	11:03	11:07	81.384	-57.345	x	xx								
087	21/02/2021	14:17	14:55	81.924	-57.690	x	xx				x				
088	24/02/2021	21:43	21:50	76.614	-55.394	x		x	xx	x	x				
089	24/02/2021	23:15	23:17	76.261	-55.190	x									
090	25/02/2021	03:29	03:36	75.384	-54.678	x		x	xx	x					
091	25/02/2021	05:14	05:17	75.030	-54.468	x		x							
092	25/02/2021	06:53	06:54	74.685	-54.262	x									
093	25/02/2021	07:26	07:55	74.571	-54.196	x		x	xx	x	x				

094	25/02/2021	09:10	09:15	74.194	-53.970	x		x	xx	x					Marion (60mL)
095	25/02/2021	20:07	20:15	73.185	-53.363	x		x	xx	x					
096	25/02/2021	22:03	22:04	72.894	-53.186	x									
097	26/02/2021	05:22	05:43	73.314	-53.281	x		x	xx	x	x				Marion (60mL)
098	26/02/2021	09:10	09:15	74.108	-52.887	x		x	xx	x		x			
099	26/02/2021	19:56	20:07	74.481	-51.643	x		x	xx	x	x				
100	26/02/2021	21:17	21:18	74.168	-51.501	x									
101	27/02/2021	01:00	01:30	73.484	-51.230	x		x			x	x	x		
102	27/02/2021	14:43	14:53	72.082	-50.661	x					x	x			
103	27/02/2021	17:10	17:10	71.590	-50.334	x									
104	27/02/2021	19:25	19:35	71.134	-50.037	x			xx	x					
105	27/02/2021	20:43	20:45	70.874	-49.867	x									
106	28/02/2021	16:45	16:50	70.881	-49.334	x	xx		xx	x			x		
107	28/02/2021	17:09	17:09	70.998	-49.290	x							x		
108	28/02/2021	17:21	17:33	71.057	-49.268	x							x		
109	28/02/2021	18:20	18:25	71.290	-49.178	x	xx						x		
110	28/02/2021	18:55	18:58	71.450	-49.121	x	xx						x		
111	28/02/2021	19:10	19:15	71.517	-49.096	x	xx		xx	x			x		
112	28/02/2021	19:43	19:43	71.664	-49.040	x	xx						x		
113	28/02/2021	20:08	20:08	71.775	-48.998	x							x		
114	28/02/2021	20:40	20:40	71.917	-48.945	x			xx	x	x		x		
115	28/02/2021	21:10	21:10	72.050	-48.894	x							x		
116	28/02/2021	21:36	21:42	72.164	-48.850	x	xx		xx	x			x		
TOTAL						110	132	53	116	58	31	14	18	4	

References

Bruland, W., Rue, E.L., Smith, G.J., DiTullio, G.R.: Iron, macronutrients and diatom blooms in the Peru upwelling regime: brown and blue waters of Peru, Marine Chemistry, 93, 81-103, doi:10.1016/j.marchem.2004.06.011

de Villiers, S., Greaves, M. and Elderfield, H. (2002) An intensity ratio calibration method for the accurate determination of Mg/Ca and Sr/Ca of marine carbonates by ICP-AES. Geochemistry, Geophysics, Geosystems 3.

Greenhalgh, R. and Riley, J.P. (1961) The determination of fluorides in natural waters, with particular reference to sea water. Analytica Chimica Acta 25, 179-188.

Heimburger, L. E., Sonke, J. E., Cossa, D., Point, D., Lagane, C., Laffont, L., Galfond, B. T., Nicolaus, M., Rabe, B. & Van Der Loeff, M. R. Shallow methylmercury production in the marginal sea ice zone of the central Arctic Ocean. Sci. Rep. 5, (2015).

Kremling, K. (1999) Determination of the major constituents, in: K. Grasshoff, K.K.a.M.E. (Ed.), Methods of Seawater Analysis. WILEY-VCH Verlag GmbH, Weinheim, pp. 229-251.

Labatut, M., Lacan, F., Pradoux, C., Chmeleff, J., Radic, A., Murray, J. W., Poitrasson, F., Johansen, A. M. and Thil, F.: Iron sources and dissolved-particulate interactions in the seawater of the western Equatorial Pacific, iron isotope perspectives, Global Biogeochemical Cycles, 28, 1044–1065, doi:10.1002/2014GB004928, 2014.

Morel, F. M. M. and Price, N. M.: The biogeochemical cycles of trace metals in the Oceans, Science, 300(5621), 944–947, DOI: 10.1126/science.1083545, 2003.

Obata, H., Karatani, H. and Nakayama, E.: Automated determination of iron in seawater by chelating resin concentration and chemiluminescence, Analytical Chemistry, 65, 1524–1528, 1993.

Schrag, D.P. (1999) Rapid analysis of high-precision Sr/Ca ratios in corals and other marine carbonates. Paleoceanography 14, 97-102.

Sarthou, G., Timmermans, K. R., Blain, S. and Tréguer, P.: Growth physiology and fate of diatoms in the ocean: a review, Journal of Sea Research, 53(1), 25–42, doi:10.1016/j.seares.2004.01.007, 2005.

Steiner, Z., Turchyn, A.V., Harpaz, E. and Silverman, J. (2018) Water chemistry reveals a significant decline in coral calcification rates in the southern Red Sea. Nature Communications 9, 3615.

Steiner Z., Sarkar A., Prakash S., Vinayachandran P.N., Turchyn A.V. (2020). Dissolved strontium, Sr/Ca ratios, and the abundance of Acantharia in the Indian and Southern Oceans. ACS Earth and Space Chemistry.

Sunda, W. G.: Trace metal/phytoplankton interactions in the sea, in Chemistry of Aquatic systems: Local and Global Perspectives, edited by G. B. and W. Stumm, pp. 213–247, ECSC, EEC, EAEC, Brussels and Luxembourg., 1994.

Tonnard, M., Planquette, H., Bowie, A. R., van der Merwe, P., Gallinari, M., Desprez de Gésincourt, F., Germain, Y., Gourain, A., Benetti, M., Reverdin, G., Tréguer, P., Boutorh, J., Cheize, M., Menzel Barraqueta, J.-L., Pereira-Contreira, L., Shelley, R., Lherminier, P. and Sarthou, G.: Dissolved iron in the North Atlantic Ocean and Labrador Sea along the GEOVIDE section (GEOTRACES section GA01), Biogeosciences Discuss., 1–53, doi:10.5194/bg-2018-147, 2018.

Warner, T.B. (1971) Normal fluoride content of seawater. Deep Sea Research and Oceanographic Abstracts 18, 1255-1263.

Wilson, T.R.S. (1975) Salinity and the major elements of seawater, in: Riley, J.P., Skirrow, G. (Eds.), Chemical Oceanography, 2nd edition ed. Academic Press, Norwich, pp. 365-414.

VI.3 Mercury speciation and mercury isotopes

Principal investigator

On shore: Lars-Eric Heimbürger-Boavida

Mediterranean Institute of Oceanography, Bât. Méditerranée, Campus de Luminy-Océanomed, 13009 Marseille.

lars-eric.heimburger@mio.osupytheas.fr

On board: Natalia Torres-Rodriguez

Mediterranean Institute of Oceanography, Bât. Méditerranée, Campus de Luminy-Océanomed, 13009 Marseille.

natalia.torres-rodriguez@mio.osupytheas.fr

Names of other participants (Clean CTD sampling team)

Bruno Hamelin (CEREGE, hamelin@cerege.fr), Wen-Hsuan Liao (LEMAR, liao.wenhsuan@univ-brest.fr), David González-Santana (LEMAR, david.gonzalezsantana@univ-brest.fr), Corentin Baudet (LEMAR, corentin.baudet@univ-brest.fr), Maria-Elena Vorrath (LEMAR, mariaelena.vorrath@univ-brest.fr), Nolwenn Lemaitre (ETH, nolwenn.lemaitre@erdw.ethz.ch)

Abstract :

Mercury is one of the trace metals with the most extravagant biogeochemical cycle, including complex photochemistry, redox-chemistry, sea-air exchange and microbial transformations, coupled with strong anthropogenic impacts.

The SWINGS cruise provides the first Hg measurements in the Indian Ocean, and is the first GEOTRACES cruise providing the full suite of Hg species, Hg stable isotope measurements and the highest Hg resolution thus far.

The precious new observations will allow to test several issues that are key to the understanding of the global Hg cycle. Notably, we will investigate hemispheric gradients, sea-air exchange, possible hydrothermal inputs, island effects, microbial MeHg production, and historic Hg deposition among others.

VI.3.1 Scientific context

The UNEP Minamata Convention[1] ratified in 2017, aims to reduce human exposure to toxic mercury (Hg). We are primarily exposed *via* the consumption of fish that bioaccumulate Hg from the ocean[2]. Current estimates of anthropogenic Hg emissions highlight a 3-fold increase in Hg levels in the surface ocean since pre-industrial times[3]. And, while decades of intense research have led to a good understanding of anthropogenic Hg fluxes, we still lack answers to some of the most fundamental questions concerning the natural Hg sources and transformations in the environment [4,5]. Hydrothermal vents represent

potentially the single most important natural source of Hg, yet flux estimates range several orders of magnitude (20 to 2000 t y^{-1}). The SWINGS cruise is a unique opportunity to sample the SWIR and also to obtain the first ever Hg measurements in the Indian Ocean.

VI.3.2 Overview of the project and objectives

- Establish the first Hg species (total mercury = tHg, dissolve gaseous mercury = DGM, methylated mercury = MeHg, monomethyl mercury = MMHg, particulate mercury = pHg, particulate monomethyl mercury = pMMHg) measurements in the Indian Ocean.
- Test with the new observations if the SWIR affects Hg species distribution.
- Test if the southern hemisphere has lower sea water Hg concentrations, similar to observed atmospheric gradients.
- Samples of tHg/DGM collected by trace metal clean surface sampler (GeoFISH) will be used to corroborate a possible latitudinal gradient, and in combination with the aerosol pHg observations, will help to evaluate Hg deposition and evasion/exchange with the atmosphere.

Hg isotopes will help to decipher sources and processes affecting Hg cycling in the study area.

VI.3.3 Methodology and sampling strategy

Unfiltered samples were collected from the TMR equipped with GOFLO bottles. Different types of bottles were used depending on the Hg species to be analysed: tHg was collected into 60 mL PFA/FEP bottles, DGM/MMHg into 125 mL PET bottles and MeHg into 380 mL PFA bottles. Right after collection THg samples were oxidized by addition of 40 µL of 180 mM BrCl and subsequently reduced to Hg^0 by addition of 40 µL of $SnCl_2$. Purged Hg° was measured onboard *via* a custom-made by purge and trap, cold vapor atomic fluorescence (CVAFS[6]). Duplicates were run for 447 samples out of 607. Dissolved gaseous Hg was measured directly using the same method without the addition of any reagent. MeHg samples were acidified with HCl to 0.4% v/v. and stored at 4°C. DGM-purged samples were treated similarly, for subsequent MMHg analysis. A total of 607 samples for tHg, 328 samples for DGM/MMHg and 562 samples for MeHg were collected (Table 21). In addition, 111 tHg and DGM samples from the GeoFISH were collected at some selected stations with an average resolution of 3 to 4 hours (see GeoFISH report for more detail).

For Hg isotopes 12 bottles of 25 L were collected at stations swg_C_11_31 and swg_C_33_85, at three depths (two bottles per depth) representing the chlorophyll maximum, oxygen minimum and the bottom waters. Total Hg analysis on board of cast swg_C_11_31 gave anomalous high Hg concentrations due to contamination with $HgCl_2$. Those bottles were emptied and a third cast (swg_C_58_150) was collected at similar depths. Furthermore, filters for pHg isotopes were collected from the *in situ* pumps at the same depths in these casts and stored at -20°C (see *in-situ* pumps report for more detail). In addition, 12 bottles of 25 L were collected by GeoFISH at six stations (see GeoFISH report for more detail).

Finally, punches for pHg analysis were collected from the *in-situ* pumps at selected depths and stored at -20°C (see in-situ pumps report for more detail).

Table 21: Collected Hg samples from TMR equipped with GO-FLO bottles.

Station	Code of operation (Station-cast)	tHg	DGM/MMHg	MeHg
1	swg_C_01_002	69	13	24
2	swg_C_02_007	20	10	20
3	swg_C_03_011	25	14	25
4	swg_C_04_014	13	11	13
5	swg_C_05_018	11	11	11
8	swg_C_08_23	18	12	18
10	swg_C_10_27	22	13	22
11	Swg_C_11_31*	11	8	11
	sgw_C_11_34	23	13	23
14	swg_C_14_41	22	11	22
16	swg_C_16_47	21	12	21
18	swg_C_18_49	22	10	22
19	swg_C_19_51	12	7	12
20	sgw_C_20_53	4	0	4
21	swg_C_21_58	12	7	12
25	swg_C_25_68	23	11	23
27	swg_C_27_74	24	11	24
29	swg_C_29_77	24	13	24
31	swg_C_31_82	24	11	24
33	swg_C_33_87	17	10	17
	swg_C_33_85*	4	3	4
35	swg_C_35_93	14	9	14
36	swg_C_36_98	24	12	24
38	swg_C_38_102	11	22	11
40	swg_C_40_109	20	9	20
42	swg_C_42_112	20	7	20
44	sgw_C_44_117	22	6	22
45	sgw_C_45_122	2	1	2
46	sgw_C_46_125	3	3	3
47	sgw_C_47_130	18	8	18
58	sgw_C_58_144	15	6	15
	Sgw_C_58_150*	4	3	4
63	sgw_C_63_156	13	11	13
65	sgw_C_65_159	3	3	3
66	sgw_C_66_163	5	5	5
67	sgw_C_67_167	5	5	5
68	sgw_C_68_169	7	7	7
Total		607	328	562

*Stations where isotopes samples were collected.

VI.3.4 Preliminary results

In general, tHg exhibited low concentrations (0.3 - 0.4 pM) in the surface waters with increasing concentrations towards the bottom (up to 1 pM; Figure 0-), with the exception of station 58 (southernmost station, Figure 0-6D) that showed tHg concentrations of up to 1.2 pM in the upper 200 m. The layers depleted in oxygen displayed the highest tHg concentrations (Figure 0-6C). Dissolved gaseous Hg displayed concentrations between 0.0 – 0.5 pM with values increasing towards the bottom and following patterns similar to tHg profiles (Figure 0-6), but the peak depth appears to be slightly different (Figure 0-6C).

VI.3.5 Post-cruise sampling analyses and envisioned timeline of working plan, people involved on shore

Samples collected for MeHg and MMHg will be analyzed *via* GC-SF-ICPMS[6], within 8 months after arrival at MIO. Sediments and *in situ* pump filters will be analyzed for pHg *via* CV-AAS within 2 months after arrival at MIO[6]. pMMHg will be analyzed similar to MeHg within 18 months, after digestion of the filter, and only if the amount of pHg is sufficient. Sea water and filters for Hg isotopes will be analyzed within 18 months after arrival at GET.

References

1 http://www.mercuryconvention.org/

2 Petrova, M. V., Ourgaud, M., Boavida, J. R., Dufour, A., Onrubia, J. A. T., Lozingot, A., & Heimbürger-Boavida, L. E. (2020). Human mercury exposure levels and fish consumption at the French Riviera. Chemosphere, 258, 127232.

3 Lamborg, C. H., Hammerschmidt, C. R., Bowman, K. L., Swarr, G. J., Munson, K. M., Ohnemus, D. C., ... & Saito, M. A. (2014). A global ocean inventory of anthropogenic mercury based on water column measurements. Nature, 512(7512), 65-68.

4 United Nations Environment Programme Global Mercury Assessment 2018.

5 Outridge, P. M., Mason, R. P., Wang, F., Guerrero, S., & Heimburger-Boavida, L. E. (2018). Updated global and oceanic mercury budgets for the United Nations Global Mercury Assessment 2018. Environmental science & technology, 52(20), 11466-11477.

6 Heimbürger, L. E., Sonke, J. E., Cossa, D., Point, D., Lagane, C., Laffont, L., Galfond, B. T., Nicolaus, M., Rabe, B. & Van Der Loeff, M. R. Shallow methylmercury production in the marginal sea ice zone of the central Arctic Ocean. Sci. Rep. 5, (2015).

VI.4 Particulate and dissolved REE

Principal investigator
Catherine Jeandel
Legos, Observatoire Midi-Pyrénées, 31400, Toulouse
33561332933
Catherine.jeandel@legos.obs-mip.fr

Names of other participants: Moustafa Belhadj (LEGOS), Hélène Planquette (LEMAR, Brest) and the team of the clean container

Abstract:

Rare Earth Elements are a family of 14 elements that slightly differ from each other by their weight and their atomic radius. These differences induce a slightly different behavior between the different REE in the physico-chemical reactions as dissolution/precipitation, adsorption/desorption and all processes involved in the dissolved/particle exchange. REE are therefore a good tracer of the dissolved/particle exchange; they also help to constrain the "apparent ageing" of the water masses: when the later encounter clouds of particles, this is quickly imprinted in their REE patterns. In the framework of SWINGS, ca 219 samples of 12L of seawater were filtered in the clean container directly from the Go-Flo sampling bottles in order to collect suspended particles and analyze PREE. Aliquots of 500 mL of filtered seawater and 25 samples of unfiltered one were immediately acidified in order to determine the dissolved and sometimes "total REE" concentrations in the seawater. Comparison of the dissolved data with the suspended particle ones help to constrain dissolve/particulate exchanges.

VI.4.1 Scientific context

Particulate and dissolved REE sampling and analyses are integrated in the general scientific framework of SWINGS. SWINGS cruise (January 11th-March 8th 2021) realized an integrated oceanographic transect in the South West Indian Ocean. This area is crucial for the Earth climate and the thermohaline circulation as it represents a major hub of heat, salt and chemical transports between the Atlantic and Indian sectors of the Southern Ocean. Combining physical oceanography and tracers can strongly help to better constrain the uncertainties on the transport estimation across the cruise track, notably by adding information on the deep-water mass export and circulation. DREE and PREE have barely been measured in the Southern Indian Ocean, except on process studies conducted around Kerguelen island (Zhang et al., 2008; Grenier, M. et al., 2018). SWINGS will also allow determining a variety of sources and sinks that influence the distribution of tracers in this area. Advective and scavenging processes, biological uptake, exchanges with the margins, atmospheric deposition, and hydrothermalism along the South West Indian Ridge (SWIR) will be investigated.

VI.4.2 Overview of the project and objectives

In this general framework, particulate REE were collected as often as possible together with the dissolved REE in order to 1) map their distribution and their physical and chemical speciation along a full-depth ocean section 2) characterize their sources and sinks and quantify their fluxes at the ocean boundaries

3) investigate the link between the REE and the production, export and remineralization of particulate organic matter

VI.4.3 Methodology and sampling strategy

This strategy allowed us to collect exactly at the same depths the dissolved and particulate REE, essential when tracing the exchanges between these 2 phases. The filters were stored at room temperature and then transferred to the laboratory on land (LEMAR, Brest, France). The full filters will be digested in LEMAR in the framework of Corentin Baudet's thesis and an aliquot of each leachate will be sent to Toulouse (LEGOS) in order to proceed to the PREE analyses.

For dissolved REE concentration analyses, 500 mL were immediately filtered onboard (PES membrane, 25mm 0.45 µm) in the clean container. This strategy allowed us to collect exactly at the same depths the dissolved and particulate REE, essential when tracing the exchanges between these 2 phases. The 500 ml aliquots were acidified to pH = 1.5 with twice-distilled HCl. The samples were stored at room temperature and then transferred to the laboratory on land (LEGOS, Toulouse, France).

PREE Planned analytical procedure:

Particulate Rare Earth Element concentrations will be measured by High Resolution Inductively Coupled Plasma Mass Spectrometers (ICP-MS) using an Element-XR (using Aridus desolvation introduction system). All the REEs present in the leaching will be determined by the external standard method. Potential sensibility variations during the measurement session are monitored by In/Re internal standard method so that the final REE concentrations are corrected accordingly.

DREE Planned analytical procedure*:*

The purification and preconcentration of DREE will be performed following the method developed in LEGOS by Viet Pham as part of his PhD thesis (Pham, 2020). Briefly, the acidified seawater samples will tri spiked with ^{150}Nd, ^{151}Eu and ^{172}Yb and brought o pH ca 5-6 using and ammonium acetate buffer. DREE will be then passed on Nobias resin cartridges using an online manifold. After elution, dissolved Rare Earth Element concentrations will be then measured by High Resolution Inductively Coupled Plasma Mass Spectrometers (ICP-MS) using an Element-XR (using Aridus desolvation introduction system). All the REEs will also be determined by the external standard method, whereas Nd and Yb are additionally determined by isotopic dilution. The values obtained for Nd and Yb concentrations by both methods enable us to determine the analytical recovery yields of these two elements in each sample, which ranges are: 88-96% and 83-94% for Nd and Yb, respectively. Efficiencies of the chemical protocol for the other REE are calculated by linear interpolation. Potential sensibility variations during the measurement session are monitored by In/Re internal standard method so that the final REE concentrations are corrected accordingly.

VI.4.4 Preliminary results

Not relevant, the following procedure will be done on land (see below)

VI.4.5 Post-cruise sampling analyses and dead-lines

Analyses of PREE and DREE require on land based clean laboratory. They cannot be done on board. We will make all what's possible to perform these analyses within the next 2 years.

Data base organization (general cruise base and/or specific data base(s))

The DREE and PREE data will be submitted in the Geotraces open source data base GDAC, hosted in BODC. The data submission will follow all the Geotraces required criteria and steps (Intercalibration, Standard and Intercalibration committee, Data Portal DOoR etc…).

The synthesis of the number of samples taken during the SWINGS cruise for dissolved and particulate REE, together with the number of samples taken for dissolved Nd isotopic composition, dissolved Pa and Th and Total Ac is proposed Table 22 (see chapter 7, section Nd IC).

References

Grenier M, Garcia-Solsona E, Lemaitre N, Trull TW, Bouvier V, Nonnotte P, van Beek P, Souhaut M, Lacan F and Jeandel C (2018) Differentiating Lithogenic Supplies, Water Mass Transport, and Biological Processes On and Off the Kerguelen Plateau Using Rare Earth Element Concentrations and Neodymium Isotopic Compositions. Front. Mar. Sci. 5:426. doi: 10.3389/fmars.2018.00426

Pham,V. (2021) Tracing the lithogenic imprint in the Coral and Solomon seas using the rare earth concentrations and neodymium isotopic compositions PhD thesis, Paul Sabatier University.

Zhang Y., Lacan F. Jeandel C.(2008) Dissolved Rare Earth Elements Trace Terrigeneous Inputs in the Wake of the Kerguelen Island (Southern Ocean) Deep-Sea Research Part II-Topical Studies in Oceanography, KEOPS special issue 55, 638-652, doi:10.1016/j.dsr2.2007.12.029.

VII. ISOTOPES AND RADIONUCLIDES

VII.1Silicon and barium biogeochemical cycles along the SWINGS transect and their links with circulation and carbon cycle

Principal investigator
On board : Damien Cardinal
LOCEAN-IPSL – CP 100 – Sorbonne Université, 4 place Jussieu, 75252 Paris Cedex 05
+33 (0)1 44 27 48 79
damien.cardinal@sorbonne-universite.fr

Names of other participants
On board: Marine Piéjus, volunteer, marine.piejus@yahoo.fr
On shore : Stéphanie Jacquet
Aix Marseille Université, CNRS/INSU, Université de Toulon, IRD, Mediterranean Institute of Oceanography (MIO), UM 110, 13288 Marseille, France
stephanie.jacquet@mio.osupytheas.fr

Abstract

The work on-board SWINGS was to collect samples for concentrations and isotopic composition of silicon (D. Cardinal) and barium (S. Jacquet) using whenever possible common seawater samples collected from standard CTD (Niskin) and filtered with the same filtration units. For particulate silicon, samples were also collected from *in situ* pumps, while for particulate barium, samples collected from clean CTD and filtered in the clean container are also available. With the wide diversity of marine environments covered by the SWINGS section and using the isotopic compositions and concentrations of both particulate and dissolved phases, we aim at better understand the silicon and barium cycles (for Si: e.g. role of diatoms, production, mixing, circulation, oceanic weathering, settling, remineralization….; for Ba: e.g. C export and remineralization, circulation, barite precipitation…).

VII.1.1 Scientific context

Si

Silicon (Si) in its dissolved form, silicic acid (DSi), is a key nutrient for silicifying organisms, mainly diatoms that are often the dominant phytoplankton in the Southern Ocean (SO) and that are important players in the biological carbon pump. The overall scientific objective of the work is to better understand the controlling factors of the ocean's silicon (Si) biogeochemical cycle by comparing different SO environments. To progress in this objective, we will use the Si isotopic signatures of silicic acid and biogenic silica (BSi). We will measure also the concentration of BSi.

Ba

We propose with the SWINGS project to set a reinforced particulate barium (P_Ba) proxy to further constrain carbon attenuation fluxes in the mesopelagic zone. One of the major questions surrounding P_Ba concerns particulate-dissolved Ba dynamics at the depth of POC remineralization. Our major

question is the following: Is dissolved Ba (D_Ba) the source of P_Ba and over what depth range does P_Ba precipitate? The overarching goal is to pinpoint POC remineralization and P_Ba formation horizons in the water column.

VII.1.2 Overview of the project and objectives

SWINGS campaign is covering a wide range of oceanic environments: continental margin of Southern Africa, Agulhas current, oligotrophic subtropical zone and along the Antarctic Circumpolar Current: the « High Nutrients Low Chlorophyll » (HNLC) regions in the Sub Antarctic, Polar Front and Antarctic Zones, and in addition, areas under the direct influence of volcanic islands (Marion, Prince Edward, Crozet, Kerguelen, Mac Donald and Heard).

With such diversity of biogeochemical regions and using silicon isotopic compositions of dissolved and biogenic silicon, the specific objectives are to provide information on the degree of Si utilization and source to the mixed layer (e.g. relative contribution of Ekman northward transport and winter vertical mixing), its fate along the water column (remineralization and/or export, including isotope systematics for application in paleoceanography) and its transport along the deep global circulation. Finally, we also aim at exploring a potential Si isotopic signature inherited from hydrothermalism and/or oceanic basalt weathering as first guessed around Heard Island during KEOPS-1 (Fripiat et al. 2011). Similar studies have already been implemented in the SO (e.g. Fripiat et al. 2012; Closset et al. 2016), but never in the ocean at such spatial resolution and covering so diverse marine environments.

Regarding barium, our hypothesis is that the D_Ba distribution and Ba-isotopic composition in seawater reflect horizons of P_Ba barite formation. The corollary to these hypotheses suggests that a water mass that experienced organic C remineralization processes should display a concurrent D_Ba depletion and Ba-isotopic fractionation. We will address it by deconvolving and quantifying the competing biogeochemical (particulate-dissolved Ba interactions, a non-conservative process) and physical (ocean circulation, a conservative process) aspects of marine Ba cycling. This will be done by utilizing D_Ba and Ba-isotopic measurements in seawater in a variety of biogeochemical provinces in the Southern Ocean.

VII.1.3 Methodology and sampling strategy

Sampling strategy

Si isotopes have been sampled and will be processed according to the GEOTRACES cookbook. Suspended particulate samples (collected from Niskin bottles) and dissolved samples (generally over the whole water column) are available from the SWINGS transect at 37 stations (all L stations, most M stations + some H and OISO stations) while settling particles (collected from in-situ pumps) have been collected at all L stations (Table 24). Because of the limited particulate material available from Niskin at depth we expect to measure BSi concentration on the upper 2000m only and BSi isotopic composition in the upper 200m. For deeper BSi concentration and isotopic composition we rely on in-situ pumps only. For P_Ba the upper 1000m is of interest only.

Sample processing on-board

Seawater collected from standard CTD with Niskin has been filtered on-board immediately after collection on PES 0.4 μm membranes (47 mm, SUPOR Pall) in 6L pressurised Perspex unit (20 psi). The pressurised air was first filtered through 0.6 μm Polycarbonate (PC) membranes.

Filtrate: Depending on the depths and stations, for Si isotopes between 2L (e.g. in surface) to 125 mL (for deep samples) of filtrate was stored in HCl pre-cleaned PP vials and kept unacidified in the dark at room temperature. For Ba isotopes a 125 ml aliquot of the same filtrate was stored in PC vials (rinsed 3 times with the filtrate) and acidified with 125 uL of ultra-clean HNO3 (69%) and stored in the dark at room temperature. For two stations filtrates were collected from clean CTD with Go-Flo filtered in the clean container (also with 0.45 μm SUPOR membranes).

Suspended particles on SUPOR membranes (between 2 to 6L depending on water availability) were rinsed with 10-20 ml of deionized water then stored in plastic Petri slides and dried for 24h on-board at 60°C. The same membranes will be used for BSi concentration, BSi and/or P_Ba by splitting the membrane in two whenever necessary. P_Ba will also be available from the clean CTD samples and processed by C. Baudet & H. Planquette (LEMAR).

¼ of in-situ pump 96 mm 0.8 μm SUPOR membranes from in-situ pumps was cut with a metallic cutter under laminar hood to measure BSi concentration and isotopic composition of settling particles.

Table 22: Exhaustive list of measured parameters for the study of Ba and Si

Parameter	Code of operation (Station-cast)	Number of samples
BSi concentration_bottle	Standard CTD, stations 2, 3, 4, 5, 8, 10, 11, 14, 15,16, 19, 20, 21,23, 25, 26, 27, 29, 33, 34, 35, 36, 38, 40, 42, 44,45, 46, 47, 58, 63, 65, 66, 67, 68, OISO E69, OISO 12	~ 250
BSi concentration_pump	PUMP stations 3, 4, 11, 14, 15, 21, 25, 33, 35, 38, 42, 44, 47, 58, 68	~ 80
BSi isotope bottle	Standard CTD, stations 2, 3, 4, 5, 8, 10, 11, 14, 15,16, 19, 20, 21,23, 25, 26, 27, 29, 33, 34, 35, 36, 38, 40, 42, 44,45, 46, 47, 58, 63, 65, 66, 67, 68, OISO E69, OISO 12	~150
BSi isotopes pump	PUMP stations 3, 4, 11, 14, 15, 21, 25, 33, 35, 38, 42, 44, 47, 58, 68	~ 80
DSi isotope bottle	Standard CTD, stations 2, 3, 4, 5, 8, 10, 11, 14, 15,16, 19, 20, 21,23, 25, 26, 27, 29, 33, 34, 35, 36, 38, 40, 42, 44,45, 46, 47, 58, 63, 65, 66, 67, 68, OISO E69, OISO 12	~ 580
D_Ba concentration bottle	Standard CTD, stations 2, 3, 4, 5, 8, 10, 11, 14, 15,16, 19, 20, 21,23, 25, 26, 27, 29, 33, 34, 35, 36, 38, 40, 42, 44,45, 46, 47, 58, 63, 65, 66, 67, 68, OISO E69, OISO 12	~ 580
P_Ba concentration bottle	Standard CTD, stations 2, 3, 4, 5, 8, 10, 11, 14, 15,16, 19, 20, 21,23, 25, 26, 27, 29, 33, 34, 35, 36, 38, 40, 42, 44,45, 46, 47, 58, 63, 65, 66, 67, 68, OISO E69, OISO 12	~ 400
D_Ba isotope bottle	Standard CTD, stations 2, 3, 4, 5, 8, 10, 11, 14, 15,16, 19, 20, 21,23, 25, 26, 27, 29, 33, 34, 35, 36, 38, 40, 42, 44,45, 46, 47, 58, 63, 65, 66, 67, 68, OISO E69, OISO 12	~ 580

VII.1.4 Post-cruise sampling analyses and envisioned timeline of working plan, people involved on shore

Si

Briefly, Mg-induced preconcentration (MAGIC) step will be performed on low DSi content and alkaline leaching for BSi followed by cation exchange chromatography and MC-ICP-MS analysis in dry plasma mode (as e.g. in Closset et al. 2016). Particulate aluminium will be measured by ICP-MS to subtract the lithogenic silicon contribution to particulate Si and calculate BSi (Ragueneau et al. 2005). Samples processing will be performed in our clean lab at LOCEAN-IPSL while isotopic analyses will be measured at LSCE-IPSL (with the help of Mustapha Benrahmoune, T_CNRS at LOCEAN and Arnaud Dapoigny, Engineer CEA in charge of MC-ICP-MS at LSCE-IPSL). Such configuration has been validated by the GEOTRACES Si isotopes intercalibration (Grasse et al. 2017).

A 6-month internship for a Master student is funded through ANR SWINGS for BSi concentration measurements in 2021-2022. Therefore, these results are expected to be available by summer 2022.

For Si isotopes, a Ph. D. topic is proposed at Doctoral School Environmental Sciences - Ile de France (ED129). If funded the scholarship is to start October 2021. Therefore, the analyses of Si isotopes are expected to last at least until 2024.

Note that with the high number of samples collected for Si isotopes we do not aim at measuring all. We will first measure at a coarser depth and spatial resolutions and then refine the profiles depending on the preliminary results. Samples for Si isotopes can be stored for years without any change.

Ba

Dissolved and particulate Ba will be measured at MIO using a HR-ICP-MS (Element XR). P_Ba will also be available from the clean CTD samples and processed by H. Planquette (LEMAR). Ba isotopes measurements will be done in collaboration with T. Horner (WHOI, US). Setting up a postdoctoral project on Ba isotopic method development is in discussion.

References

Allmen, Katja von, Michael E. Böttcher, Elias Samankassou, and Thomas F. Nägler. “Barium Isotope Fractionation in the Global Barium Cycle: First Evidence from Barium Minerals and Precipitation Experiments.” Chemical Geology 277, no. 1 (2010): 70–77. doi:https://doi.org/10.1016/j.chemgeo.2010.07.011.

Closset, I., Cardinal, D., Rembauville, M., Thil, F., & Blain, S. (2016). Unveiling the Si cycle using isotopes in an iron fertilized zone of the Southern Ocean: from mixed layer supply to export. Biogeosciences, 13, 6049–6066. https://doi.org/10.5194/bg-2016-236

Fripiat, F., Cavagna, A.-J., Savoye, N., Dehairs, F., André, L., & Cardinal, D. (2011). Isotopic constraints on the Si-biogeochemical cycle of the Antarctic Zone in the Kerguelen area (KEOPS). Marine Chemistry, 123(1–4), 11–22. https://doi.org/10.1016/j.marchem.2010.08.005

Fripiat F., Cavagna A.-J., Dehairs F., de Brauwere A., André L., & Cardinal D. (2012). Processes controlling the Si-isotopic composition in the Southern Ocean and application for paleoceanography. Biogeosciences, 9, 2443–2457. http://www.biogeosciences.net/9/2443/2012/bg-9-2443-2012.html

Grasse, P., Brzezinski, M. A., Cardinal, D., de Souza, G. F., Andersson, P., Closset, I., Cao, Z., Dai, M., Ehlert, C., Estrade, N., Francois, R., Frank, M., Jiang, G., Jones, J. L., Kooijman, E., Liu, Q., Lu, D., Pahnke, K., Ponzevera, E., … Zhang, Z. (2017). GEOTRACES inter-calibration of the stable silicon isotope composition of dissolved silicic acid in seawater. Journal of Analytical Atomic Spectrometry, 32(3), 562–578. https://doi.org/10.1039/C6JA00302H

Horner, Tristan J., Christopher W. Kinsley, and Sune G. Nielsen. “Barium-Isotopic Fractionation in Seawater Mediated by Barite Cycling and Oceanic Circulation.” Earth and Planetary Science Letters 430 (November 15, 2015): 511–22. doi:10.1016/j.epsl.2015.07.027.

Jacquet, S. H. M., F. Dehairs, D. Lefèvre, A. J. Cavagna, F. Planchon, U. Christaki, L. Monin, L. André, I. Closset, and D. Cardinal. “Early Spring Mesopelagic Carbon Remineralization and Transfer Efficiency in the Naturally Iron-Fertilized Kerguelen Area.” Biogeosciences 12, no. 6 (March 17, 2015): 1713–31. doi:10.5194/bg-12-1713-2015.

Jacquet, S. H. M., F. Dehairs, N. Savoye, I. Obernosterer, U. Christaki, C. Monnin, and D. Cardinal. “Mesopelagic Organic Carbon Remineralization in the Kerguelen Plateau Region Tracked by Biogenic Particulate Ba.” Deep Sea Research Part II: Topical Studies in Oceanography, KEOPS: Kerguelen Ocean and Plateau compared Study, 55, no. 5–7 (March 2008b): 868–79. doi:10.1016/j.dsr2.2007.12.038.

Jacquet, S.H.M., C. Monnin, V. Riou, L. Jullion, and T. Tanhua. "A High Resolution and Quasi-Zonal Transect of Dissolved Ba in the Mediterranean Sea." Marine Chemistry 178 (January 20, 2016): 1–7. doi:10.1016/j.marchem.2015.12.001.

Jullion, L., S. H. M. Jacquet, and T. Tanhua. "Untangling Biogeochemical Processes from the Impact of Ocean Circulation: First Insight on the Mediterranean Dissolved Barium Dynamics." Global Biogeochemical Cycles 31, no. 8 (2017): 1256–70. doi:10.1002/2016GB005489.

Ragueneau, O., Savoye, N., Del Amo, Y., Cotten, J., Tardiveau, B., & Leynaert, A. (2005). A new method for the measurement of biogenic silica in suspended matter of coastal waters: using Si:Al ratios to correct for the mineral interference. Continental Shelf Research, 25(5–6), 697–710. https://doi.org/10.1016/j.csr.2004.09.017

VII.2 Dissolved and particulate Nd isotopes

Principal investigator
On board: Catherine Jeandel
Legos, Observatoire Midi-Pyrénées, 31400, Toulouse
+33 (0) 561332933
Catherine.jeandel@legos.obs-mip.fr

Names of other participants:
On board: Moustafa Belhadj (AI, CNRS, LEGOS, Toulouse), Marion Lagarde (PhD student, LEGOS, Toulouse), Christophe Cassou (DR, CNRS, CECI, CERFACS)

Abstract:

Among the REE elements, Nd is characterized by 7 isotopes. "Nd isotopic composition" refers to the very precise analysis of the $^{143}Nd/^{144}Nd$ ratio. The variation of this ratio in the different oceanic compartments (water masses, particles…) is a good tracer of 1) the sources of chemical element to the water masses at the ocean boundaries and 2) trajectory and history of the water masses in a low frequency circulation dynamic.

In the framework of SWINGS, we collected 247 samples (average V= 10 L) of filtered seawater and 25 samples of unfiltered one in order to determine the dissolved Nd isotopic composition of the different water masses. Comparison of these dissolved data with the suspended particle ones collected by the filtration of large volumes of water using *in situ* pumps will help to constrain dissolved/particulate exchanges.

VII.2.1 Scientific context

Nd isotopes sampling and analyses are integrated in the general scientific framework of SWINGS. SWINGS cruise (January 11th-March 8th 2021) realized an integrated oceanographic transect in the South West Indian Ocean. This area is crucial for the Earth climate and the thermohaline circulation as it represents a major hub of heat, salt and chemical transports between the Atlantic and Indian sectors of the Southern Ocean. Combining physical oceanography and tracers can strongly help to better constrain the uncertainties on the transport estimation across the cruise track, notably by adding information on the deep-water mass export and circulation. Tracers like Nd isotopes are precious in this context. SWINGS will also allow determining a variety of sources and sinks that influence the distribution of tracers in this area. The relative roles of advective and scavenging processes, biological uptake, exchanges with the

margins, atmospheric deposition, and hydrothermalism along the South West Indian Ridge (SWIR) in the Nd IC distribution will be investigated.

VII.2.2 Overview of the project and objectives

The oceanic waters are strongly suspected to acquire their Nd concentrations and isotopic signatures at the continent/ocean interface, mostly through a significant exchange of Nd between water masses and the margin along which they flow. This isotopic signature reflects the abundance variation of ^{143}Nd isotope. It is commonly expressed as $\varepsilon_{Nd} = \left(\frac{\left(\frac{^{143}Nd}{^{144}Nd}\right)_{Sample}}{\left(\frac{^{143}Nd}{^{144}Nd}\right)_{CHUR}} - 1 \right) \times 10^4$ where "CHUR" is a reference, representing the average 143Nd/144Nd earth value. The continental margins surrounding the world ocean display different isotopic signature, mostly reflecting their different geological origin and story: from margins covered by old granitic sediments with a low ^{143}Nd/^{144}Nd ratios (i.e. negative εNd values, South Africa is a good example) to the volcanic ones, with high ^{143}Nd/^{144}Nd ratios (εNd values positive or close to 0, Crozet and Kerguelen islands for example). This property allows the quantification of the fraction of weathered material that dissolves at the continent/ocean or island/ocean interface (Lacan and Jeandel, 2005; Arsouze et al, 2009). Once water masses have acquired their Nd isotopic composition in a specific area, Nd isotopes behave quasi conservatively and can be assimilated to a "color" used to trace the pathways of the water masses (Piepgras and Wasserburg, 1983; Jeandel, 1993; Lacan and Jeandel, 2004). Nd isotopes have barely been measured in the Southern Indian Ocean, except on process study conducted around Kerguelen island (Zhang et al., 2008; Grenier, M. et al., 2018). Owing to the importance of the Nd parameters as "tags" of the low frequency circulation, as imprinted for example in the deep water corals or foraminifera shells, solving these issues is essential. In addition, close analyses of the dissolved/particulate exchange -conducted with that dedicated to the Fe speciation at the particle surface- will allow understanding better the processes yielding the release of REE at the sediment/water (or particle/water) interface.

In this goal, dissolved and particulate Nd isotopes were collected as often as possible in order to 1) map their distribution and their physical and chemical speciation along a full-depth ocean section 2) characterize their sources and sinks and quantify their fluxes at the ocean boundaries 3) investigate the link between the isotope transport and the production, export and remineralization of particulate organic matter.

VII.2.3 Methodology and sampling strategy

For dissolved Nd isotope analyses, ~247 samples of 10 L of seawater were collected from Niskin bottles of the classic rosette at each L stations and some M and H stations in order to ensure the best vertical and horizontal resolutions, and "tag" the water masses as precisely as possible (Table 23). Samples were immediately filtered onboard through ACROPACK cartridges under pressured clean air. They were immediately loaded on C18 pre-cleaned cartridges at pH 3.7, following the procedure initially described in Tachikawa et al (1999).

For particulate Nd isotope analyses, 115 samples were filtered on SUPOR membranes using in situ pumps deployed at the same depths as most of the sampling bottles dedicated to the dissolved Nd (see ISP report section in this chapter). Filters were then dried and stored in clean Petri boxes. Note that these

filters will be dedicated to the analysis of particulate Th and Pa isotopes too: the leaching solution will be shared between the LSCE and LEGOS partners after a first extraction on the "unique column" developed by Jeandel et al (2011).

Planned Analytical procedure

Back to the laboratory, Nd will be extracted from the water sample following a procedure based on reverse liquid chromatography and then isotopic ratios are measured using a mass spectrometer. Details are given in Lacan and Jeandel (2001)

Units

The isotopic neodymium composition (ε_{Nd}) corresponds to the $^{143}Nd/^{144}Nd$ ratio (no units) defined by:

$$\varepsilon_{Nd} = ([(^{143}Nd/^{144}Nd)_{sample}/(^{143}Nd/^{144}Nd)_{CHUR}]-1)*10000$$

VII.2.1 Post-cruise sampling analyses and deadlines

Analyses of Nd isotopic compositions require a chemical purification of the matrix that is concentrated on the cartridges. Dissolved Nd IC are extracted by passing 30 ml of 6N HCl on the cartridges. Particulate Nd IC are recovered from the filters by an appropriate leaching using concentrated acids. Once extracted and purified from their respective initial matrix, Nd mass ratios are analyzed in a mass spectrometer at multicollection and thermo ionization (TIMS). This protocol is long and requires on land clean conditions. We will make all what's possible to perform these analyses within the next 3 years.

The Nd IC data will be submitted in the Geotraces open source data base GDAC, hosted in BODC. The data submission will follow all the Geotraces required criteria and steps (Intercalibration, Standard and Intercalibration committee, Data Portal DOoR etc…).

References

Arsouze, T., Treguier, A.M., Peronne, S., Dutay, J.-C., Lacan, F. and Jeandel, C., 2010. Ocean Sci., 6: 789-797.

Arsouze, T., Dutay, J.-C., Lacan, F. and Jeandel, C., 2009. Biogeosciences, 6: 1-18.

Grenier M, Garcia-Solsona E, Lemaitre N, Trull TW, Bouvier V, Nonnotte P, van Beek P, Souhaut M, Lacan F and Jeandel C (2018) Differentiating Lithogenic Supplies, Water Mass Transport, and Biological Processes On and Off the Kerguelen Plateau Using Rare Earth Element Concentrations and Neodymium Isotopic Compositions. Front. Mar. Sci. 5:426. doi: 10.3389/fmars.2018.00426

Jeandel, C. (1993), Earth and Planetary Science Letters, 117, 581-591.

Jeandel, C., Venchiarutti, C., Bourquin, M., Pradoux, C., Lacan, F., van Beek, P. and Riotte, J. (2011), Single Column Sequential Extraction of Ra, Nd, Th, Pa and U from a Natural Sample. Geostandards and Geoanalytical Research, 35: doi: 10.1111/j.1751-908X.2010.00087.x.

Lacan, F. and Jeandel, C., 2004. Geochemistry, Geophysics, and Geosystems, 5, doi:10.1029/2004GC000742.

Lacan, F. and Jeandel, C., 2005. Earth Planet. Sci. Lett., 232(3-4): 245-257.

Piepgras, D. J., and G. J. Wasserburg (1983), Journal of Geophysical Research, 291 88, 5997-6006.

Tachikawa K., Jeandel C. and Roy-Barman M., 1999. Earth Planet. Sci. Lett. 170, 433-446.

Zhang Y., Lacan F. Jeandel C.(2008) Dissolved Rare Earth Elements Trace Terrigeneous Inputs in the Wake of the Kerguelen Island (Southern Ocean) Deep-Sea Research Part II-Topical Studies in Oceanography, KEOPS special issue 55, 638-652, doi:10.1016/j.dsr2.2007.12.029.

Table 23: Synthesis of the number of samples taken during the SWINGS cruise for dissolved and particulate REE, dissolved Nd isotopic composition, dissolved Pa and Th and Total Ac.

station#	# DNd IC	# PNd IC (ISP)	# DPa/Th	# PPa/Th (ISP)	# T Ac	#D&P REE (Clean)
1	8	4	0	4	0	16
2	11	0	0	0	0	0
3	10	10	0	10	0	9
4	5	6	0	6	0	13
5	8	0	0	0	0	8
6	3	0	0	0	0	0
9	13	0	0	0	0	0
11	11	10	11	10	0	10
13	7	0	7	0	7	0
14	7	7	7	7	11	11
15	0	0	0	0	0	9
17	11	0	12	0	0	0
18	8	0	14	0	0	4
19	9	0	13	0	0	8
20	3	0	0	0	0	7
21	7	5	0	5	0	8
25	11	11	15	11	7	11
26	2	0	0	0	0	18
29	0	0	14	0	0	13
30	11	0	11	0	0	0
31	3	0	0	0	0	0
33	8	9	13	9	0	8
34	4	0	0	0	0	0
35	7	0	10	0	0	3
36	12	8	12	8	9	10
38	3	6	0	6	0	0
42	9	5	14	5	7	11
44	4	5	8	5	5	7
45	4	0	0	0	0	2
46	2	0	0	0	0	3
47	4	10	13	10	0	4
48	0	0	0	0	8	0
52	7	0	7	0	4	0
53	0	0	3	0	9	0
58	0	13	11	13	0	0
59	14	0	0	0	0	0
61	6	0	0	0	0	6
62	4	0	0	0	0	4
65	2	0	0	0	0	3
66	2	0	0	0	0	4
67	2	0	0	0	0	4
68	5	6	13	6	0	5
TOTAL	**247**	**115**	**208**	**115**	**67**	**219**

VII.3Dissolved and particulate Th-Pa isotopes and Total Ac isotopes (by Mass spectrometry)

Principal investigator
On shore: Matthieu Roy-Barman
LSCE, UMR8212 (CEA/CNRS/UVSQ - IPSL), Univ Paris Saclay
Orme des Merisiers - centre de Saclay 91 191 Gif-sur-Yvette Cedex
+33(0)1 69 08 27 57
matthieu.roy-barman@lsce.ipsl.fr

Names of other participants :

On board : Catherine Jeandel (DR, CNRS, LEGOS, Toulouse), Moustafa Belhadj (AI, CNRS, LEGOS, Toulouse), Damien Cardinal (Pr Sorbonne Université)

On shore: Lorna Foliot (AI, UVSQ, LSCE, Gif sur Yvette),

Abstract:

The natural radioactive isotopes 230Th, 231Pa and 227Ac are useful chronometers of particle fluxes and deep oceanic mixing. In the framework of SWINGS, we collected 198 filtered seawater samples (average V= 2 L) to determine 230Th and 231Pa and 69 filtered seawater samples (average V= 2 L) for the analysis of dissolved 227Ac. Comparison of these dissolved data with the particulate data will help to constrain dissolve/particulate exchanges.

VII.3.1 Scientific context

Th, Pa and Ac isotopes sampling and analyses are integrated in the general scientific framework of SWINGS. SWINGS cruise (January 11th-March 8th 2021) realized an integrated oceanographic transect in the South West Indian Ocean. This area is crucial for the Earth climate, the thermohaline circulation and the carbon cycle, as it represents a major hub of heat, salt and chemical transports between the Atlantic and Indian sectors of the Southern Ocean. Combining physical oceanography and tracers allows better constraining the dissolved and particulate transport across the cruise track, notably by adding information diapycnal and isopycnal mixing (^{231}Pa-^{227}Ac disequilibrium, Geibert et al, 2002) and on particle dynamics (^{231}Pa-^{230}Th, Venchiarutti et al., 2011, Roy-Barman et al., 2019). The SWINGS cruise is particularly well located for studying Pa-Ac will as it includes 2 hot spots of the vertical mixing in the ACC (SWIR and Kerguelen, Tamsitt et al., 2017). The impact of hydrothermal activity along the South West Indian Ridge (SWIR) as a source of Ac will be also investigated.

VII.3.2 Overview of the project and objectives

The natural radioactive isotopes 230Th, 231Pa and 227Ac are valuable chronometers of particle fluxes and deep oceanic mixing.

^{230}Th and ^{231}Pa are particle-reactive isotopes produced uniformly in the ocean by radioactive decay of soluble uranium isotopes. After being produced in seawater, they stick to particles and become chronometers of particle dynamics. They are used as tracer of particle scavenging rate, settling rates, dissolved-particulate exchange. In "clear and deep" waters, the Pa/Th disequilibrium can also be used as tracer of slow ventilation. The ^{230}Th/^{231}Pa ratio is sensitive to the particle composition, refining the estimation of D/P exchange rate & boundary scavenging. ^{232}Th is a direct lithogenic tracer and the ^{230}Th/^{232}Th ratio is used to quantify atmospheric dust flux in the surface mixed layer.

^{227}Ac is a soluble daughter product from the decay of ^{231}Pa which has a strong affinity to the marine particle. This difference of behavior produces a disequilibrium between actinium and protactinium distribution in seawater column. There is an excess of ^{227}Ac in deep water, because ^{227}Ac diffuses from the sediment where ^{231}Pa accumulates. Hence, we can use the distribution of the excess of ^{227}Ac like a clock of the vertical mixing in deep water during about 30 years (^{227}Ac approximate mean life time). It can then be used to estimate the diffusion flux from the sediment of other elements, like rare earth element or nutrient.

The scientific issues addressed will be:

1) the spatial evolution of sedimentation of particles with the hydrological structures will be studied with ^{230}Th and ^{231}Pa.

2) the effect of the topography on the intensity of the deep oceanic mixture will be timed by the ^{231}Pa - ^{227}Ac chronometer.

3) the combined effect of particulate transport and deep mixing on the storage of trace elements and carbon in the deep ocean.

VII.3.3 Methodology and sampling strategy

For dissolved Pa-Th isotope analyses, ~208 samples of 10 L of seawater were collected from Niskin bottles of the classic rosette at each L stations and some M and H stations in order to ensure the best vertical and horizontal resolutions, and follow the water masses along isopycnals (Table 24). Particulate Pa and Th analyses will be measured on 115 *in situ* pump (ISP) samples collected at corresponding depths on SUPOR membrane filters (see ISP report). The same filters as for Nd IC will be used for this purpose: the leaching solution will be shared between the LSCE and LEGOS partners after a first extraction on the "unique column" developed by Jeandel et al (2011).

For total ^{227}Ac analyses, 67 samples of 10 L of seawater where collected with an improved resolution close to the seafloor. Samples were immediately filtered onboard through ACROPACK cartridges under pressured clean air or with Perspex system. They were then acidified with ultraclean HCl.

Planned Analytical procedure

Back to the laboratory, Th, Pa and Ac analysis requires spiking with artificial tracers, a chemical preconcentration and further purification by column chromatography. After purification, Nd IC on the one hand and Th, Pa concentrations on the other hand are analyzed by TIMS and MC-ICPMS respectively. This protocol is long and requires on land clean conditions. We will make all what's possible to perform these analyses within the next 3 years. Details are given in Jeandel et al., 2011, Gdaniec et al., 2019 and Levier et al., 2021.

Note that an exhaustive compilation of the samples collected per station and cast is proposed in Table 22 above (see Nd IC section of this chapter)

Table 234: List of measured parameters, with their units

Parameter	code of operation *	units
1. Dissolved Th	Classic CTD	fg/kg (^{230}Th), pg/kg (^{232}Th)
2. Dissolved Pa	Classic CTD	fg/kg (^{231}Pa)
3. Dissolved Ac	Classic CTD	ag/kg (^{227}Ac)

VII.3.4 Post-cruise sampling analyses and dead-lines

Analyses of Nd IC, Th, Pa and Ac require a chemical preconcentration and further purification by column chromatography. Once extracted, Nd Th, Pa concentrations are analyzed by mass spectrometry. This protocol is long and requires on land clean conditions. We will make all what's possible to perform these analyses within the next 3 years.

Data base organization (general cruise base and/or specific data base(s))

The Th, Pa and Ac data will be submitted in the Geotraces open source data base GDAC, hosted in BODC. The data submission will follow all the Geotraces required criteria and steps (Intercalibration, Standard and Intercalibration committee, Data Portal DOoR etc…).

References

Gdaniec et al. (2018). Thorium and protactinium isotopes as tracers of marine particle fluxes and deep water circulation in the Mediterranean Sea. Marine Chemistry 199, 12-23.

Geibert, W. et al.. (2002). Actinium-227 as a deep-sea tracer: sources, distribution and applications. Earth and Planetary Science Letters, 198(1-2), 147-165.

Jeandel, C., Venchiarutti, C., Bourquin, M., Pradoux, C., Lacan, F., van Beek, P. and Riotte, J. (2011), Single Column Sequential Extraction of Ra, Nd, Th, Pa and U from a Natural Sample. Geostandards and Geoanalytical Research, 35: doi: 10.1111/j.1751-908X.2010.00087.x.

Levier et al. (2021). Determination of low level of actinium 227 in seawater and river water by isotope dilution and mass spectrometry.Mar. Chem. accepted with minor revisions.

Roy-Barman M.et al. (2019) Thorium isotopes in the Southeast Atlantic Ocean: Tracking scavenging during water mass mixing along neutral density surfaces. Deep Sea Res. Part I 149, 103042

Tamsitt, V. et al. (2017). Spiraling pathways of global deep waters to the surface of the Southern Ocean. Nature communications, 8(1), 1-10.

Venchiarutti et al. (2011) Influence of intense scavenging on Pa-Th fractionation in the wake of Kerguelen Island (Southern Ocean), Biogeosciences, 8, 3187-3201.

VII.4 Dissolved and particulate Radium and Ac isotopes (by gamma counting)

Principal investigator
On board: Pieter van Beek
LEGOS, Observatoire Midi Pyrénées, 14 avenue Edouard Belin 31400 Toulouse - France
+33(0)561333051
vanbeek@legos.obs-mip.fr

Names of other participants
On board: Virginie Sanial (assistant professor, Toulon University / MIO), Morgane Leon (PhD Student, Toulouse III University/ LEGOS); on shore: Marc Souhaut (engineer, LEGOS), Matt Charette (WHOI, USA), Paul Henderson (WHOI, USA), Thomas Zambardi (OMP/ LAFARA underground laboratory)

Abstract

We will analyze Ra isotopes and ^{227}Ac along the SWINGS section in the South West Indian Ocean. With a shorter half-life, ^{224}Ra, ^{223}Ra and ^{228}Ra will be used to trace recent (weeks to years) interaction of the water masses with margin or deep-sea sediments. Ra isotopes and ^{227}Ac will be used as tracers of hydrothermal vents. With a longer half-life, ^{226}Ra will be used as a tracer of water masses at larger scale. We will also investigate the relationship between the distributions of ^{226}Ra, Ba and DSi, following what was done during the GEOSECS programme. Vertical profiles of ^{226}Ra, ^{228}Ra and ^{227}Ac will allow us to estimate vertical eddy diffusion coefficients (K_z). Offshore several islands, horizontal eddy diffusion coefficients (K_h) will be estimated as well. Kz and Kh coefficients can be combined with vertical gradients above sediments and offshore gradients from islands of chemical elements, respectively to estimate elements transferred from deep and shallow sediments toward the water column.

VII.4.1 Scientific context

Radium isotopes have been widely used as tracers to study i) the oceanic circulation and mixing and ii) the flux of chemical elements transferred at the continent-ocean or deep sea-ocean interfaces. Radium has four isotopes that display various half-lives, which allow us to study processes at different time and spatial scales: ^{224}Ra ($T_{½}$= 3.66 d), ^{223}Ra ($T_{½}$= 11.3 d), ^{228}Ra ($T_{½}$= 5.75 y) and ^{226}Ra ($T_{1/2}$= 1602 y). In the Crozet-Kerguelen-Heard region, Ra isotopes have been used in past projects to investigate the mechanisms and time-scale of iron fertilization (Charette et al., 2007; van Beek et al., 2008; Sanial et al., 2014, 2015) and to derive vertical and horizontal fluxes of iron offshore these islands (Charette et al., 2007; van Beek et al., 2008). ^{227}Ac (21.8 y) has also been used to study vertical mixing in the ocean (Nozaki et al., 1984) and as a tracer of hydrothermal vents (Kipp et al., 2017).

VII.4.2 Overview of the project and objectives

Distributions of Ra isotopes and ^{227}Ac will be plotted along the section of the South West Indian Ocean. ^{224}Ra, ^{223}Ra, and ^{228}Ra will be used to trace the transfer of the chemical elements released by sediments from offshore islands and continental margins. Vertical eddy diffusion coefficients (K_z) will be estimated from the vertical profiles of radionuclides. Eddy diffusion coefficients will be combined with the gradient of chemical elements to derive chemical fluxes.

A section of ^{226}Ra will also be reported. ^{226}Ra is used as a water mass tracer at large scale. The radium-barium relationship will be investigated along that section because Ba has been proposed as the "stable isotope" of radium for the use of the ^{226}Ra/Ba ratio as a clock - in a similar manner as the ^{14}C/^{12}C ratio, since ^{226}Ra and Ba are chemical analogues (see e.g., Le Roy et al. 2017). Dissolved Barium concentration will be determined at MIO, Marseille by Stephanie Jacquet. The Ra-Ba-DSi relationships will be investigated.

Ra isotopes and ^{227}Ac will also be used to investigate hydrothermal inputs (eg., stations 14 and 15).

VII.4.3 Methodology and sampling strategy

Sampling

Niskin bottles: discrete 10-12L samples were collected using Niskin bottles. The seawater samples were filtered through 10 g of acrylic fibers impregnated with MnO_2 ("Mn Fiber"), which adsorbs Ra and ^{227}Ac quantitatively.

In situ pumps: large volumes of seawater were filtered *in situ* onto two cartridges impregnated with MnO_2 placed in series and mounted on McLane in situ pumps. The yield of Ra fixation onto the Mn-cartridges will be determined from the ^{226}Ra activity determined in the discrete samples. The yield of ^{227}Ac fixation will be determined using the two cartridges placed in series (Le Roy et al., 2019).

Underway samples: We also collected surface samples using either the large volume pump of Bill Landing, the ship seawater intake, the towed fish and a teflon pump from the moon hole ("Chips").

Analysis

^{226}Ra activity will be determined in the discrete samples using the Rn emanation technique, in collaboration with Matt Charette at WHOI, USA, as was done by Le Roy et al. (2018).

The Mn-cartridges were analyzed on board right after sampling to quantify the short-lived Ra isotopes (^{223}Ra and ^{224}Ra) using Radium Delayed Coincidence Counters (RaDeCC; Moore and Arnold, 1996). The samples have to be analyzed again three weeks after sampling and then three months after sampling to quantify the ^{224}Ra supported by ^{228}Th and the ^{223}Ra supported by ^{227}Ac, respectively. Part of the second counting was therefore done onboard. The third analysis allows us to quantify the ^{227}Ac activity in the samples (Le Roy et al., 2019). The Mn-cartridges will be then analyzed using the low-background gamma spectrometers placed at the underground laboratory of Ferrières (LAFARA facility belonging to the university of Toulouse III; https://lafara.obs-mip.fr/; van Beek et al., 2013). This latter analysis will provide the ^{226}Ra, ^{228}Ra and ^{228}Th activities in the samples.

Dissolved Ba concentrations will be analyzed at MIO by ICP-MS (S. Jacquet). Seawater samples were collected using Niskin bottles and acidified on board using 65% HNO_3. The compilations of samples collected per sampling tools are proposed in Tables 25, 26, 27.

Table 25: Samples collected for the dissolved radionucleides using in situ pumps

Sample ID	Station #	Cast #	Pump ID	Depth (m)	Total vol. (L)	Pump duration (h)
SWG_P_01_03_0020	1	3	ISPCa3	1000	169	1
SWG_P_01_03_1000	1	3	ISPCa4	0020	339	1
SWG_P_03_013_2147	3	13	ISPCa3	2147	866	3
SWG_P_03_013_2100	3	13	ISPCa4	2100	1007	3
SWG_P_03_013_1750	3	13	ISPCa6	1750	1013	3
SWG_P_03_013_1480	3	13	ISPCa7	1480	868	3
SWG_P_03_013_1020	3	13	PIS007	1020	1158	3
SWG_P_03_013_0750	3	13	PIS009	0750	1047	3
SWG_P_03_013_0500	3	13	PIS010	0500	1149	3
SWG_P_03_013_0160	3	13	PIS011	0160	844	3
SWG_P_03_013_0100	3	13	PIS012	0100	282	3
SWG_P_03_013_0030	3	13	PIS013	0030	139	3
SWG_P_04_016_0616	4	16	ISPCa4	0616	979	3
SWG_P_04_016_0500	4	16	ISPCa6	0500	555	3
SWG_P_04_016_0400	4	16	ISPCa7	0400	917	3
SWG_P_04_016_0250	4	16	PIS013	0250	748	3
SWG_P_04_016_0090	4	16	PIS007	0090	1074	3
SWG_P_04_016_0015	4	16	PIS009	0015	416	3
SWG_P_11_035_5000	11	35	ISPCa4	5000	839	3
SWG_P_11_035_4500	11	35	ISPCa6	4500	875	3
SWG_P_11_035_4000	11	35	PIS010	4000	914	3
SWG_P_11_035_3500	11	35	ISPCa7	3500	783	3
SWG_P_11_035_3000	11	35	PIS012	3000	735	3
SWG_P_11_035_2200	11	35	PIS013	2200	751	3
SWG_P_11_035_1550	11	35	PIS011	1550	762	3
SWG_P_11_035_1000	11	35	ISPCa3	1000	911	3
SWG_P_11_035_0250	11	35	PIS007	0250	1113	3
SWG_P_11_035_0030	11	35	PIS009	0030	398	3
SWG_P_14_043_1260	14	43	ISPCa4	1260	646	3
SWG_P_14_043_1200	14	43	ISPCa6	1200	674	3
SWG_P_14_043_1160	14	43	ISPCa7	1160	584	3
SWG_P_14_043_1100	14	43	PIS012	1100	548	3
SWG_P_14_043_1000	14	43	PIS013	1000	528	3
SWG_P_14_043_0900	14	43	ISPCa3	0900	615	3
SWG_P_14_043_0210	14	43	PIS009	0210	601	3
SWG_P_14_043_0050	14	43	PIS011	0050	427	3
SWG_P_15_045_1690	15	45	ISPCa4	1690	630	3
SWG_P_15_045_1370	15	45	ISPCa6	1370	677	3
SWG_P_15_045_1260	15	45	PIS010	1260	665	3
SWG_P_15_045_1200	15	45	PIS013	1200	503	3
SWG_P_15_045_1160	15	45	ISPCa3	1160	579	3
SWG_P_15_045_0700	15	45	PIS011	0700	532	3
SWG_P_21_056_1270	21	56	ISPCa6	1270	978	3
SWG_P_21_056_1000	21	56	ISPCa7	1000	817	3
SWG_P_21_056_0500	21	56	PIS012	0500	700	3

Table 26: Samples collected for the dissolved radionucleides using Niskin bottles

SWINGS ID	Station #	Cast #	Nb samples #	Nom. Depth (m)	Ba #	DSi #
SWG_S_01_004_	01	4	1	15	X	
SWG_S_02_005_	02	5	8	2000.1800.1200.500.250.125.80.30	X	
SWG_S_03_008_	03	8	11	2144.2100.1750.1480.1020.750.500.160.100.30.15	X	
SWG_S_03_012_	03	12	1	1050	X	
SWG_S_04_015_	04	15	7	623.500.400.250.90.38.15	X	
SWG_S_05_017_	05	17	8	1018.800.600.400.250.90.50.15	X	
SWG_S_09_025_	09	25	9	5900.5050.4500.3500.3050.1750.1250. 680.180	X	X
SWG_S_11_029_	11	28	9	5000.4500.4000.3500.3000.2200.1550. 1000.250	X	
SWG_S_11_032_	11	32	5	150.100.75.30.15	X	
SWG_S_11_036_	11	36	4	750.550.400.350	X	
SWG_S_13_039_	13	39	7	1600.1250.1000.800.500.300.150	X	
SWG_S_14_040_	14	40	11	1400.1350.1300.1250.1200.1150.1100. 1000.900.200.50	X	X
SWG_S_15_044_	15	44	7	1755.1690.1500.1370.1260.1200.1160	X	X
SWG_S_17_048_	17	48	11	3340.2800.2400.1800.1200.1000.700.500.250.70.30	X	X
SWG_S_20_054_	20	54	1	15		
SWG_S_21_057_	21	57	7	1294.1000.750.500.250.50.15	X	
SWG_S_21_059_	21	59	1	375	X	
SWG_S_25_065_	25	65	12	3678.3250.3500.3000.2250.1800.1200. 800.500.220.120.30	X	
SWG_S_25_065_	25	71	1	15	x	
SWG_S_26_073_	26	73	12	3838.3200.2500.1800.1250.800.600.400.250.120.80.15	X	X
SWG_S_30_079_	30	79	11	4622.4000.3500.3000.2500.1750.1250. 800.500.200.50	X	
SWG_S_31_080_	31	80	4	1500.800.500.250	X	
SWG_S_31_083_	31	83	4	200.150.85.15	X	
SWG_S_33_090_	33	90	7	2204.1950.1750.175.135.40.15	X	
SWG_S_36_095_	36	95	11	4250.4000.3750.3500.3250.3000.2500. 2000. 1500.1000.750	X	
SWG_S_36_099_	36	99	2	290.30	x	
SWG_S_36_100_	36	100	7	500.250.200.140.60.30.15	x	
SWG_S_42_114_	42	114	8	1680.1500.1000.700.500.300.200.20	x	
SWG_S_44_120_	44	120	6	264.220.150.110.70.30	x	
SWG_S_45_121_	45	121	2	75.27	x	
SWG_S_45_123_	45	123	4	75.60.40.30	x	
SWG_S_46_124_	46	124	2	106.3	x	
SWG_S_46_126_	46	126	4	100.60.30.10	x	

SWG_S_47_131_	47	131	10	2160.2000.1500.1000.600.400.300.195. 100.20	x	
SWG_S_48_133_	48	133	8	1686.1500.1000.675.500.320.190.20	x	
SWG_S_53_139_	53	139	13	2702.2650.2350.2000.1500.1300.1000. 700.400.200.108.80.20	X	X
SWG_S_61_153_	61	153	14	2068.1950.1750.1500.1000.750.500.350.230.150.100.65.40.2 0	X	
SWG_S_62_154_	62	154	11	1750.1600.1400.1000.800.500.220.150. 100.75.40	X	X
SWG_S_65_158_	65	158	2	120.30	X	
SWG_S_65_160_	65	160	4	120.60.30.10	X	
SWG_S_66_162_	66	162	4	480.375.200.30	X	
SWG_S_66_164_	66	164	2	100.30	X	
SWG_S_66_165_	66	165	2	400.180	X	
SWG_S_68_170_	68	170	8	460.400.320.250.175.150.100.30	X	
SWG_S_68_172_	68	172	2	50.20	X	

Table 27: Surface samples collected underway for radionucleide analyses, using either the ship seawater intake, the Be pump, teflon pumps (FISH and CHIPS), a hand pump or LEGOS pump.

Sample ID	Station	Type	Init Lat. (°S)	Init Long. (°E)	Weight (kg)	Barium
SWG_03_UW	3	Intake	-30,1333	32,8001	164,5	
SWG_03b_UW		Intake	-30,5403	31,8061	87	
SWG_03c_UW		Intake	-29,8063	31,1572	86,6	
SWG_04_UW	4	Intake	-29,8187	31,6882	84,1	
SWG_05_UW	5	Intake	-30,0864	31,7909	87,4	
SWG_06_UW	6	Intake	-30,6547	32,1507	110,4	
SWG_06b_UW		Intake	-31,6748	32,8023	109,1	
SWG_07_UW	7	Intake	-32,6002	33,4202	105,7	
SWG_08_UW	8	Intake	-35,2169	34,4710	109,3	
SWG_09_UW	9	Intake	-37,1024	36,0167	112,4	X
SWG_10b_UW		Intake	-38,3365	36,0609	112,7	X
SWG_11_UW	11	Intake	-39,8007	36,3517	112,7	X
SWG_11b_UW		Intake	-40,3155	31,6433	22,6	X
SWG_11c_UW		Intake	-40,6584	36,7461	22,5	X
SWG_12b_UW		Intake	-41,8853	36,7051	22,3	X
SWG_12c_UW		Intake	-43,1195	36,4588	22,4	X
SWG_13_UW	13	Intake	-44,8582	36,1081	108,5	X
SWG_14_UW	14	Intake	-44,8616	36,1743	112	X
SWG_18_UW	18	Intake	-47,0596	38,1503	110	X
SWG_19_UW	19	Intake	-46,9699	38,0598	111,5	X
SWG_20_UW	20	Intake	-46,8900	37,9496	111,4	X
SWG_21_UW	21	Intake	-46,6006	37,7791	112,4	X
SWG_21b_UW		Intake	-47,0639	38,5523	108,9	X
SWG_22_UW	22	Intake	-47,5001	39,2997	130,7	X
SWG_Be_22	22	Be Pump	-47,5001	39,2997	130,6	X
SWG_25_CHIPS	25	CHIPS	-47,3094	43,1094	129,2	X
SWG_CR0_CHIPS	Crozet	CHIPS	-46,4272	51,8736	109,7	X
SWG_CR1_CHIPS		CHIPS	-46,3392	51,8868	109,2	X
SWG_CR2_CHIPS		CHIPS	-46,2487	51,8900	110,5	
SWG_CR3_CHIPS		CHIPS	-46,1639	51,8928	110,2	
SWG_33_CHIPS	33	CHIPS	-46,2027	51,8920	106,7	X
SWG_34_CHIPS	34	CHIPS	-45,2033	51,9983	107,7	X
SWG_34_Be	34	Be Pump	-45,2033	51,9983	108	X
SWG_38_CHIPS	38	CHIPS	-47,3216	59,7839	130,2	X
SWG_38_Be	38	Be Pump	-47,3216	59,7839	129,3	X
SWG_58_CHIPS	58	CHIPS	-57,6883	81,9106	131,7	X
SGW_58_Be	58	Be Pump	-57,6883	81,9106	130,5	X
SWG_66_FISH	66	FISH	-51,6397	74,4709	108,6	X
SWG_67_FISH	67	FISH	-51,3141	73,7138	109,5	X
SWG_KER0	Baie du Morbihan	LEGOS Pump	-49,3593	70,2123	130,5	X
SWG_PAF	Beach Port-aux-Français	Hand pump			88,8	
SWG_KER1_CHIPS		CHIPS	-49,3674	70,7938	88,8	
SWG_KER2_FISH		FISH	-49,2534	71,0926	88,7	
SWG_KER3_FISH		FISH	-49,1067	71,4852	89	
SWG_KER4_FISH		FISH	-48,9461	71,9120	88,9	

VII.4.4 Preliminary results

The water samples collected at stations 14 and 15 were analysed on board using RaDeCC. The ^{223}Ra activities were higher than the ^{224}Ra activities below 800 m. The high ^{223}Ra activities found near the bottom (Figure VII-1) suggest that the Ra activity is associated with a hydrothermal plume, a pattern that was also observed in other oceanic basins (see e.g. Kipp et al., 2017). Further analysis will allow us to quantify the excess ^{223}Ra and ^{224}Ra activities, as well as ^{228}Ra, ^{226}Ra and ^{227}Ac activities that will be used to confirm (or infirm) the preliminary conclusions.

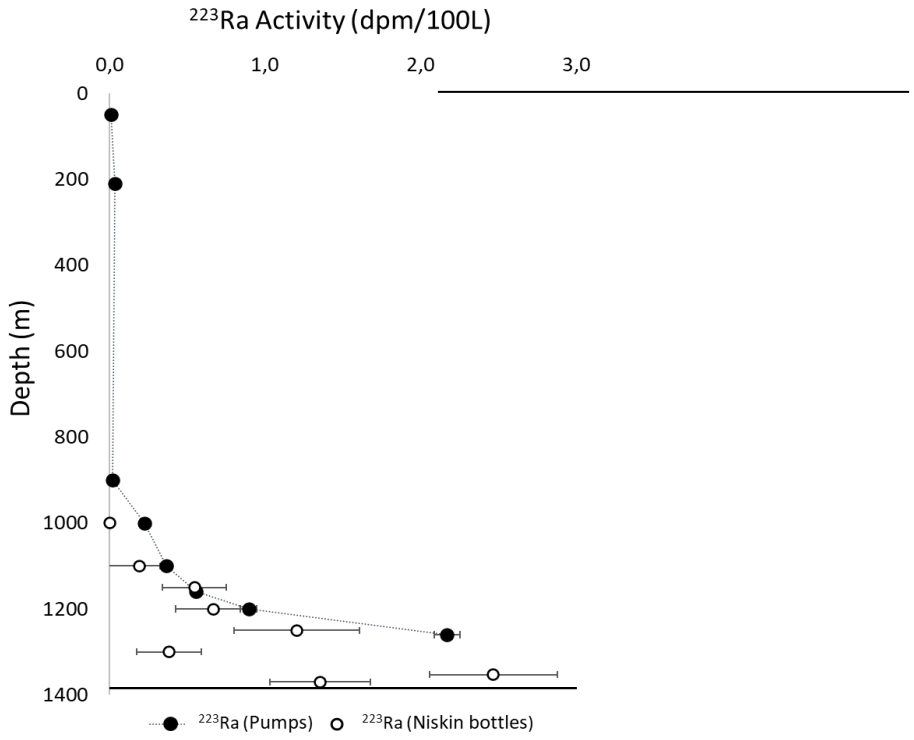

Figure VII-1: *Preliminary vertical profiles of ^{223}Ra activities determined in Mn cartridges mounted on in situ pumps (closed circles) and in Mn fibers (Niskin bottles; open circles) at station 14. Excess Ra activities (and correction for radioactive decay) still need to be quantified in these samples. dpm: disintegration per minute.*

VII.4.5 Post-cruise sampling analyses and envisioned timeline of working plan, people involved on shore

Morgane Léon (LEGOS) will conduct a PhD Thesis on the Ra-Ac data from the SWINGS project, under the supervision of P. van Beek (Univ. Toulouse) and V. Sanial (Univ. Toulon). The thesis started in October 2020. Once back in the laboratory, Morgane will analyze the Mn-fiber and Mn-cartridge samples using the RaDeCC, to quantify the Ra supported by ^{228}Th and ^{227}Ac. In spring 2022, Morgane will spend 3 months at WHOI (collaboration with Matt Charette) to analyze the ^{226}Ra activity in the discrete samples collected with Niskin bottles (EUR TESS funding). The Mn-cartridges will then be analyzed at the LAFARA underground laboratory (M. Souhaut, T. Zambardi). The Ba samples will be analyzed no later than year 2022 (S. Jacquet). All the data of the SWINGS project will be acquired during the PhD Thesis.

References

Charette M. A., Gonneea M. E., Morris P. J., Statham P., Fones G., Planquette H., Salter I. and Garabato A. N., 2007. Radium isotopes as tracers of iron sources fueling a Southern Ocean phytoplankton bloom, Deep Sea Research Part II: Topical Studies in Oceanography, 54(18–20), 1989–1998, https://doi.org/10.1016/j.dsr2.2007.06.003.

Kipp L.E., Sanial V., Henderson P.B., van Beek P., Reyss J.-L., Hammond D.E., Moore W.S., Charette M.A., 2017. Radium isotopes as tracers of hydrothermal inputs and neutrally buoyant plume dynamics in the deep ocean, Marine Chemistry 201, 51-65.

Le Roy E., Sanial V., Charette M.A., van Beek P., Lacan F., Jacquet S.H.M., Henderson P.B., Souhaut M., García-Ibáñez M.I., Jeandel C., Pérez F.F., Sarthou G., 2018. The 226Ra–Ba relationship in the North Atlantic during GEOTRACES-GA01.Biogeosciences 15, 3027–3048.https://doi.org/10.5194/bg-15-3027-2018.

Le Roy E., Sanial V., Lacan F., van Beek P., Souhaut M., Charette M.A., P.B. Henderson, 2019. Insight into the measurement of dissolved 227Ac in seawater using radium delayed coincidence counter, Marine Chemistry 212, 64-73.

Moore W.S., Arnold R., 1996. Measurement of 223Ra and 224Ra in coastal waters using a delayed coincidence counter. J. Geophys. Res. Oceans 101, 1321–1329. https://doi.org/10.1029/95JC03139

Nozaki Y., 1984. Excess 227Ac in deep ocean water. Nature 310, 486–488.https://doi.org/10.1038/310486a0.

Sanial V., van Beek P., Lansard B., d'Ovidio F., Kestenare E., Souhaut M., Zhou M. and Blain S., 2014. Study of the phytoplankton plume dynamics off the Crozet Islands (Southern Ocean): A geochemical-physical coupled approach, J. Geophys. Res. Oceans, 119(4), 2227–2237, https://doi.org/10.1002/2013JC009305.

Sanial V., van Beek P., Lansard B., Souhaut M., Kestenare E., d'Ovidio F., Zhou M. and Blain S., 2015. Use of Ra isotopes to deduce rapid transfer of sediment-derived inputs off Kerguelen, Biogeosciences, 12(5), 1415–1430, https://doi.org/10.5194/bg-12-1415-2015.

van Beek P., Bourquin M., Reyss J.-L., Souhaut M.,Charette M. A., and Jeandel C., 2008. Radium isotopes to investigate the water mass pathways on the Kerguelen Plateau (Southern Ocean), Deep Sea Res. Pt. II, 55, 622–637,doi:10.1016/j.dsr2.2007.12.025.

van Beek P., Souhaut M., Lansard B., Bourquin M., Reyss J.-L., Von Ballmoos P., and Jean P., 2013. LAFARA: a new under-ground laboratory in the French Pyrenees for ultra low-level gamma-ray spectrometry, J. Environ. Radioactivity, 116, 152–158,doi:10.1016/j.jenvrad.2012.10.002, 2013.

VIII. PARTICLES, EXPORT AND SEDIMENT CORES

VIII.1 *In-situ* Pumps (POC, PON, BSi, LSi, Hg, Fe, Mn, Al, Cu, Co, Zn, Ba, P, Y, Cd, Ti, V, Ni, Ca, Mo, ε_{Nd}, $\delta^{13}C$, $\delta^{15}N$, $\delta^{66}Zn$, $\delta^{60}Ni$, $\delta^{30}Si$, ^{223}Ra, ^{224}Ra, ^{226}Ra, ^{228}Ra, ^{227}Ac, ^{231}Pa, ^{232}Th, ^{234}Th, bio markers, proteins)

Principal investigators

On board : de Saint-Léger Emmanuel (DT-INSU, Plouzané, emmanuel.desaint-leger@cnrs.fr), **Perault Fabien** (DT-INSU, Plouzané, fabien.perault@cnrs.fr), **Planquette Hélène (**LEMAR, Plouzané, helene.planquette@univ-brest.fr), **Jeandel Catherine** (LEGOS, Toulouse, catherine.jeandel@legos.obs-mip.fr), **Planchon Frederic** (LEMAR, Plouzané, frederic.planchon@univ-brest.fr), **van Beek Pieter** (LEGOS, Toulouse, pieter.van-beek@legos.obs-mip.fr), **Lemaitre Nolwenn** (ETH Zürich, Suisse, nolwenn.lemaitre@erdw.ethz.ch), **Lagarde Marion** (LEGOS, Toulouse, marion.lagarde@legos.obs-mip.fr, **Sanial Virginie** (Université de Toulon, La Garde, virginie.sanial@univ-tln.fr), **Léon Morgane** (LEGOS, Toulouse, morgane.leon@legos.obs-mip.fr), Cotard Edwin (LEMAR, Plouzané, cotard.edwin@gmail.com), **Natalia Torres-Rodriguez** (MIO, Marseille, natalia.torres-rodriguez@mio.osupytheas.fr)
On shore : Roy Barman Matthieu (LSCE, Gif-sur-Yvette, matthieu.roy-barman@lsce.ipsl.fr), **Heimburger Lars-Eric** (MIO, Marseille, lars-eric.heimburger@mio.osupytheas.fr), **Vance Derek** (ETH Zürich, Suisse, derek.vance@erdw.ethz.ch),), **Souhaut Marc** (LEGOS, Toulouse, marc.souhaut@legos.obs-mip.fr),

Names of other participants:
On board: Ingrid Obernosterer (LOMIC, Banyuls sur mer), Damien Cardinal (LOCEAN, Paris)
On shore: Mak Saito (WHOI, USA)

Abstract:

In-situ pumps (ISP) are mainly used to collect particles from large volumes of filtered seawater. The large filtered volumes allow us to get sufficient quantities of particles to analyze major, trace elements and isotopes on suspended and/or sinking particles. Additionally, specific cartridges placed after the filter allowed us to preconcentrate radionuclides from seawater.

VIII.1.1 Scientific context

SWINGS is a multidisciplinary project fully dedicated to elucidate trace element sources, transformations and sinks along a section crossing key areas of the Southern Ocean (SO).

SWINGS aims at 1) establishing the relative importance of sedimentary, atmospheric, and hydrothermal sources of trace elements and isotopes (TEIs) in the Indian sector of the SO, 2) investigating the drivers of the internal trace element cycles: biogenic uptake, remineralization, particle fate, and export, and 3) quantifying TEI transport by the Antarctic Circumpolar Current and the complex frontal areas at the confluence between Indian and Atlantic Oceans. This is of prime importance as the SO is identified as the most sensitive ocean to climate change.

VIII.1.2 Overview of the project and objectives

In this project, our main objective is to study the distributions, sources, and internal cycles of different particulate elements (POC, PON, BSi, LSi, Hg, REE, Fe, Mn, Al, Cu, Co, Zn, Ba, P, Y, Cd, Ti, V, Ni, Ca, Mo, ε_{Nd}, $\delta^{13}C$, $\delta^{15}N$, $\delta^{66}Zn$, $\delta^{60}Ni$, $\delta^{30}Si$, ^{231}Pa, ^{232}Th, ^{234}Th, bio-markers, proteins) as well as the distributions of natural radioactive elements (^{223}Ra, ^{224}Ra, ^{226}Ra, ^{228}Ra, ^{227}Ac) in the dissolved phase. The comparison with the dissolved samples will help to better understand the exchanges between the particulate and dissolved phases.

VIII.1.3 Methodology and sampling strategy

Two pump casts were done for half of the stations: one called trace metal and Thorium cast (for analysing ^{234}Th, POC, PN, BSi, LSi, Ca, $\delta^{13}C$, $\delta^{15}N$, biomarkers, Hg, trace metal concentrations, Zn, Ni and Si isotopes and proteins) and another one called isotope cast (for analysing εNd, Ra isotopes, and Th/Pa isotopes).

Pump heads were prepared in three different ways: 1) for trace metal and Thorium casts: QMA 1 µm + Petex 5µm + Petex 50µm (hereafter QMA/P1/P2 head). 2) for trace metal and Thorium casts: Supor 0.8 µm (hereafter Supor HP head). 3) for isotope casts: Supor 0.8 µm (hereafter Supor CJ head). For the isotope cast, cartridges impregnated with manganese (Mn cartridges) were placed in series on the pumps equipped with plastic cartridge holders. For the other half of the stations, time and/or weather conditions did not allow to put two casts, so one cast was shared for trace metals, Th, isotopes and radionuclides. All the pumps were equipped with one-way valves placed below the filter and outgassing systems.

Before being used for sampling, both CJ and HP Supor filters were preconditioned as follows: filters were placed in an acid cleaned container or a 1L-LDPE bottle containing 1.2M HCl (Suprapur grade, Merck). The containers were then double bagged in Ziploc bags and placed in an oven at 60°C overnight. After cooling, the acid solution was removed and filters were thoroughly rinsed three times with Milli-Q water. Filters on board are stored in containers with Milli-Q water. Similarly, QMA filters were precombusted at 450°C for 4h and stored in aluminium foils. Petex filters were acid cleaned on board with 1.2M HCl (Suprapur grade, Merck) solution and rinsed with Milli-Q.

Before deployment, filters were placed in the *in-situ* pump heads under a laminar flow unit in a clean lab (bubble), except QMA filters that were processed outside the bubble in a standard cleaned room. Pump heads were then covered with plastic bags to minimize contamination and stored in boxes until mounted on the ISPs just before the deployment of the cast. After this, the ISPs were programmed. The ISPs were then primed as: the pump tubing system was filled with fresh water from the ship, the tubing was then

connected to the head, which was finally filled with Milli-Q water. In-situ pumps were then deployed using a Dyneema cable thanks to the crew. Plastic bags, covering the heads, were removed at the last minute when the pump was attached to the cable.

After recovery, the volume filtered by the pumps was double checked and reported; then the pump heads with filters were removed after pumping the excess water on top of the filters. Then the Mn cartridges were removed. The Mn cartridges were rinsed using Ra-free water, dried and analysed on the ship for the short-lived Ra isotopes (reported in Table 28). In-situ pump heads were covered with a plastic bag, stored in boxes, and transferred into the bubble for sub-sampling. Aliquots for sensitive tracers (on Supor and Petex filters) were processed under the laminar flow unit in the bubble. Aliquots for the remaining tracers (on QMA filters) were processed in a standard cleaned room. At stations 44, 47 and 58, a second Supor filter was added to the first one for the surface and bottom pumps. It was processed as a sample filter in the bubble, and will be leached the same way in the home laboratory in order to determine the process blank.

After the last station (Station 68), we processed and stored 5 cleaned and unused filters as if they were samples.

The processing of the filters depended on the targeted elements:

Trace metal and Thorium casts:

1) Supor HP heads: 2 punches of 13mm of diameter are dedicated to trace metal concentrations (for Hélène Planquette et al), 5 punches are dedicated to δ66Zn and δ60Ni (Nolwenn Lemaitre), one quarter to δ30Si (Damien Cardinal). For the filters deployed in the upper 400m of depth, one eighth is dedicated to proteins (Mak Saito). The left over is kept for analysing εNd (Catherine Jeandel & Marion Lagarde et al). Samples for proteins are stored at -80°C. Samples for trace metal concentrations, Ni and Zn isotopes are stored at -20°C. Samples for δ30Si as well as the left overs for εNd are dried under the hood and stored at ambient temperature.

2) QMA/P1/P2 heads: Petex P1 (50 µm) and P2 (5 µm) were divided in quarters using a scalpel. One eighth of each Petex was placed in cleaned tubes for analysing trace metal concentrations and stored at -20°C. The rest of each Petex filters was given back outside the bubble. One quarter was dedicated to POC, PN, $\delta^{13}C$, $\delta^{15}N$, and ^{234}Th determination: particles were resuspended with filtered seawater and recollected on a 25 mm QMA filters. Another quarter was dedicated to BSi and LSi: particles were resuspended with filtered seawater and recollected on a 25 mm polycarbonate (PC) filter. The 25 mm QMA and PC filters were dried overnight (T=60°C). PC filters were stored at room temperature and the 25 mm QMA filters were mounted on polyacrylamide support filter for beta counting onboard. The last quarters dedicated to biomarkers were placed in 15 ml tube and kept frozen (T=-80°C).

The 142 mm QMA filter was subsampled using a 25 mm plexiglass punch as follows: 2 punches for ^{234}Th, POC, PN, $\delta^{13}C$, $\delta^{15}N$, 4 punches for particulate Hg, one punch for POP, Al, Ca, Na, 6 punches for biomarkers (lipid and amino acids), and 3 punches for genomics. The remaining part of the QMA filter was frozen (-80°C) and kept as a backup for biomarkers analysis. Punches dedicated to ^{234}Th, POC, PN, $\delta^{13}C$, $\delta^{15}N$ were dried overnight at 60°C, and one punch was mounted on a polyacrylamide support filter for beta counting on board.

Isotope casts:

Supor CJ filters were moved from the heads to Petri dishes. Filters were dried under the hood and stored at room temperature. Filters sampled at the same depth +/- 20 m from the two different casts were stored in the same Petri dish.

Pictures of all filters are taken and are available for everyone upon request.

Table 28: List of stations and filters sampled during the SWINGS cruise using in-situ pumps

Station #	Cast number	Number of Supor filters	Number of QMA filters	Number of Mn cartridges
1	3	4 CJ + 3 HP	2	2
3	9	7 HP	8	0
3	13	10 CJ	0	20
4	16	4 HP + 6 CJ	5	12
11	30	7 HP	7 + 1 Hg	0
11	35	12 CJ	3 Hg	20
14	43	4 HP + 7 CJ	4	13
15	45	7 HP + 6 CJ	2 Hg	10
21	56	4 HP + 5 CJ	6	10
25	66	8 HP	7	0
25	70	11 CJ	0	20
31	81	2 HP	7	0
33	86	0	7 + 2 Hg	0
33	89	4 HP + 8 CJ	2 Hg	16
36	96	5 HP + 10 CJ	0	16
38	104	5 HP	7	0
42	113	3 HP + 5 CJ	7	10
44	119	3 HP + 5 CJ	4	10
47	129	8 HP	7	0
47	132	12 CJ	0	20
58	145	8 HP	7	0
58	149	15 CJ	0	20
68	171	3 HP + 6 CJ	6	10

VIII.1.4 Post-cruise sampling analyses and dead-lines

The analyses of all the parameters should be completed in the next 24 months.

For ^{234}Th activity, samples will be re-counted after a delay of six ^{234}Th half-lifes (~6 months) after sampling in order to correct for any residual beta activity due to longer beta emitter than ^{234}Th. This will be performed at the home laboratory

Data will be posted on the SWINGS database in a timely manner after analysis and processing. For TEIs, data will be submitted to the GEOTRACES data base.

VIII.2 Carbon, major and trace elements export deduced from the ^{234}Th deficiency method

Principal investigator
On board : Planchon Frédéric
LEMAR, Institut Universitaire Européen de la Mer (IUEM), Rue Dumont d'Urville, F-29280 Plouzané
+33 2 98 49 86 98
frederic.planchon@univ-brest.fr

Names of other participants
On board : Cotard Edwin
LEMAR, Institut Universitaire Européen de la Mer (IUEM), Rue Dumont d'Urville, F-29280 Plouzané
cotard.edwin@gmail.com

Abstract

This work aims at studying the vertical export of carbon and associated bioactive trace and major elements in the contrasting biogeochemical provinces sampled during the SWINGS campaign. Export fluxes will be deduced using the ^{234}Th deficiency method relying on high resolution vertical profiles of total ^{234}Th activity in the upper water column combined with element to ^{234}Th ratios of three size fractions of suspended particles (small, 1-5 µm, medium, 5-50 µm, and large, >50 µm) collected using large volume in-situ pumping systems (ISP). Export fluxes of POC, PN, POP, PIC, biogenic silica (BSi), lithogenic material as well as a suite of trace elements including Fe will be obtained at different depth horizons, at the base of the euphotic zone corresponding to 1% of photosynthetically available radiation (PAR), the sub-photic zone (0.1% PAR) and also 100 m below the sub-photic zone. In addition to fluxes, a suite of biomarkers including fatty acids, sterols, and amino-acids will be used to constrain the source and transformation pathways of suspended organic matter.

VIII.2.1 Scientific context

Export of Particulate Organic Carbon (POC) via the biological carbon pump (BCP) is an essential component of the marine carbon cycle that affects the air-sea transfer of carbon dioxide (CO_2) and therefore climate. In addition to carbon, the BCP is also an active removal process of several key elements including major (N, P, Si) and trace (Fe, Cu, Zn) components of organic matter produced by marine phytoplankton in the surface euphotic zone. This removal term is important to consider as it contributes to establish limiting conditions for photosynthetic activity and control ecosystem productivity. In the Southern Ocean, data remain scarce on the magnitude of the sinking flux of POC and by extension on associated bioactive elements, especially trace metals like Fe. Comprehensive data have been obtained in high productive regions found in the vicinity of subantarctic Islands such as Kerguelen (Planchon et al., 2015; Rembauville et al., 2015; Savoye et al., 2008), Crozet (Morris et al., 2007; Salter et al., 2007), and South Georgia (Manno et al., 2015), as well as in the Polar Front Region (Roca-Martí et al., 2017). However, only few data exist for the Antarctic Circumpolar Current (ACC) area and the few existing data indicate that export processes vary widely according to the biogeochemical provinces considered, in line

with changing primary production regimes, phytoplankton species, and the overall ecosystem structure (Planchon et al., 2013; Puigcorbé et al., 2017; Rosengard et al., 2015).

VIII.2.2 Overview of the project and objectives

The principal aim of this study is to assess the spatial variability of the BCP in the various biogeochemical provinces of the South West Indian ocean sampled during the SWINGS campaign. It includes the subtropical zone close to the South African margin, the subantarctic zone close to Marion Island, the polar frontal zone close and downstream of the Crozet Island, and the Antarctic zone of the Kerguelen Plateau. Our focus is to estimate export fluxes of POC and associated major (N, P, Si) and trace elements including Fe taking place in the upper part of the water column, from the surface euphotic zone to the upper mesopelagic (200-300 m). We intend to study some of the controlling factors of the sinking flux of biogenic material including the ballast effect associated to biominerals such as calcium carbonate ($CaCO_3$) and biogenic silica (BSi), as well as the heterotrophic interactions with zooplankton through grazing and repacking.

For carbon, export fluxes estimated at different depth horizons, at the base of the euphotic zone corresponding to 1% of photosynthetically available radiation (PAR), the sub-photic zone (0.1% PAR) and also 100 m below the sub-photic zone, will allow to obtain relevant metrics (vertical transfer and surface export efficiencies) allowing a complete description of the BCP in the upper water column. Finally, and using a suite of biomarkers including fatty acids, sterols, and amino-acids, we intend to constrain the origin and transformation pathways of suspended organic matter in the first 800 m.

VIII.2.3 Methodology and sampling strategy

The methodological approach for estimating the vertical export fluxes of POC and by extension of PN, POP, BSi, $CaCO_3$, lithogenic particles, and trace elements is based on ^{234}Th deficiency method (Lemaitre et al., 2016; Planchon et al., 2013). Briefly, ^{234}Th is a short-lived radionuclide ($T_{1/2}$=24.1 d) produced by the radioactive decay of ^{238}U. Unlike ^{238}U which is highly soluble and conservative in seawater, ^{234}Th has a strong affinity for particles and can rapidly be scavenged by the vertical export of particles. This loss of ^{234}Th creates a disequilibrium with its parent nuclide in surface waters, which can be quantitatively and temporally related to the export flux of particles (Savoye et al., 2006). Using the POC (or element) to ^{234}Th ratio of sinking particles, the net ^{234}Th export flux can then be converted into a POC or any elemental export flux.

The sampling strategy (Table 29) has consisted first in resolving the distribution of total ^{234}Th activity in the first 1000 m of the water column at a high vertical resolution. At high bathymetry (>1500 m) stations, 20-21 depths were sampled with 12 sampled depths between the surface and 200 m depth, and 6 sampled depths between 200 and 800 m depth. The deepest samples were taken at 1000 and 1500 m depth for calibration purpose, with the assumption that ^{234}Th and ^{238}U are in secular equilibrium at these depths. For stations with a low bathymetry, sampling was adjusted according to bottom depth and the same resolution was taken in the upper interval. Total ^{234}Th activity was obtained with 4 L of seawater samples collected at the classic CTD rosette from NISKIN bottle. Seawater samples were processed following the methodology developed by Pike et al. (2005) and adapted by Planchon et al. (2013). Seawater samples are first acidified with nitric acid (pH = 2) and spiked with ^{230}Th as a yield tracer, then samples were co-precipitated with MnO_2 and filtered on 25 mm QMA filters. Filters were then dried (T=60°C) overnight and mounted on polyacrylamide support filter for beta counting on-board. Beta

counting were performed using a two low-level beta counter (RISO Scientific), protected with a lead shield. Activities were measured until counting uncertainty (2σ) reached 2%. Each sample for total activity was measured twice.

In addition to total ^{234}Th activity, the good application of the deficiency method requires particulate ^{234}Th and co-occurring elements (C, N, P, Si, Ca, TE) to be measured in the particulate phase. Suspended particles were sampled using large volume in-situ pumping systems (ISP) deployed at 13 stations. According to the bathymetry, between 4 and 8 ISP were deployed between the surface and 800 m depth. Suspended particles were collected at each depth according to size with the following filter configuration: 50 µm PETEX, 5 µm PETEX, 1 µm QMA allowing three size fractions of particles to be obtained (Large >50 µm, medium 5-50 µm, and small 1-5 µm). After ISP recovery, filters were processed onboard with a first step of subsampling performed in the clean bubble for TE determination on the two PETEX filters. For total ^{234}Th activity, one quarter of each PETEX filter was processed as follow: particles were washed from the PETEX using filtered (0.4 µm) seawater collected at deep depth (>1000 m) and then recollected on 25mm QMA filters. 25mm QMA filters were then dried (T=60°C) and treated similarly as co-precipitated samples for beta counting. For the 142mm QMA filters, 25mm punches were taken and processed as described above. For each sample, beta activity was measured until counting uncertainty (2σ) reached 3%. POC, PN concentrations and natural isotopic composition of C and N (δ^{13}C, δ^{15}N) will be obtained on the same subsamples processed for particulate ^{234}Th activity. BSi and lithogenic Si (LSi), major (Ca, Na, P) and TE concentrations, and biomarkers abundances will be measured on separate subsamples of the PETEX filters. For biomarkers, punches on the 142 mm QMA were taken.

Table 249: Exhaustive list of measured parameters for Carbon, major and trace elements export determination

Parameter	Code of operation (Station-cast)	Number of samples
Total ^{234}Th	SWG-03-010-S	21
Particulate ^{234}Th, major (C, N, P, BSi, LSi, Ca, Na) and TE particulate concentrations	SWG-03-009-P	8
3. Total ^{234}Th	SWG-04-014-C	8
4. Total ^{234}Th	SWG-04-015-S	3
Particulate ^{234}Th, major (C, N, P, BSi, LSi, Ca, Na) and TE particulate concentrations	SWG-04-016-P	5
Total ^{234}Th	SWG-11-033-S	19
Particulate ^{234}Th, major (C, N, P, BSi, LSi, Ca, Na) and TE particulate concentrations	SWG-11-030-P	7
Total ^{234}Th	SWG-14-042-S	8

Particulate ^{234}Th, C, N, P, Ca, Na particulate concentrations	SWG-14-043-P	4
Total ^{234}Th	SWG-21-055-S	20
Particulate ^{234}Th, major (C, N, P, BSi, LSi, Ca, Na) and TE particulate concentrations	SWG-21-056-P	6
Particulate ^{234}Th, major (C, N, P, BSi, LSi, Ca, Na) and TE particulate concentrations	SWG-25-066-P	7
Total ^{234}Th	SWG-25-067-S	19
Total ^{234}Th	SWG-31-080-S	17
Particulate ^{234}Th, major (C, N, P, BSi, LSi, Ca, Na) and TE particulate concentrations	SWG-31-081-P	7
Particulate ^{234}Th, major (C, N, P, BSi, LSi, Ca, Na) and TE particulate concentrations	SWG-33-086-P	7
Total ^{234}Th	SWG-33-088-S	14
Total ^{234}Th	SWG-33-090-S	2
Particulate ^{234}Th, major (C, N, P, BSi, LSi, Ca, Na) and TE particulate concentrations	SWG-38-104-P	7
Total ^{234}Th	SWG-38-105-S	19
Total ^{234}Th	SWG-42-111-S	18
Particulate ^{234}Th, major (C, N, P, BSi, LSi, Ca, Na) and TE particulate concentrations	SWG-42-113-P	7
Particulate ^{234}Th, major (C, N, P, BSi, LSi, Ca, Na) and TE particulate concentrations	SWG-44-119-P	4
Total ^{234}Th	SWG-44-120-S	13
Total ^{234}Th	SWG-47-128-S	20

Particulate ^{234}Th, major (C, N, P, BSi, LSi, Ca, Na) and TE particulate concentrations	SWG-47-129-P	7
Particulate ^{234}Th, major (C, N, P, BSi, LSi, Ca, Na) and TE particulate concentrations	SWG-58-145-P	7
Total ^{234}Th	SWG-58-148-S	20
Total ^{234}Th	SWG-68-168-S	16
Particulate ^{234}Th, major (C, N, P, BSi, LSi, Ca, Na) and TE particulate concentrations	SWG-68-171-P	6

VIII.2.4 Post-cruise sampling analyses and envisioned timeline of working plan, people involved on shore

^{234}Th activity: All samples will be re-counted after a delay of six ^{234}Th half-lives after sampling in order to correct for the residual beta activity due to longer beta emitter than ^{234}Th. This will be performed at the home laboratory from September 2021.

Samples for Total ^{234}Th will be also processed for coprecipitation recovery. This will be carried out using a double spike technique using ^{229}Th as a second yield tracer. Recovery will be estimated from the ^{230}Th/^{229}Th ratio measured by ICP-SFMS (Jan. 2022).

Particulate samples (three size fractions) will be analyzed for POC, PN, δ13C, δ15N at the LEMAR by EA-IRMS after carbonate removal and encapsulation.

Particulate samples (large and medium size fractions) will be analyzed for BSi and LSi (lithogenic silica). Subsamples of ISP filters will be processed using the three steps alkaline digestion procedure of Ragueneau et al. (2005) followed by online colorimetric (Technicon) for silicic acid and fluorimetric analysis for Al determination. The combined determination of dissolved Si (as Si(OH)4) and Al will allow to correct for the particulate Si contribution of lithogenic origin and to obtain a more reliable estimate of BSi content in SPM. Analytical determination will be carried out at the LEMAR.

In addition, subsamples of ISP filters (three size fractions) will be processed Ca, Na, Al and P content in two size fractions (small and large). These elements will be determined after tri-acid (HCl/HNO3/HF) digestion described in Cardinal et al. (2001) and conversion to analytical matrix (2% HNO_3). Ca, Al, Na and P content will be determined by ICP-QMS and using different certified reference materials BHVO-1, JB-3, JGb-1 and SLRS-5. Analysis is expected to be done in 2022

For trace elements, analysis will be performed following the method of Planquette and Sherrell (2012) on two size fractions (large and medium). The final database for ^{234}Th, major and trace elements is expected to be available at the end of 2022.

For lipids including fatty acids and sterols, the determination will include the following steps:

Lipid extraction using 2:1 chloroform:methanol (Folch et al., 1957)

2:1 chloroform:methanol lipid extracts will be further separated into Neutral and Polar fraction using Solid Phase Extraction and with Neutral (98:2 Chloroform:methanol) and Polar (methanol) solvents.

The two fractions (neutral and polar) will be then transmethylated to allow FA determination by GC-FID. Molecular identification and quantification will be performed according to retention time and using an internal standard of known composition (23:0) (Soudant et al., 1999)

Analysis will be performed according to funding availability and no timeline can be given.

References

Cardinal, D., Dehairs, F., Cattaldo, T., André, L., 2001. Geochemistry of suspended particles in the Subantarctic and Polar Frontal Zones south of Australia: Constraints on export and advection processes. J. Geophys. Res. 106, 31637-31656.

Folch, J., Lees, M., Stanley, G.H.S., 1957. A simple methods for the isolation and purification of total lipids from animal tissues. J. Biol. Chem. 226, 497–509.

Lemaitre, N., Planquette, H., Dehairs, F., van der Merwe, P., Bowie, A.R., Trull, T.W., Laurenceau-Cornec, E.C., Davies, D., Bollinger, C., Le Goff, M., Grossteffan, E., Planchon, F., 2016. Impact of the natural Fe-fertilization on the magnitude, stoichiometry and efficiency of particulate biogenic silica, nitrogen and iron export fluxes. Deep Sea Research Part I: Oceanographic Research Papers 117, 11-27.

Manno, C., Stowasser, G., Enderlein, P., Fielding, S., Tarling, G.A., 2015. The contribution of zooplankton faecal pellets to deep-carbon transport in the Scotia Sea (Southern Ocean). Biogeosciences 12, 1955-1965.

Morris, P.J., Sanders, R., Turnewitsch, R., Thomalla, S., 2007. 234Th-derived particulate organic carbon export from an island-induced phytoplankton bloom in the Southern Ocean. Deep Sea Research Part II: Topical Studies in Oceanography 54, 2208-2232.

Pike, S.M., Buesseler, K.O., Andrews, J., Savoye, N., 2005. Quantification of 234Th recovery in small volume sea water samples by inductively coupled plasma-mass spectrometry. Journal of Radioanalytical and Nuclear Chemistry 263, 355-360.

Planchon, F., Ballas, D., Cavagna, A.J., Bowie, A.R., Davies, D., Trull, T., Laurenceau-Cornec, E.C., Van Der Merwe, P., Dehairs, F., 2015. Carbon export in the naturally iron-fertilized Kerguelen area of the Southern Ocean based on the 234Th approach. Biogeosciences 12, 3831-3848.

Planchon, F., Cavagna, A.J., Cardinal, D., André, L., Dehairs, F., 2013. Late summer particulate organic carbon export and twilight zone remineralisation in the Atlantic sector of the Southern Ocean. Biogeosciences 10, 803-820.

Planquette, H., Sherrell, R.M., 2012. Sampling for particulate trace element determination using water sampling bottles: methodology and comparison to in situ pumps. Limnology and Oceanography Methods 10, 367-388.

Puigcorbé, V., Roca-Martí, M., Masqué, P., Benitez-Nelson, C.R., Rutgers v. d. Loeff, M., Laglera, L.M., Bracher, A., Cheah, W., Strass, V.H., Hoppema, M., Santos-Echeandía, J., Hunt, B.P.V., Pakhomov, E.A., Klaas, C., 2017. Particulate organic carbon export across the Antarctic Circumpolar Current at 10°E: Differences between north and south of the Antarctic Polar Front. Deep Sea Research Part II: Topical Studies in Oceanography 138, 86-101.

Ragueneau, O., Savoye, N., Del Amo, Y., Cotten, J., Tardiveau, B., Leynaert, A., 2005. A new method for the measurement of biogenic silica in suspended matter of coastal waters: using Si:Al ratios to correct for the mineral interference. Continental Shelf Research 25, 697-710.

Rembauville, M., Salter, I., Leblond, N., Gueneugues, A., Blain, S., 2015. Export fluxes in a naturally iron-fertilized area of the Southern Ocean – Part 1: Seasonal dynamics of particulate organic carbon export from a moored sediment trap. Biogeosciences 12, 3153-3170.

Roca-Martí, M., Puigcorbé, V., Iversen, M.H., van der Loeff, M.R., Klaas, C., Cheah, W., Bracher, A., Masqué, P., 2017. High particulate organic carbon export during the decline of a vast diatom bloom in the Atlantic sector of the Southern Ocean. Deep Sea Research Part II: Topical Studies in Oceanography 138, 102-115.

Rosengard, S.Z., Lam, P.J., Balch, W.M., Auro, M.E., Pike, S., Drapeau, D., Bowler, B., 2015. Carbon export and transfer to depth across the Southern Ocean Great Calcite Belt. Biogeosciences 12, 3953-3971.

Salter, I., Lampitt, R.S., Sanders, R., Poulton, A., Kemp, A.E.S., Boorman, B., Saw, K., Pearce, R., 2007. Estimating carbon, silica and diatom export from a naturally fertilised phytoplankton bloom in the Southern Ocean using PELAGRA: A novel drifting sediment trap. Deep Sea Research Part II: Topical Studies in Oceanography 54, 2233-2259.

Savoye, N., Benitez-Nelson, C., Burd, A.B., Cochran, J.K., Charette, M., Buesseler, K.O., Jackson, G.A., Roy-Barman, M., Schmidt, S., Elskens, M., 2006. 234Th sorption and export models in the water column: A review. Marine Chemistry 100, 234-249.

Savoye, N., Trull, T.W., Jacquet, S.H.M., Navez, J., Dehairs, F., 2008. 234Th-based export fluxes during a natural iron fertilization experiment in the Southern Ocean (KEOPS). Deep Sea Research Part II: Topical Studies in Oceanography 55, 841-855.

Soudant, P., Ryckeghem, K.V., Marty, Y., Moal, J., Samain, J.F., Sorgeloos, P., 1999. Comparison of the lipid class and fatty acid composition between a reproductive cycle in the nature and a standart hatchery conditioning of the Pacific Oyster Crassostrea gigas. Comp. Biochem. Physiol. B 123, 209–222.

VIII.3 Sediment coring

People involved:

On board: Maria-Elena Vorrath (LEMAR, Plouzané), Bruno Hamelin (CEREGE, Aix-en-Provence), Natalia Torres-Rodriguez (MIO, Marseille), Fabien Perault (DT INSU, Plouzané), Emmanuel de Saint Léger (DT INSU, Plouzané). On shore : Lars-Eric Heimbürger-Boavida (MIO, Marseille)

Sediment samples were collected to investigate the cycling of different trace metals and isotopes from the water column into the upper sediments. At several stations a mono-corer was attached to the *in-situ* pumps. Due to the high sensitivity of the mono-corer to the moving ship many casts failed and only 8 sediment cores were retrieved successfully (Table 30). The sediment core was sliced with plastic plates into 0.2mm to 0.5mm slices and stored frozen (-20°C) in a box to be transported to the University Marseille for further processing. Additionally, supernatant water, here "bottom water", was also sampled to measured trace metals concentrations within the 20 cm above the seafloor. At every station, Hg concentrations in bottom water were directly measured on board from Natalia Torres-Rodriguez, while all other water samples were stored frozen (-20°C) in a box to be transported to the LEMAR, Brest, for analysis of particulate trace metals. For the sediments, several analyses are planned on land to reveal the cycling of certain trace metals. The concentrations of different trace metals, e.g. Mn, Fe, will be examined by Hélène Planquette (LEMAR, Brest), Zn and Ni isotopes by Nolwenn Lemaitre (ETH Zurich), Pb isotopes by Bruno Hamelin (AMU-CEREGE, Aix-Marseille), REE and Nd isotopes by Catherine Jeandel (LEGOS, Toulouse), Hg isotopes by Lars-Eric Heimbürger-Boavida (AMU-MIO, Marseille) and Ba isotopes by Stephanie Jacquet (AMU-MIO, Marseille; Table 31).

Table 30: Overview of station, sediment length, water depth, samples and core description.

Station ID	Water Depth [m]	Core Length [cm]	No. of sediment and water samples	Core description
SWG_03_09	2182	16	1x50ml bottom water* 2x60ml bottom water 27x sediment (0-13,5cm á 0,5cm)	Muddy clay
SWG_25_70	3714	12	1x50ml bottom water* 3x60ml, 1x20ml bottom water 27x sediment (0-3cm á 0,2cm, 3-9cm	Calcareous ooze
SWG_33_89	2164	12	1x50ml bottom water* 3x60ml bottom water 27x sediment (0-3cm á 0,2cm, 3-9cm	Fine sand
SWG_42_113		9	1x50ml bottom water* 4x60ml bottom water 20x sediment (0-3cm á 0,2cm, 3-5,5cm	Calcareous fine sand
SWG_46_127			1x sediment 0-4cm	
SWG_47_132			26 x sediment (0-8 cm á 0,2cm)	
SWG_66_166			16x sediment (0-8cm á 0,5cm)	
SWG_68_172			28x sediment (0-9 cm á 0,2cm)	

Table 31: Overview of investigated parameters from the core samples once freeze-dried at M.I.O

PI	Parameters	Dry weight required (g)
N. Lemaitre (ETH)	Ni & Zn isotopes	1
H. Planquette (LEMAR)	Fe, Al, Mn, Co, Cu, Ni, Zn, Mo, Pb, Ti, Cr, Zr, Ba, P, Zr, Sr, Cd and Fe isotopes	2
S. Jacquet (M.I.O)	Ba & Ba isotopes	3
B. Hamelin (CEREGE)	Pb isotopes	0.2
L.-E. Heimbüger (M.I.O)	Hg and Hg isotopes	0.5
C. Jeandel (LEGOS)	REE and Nd isotopes	0.3
R. Granger (UCT)	foraminifera	6

IX. OUTREACH ACTIVITIES

Principal investigators
Catherine Jeandel (LEGOS, Toulouse) & Hélène Planquette (LEMAR, Plouzané)

Names of other participants
Most of the cruise participants
Sibylle le Barrois d'Orgeval (sibdor@gmail.com)
Laurent Godard (godass9@gmail.com)

Abstract

The SWINGS outreach activity is structured following 4 main actions: 1) a documentary maker, Sibylle le Barrois d'Orgeval is realizing a documentary on the cruise. With the help of Laurent Godard, they did videos, rushes and will finish on land; 2) an online journal, eXploreur from the Toulouse University, was weekly edited (8 articles), 3) a daily web site, maintained in Toulouse, which received 28 articles from the cruise participants 4) a special communication towards the schools, including an exchange with convicts.

In addition, we edited a logo (with the help of F. Perault (DT INSU) and S. Hervé (IUEM) and realized T-shirts and hoodies, that were distributed to all the people on board (including the crew).

IX.1.1 Scientific context

Outreach is an essential activity of the SWINGS project and we developed efficient ways to communicate on our activities

IX.1.2 Overview of the project and objectives

The objectives were to broadcast as largely as possible the research activity developed on boardMethodology and sampling strategy

The scheme reported in Figure IX-1 summarizes the structure of the scientific mediation made from the *Marion Dufresne* by the people on board and how it was relayed on land by Elena Masferrer (web site, (https://swings.geotraces.org/)) and Anne-Claire Jolivet (journal eXploreur : https://exploreur.univ-toulouse.fr/). These 2 sources of information were thus used by many actors like the CNRS, the IUEM at university of Bretagne Occidentale, the professors of schools, including the service éducatif de l'Observatoire Midi-Pyrénées, Toulouse (https://edu.obs-mip.fr/a-propos/) and journalists.

In addition to what was written by the scientists, Sibylle d'Orgeval and Laurent Godard were taking images and videos in order to make a documentary relating the work at sea, the daily on-board life and the personal motivations of scientists involved.

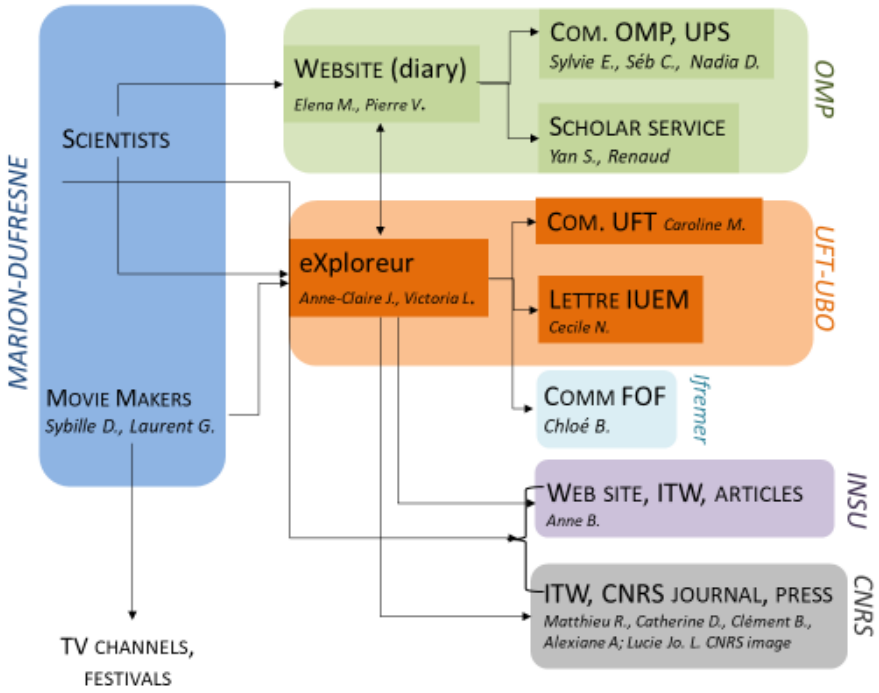

Figure IX-1: Structure of the outreach organized in the framework of SWINGS. In blue: the source of information; the other colours are distinguishing the different actors that were using this information.

IX.1.3 Preliminary results

We have got 12 institutional articles (including 8 with eXploreur), 6 radio interviews including a special broadcast "la Terre au Carré" on France Inter the public radio on march 29th, 2021, more than 14 articles in different journals and many interactions with schools (different levels) including the Seysses jail in the area of Toulouse. The movie will be realized by Sibylle d'Orgeval within the coming year. Our activites were also included in a video realized by NSF.

The media coverage of SWINGS activities is compiled following

https://www.geotraces.org/geotraces-french-swings-gs02-cruise-press-review/

and reported below:

EXPLOREUR journal (Université de Toulouse): Expedition SWINGS. This journal has followed the SWINGS expedition publishing one article per week: https://exploreur.univ-toulouse.fr/swings-expedition-english
News, University of Liverpool, UK (25 February 2021): Studying iron cycling in the Southern Ocean Download the pdf version of this article.
Embassy of France in Australia (24 February 2021): Let's swing together on the Southern Ocean! Download the pdf version of this article.
CNRS, News: Exploring the world's largest ocean current (26 January 2021): Exploring the world's largest ocean current Download the pdf version of this article.
News, Florida International University (21 April 2021: 52 days at sea — with someone else's research

In other languages:

Journal articles

(French) EXPLOREUR journal (Université de Toulouse): Expedition SWINGS. This journal has followed the SWINGS expedition publishing one article per week: https://exploreur.univ-toulouse.fr/expedition-swings

The French CNRS have broadcasted these articles as well.

(French) Ouest France Journal (1st January 2021): PORTRAIT. Hélène Planquette recherche les poussières de fer dans l'océan

(French) France Bleu (5th January 2021): Des Bretons se préparent à embarquer sur le Marion-Dufresne II

(French) CNRS INSU News (13 January 2021): En route pour l'Océan austral avec la campagne SWINGS. Download the pdf version of this article.

(French) Ouest France Journal (18th January 2021): Deux mois sur le « Marion Dufresne » pour tenter de percer les secrets de l'océan

(French) Ouest France Journal (19th January 2021): Deux cheffes de mission océanographique comblées

(French) La Dépêche Journal (19th January 2021): Depuis Toulouse, cette chercheuse participe à l'expédition océanographique SWINGS. Download the pdf version of this article.

(French) Ouest France Journal (29th January 2021): « Embrassez qui vous voudrez » dans l'océan Austral

(French) Ouest France Journal (2nd February 2021): La Brestoise Hélène Planquette raconte son voyage scientifique dans les mers australes.

(French) La Dépêche Journal (7th March 2021): Toulouse. Science : l'incroyable odyssée d'un équipage toulousain dans les mers australes

(French) France Info, Occitanie (9th March 2021): Retour des chercheurs toulousains partis 8 semaines en mer australe étudier comment l'océan régule le climat Download the pdf version of this article.

(French) France 3 – Occitanie (10th March 2021): Retour des chercheurs toulousains partis 8 semaines en mer australe étudier comment l'océan régule le climat. Download the pdf version of this article.

(French) Ouest France Journal (13 April 2021): La mer notre avenir, interview to Nolwenn Lemaitre (journal supplement: La génération sur la pont). Download the pdf version of this supplement.

(French) Le Monde (27 April 2021): De Jean-Louis Etienne à Swings : la quête des mystères de l'océan Austral, crucial dans la régulation du climat

(French) Les étoiles brillent pour tous, website (27 Mai 2021): Les détenus de Seysses à bord du Marion Dufresne par temps de COVID

Radio podcasts or TV videos in French:

(French) Interview on France Inter Radio show "Le 7/9" (12 January 2021), listen the podcast here: https://www.franceinter.fr/emissions/le-7-9/le-7-9-12-avril-2021

(French) Interview to Hélène Planquette on RCF Radio show "La matinale" (20 January 2021), listen the podcast here: https://rcf.fr/la-matinale/swings-une-expedition-pour-comprendre-la-regulation-du-climat-22

(French) Interview to Catherine Jeandel on France 3 – Occitanie TV (16 March 2021) starting at minute 17'44": https://france3-regions.francetvinfo.fr/occitanie/emissions/jt-1920-midi-pyrenee

(French) Interview to Hélène Planquette on RCF Radio show "La matinale" (17 March 2021), listen the podcast here: https://rcf.fr/la-matinale/swings-mission-reussie-bord-du-marion-dufresne

***(French) Interview to Nolwenn Lemaitre on* RTS Radio 'CQFD' (25 March 2021) : Expédition SWINGS :**
https://pages.rts.ch/la-1ere/programmes/cqfd/25-03-2021

(French) Interview to Catherine Jeandel and Hélène Planquette on France Inter Radio show "La Terre au Carré" (29 March 2021), listen the podcast here: https://www.franceinter.fr/emissions/la-terre-au-carre/la-terre-au-carre-29-mars-2021

X. APPENDIX

X.1 Bilan technique CTD & LADCP

Principal Investigator :
Elodie Kestenare, LEGOS
Elodie.Kestenare@legos.obs-mip.fr

Généralités

- Pour le post-processing des CTDs et des LADCPS, sur Windows: utilisation d'un package de l'US IMAGO (IRD Brest). Nous avons eu besoin d'adapter le software pour les CTD (Clean et Standard). Le batch pour le SBE processing a aussi été modifié à bord.

- La turbidité n'ayant pas été incluse dans la configuration initiale des batch du processing des CTD Standard, il faudra prévoir de le faire pour le reprocessing final post campagne. Prévoir aussi d'intégrer l'altimètre dans le jeu final.

- Les profils CTD ont été envoyés à CODAC (SISMER) tous les 2 ou 3 jours.

- Un journal rosette a été réalisé incluant tous les capteurs mesurés au moment de la fermeture des bouteilles, ainsi que les paramètres dérivés (tels que densité, température potentielle, etc). Ce journal rosette a été distribué régulièrement (environ tous les 2 ou 3 jours) à l'ensemble des scientifiques à bord.

- Concernant le code de traitement des LADCPs, nous avons utilisé le code distribué par Andréas Thurnherr, version 10.16 (2013). Nous avons rencontré quelques difficultés avec le package de l'US Imago, sur le PC Windows dédié à la mission : le code de traitement LADCP a initialement été installé (et adapté) sur l'ordinateur portable d'Elodie Kestenare.

Détails par instrument

CTD Standard

- sur 3 casts, des lignes de hiéroglyphes dans les fichiers d'en têtes et sur certaines trames de données, ce qui rend les fichiers illisibles => Cause: peut-être un défaut de transmission au niveau du Deck Unit (défaut qui pourrait être lié à l'ancienneté du Deck Unit ou incompatibilité de version de Seasave versus SBEprocessing => demander à Emmanuel de Saint Léger)
=> solution : une édition manuelle a été faite pour retirer ces lignes avec mauvais caractères.

-problème des spikes: ST01_001 a ST11_036:
le nombre de spikes augmentent au cours de ces casts (visibles au cours du profil en temps réel, affichage 1 seconde)=> Analyse du pb: pour ces stations, tracé de toutes les mesures acquises -en temps différé- c'est a dire 24hz pour confirmer ce constat => alerte à Emmanuel de Saint Léger: nettoyage du contacteur tournant après ST11_029: les spikes sont moins présents, mais ils persistent

-ST12_038: panne du Deck Unit:
solution: réparation par DT INSU et GENAVIR (pour avoir les détails sur la pièce 'fautive', demander à Emmanuel de Saint Léger), la cause des spikes (cf 1.2) est donc déterminée.

Pour s'affranchir des spikes, le processing des CTD a été modifié; tous les casts ont du être rejoués depuis le début de la mission avec une modification du filtre des données, modification qui sera conservée pour toute la campagne. Néanmoins, pour les casts ST1_001 a ST12_038, certains spikes persistent et doivent être supprimés manuellement. A partir du cast ST13_039, les spikes ont totalement disparu.

-pas de SPAR (donc de CPAR) entre ST13_039 et ST23_062:
cause: le SPAR avait été rebranché sur la mauvaise fiche lors du remontage du Deck Unit (cf point 1.3)
solution: le SPAR a été rebranché sur la bonne entrée du Deck unit

- S_25_067: pb capteur 1 conductivité au cours de la descente vers 1150m induisant un offset variant de -.4 a -.3 sur la salinité => cause: filament de méduse observé au retour de la CTD à bord => solution: utiliser les mesures (T,S) du capteur 2

- bouteille 9 non fermée à partir des 3 (?) derniers casts ... à préciser avec les préleveurs (pas retrouvé les infos sur les feuilles de station, Elodie) => Cause: pb mécanique ou défaillance du moteur du carrousel: à confirmer avec Emmanuel de Saint Léger

CTD Clean

Pas d'anomalie relevée (par les personnes en quart CTD, à confirmer par les préleveurs).

LADCP
- PC LADCP pour lancer l'acquisition des instruments était en avance de 1h12mn par rapport au temps TU: casts ST01_001 a ST03_012 => solution : à partir du cast 15, mise à l'heure du PC LADCP avec synchronisation automatique à l'heure TU

- pb de spikes avec les CTD Standard ne permettent pas de traiter les LADCPs
Rappel: profils concernés ST01_001 a ST12_038 (cf point 1.3 ci dessous)
solution: les CTD standard ont été rejoués en changeant le processing. Quelques spikes restant seront supprimés manuellement (cf point 1.3 ci-dessous)

- trois casts sans doute irrécupérables; pour l'un d'eux (ST43_115), le pb est clairement identifié: perte de portée du LADCP down d'environ 150m au lieu de 300 a 350m, mais la raison n'est pas déterminée. Pour d'autres stations/casts, un travail d'analyse doit être effectué pour essayer de comprendre l'origine du bug et tenter de sauver les profils.

- problème "majeur" lors de acquisition des LADCPs: dans les fichiers de configurations (fournis par l'US Imago) pour lancer l'acquisition du 150kHz (downlooker), la commande Bottom Track (BT) n'a pas été donnée
Conséquence: pas de RDI BT (c'est à dire le bottom track effectué par l'instrument lui même). Seul le User bottom track est possible avec le logiciel de traitement, méthode qui semble avoir ses limites pour bien contraindre les profils au fond (analyse sur 15 casts). Ce point concerne un grande majorité des profils acquis lorsque la CTD allait jusqu'au fond.

Commentaire général :

Il est possible que l'origine des soucis du traitement de certains profils LADCP soit liée à d'autres causes (telle qu'une mauvaise synchronisation des 2 LADCPs): l'analyse de ces profils est en cours en collaboration avec Frédéric Marin (Legos). En tout état de cause, tous les profils seront rejoués post-campagne, et sauf exception, ils devraient être entièrement fiables, après un ajustement de certains paramètres dédiés au traitement.

X.1.1 Bilan

Nombre de profils CTD Standard: 94 (+ 5 OISO sur le transit Kerguelen - La Réunion)
Nombre de profils CTD Clean: 40
Nombre de profils avec LADCP: 62

X.1.2 Annexe

Liste des étapes de traitement des fichiers CTD (avec SBEprocessing) : exemple pour la station S_39_107

(1) Fichier avec le profil complet
datcnv_date = Feb 14 2021 09:59:32, 7.26.7.114 [datcnv_vars = 19]
datcnv_in = c:\Cruises\SWINGS\data-processing\CTD_CLASSIC\data\raw\swg_s_39_107.hex c:\Cruises\SWINGS\data-processing\CTD_CLASSIC\data\raw\swg_s_39_107.XMLCON
datcnv_skipover = 0
datcnv_ox_hysteresis_correction = yes
datcnv_ox_tau_correction = no
wfilter_date = Feb 14 2021 09:59:41, 7.26.7.114
wfilter_in = c:\Cruises\SWINGS\data-processing\CTD_CLASSIC\data\tmp\swg_s_39_107.cnv
wfilter_excl_bad_scans = yes
wfilter_action prDM = median, 24
wfilter_action depSM = median, 24
wfilter_action t090C = median, 5
wfilter_action t190C = median, 5
wfilter_action c0S/m = median, 5
wfilter_action c1S/m = median, 5
wildedit_date = Feb 14 2021 09:59:42, 7.26.7.114
wildedit_in = c:\Cruises\SWINGS\data-processing\CTD_CLASSIC\data\tmp\swg_s_39_107.cnv

wildedit_pass1_nstd = 2.0
wildedit_pass2_nstd = 20.0
wildedit_pass2_mindelta = 0.000e+000
wildedit_npoint = 100
wildedit_vars = latitude longitude prDM depSM t090C t190C c0S/m c1S/m sbeox0V sbeox1V sbox0dV/dT sbox1dV/dT CStarTr0 flC par spar cpar
wildedit_excl_bad_scans = yes
filter_date = Feb 14 2021 09:59:43, 7.26.7.114
filter_in = c:\Cruises\SWINGS\data-processing\CTD_CLASSIC\data\tmp\swg_s_39_107.cnv
filter_low_pass_tc_A = 0.030
filter_low_pass_tc_B = 0.150
filter_low_pass_A_vars = latitude longitude sbox0dV/dT sbox1dV/dT flC par spar cpar
filter_low_pass_B_vars = prDM
alignctd_date = Feb 14 2021 09:59:45, 7.26.7.114
alignctd_in = c:\Cruises\SWINGS\data-processing\CTD_CLASSIC\data\tmp\swg_s_39_107.cnv
alignctd_adv = sbeox0V 2.000, sbeox1V 2.000
celltm_date = Feb 14 2021 09:59:46, 7.26.7.114
celltm_in = c:\Cruises\SWINGS\data-processing\CTD_CLASSIC\data\tmp\swg_s_39_107.cnv
celltm_alpha = 0.0300, 0.0300
celltm_tau = 7.0000, 7.0000
celltm_temp_sensor_use_for_cond = primary, secondary
loopedit_date = Feb 14 2021 09:59:47, 7.26.7.114
loopedit_in = c:\Cruises\SWINGS\data-processing\CTD_CLASSIC\data\tmp\swg_s_39_107.cnv
loopedit_minVelocity = 0.000
loopedit_surfaceSoak: do not remove
loopedit_excl_bad_scans = yes
Derive_date = Feb 14 2021 09:59:49, 7.26.7.114 [derive_vars = 10]
Derive_in = c:\Cruises\SWINGS\data-processing\CTD_CLASSIC\data\tmp\swg_s_39_107.cnv c:\Cruises\SWINGS\data-processing\CTD_CLASSIC\data\raw\SWG_S_39_107.xmlcon
derive_time_window_docdt = seconds: 2
derive_ox_tau_correction = no
binavg_date = Feb 14 2021 09:59:51, 7.26.7.114
binavg_in = c:\Cruises\SWINGS\data-processing\CTD_CLASSIC\data\tmp\swg_s_39_107.cnv
binavg_bintype = decibars
binavg_binsize = 1
binavg_excl_bad_scans = yes
binavg_skipover = 0
binavg_omit = 0
binavg_min_scans_bin = 1
binavg_max_scans_bin = 2147483647
binavg_surface_bin = yes, min = 0.000, max = 2.000, value = 0.000
file_type = ascii

(2) Fichier bouteilles

datcnv_date = Feb 14 2021 09:59:32, 7.26.7.114
datcnv_in = c:\Cruises\SWINGS\data-processing\CTD_CLASSIC\data\raw\swg_s_39_107.hex c:\Cruises\SWINGS\data-processing\CTD_CLASSIC\data\raw\swg_s_39_107.XMLCON
datcnv_ox_hysteresis_correction = yes
datcnv_ox_tau_correction = no
datcnv_bottle_scan_range_source = scans marked with bottle confirm bit, -4, 8
datcnv_scans_per_bottle = 193
bottlesum_date = Feb 14 2021 10:00:06, 7.26.7.114
bottlesum_in = c:\Cruises\SWINGS\data-processing\CTD_CLASSIC\data\tmp\swg_s_39_107.ros c:\Cruises\SWINGS\data-processing\CTD_CLASSIC\data\raw\SWG_S_39_107.xmlcon
bottlesum_ox_tau_correction = no

Fichier spécifique nécessaire pour le traitement du LADCP, en complément du fichier avec le profil entier, cf (1)

datcnv_date = Feb 14 2021 09:59:57, 7.26.7.114 [datcnv_vars = 7]
datcnv_in = c:\Cruises\SWINGS\data-processing\CTD_CLASSIC\data\raw\swg_s_39_107.hex c:\Cruises\SWINGS\data-processing\CTD_CLASSIC\data\raw\SWG_S_39_107.xmlcon
datcnv_skipover = 0
wildedit_date = Feb 14 2021 10:00:01, 7.26.7.114
wildedit_in = c:\Cruises\SWINGS\data-processing\CTD_CLASSIC\data\ladcp\swg_s_39_107_ladcp.cnv
wildedit_pass1_nstd = 2.0
wildedit_pass2_nstd = 20.0
wildedit_pass2_mindelta = 0.000e+000
wildedit_npoint = 100
wildedit_vars = prDM t090C sal00 latitude longitude
wildedit_excl_bad_scans = yes
binavg_date = Feb 14 2021 10:00:02, 7.26.7.114
binavg_in = c:\Cruises\SWINGS\data-processing\CTD_CLASSIC\data\ladcp\swg_s_39_107_ladcp.cnv
binavg_bintype = seconds
binavg_binsize = 1
binavg_excl_bad_scans = yes
binavg_skipover = 0
binavg_omit = 0
binavg_min_scans_bin = 1
binavg_max_scans_bin = 2147483647
binavg_surface_bin = no, min = 0.000, max = 0.000, value = 0.000
file_type = ascii

(4) Fichier pour envoi CODAC (SISMER)
datcnv_date = Feb 14 2021 09:59:26, 7.26.7.114 [datcnv_vars = 4]

datcnv_in = c:\Cruises\SWINGS\data-processing\CTD_CLASSIC\data\raw\swg_s_39_107.hex c:\Cruises\SWINGS\data-processing\CTD_CLASSIC\data\raw\SWG_S_39_107.xmlcon
datcnv_skipover = 0
wfilter_date = Feb 14 2021 09:59:29, 7.26.7.114
wfilter_in = c:\Cruises\SWINGS\data-processing\CTD_CLASSIC\data\codac\swg_s_39_107.cnv
wfilter_excl_bad_scans = yes
wfilter_action prDM = median, 24
wfilter_action depSM = median, 24
wfilter_action t090C = median, 5
wfilter_action c0S/m = median, 5
wildedit_date = Feb 14 2021 09:59:30, 7.26.7.114
wildedit_in = c:\Cruises\SWINGS\data-processing\CTD_CLASSIC\data\codac\swg_s_39_107.cnv
wildedit_pass1_nstd = 2.0
wildedit_pass2_nstd = 20.0
wildedit_pass2_mindelta = 0.000e+000
wildedit_npoint = 100
wildedit_vars = prDM depSM t090C c0S/m
wildedit_excl_bad_scans = yes
celltm_date = Feb 14 2021 09:59:30, 7.26.7.114
celltm_in = c:\Cruises\SWINGS\data-processing\CTD_CLASSIC\data\codac\swg_s_39_107.cnv
celltm_alpha = 0.0300, 0.0000
celltm_tau = 7.0000, 0.0000
celltm_temp_sensor_use_for_cond = primary,
filter_date = Feb 14 2021 09:59:30, 7.26.7.114
filter_in = c:\Cruises\SWINGS\data-processing\CTD_CLASSIC\data\codac\swg_s_39_107.cnv
filter_low_pass_tc_A = 0.030
filter_low_pass_tc_B = 0.150
filter_low_pass_A_vars = c0S/m
filter_low_pass_B_vars = prDM depSM
loopedit_date = Feb 14 2021 09:59:30, 7.26.7.114
loopedit_in = c:\Cruises\SWINGS\data-processing\CTD_CLASSIC\data\codac\swg_s_39_107.cnv
loopedit_minVelocity = 0.250
loopedit_surfaceSoak: do not remove
loopedit_excl_bad_scans = yes
binavg_date = Feb 14 2021 09:59:31, 7.26.7.114
binavg_in = c:\Cruises\SWINGS\data-processing\CTD_CLASSIC\data\codac\swg_s_39_107.cnv
binavg_bintype = decibars
binavg_binsize = 5
binavg_excl_bad_scans = yes
binavg_skipover = 0
binavg_omit = 0
binavg_min_scans_bin = 1
binavg_max_scans_bin = 2147483647
binavg_surface_bin = yes, min = 0.000, max = 2.000, value = 0.000
Derive_date = Feb 14 2021 09:59:32, 7.26.7.114 [derive_vars = 1]

Derive_in = c:\Cruises\SWINGS\data-processing\CTD_CLASSIC\data\codac\swg_s_39_107.cnv c:\Cruises\SWINGS\data-processing\CTD_CLASSIC\data\raw\SWG_S_39_107.xmlcon
file_type = ascii

X.2 Evaluation of salinity and oxygen sensor data collected during the SWINGS cruise

By Claire LO MONACO (LOCEAN), Coraline LESEURRE (LOCEAN) and Christophe CASSOU (CERFACS)

The standard rosette and clean rosette were both equipped with two sets of temperature, salinity and oxygen sensors (Seabird, provided by DT INSU, France). Temperature data were checked against underway surface data (SBE38), showing a good agreement (within ± 0.14°C). Salinity and oxygen were checked against bottle measurements. Salinity and oxygen samples were collected from the standard rosette at most of the stations (table A), whereas for the clean rosette, salinity samples were collected at 12 stations and oxygen samples at 2 stations (table B).

Table A: List of the stations where salinity and oxygen samples were collected from the standard rosette, corresponding cast number, and number of salinity and oxygen samples per station (the total number of samples is 436 for salinity and 649 for oxygen).

Station	Cast	Sal	O2	Station	Cast	Sal	O2	Station	Cast	Sal	O2
1	1	20	20	**21**	57	7	7	**41**	110	5	6
2	6	11	22	**22**	60	10	10	**42**	111	7	16
3	12	9	19	**23**	62	9	8	**43**	115	8	14
4	15	6	6	**24**	63	8	10	**44**	120	6	5
5	17	4	4	**25**	69	8	10	**45**	123	4	5
5	19	5	5	**26**	73	7	10	**47**	131	4	9
7	21	8	20	**27**	75	9	11	**48**	133	6	8
8	24	7	8	**28**	76	9	8	**52**	138	5	4
9	25	3	5	**29**	78	10	10	**57**	143	11	11
10	28	10	20	**30**	79	5	7	**58**	146	7	12
11	36	10	22	**31**	80	9	8	**62**	154	8	13
13	39	6	6	**33**	88	8	7	**63**	155	8	11
14	42	10	10	**34**	91	7	18	**66**	162	6	6
15	44	10	11	**35**	94	8	9	**68**	170	5	12
16	46	8	9	**36**	97	9	10	**69**	173	8	19
17	48	6	8	**37**	101	7	17	**70**	174	8	20
18	50	11	11	**38**	103	8	9	**71**	175	8	18
19	52	7	7	**39**	107	7	18	**72**	177	8	19

20	54	3	4		**40**	108	7	18		**73**	178	8	19

Table B: List of the stations where salinity and oxygen samples were collected from the clean rosette, corresponding cast number, and number of salinity and oxygen samples per station (the total number of samples for salinity is 218).

Station	Cast	Sal	O2
1	2	20	
2	7	18	
3	11	20	
4	14	13	
5	18	11	
8	23	18	
10	27	23	
11	34	24	
12	38	7	10
14	41	22	
16	47		9
40	109	19	
48	134	23	

Evaluation of salinity data from the standard rosette

The comparison of the 2 salinity sensors data with bottle salinity measurements shows a general good agreement (Figure A). The mean difference (Sctd – Smeas) in deep and bottom waters (below 1000m) is -0.001 ±0.001 for sensor 1. However, it appears slightly higher at the last two station (72 and 73) with a mean value of -0.004 ±0.001. The mean difference in deep and bottom waters for sensor 2 is -0.001 ±0.002 for stations 1 to 38 and -0.005 ±0.002 for stations 39 to 73.

Recommendations: apply a correction of +0.004 for sensor 1 at stations 72 and 73 and +0.005 for sensor 2 at stations 39 to 73.

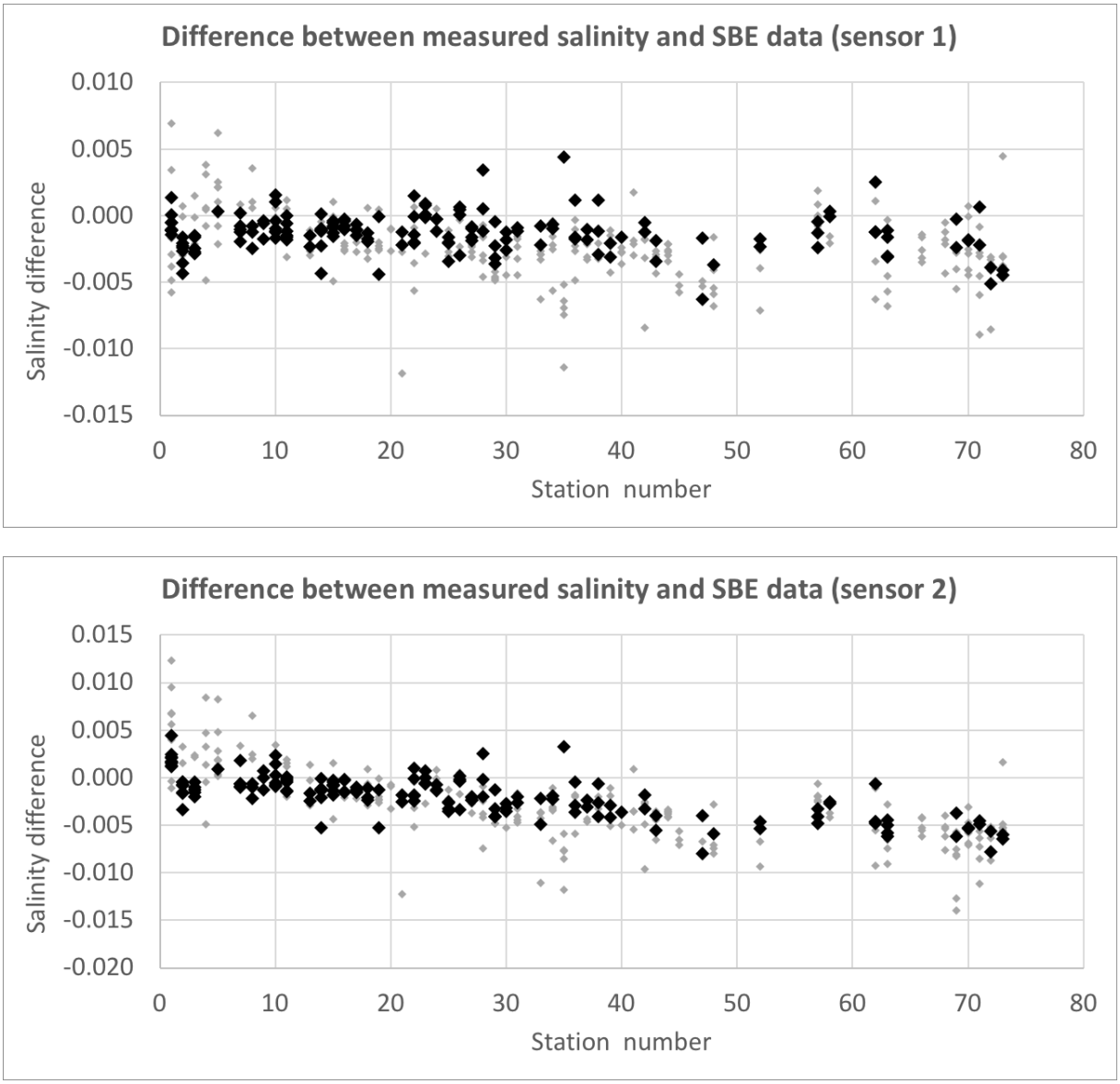

Figure A: Difference between the sensors data and bottle measurements (Sctd – Smeas) for sensor 1 (top) and sensor 2 (bottom) from the standard rosette. The gray dots show all samples whereas the black dots are for deep and bottom water (below 1000m).

Evaluation of oxygen data from the standard rosette

The comparison of the 2 oxygen sensors data with bottle salinity measurements show a significant offset of the 2 sensors and a sudden increase of the offset at station 9 (Figure B). This shift is probably due to the high pressure at the bottom of station 9 (down to 5800m). Consequently, the offset at station 9 was higher during the upcast than during the downcast.

- **Recommended corrections (station per station)**

The sensors data should be corrected according to Table C. These corrections were evaluated by comparing the bottle data with the upcast profile. For station 9, the correction is thus not suitable for the downcast profile. At this station, the sensors data during the upcast should be corrected using the coefficients evaluated at station 8. At all stations, the regression curve changes below the minimum oxygen layer. For this reason, a different correction should be applied in upper and lower waters (Table 3). Within the minimum oxygen layer, one or the other correction can be applied, leading to very similar results. The residuals are generally lower than 2 µmol/kg (Figure C). The standard (root mean square) error is 0.8 µmol/kg for sensor 1 and 0.9 µmol/kg for sensor 2.

- **Global corrections**

A rough correction could also be applied to the sensors data by combining stations 1 to 8 (+downcast of station 9) and stations 9 (upcast) to 73 (Figure D), as follows:

stations 1 to 8 (+ the downcast of station 9), sensor 1: O2corr = 1.0512x + 5.04

stations 1 to 8 (+ the downcast of station 9), sensor 2: O2corr = 1.0591x + 10.82

stations 9 (upcast) to 73, sensor 1: O2corr = 1.0548x + 12.53

stations 9 (upcast) to 73, sensor 2: O2corr = 1.0814x + 15.57

The residuals can reach 10 µmol/kg (Figure E). The standard (root mean square) error is 2.2 µmol/kg for sensor 1 and 2.8 µmol/kg for sensor 2.

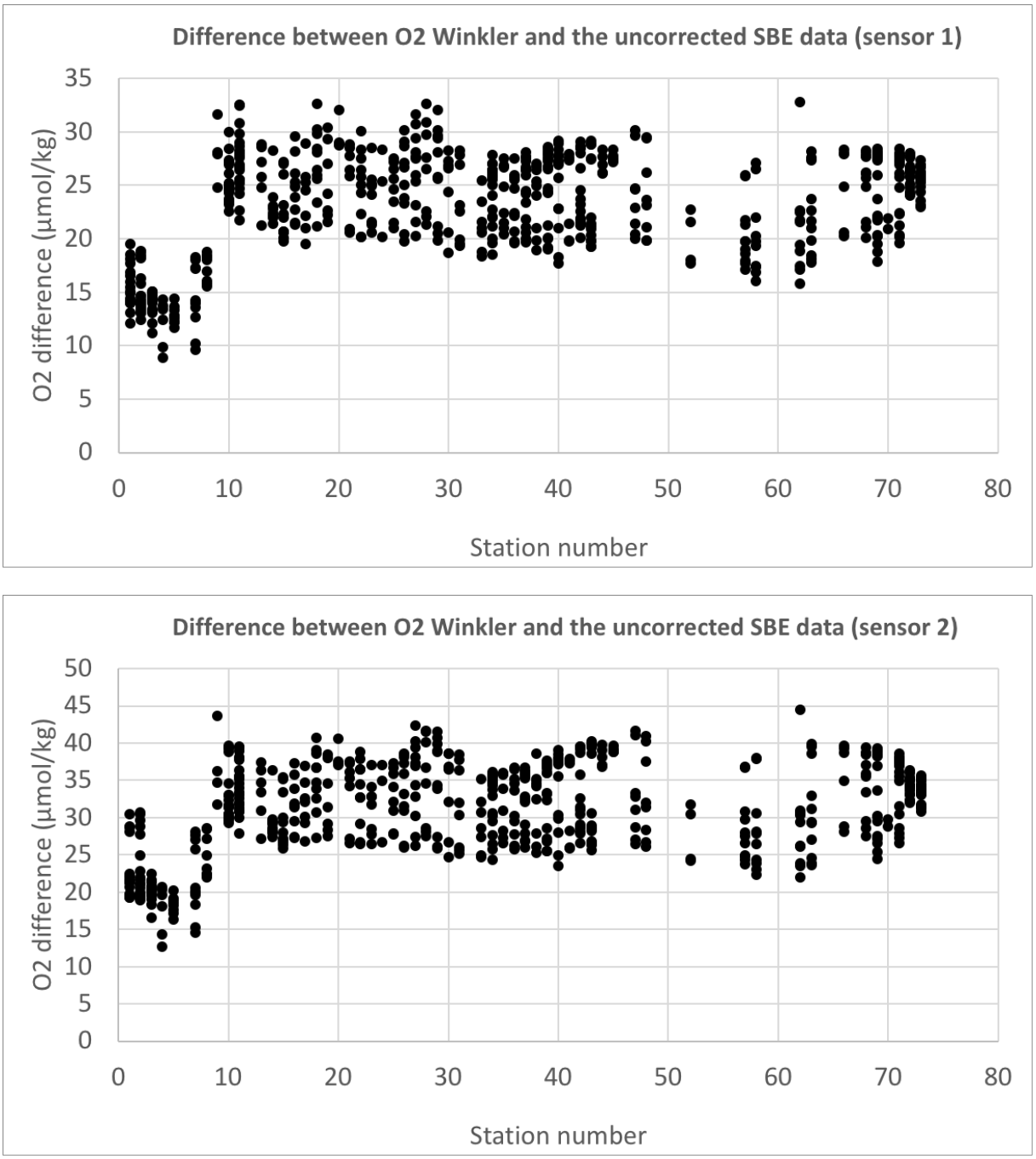

Figure B: Difference between the sensors uncorrected data and bottle measurements (O2meas - O2ctd) for sensor 1 (top) and sensor 2 (bottom) from the standard rosette.

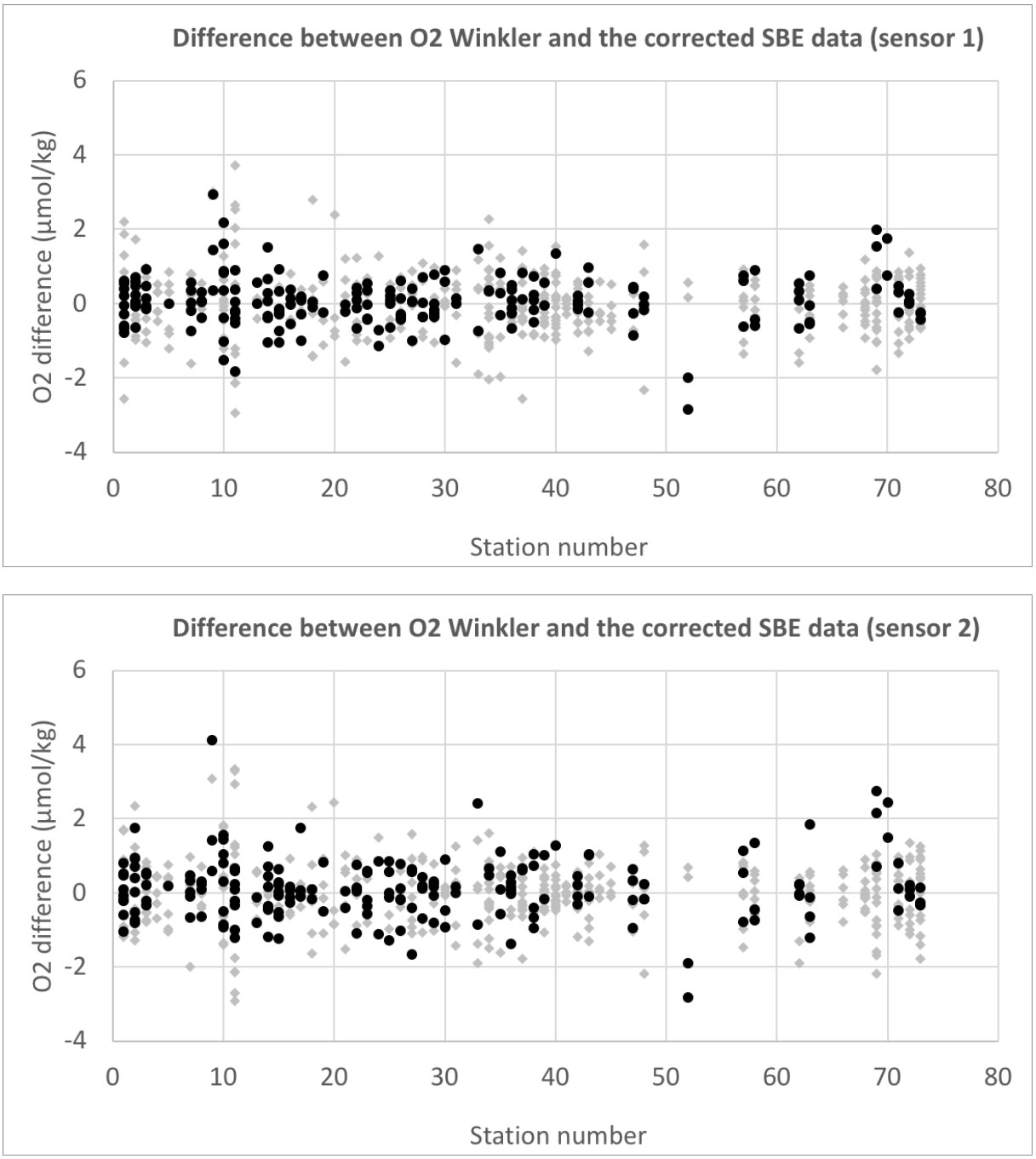

Figure C: Difference between the sensors corrected data and bottle measurements (O2meas - O2ctd) for sensor 1 (top) and sensor 2 (bottom) from the standard rosette. The sensors data were corrected according to Table 3. The gray dots show all samples whereas the black dots are for deep and bottom water (below 1000m).

Table C: Corrections for oxygen data from the 2 sensors on the standard rosette. The corrected sensor data (O2corr) are calculated following: O2corr = a.x + b, where x is the uncorrected data. A different correction is given be applied above and below the minimum oxygen layer (upper and lower waters, respectively). Within the minimum oxygen layer, one or the other correction can be applied.

			Sensor 1		Sensor 2	
Station	**Cast**	**Depth**	**a**	**b**	**a**	**b**
S01	1	**upper**	1.000	14.7	0.979	24.8
S01	1	**lower**	1.113	-2.8	1.215	-9.2
S02	6	**upper**	1.019	10.2	1.008	18.9
S02	6	**lower**	1.110	-3.3	1.216	-11.1
S03	12	**upper**	1.048	4.8	1.060	8.9
S03	12	**lower**	1.083	-0.2	1.155	-3.9
S04	15	**upper**	1.086	-2.9	1.136	-5.2
S05	17	**upper**	1.040	6.0	1.071	6.2
S05	19	**upper**	1.040	6.0	1.071	6.2
S06	20	**upper**	1.040	6.0	1.071	6.2
S06	20	**lower**	1.109	-3.6	1.193	-8.7
S07	21	**upper**	1.124	-10.1	1.152	-8.9
S07	21	**lower**	1.109	-3.5	1.192	-8.5
S08	24	**upper**	0.948	26.5	0.947	32.9
S08	24	**lower**	1.004	17.6	1.085	12.2
S09	25	**upper**	1.041	16.7	1.025	26.8
S09	25	**lower**	1.095	10.2	1.230	-2.4
S10	28	**upper**	1.035	17.7	1.019	27.5
S10	28	**lower**	1.091	10.2	1.221	-1.9
S11	36	**upper**	1.165	-4.2	1.177	0.7
S11	36	**lower**	1.139	0.8	1.250	-8.6
S13	39	**upper**	1.068	10.1	1.090	13.1
S13	39	**lower**	1.135	1.4	1.255	-9.5
S14	42	**upper**	1.055	13.2	1.077	16.2
S15	44	**upper**	1.060	11.0	1.078	15.0
S15	44	**lower**	1.180	-8.7	1.258	-13.6
S16	46	**upper**	1.067	10.4	1.083	14.1
S16	46	**lower**	1.140	-1.0	1.213	-5.6
S17	48	**upper**	1.074	8.4	1.070	17.6
S17	48	**lower**	1.155	-4.1	1.273	-15.4
S18	50	**upper**	1.074	8.9	1.097	11.8
S18	50	**lower**	1.179	-8.2	1.308	-21.3
S19	52	**upper**	1.069	10.4	1.091	13.5
S20	54	**upper**	1.067	10.6	1.089	13.6
S21	57	**upper**	1.065	10.3	1.090	12.8
S22	60	**upper**	1.074	7.6	1.101	9.9
S22	60	**lower**	1.158	-5.3	1.273	-16.1

			Sensor 1		Sensor 2	
Station	**Cast**	**Depth**	**a**	**b**	**a**	**b**
S29	78	**upper**	1.078	7.7	1.108	9.4
S29	78	**lower**	1.164	-5.5	1.300	-20.0
S30	79	**upper**	1.064	8.4	1.099	9.5
S30	79	**lower**	1.156	-5.5	1.284	-18.6
S31	80	**upper**	1.063	8.9	1.096	10.1
S31	80	**lower**	1.134	-2.0	1.240	-11.6
S33	88	**upper**	1.040	12.7	1.064	15.5
S34	91	**upper**	1.058	10.0	1.084	12.4
S35	94	**upper**	1.045	13.4	1.068	16.7
S36	97	**upper**	1.063	9.5	1.087	12.4
S36	97	**lower**	1.166	-7.4	1.310	-22.7
S37	101	**upper**	1.057	10.6	1.081	13.7
S38	103	**upper**	1.070	7.9	1.096	10.6
S38	103	**lower**	1.172	-8.1	1.333	-26.3
S39	107	**upper**	1.070	7.9	1.094	11.2
S40	108	**upper**	1.075	6.0	1.110	7.0
S40	108	**lower**	1.172	-8.1	1.333	-26.3
S41	110	**upper**	1.061	10.2	1.094	11.7
S42	111	**upper**	1.060	10.8	1.097	11.8
S42	111	**lower**	1.116	1.8	1.191	-2.5
S43	115	**upper**	1.061	10.1	1.096	12.0
S44	120	**upper**	1.061	10.1	1.096	12.0
S45	123	**upper**	1.061	10.1	1.096	12.0
S47	131	**upper**	1.069	9.2	1.107	10.2
S47	131	**lower**	1.132	-0.2	1.201	-3.0
S48	133	**upper**	1.059	10.5	1.095	12.0
S48	133	**lower**	1.140	-2.0	1.216	-5.5
S52	138	**upper**	1.058	8.4	1.093	9.7
S52	138	**lower**	1.140	-2.0	1.216	-5.5
S57	143	**upper**	1.058	8.4	1.093	9.7
S57	143	**lower**	1.132	-4.5	1.250	-16.3
S58	146	**upper**	1.075	4.6	1.114	5.1
S58	146	**lower**	1.160	-9.7	1.244	-15.6
S59	151	**upper**	1.075	4.6	1.114	5.1
S59	151	**lower**	1.160	-9.7	1.244	-15.6
S61	153	**upper**	1.075	4.6	1.114	5.1
S61	153	**lower**	1.160	-9.7	1.244	-15.6

S23	62	**upper**	1.058	11.2	1.082	13.7
S23	62	**lower**	1.158	-4.9	1.239	-10.4
S24	63	**upper**	1.058	11.2	1.082	13.7
S24	63	**lower**	1.158	-4.9	1.239	-10.4
S25	69	**upper**	1.070	9.3	1.093	12.5
S25	69	**lower**	1.147	-2.4	1.272	-14.9
S26	73	**upper**	1.073	8.1	1.100	10.5
S26	73	**lower**	1.199	-12.4	1.341	-27.7
S27	75	**upper**	1.072	9.3	1.106	10.2
S27	75	**lower**	1.154	-3.4	1.291	-17.9
S28	76	**upper**	1.086	6.5	1.117	7.4
S28	76	**lower**	1.171	-6.0	1.318	-22.1

S62	154	**upper**	1.109	-0.8	1.151	-0.3
S62	154	**lower**	1.171	-9.8	1.256	-15.5
S63	155	**upper**	1.065	7.6	1.108	7.5
S63	155	**lower**	1.156	-6.6	1.264	-16.2
S66	162	**upper**	1.073	6.0	1.105	8.6
S68	170	**upper**	1.062	9.7	1.096	11.6
S69	173	**upper**	1.062	9.5	1.096	11.5
S70	174	**upper**	1.062	9.5	1.096	11.5
S71	175	**upper**	1.069	8.8	1.099	11.9
S72	177	**upper**	1.075	10.0	1.078	18.1
S73	178	**upper**	1.077	9.4	1.080	17.3

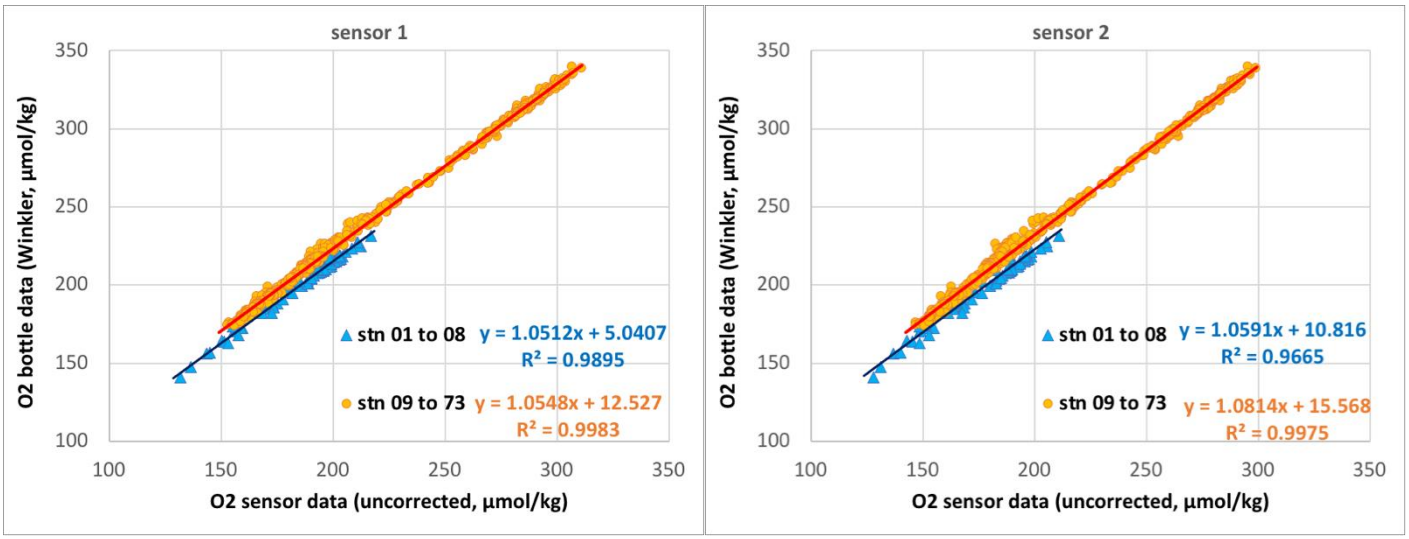

Figure D: Regression between the bottle measurements and the sensors data for sensor 1 (left) and sensor 2 (right) from the standard rosette. A global regression is given for stations 1 to 8 + the downcast of station 9 (in blue) and for the upcast of station 9 to station 73 (in orange).

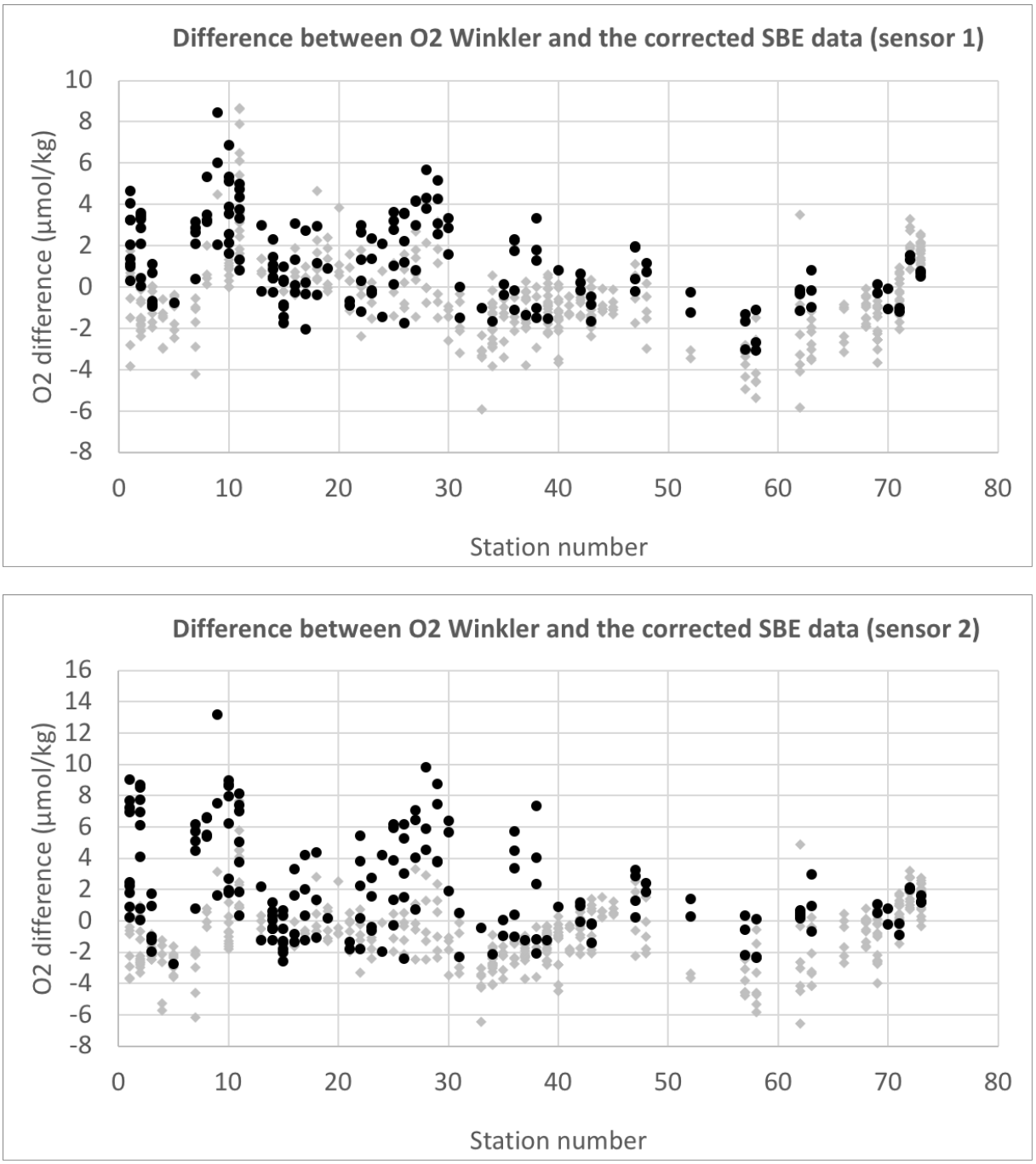

Figure E: Difference between the sensors corrected data and bottle measurements (O2meas - O2ctd) for sensor 1 (top) and sensor 2 (bottom) from the standard rosette. The sensors data were corrected according to the regression curves shown in Figure 4. The gray dots show all samples whereas the black dots are for deep and bottom water (below 1000m).

Evaluation of salinity data from the clean rosette

The comparison of the 2 salinity sensors data with bottle salinity measurements shows a small, but significant offset for sensor1 (Figure F): the mean difference (Sctd – Smeas) in deep and bottom waters (below 1000m) is -0.005 ±0.004 for sensor 1 and -0.003 ±0.005 for sensor 2.

Recommendations: apply a correction of +0.005 for sensor 1 at all stations.

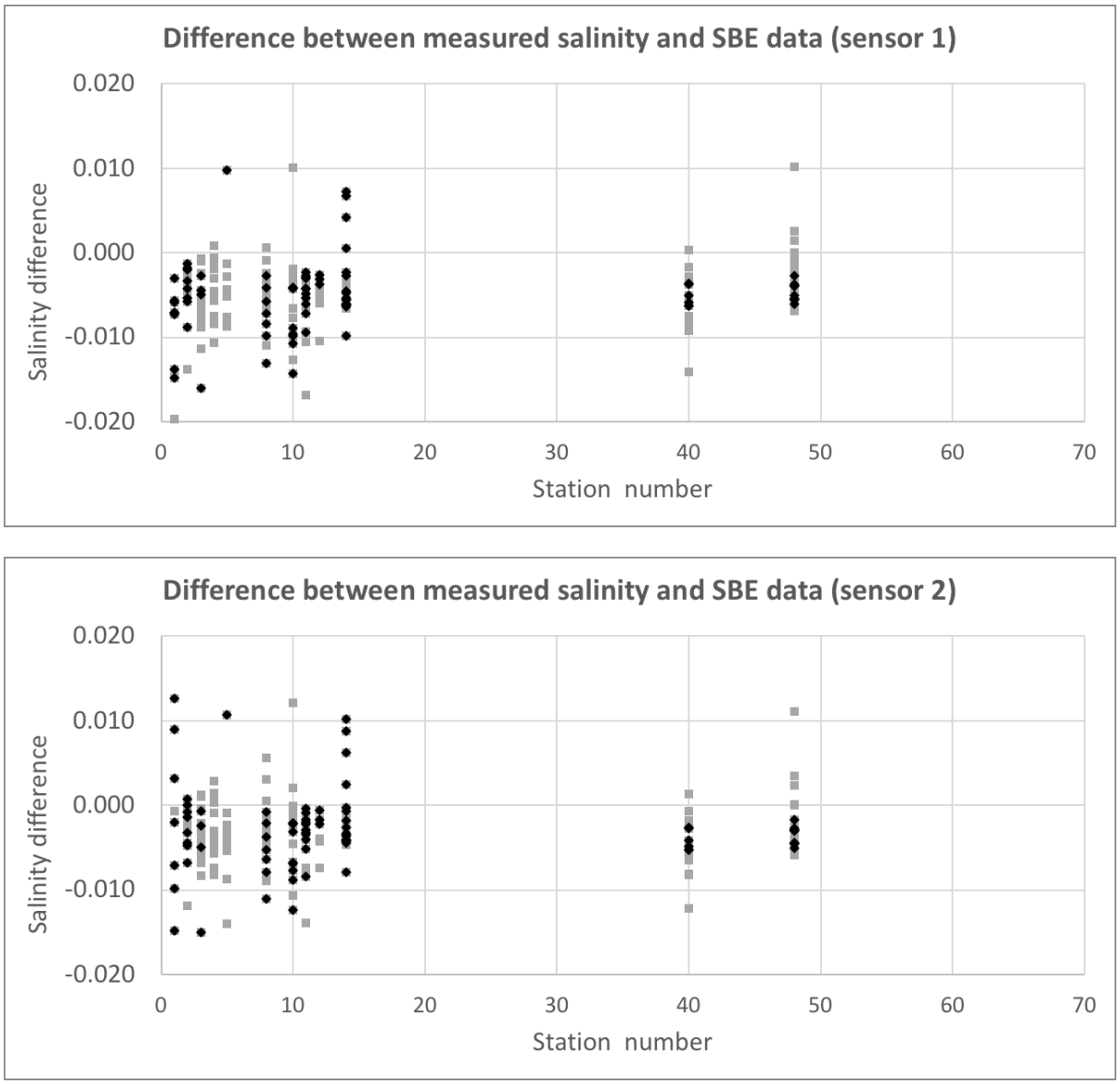

Figure F: Difference between the sensors data and bottle measurements (Sctd – Smeas) for sensor 1 (top) and sensor 2 (bottom) from the clean rosette. The gray dots show all samples whereas the black dots are for deep and bottom water (below 1000m).

Evaluation of oxygen data from the clean rosette

Oxygen samples from the clean rosette were only collected at stations 12 and 16 (Figure G). Oxygen data from sensor 1 were lower than bottle data by 15 to 21 µmol/kg, while the data from sensor 2 were lower by 16 to 24 µmol/kg. By combining data from stations 12 and 16 (Figure G), we obtained the following corrections:

Sensor 1, upper waters (above the oxygen minimum): O2corr = 1.0115x + 14.78

Sensor 1, lower waters (below the oxygen minimum): O2corr = 1.1562x - 8.8172

Sensor 2, upper waters (above the oxygen minimum): O2corr = 1.0206x + 11.917

Sensor 2, lower waters (below the oxygen minimum): O2corr = 1.1331x - 6.4119

Same as for the sensors on the standard rosette, the regression curve changes below the minimum oxygen layer (Figure G). For this reason, a different correction should be applied for upper and lower waters. Within the minimum oxygen layer, one or the other correction can be applied, leading to very similar results. The residuals at station 12 and 16 are lower than 2 µmol/kg.

The corrections proposed above appear to be suitable for stations 10 to 68, but not for stations 1 to 8 (Figure H). For the latter, an intermediate correction should be applied.

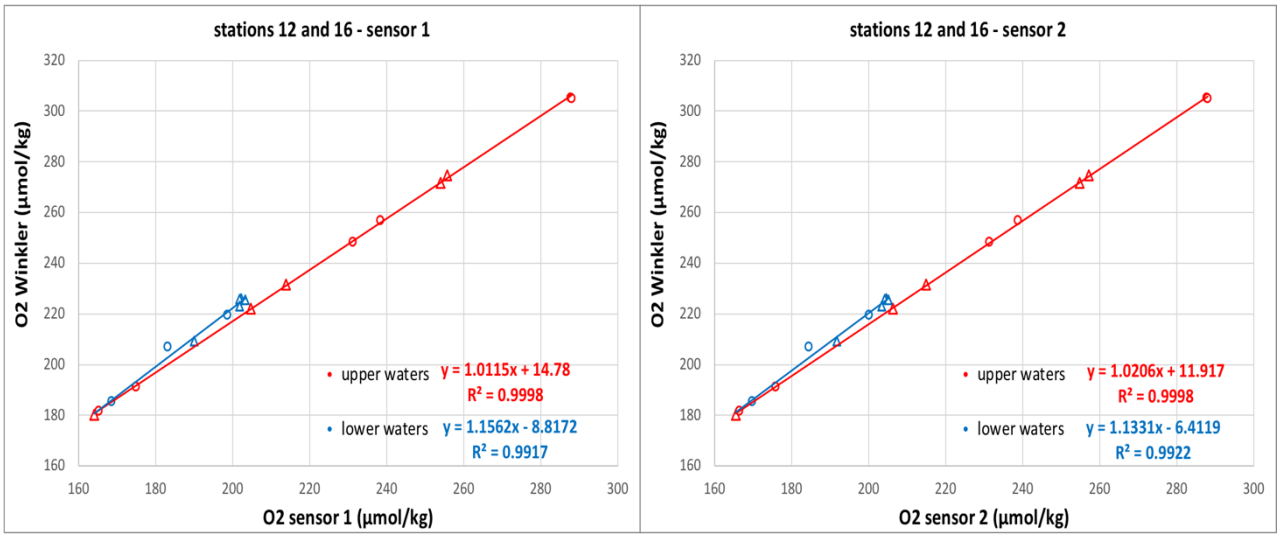

Figure G: Regression between the bottle measurements and the sensors data for sensor 1 (left) and sensor 2 (right) from the clean rosette at stations 12 (triangles) and 16 (dots). The regression curves were obtained by combining in upper waters (above the oxygen minimum, in red) and lower waters (in blue).

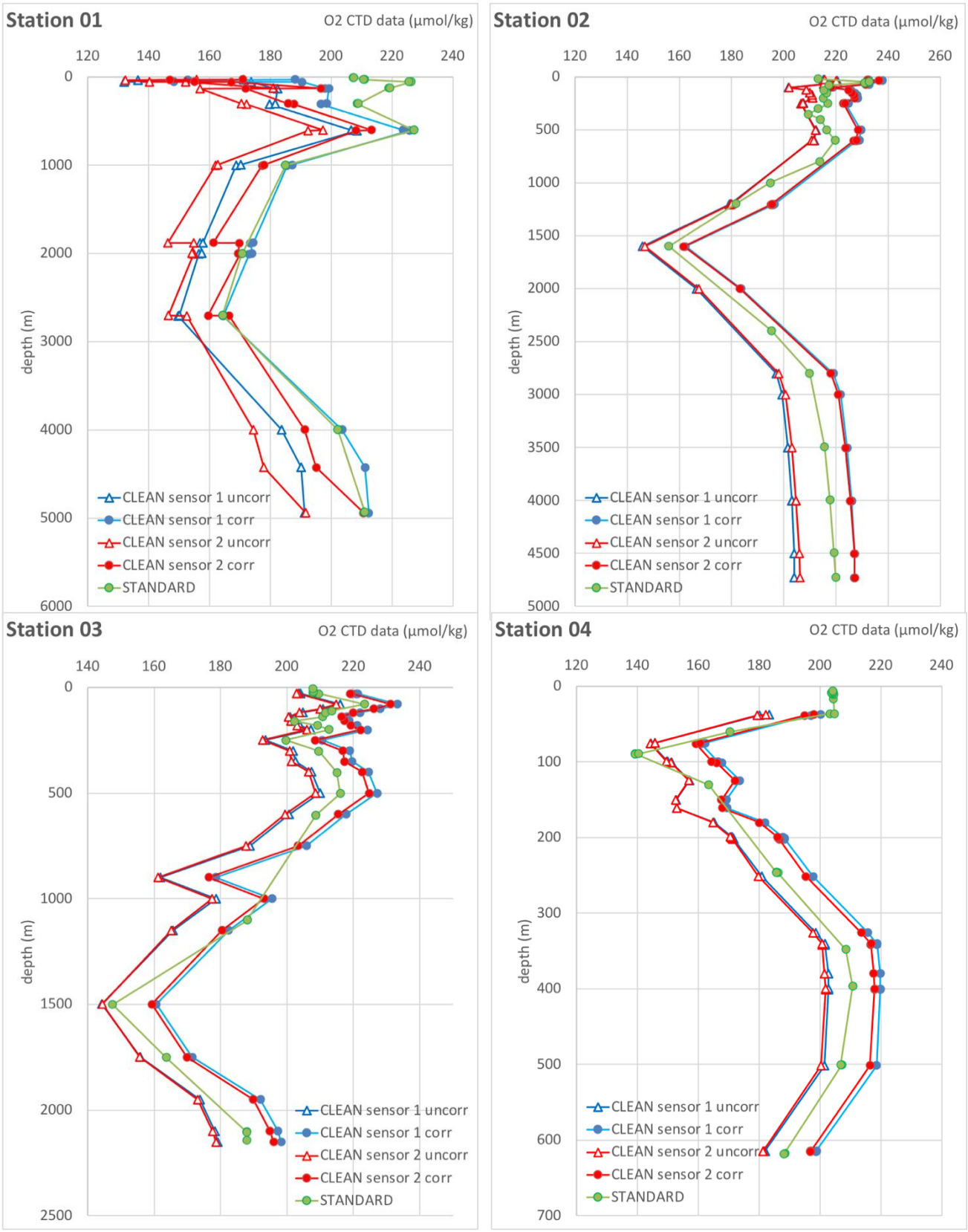

Figure H: Profiles of oxygen data at stations 1 to 8, 10 and 68 obtained from the standard rosette (in green, data from sensor 1 corrected according to Table 3) and the clean rosette (in blue for sensor 1 and red for sensor 2). Uncorrected data (triangles) are compared to data corrected according to Figure 7 (blue and red dots).

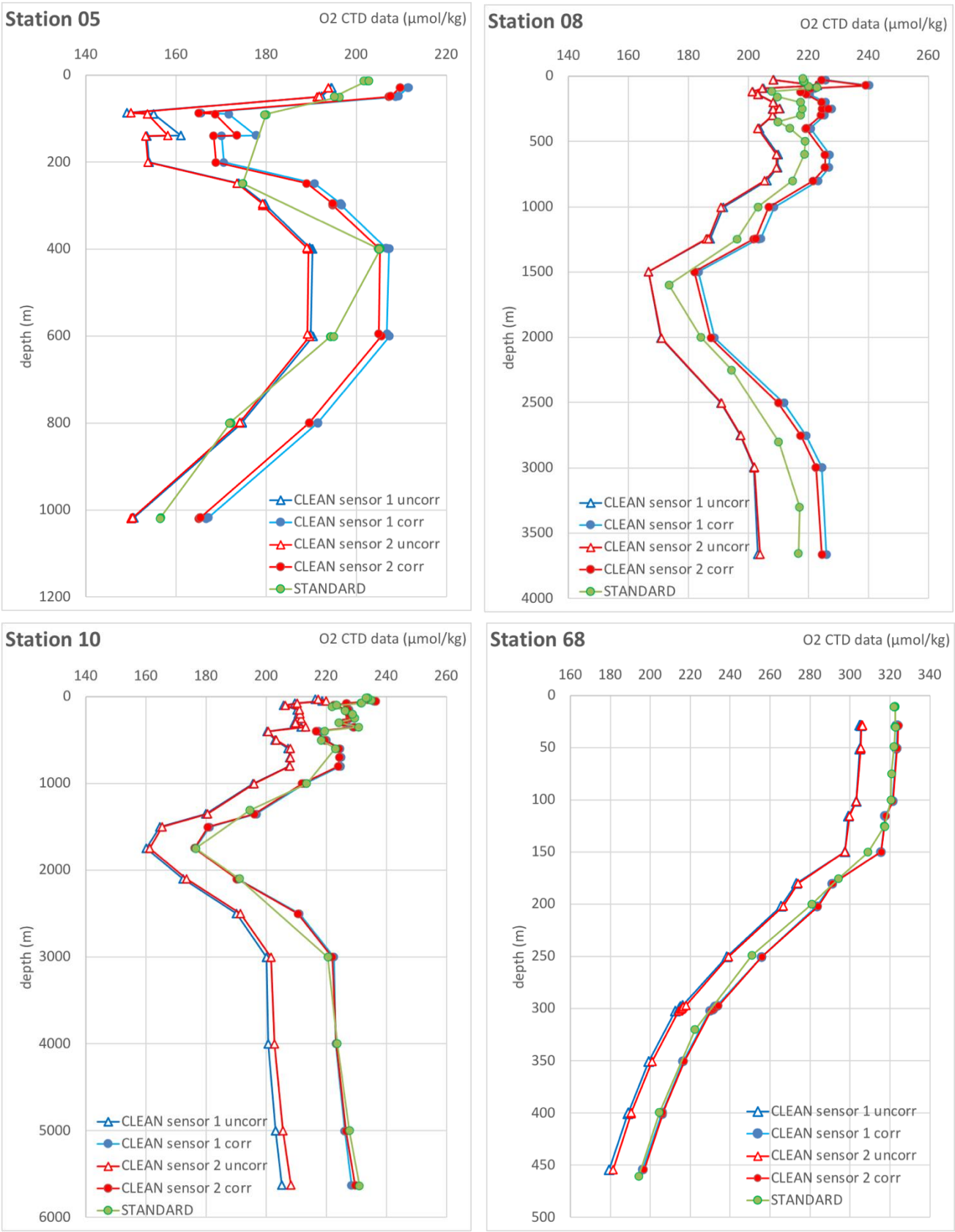

Figure H continued

X.3 Elements techniques à rapporter en lien avec l'exploitation de l'EK80 et l'acquisition de données de qualité.

Lors des campagnes précédentes (notamment MD217), un problème de bruit de carène avait été indentifié. Selon les tirants d'eau et l'assiette du navire, l'état de la mer et le tanguage, l'EK80 peut être bullé entre 10,5 et 14 noeuds. Un ajustement de la vitesse semble donc être nécessaire afin d'obtenir des données de qualité optimale.
Lors de la campagne SWINGS, nous avons identifié une influence des flaps (système d'ouverture/fermeture des propulseurs d'étrave) sur les données acoustiques de l'EK80. Nous avons ainsi pu pratiquer plusieurs phases de test pendant lesquels une différence de qualité des données acoustiques a été observée suite à l'ouverture ou à la fermeture des flaps. Ces cas ont été rapportés dans le document de Vincent Gabriel transmis par Genavir.

Cas 1 :
Nous avons réalisé un premier test au départ de la Réunion, le 13/01/2021 avec un état de mer très propre, pas de houle et 10kts de vent.
Nous avons effectué une montée en allure entre 10 et 14 knts, flaps fermés, puis flaps ouverts. A notre surprise, nous avions un meilleur résultat flaps ouverts, notamment sur l'EK80, où nous pouvons constater l'absence de perturbations (traits blancs verticaux). L'infuence de la vitesse n'est par contre pas notable, dans l'une ou l'autre configuration (mer très propre).

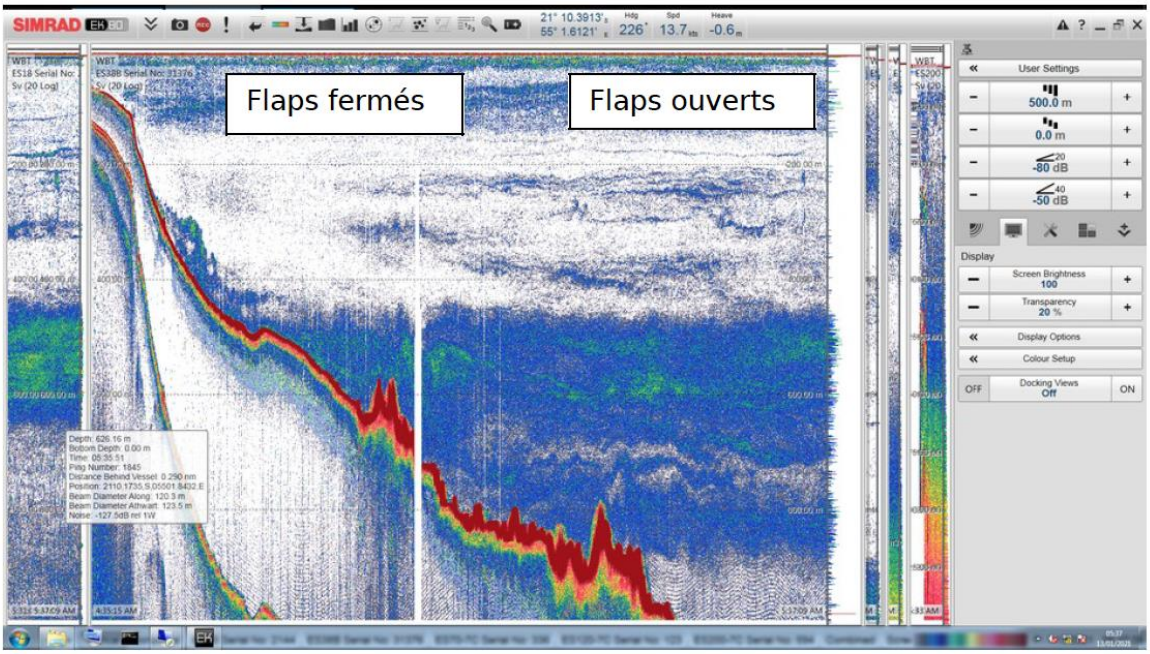

Cas 2 :
Un deuxième test a ensuite pu être réalisé le 24/01, avec des conditions météorologiques plus dégradées, mer formée et 40knts.
Nous constatons alors une nette amélioration sur les fréquences 18kHz et 38kHz à la fermeture des flaps. Nous pensons que le tangage et le roulis induisent une vibration lorsque les flaps sont ouverts. Nous ne retrouvons pas la signature du bullage qui se traduit par des traits blancs verticaux, mais plutôt des caractéristiques de perturbations de type électriques (lignes rouges dans les échogrammes).

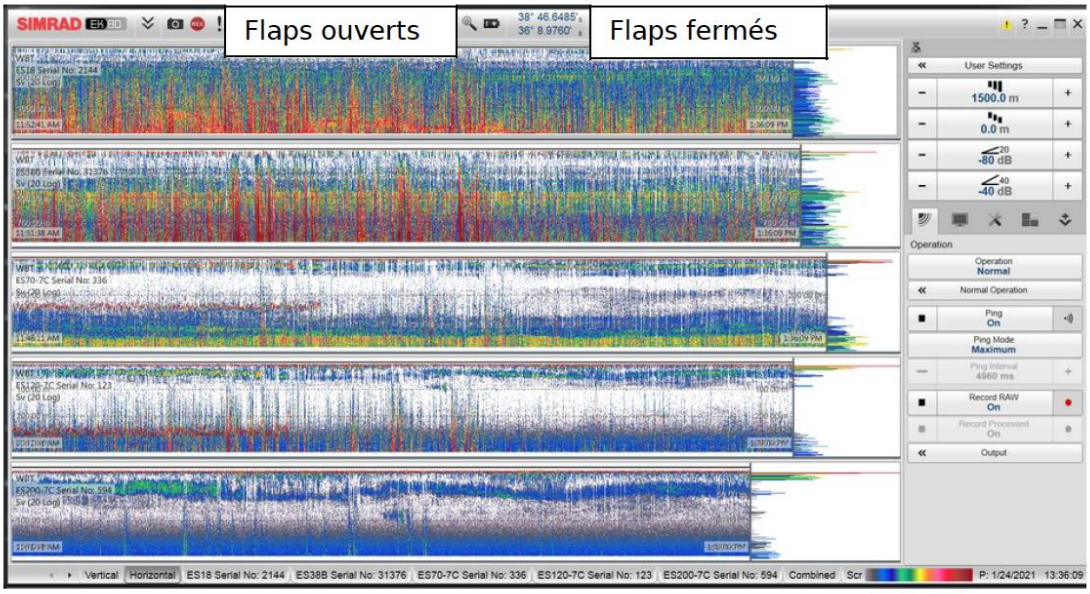

Cas 3 :

Une dernière expérience a été menée le 06/02/2021, avec des conditions encore une fois dégradées (mer agitée). Après avoir constaté une dégradation des données sur l'EK80 18kHz et 38kHz due aux conditions de mer et au mouvement du bateau, le problème de bullage semble être atténué par l'ouverture des flaps (moins de traits blancs).

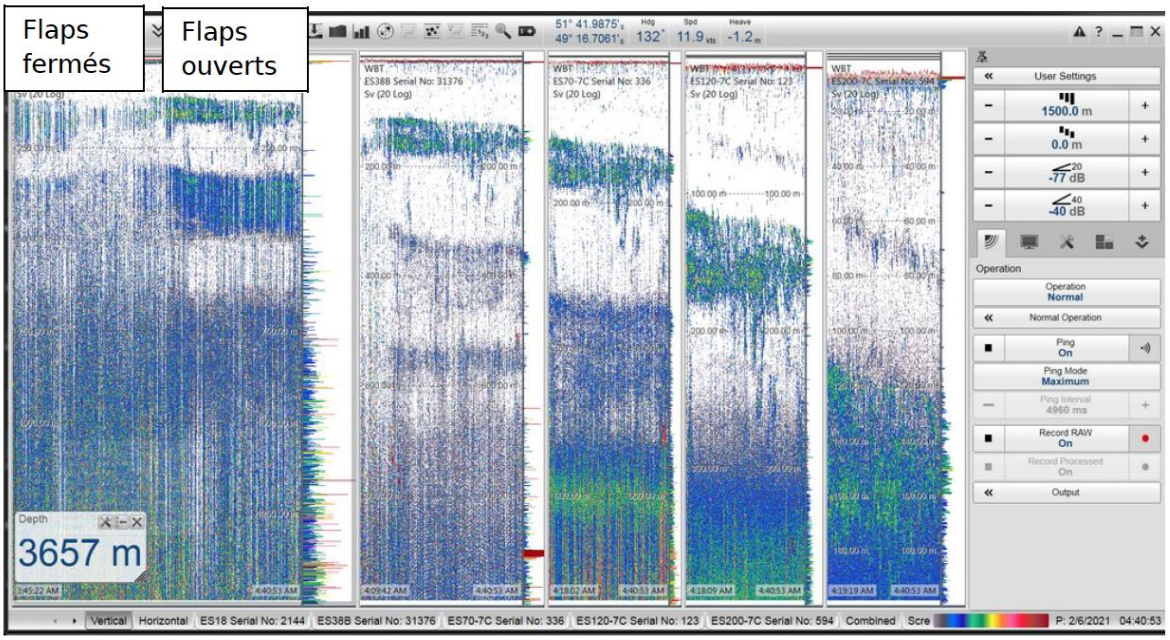

Conclusion

Nous constatons donc un effet de la position des flaps sur les données acoustiques, en particulier sur les basses fréquences, plus impactées par les perturbations. Le choix de la position des flaps pour des données de qualité optimale n'est pas figé, car il dépend des conditions de mer principalement. Nous constatons que les conditions de mer, en particulier la direction, la hauteur et la période de la houle ont une influence majeure sur le comportement des EK80 : il ne se comportera pas de la même manière avec une mer de face, où les flaps ouverts peuvent améliorer le flux et l'évacuation des bulles (par rapport à la position de la gondole acoustique) alors qu'une mer par le travers pourra conduire à des vibrations des flaps.

Il est à noter que le système d'ouverture et de fermeture des flaps étant déjà déterioré, un jeu important existe au niveau des axes des flaps. En raison de la détérioration avancée constatée du système, ayant entrainé une voie d'eau au niveau de la tringlerie, il a été décidé en milieu de mission de garder les flaps en position d'ouverture pour éviter une potentielle avarie. Le forçage mécanique a limité les vibrations.